

The Effects of Oxidation on Striated Muscle

© Daren Elkrief

Department of Physiology
Faculty of Medicine and Health Sciences
McGill University, Montreal



August, 2023

A thesis submitted to McGill University in partial fulfillment of the requirements of the degree of
Doctor of Philosophy in Physiology

Table of Contents

Abstract	4
Résumé.....	5
Acknowledgments.....	6
Contribution to Original Knowledge	7
Contribution of Authors.....	8
List of Figures.....	9
List of Tables	14
List of Abbreviations	16
Introduction to Thesis	19
Literature Review.....	20
From Amino-acid to Disease: The Effects of Oxidation on Actin-Myosin Interactions in Muscle	21
Abstract	22
Introduction.....	23
Actin-myosin interactions.....	26
Major Sources of muscle oxidation	28
Oxidative alterations in thick filament proteins.....	30
Oxidative alterations in thin filament proteins.....	36
Impacts of oxidation actin-myosin interactions	40
Oxidation of contractile proteins in disease and aging	42
Arthritis.....	43
Heart disease	44
Muscular dystrophy	46
Aging.....	47
Transgenic models in redox regulation.....	50
Conclusion	52
Experimental Study 1.....	62
Oxidation alters myosin-actin interaction and force generation in skeletal muscle filaments .	63
Abstract.....	64
Introduction.....	65

Methods.....	67
Results.....	74
Discussion.....	77
References.....	81
Bridging text between study 1 and study 2.....	88
Experimental Study 2.....	89
Oxidation of striated muscle thin filaments.....	90
Abstract.....	91
Introduction.....	91
Methods.....	93
Results.....	101
.....	104
Discussion.....	103
Conclusion.....	111
References.....	112
Bridging text between study 2 and 3.....	145
Experimental Study 3.....	146
Oxidation-induced structural changes in actin and myosin evaluated by computational simulation and high-speed AFM.....	147
Abstract.....	148
Significance Statement.....	148
Introduction.....	149
Results and Discussion.....	151
Methods.....	165
References.....	170
Thesis Discussion.....	185
Conclusion and Summary of Thesis.....	192
Appendices and Supplemental Information.....	195
First Authorship Agreement for Study 3.....	196
Thesis References.....	198

Abstract

Muscle function is governed by interactions between actin, myosin, and regulatory proteins, which are the key constituents of striated muscle fibers. Despite extensive research, the understanding of the impact of oxidation on these proteins and the consequent alterations in muscle contraction remains fragmented. As oxidation events play a significant role in aging and various diseases, comprehending these impacts holds a great therapeutic potential. This thesis addresses this gap by providing a comprehensive investigation of the structural and functional impacts of protein oxidation in striated muscles, particularly focusing on myosin-actin interactions. Spanning from the molecular level of amino acids to macroscopic muscle structures, this study is composed of three main investigations. The first explores how oxidation of actin and myosin, induced by the oxidant SIN-1, impacts their interaction and the consequent force generation. We found that oxidation significantly affects actin-myosin interactions and results in a decrease in force generated by myosin and actin filaments, thereby reducing muscle contractile activity. The second investigation extends this understanding by examining the oxidation of thin filament proteins. Our results indicate that oxidation alters their interaction with myosin and potentially modifies the calcium handling properties of the thin filament. Mass spectrometry data further identified numerous oxidized residues, hinting at possible mechanisms behind the observed functional alterations. The final investigation employs high-speed atomic force microscopy (HS-AFM) and molecular dynamics simulations to evaluate oxidation-induced structural changes in actin and myosin. We observed that oxidation destabilizes the molecular structure of G-actin and alters myosin displacement on a single-molecule level, suggesting decreased force generation by myosin motors under oxidative conditions. The insights garnered from these studies can pave the way for future research and potential therapeutic interventions targeting oxidation-induced muscle dysfunctions, thereby emphasizing its significance not only to muscle physiology but also to the broader understanding of biological aging and disease processes.

Résumé

La fonction musculaire dépend des interactions entre l'actine, la myosine, et d'autres protéines régulatrices, essentielles aux fibres musculaires striées. Parmi les modifications chimiques affectant ces protéines, l'oxydation est l'une des plus courantes. Malgré de nombreuses études, les effets précis de l'oxydation sur ces protéines et la contraction musculaire ne sont pas entièrement compris. L'oxydation est importante dans le vieillissement et dans de nombreuses maladies, offrant un potentiel thérapeutique. Cette thèse étudie en profondeur les effets de l'oxydation sur les protéines musculaires, en mettant l'accent sur les interactions entre myosine et actine. Elle comprend trois investigations principales: I. Comment l'oxydation, causée par SIN-1, influence l'interaction entre l'actine et la myosine et la force produite. Nous avons découvert que l'oxydation réduit la force produite par ces protéines, diminuant l'activité musculaire. II. L'étude de l'oxydation des protéines du filament mince. Nos résultats montrent que l'oxydation change leur interaction avec la myosine et pourrait affecter la gestion du calcium. De plus, nous avons identifié plusieurs zones oxydées sur ces protéines. III. L'utilisation de la microscopie à force atomique (HS-AFM) et des simulations pour observer les changements structuraux causés par l'oxydation. Nous avons observé que l'oxydation déstabilise la structure moléculaire de G-actine et modifie le déplacement de la myosine à un niveau de molécule unique, suggérant une diminution de la génération de force par les moteurs de myosine sous des conditions oxydatives. Collectivement, ces résultats contribuent significativement à la compréhension du rôle de l'oxydation dans la fonction musculaire striée et soulignent ses implications pathologiques potentielles. Ces découvertes pourraient guider des recherches futures et des interventions thérapeutiques potentielles par rapport aux dysfonctions musculaires induites par l'oxydation. Selon sont importat non seulement pour la physiologie musculaire mais aussi pour la compréhension plus large des processus de vieillissement biologique et des maladies.

Acknowledgments

Before anything, my heartfelt thanks go to my supervisor, Dr. Dilson Rassier, for his unwavering support, financial assistance through his granting agencies, and the trust he placed in me. He consistently provided the necessary resources and a keen editing and directional guidance which was critical to the degree direction. I would like to thank my committee members, Dr. Claire Brown, Dr. Peter Grutter and Dr. Adam Hendricks who have held me accountable and provided feedback over my degree; their assistance was invaluable and encouraging. I would like to extend special gratitude to Dr. Claire Brown who has agreed to serve as my supervisor during the end of my degree and continues to provide valuable support. I wish to express my deepest gratitude to Dr. Yu-Shu Cheng, whose invaluable guidance and immense knowledge have been instrumental in the completion of my degree. His keen insights greatly enhanced our joint manuscripts, particularly in the areas of thin filament analyses and experimentation. I am deeply indebted to Dr. Oleg Matusovsky, whose steadfast support, sage advice, and expertise in atomic force microscopy study were invaluable. My sincere thanks go out to my current and former laboratory colleagues over the years, including Ricarda Haeger, PhD, Caitlin MacEachen, MS, Rezuhanul Haque Saikat, MD, MS, Andrea Mendoza, MS, Chelsea Eng and the greater McGill community. Their collective support, advice during challenging times, and contributions to a healthy laboratory environment were critical. A special acknowledgment goes to Dr. Galina Matusovsky, whose consistently positive attitude and remarkable efficiency in handling chemical and laboratory equipment acquisition significantly facilitated our work. I also extend my appreciation to the valuable collaborators at McGill: Gijs Ipjma, whose *in vitro* motility assay analysis software saved me substantial time, and Lorne Taylor and Amy Wong of the McGill Proteomics platform, who rescued the thin filament analysis study from the brink of failure. I would like to thank collaborators early in my degree at the Karoliska Instiutet, Dr. Alf Mansson who provided the first version of the analysis software and Dr. Malin Persson who helped conceive the original idea for the first project in this thesis. Finally, I would like to express my deepest gratitude to my siblings and my parents. Their unwavering belief in my abilities was the backbone of my persistence. Their encouragement inspired me to put forth my greatest effort.

Contribution to Original Knowledge

Encompassing molecular dynamics and visualization to amino acid modifications identified through mass spectrometry (MS), this study represents a pioneering effort in understanding the effects of oxidation at such a scope. Moreover, we have run studies in parallel on functional and structural alterations resulting from oxidation, allowing us to draw strong conclusions on the effects of oxidation on contractile protein function.

Our utilization of the Filament Force Microscopy System (FFMS) to evaluate filament force changes in the presence of oxidation is unprecedented. When combined with the In Vitro Motility Assay (IVMA), our findings underscore the pivotal role of actin in the observed decline of contractile function under oxidative conditions. Although previous research has illuminated the behavior of myosin II using High-Speed Atomic Force Microscopy (HS-AFM), our HS-AFM data is ground-breaking in its exploration of oxidation's impact and the molecular simulations implying decreased myosin force due to structural alterations.

A significant revelation from our study is the demonstrable effect of actin oxidation on myosin binding properties, offering compelling evidence of both structural and computational alterations. Furthermore, we have meticulously analyzed potential modifications on thin filament proteins using the IVMA and have drawn correlations with MS-derived data on amino acid modifications.

In summary, our study provides an intricate yet expansive examination of the influence of oxidation on actin-myosin and regulatory protein function. By seamlessly integrating insights from functional, structural, and amino acid modifications, our research offers both a panoramic view and a detailed analysis, underscoring the depth and breadth of the thesis.

Contribution of Authors

Chapter 1: For the first study, I conceived and directed the study, data analysis, manuscript writing, and oversaw the submission and revision process. The study's successful completion was due in no small part to the input of Dr. Yu-Shu Cheng, who directed the thin filament experimentation and analyses, offering critical insights and lending his expertise to the study. Additionally, Dr. Oleg Matusovskiy offered valuable advice during the development of the manuscript and approved its final version, while Dr. Dilson Rassier supervised the study and provided the final approval for the manuscript. Chapter 2: For the second study, I conceived and directed the project, emphasizing the oxidation of thin filament proteins. I conducted mass spectrometry analysis, SDS-PAGE gels, and the IVMA for thin filament experimentation and analysis. Dr. Yu-Shu Cheng contributed his expertise to the SDS-PAGE, and Dr. Dilson Rassier supervised and provided his approval for the manuscript, affirming the validity and impact of the work. Chapter 3: The final study represents an innovative application of high-speed atomic force microscopy (HS-AFM) and molecular dynamics simulations to explore oxidation-induced structural changes in actin and myosin. While Dr. Oleg Matusovskiy was critical to the experimentation using the HS-AFM, my contribution was pivotal at the onset. I provided the idea for the study and isolated the protein filaments used in the study. HS-AFM data which I had produced was removed from an earlier study and placed into this study instead. Although the study grew beyond my initial involvement, I contributed to the genesis, review and writing of the work, and my involvement was essential in getting this ambitious project off the ground. I contributed to writing, final edits, and review of the manuscript. Dr. Dilson Rassier provided support for this study by editing, reviewing, and approving the final manuscript.

List of Figures

Literature Review Figures

Figure 1. Myosin cross-bridge cycle. Circles represent actin monomers. A: Actin, M: Myosin, D: ADP (adenosine diphosphate), T: ATP (adenosine triphosphate), Pi: Inorganic phosphate. 27

Figure 2. The ribbon diagram of the myosin II molecule in four structure states: rigor, post-rigor, pre-power stroke and post-power stroke. The lever arm position is controlled by the position of the converter, which swings relative to the rest of the motor domain. Model designed by Y.S. Cheng. 28

Figure 3. Oxidation of the actin-myosin cross-bridge. **a.** Oxidative PTMs have a preferential effect on the weak to strong transition, and thus reduction in force. A greater reduction in proportion of strong binding cross-bridges at steady state. Oxidation of MHC Cys-707 and Cys-697 may impair transition state. **b.** Decreased access of oxidizable residues in strong binding states in absence of ATP, when actin is blocking sensitive residues on the S1 may prevent oxidation of key cysteines. **c.** Nitrosylation of actin Cys-374 and Cys-285 increases the time which actin is bound to myosin or decreases the detachment rate. **d.** Oxidation can preferentially modify actin and myosin during the relaxing state because the actin myosin binding pockets are exposed. **e.** Multiple targets alter ATPase directly, such as Lys-84. 35

Figure 4. Oxidation in thin filament proteins. **a.** TnC binds Ca^{2+} and undergoes conformational change that exposes a hydrophobic region. there is no evidence that oxidation of TnC alters Ca^{2+} binding however, oxidation of TnC Cys-98 has been shown to reduce binding to TnI. Oxidation of TnI Cys-133 increases Ca^{2+} sensitivity. **b.** After Ca^{2+} binding, TnC-TnI dissociates from actin allowing Actin-myosin binding. TnT moves Tm to expose myosin binding site on actin. Oxidation of Tm Cys-190 increases Ca^{2+} sensitivity by crosslinking with actin Cys-257, biasing Tm to an open configuration. 40

Experimental Study 1 Figures

Figure 1. Myosin-propelled actin sliding velocities. A: comparison between control and SIN-1 oxidized actin filament and HMM in the IVMA. There was a significant decrease for SIN-1-treated actin (n = 14), SIN-1-treated HMM (n = 10), and SIN-1-treated actin + HMM (n = 10, videos) (P

< 0.01) when compared with untreated filaments (n = 13, videos). B: relative decrease in motility velocity relative to control experiments. There was an ~10% decrease when actin was oxidized and a 15% decrease when HMM was oxidized. When both actin and HMM were oxidized, there was a 55% decrease in velocity. C: motile fractions were similar between control (n = 12, videos), SIN-1 actin (n = 13), SIN-1 HMM (n = 10), and SIN-1 actin + SIN-1 HMM (n = 17) (P = 0.09). All values are shown as means ± SE. HMM, heavy meromyosin; IVMA, in vitro motility assay; SIN-1, 5-amino-3-(4-morpholinyl)-1,2,3-oxadiazolium chloride. 74

Figure 2. The effects of antioxidant in the myosin-propelled actin sliding. HMM was incubated with SIN-1 (n = 10). After initial imaging, the proteins were left on the coverslip in the dark for 15 min and the velocity decreased (P < 0.001). Catalase was added, and videos were taken 15 min later. At this point, velocity of actin motility was restored with values that were not statistically different from control (P = 0.02). Another 15-min period did not change the results (P = 0.152), and the velocity remained similar to control levels. All values are shown as means ± SE. HMM, heavy meromyosin; SIN-1, 5-amino-3-(4-morpholinyl)-1,2,3-oxadiazolium chloride. 75

Figure 3. Filament force measurement in control and SIN-1-treated filaments. A: representative images of thick and thin filaments attached to the cantilevers. I) filaments are separated before actin-myosin interaction (boxed area). II): cantilevers are brought closer together, and actin and myosin interact. III): myosin filaments exert force on actin filaments, bending the cantilever. IV): actin-myosin interaction is disrupted when the filaments detach. B: there was a decrease in force observed in SIN-1-treated actin filaments (82.75 pN/μm, n = 11) and SIN-1-treated thick filaments (66.98 pN/μm, n = 11) when compared with control filaments (113.4 pN/μm, n = 15) (P = 0.0001). Scale bars: 10 μm. All values are shown as means ± SE. SIN-1, 5-amino-3-(4-morpholinyl)-1,2,3-oxadiazolium chloride. 76

Experimental Study 2 Figures

Figure 1 Velocity comparison between (A) unregulated (Actin) and regulated thin filaments (TF) in non-oxidized (A) and oxidized (B) (SIN-1) conditions. Velocities were normalized to actin filaments in non-oxidized (C) and oxidized (D) conditions. Data presented as mean ± S.E.M. 101

Figure 2. Semi log plot of the velocity of regulated thin filament as a function of the free calcium concentration for (A) control and SIN-1-treated thin filaments. (B) Plots were normalized to their

respective V_{max} . Average frame filament velocities are shown for control (C) and oxidized (D) thin filaments. Each point represents an entire frame from the video, and all velocities are averaged for each frame. Data was fitted to the Hill equation. Data presented as mean \pm S.E.M. 102

Figure 3 Amino acid oxidation locations as determined by MS. Oxidation locations were determined thin filament proteins including: (A) tropomyosin (B) TnT (C) G-actin (D) TnI and (E) TnC. Amino acids designated by letter and position. Oxidation sites were highlighted in green. Coloring on model corresponds to model structure confidence, where blue is very high, light blue confident, yellow is low, and orange is low confidence. Models were generated in alpha fold. 103

Experimental Study 3 Figures

Figure. 1. **Computational oxidative nitration of the G-actin.** (a) The non-oxidized and (b) computationally oxidized G-actin (PDB 2ZWH). The modified residues shown as blue sticks with the phenyl ring in each subdomain (SD1-SD4). Oxidative modifications were performed in the pyMOL using pyTM plugin (v.1.2) (Warnecke, Sandalova, Achour, & Harris, 2014). The oxidized atoms in the residues highlighted by pink color. (c) The successive y-axis rotation of the non-oxidized and oxidized G-actin structures with 45° step from initial position showed the local changes in the electrostatic potential energy around oxidized residues. The matched colored boxes for each orientation were magnified to show the charge differences more precisely. The map scale represents the electrostatic potential energy from -5.0 k_BT (red) to 5.0 k_BT (blue). 153

Figure 2. **Molecular dynamics (MD) simulation of the G-actin structure with non-oxidized and Tyr-3NT oxidized residues.** An example of solvation (a) and ionization (b) of the G-actin structure. The structure was placed in a rectangular box filled with water molecules. The cyan and yellow spheres represent Na²⁺ and Cl⁻ ions, respectively. (c) The root-mean-square deviation (RMSD) calculated for G-actin structures with non-oxidized and Tyr-3NT oxidized residues. 155

Figure 3. **Cross-sectional analysis in the simulated G-actin and G-actin-3NT HS-AFM images.** (a) The initial conformation of the G-actin monomer structure (PDB: 2ZWH) rotated with 45° step around y-axis and corresponding simulated HS-AFM images (Sim HS-AFM) obtained with BioAFM viewer with the tip radius 0.1 nm and the apex angle 5°. (b, c) G-actin structures with non-oxidized Tyr and Tyr-3NT residues, indicating the x, y-axis used to obtain the local height values (b) and global height values (c) with corresponding simulated HS-AFM images of

the G-actin structures with tip radius 1.0 nm with schematic directions of the scanned surfaces. **(d, e)** local and global height profiles for the G-actin structures with non-oxidized Tyr (blue) and Tyr-3NT (red) residues with the frequency analysis of the height values from entire surface. The red arrow shows a higher frequency of 1.8-2.2 nm height values in the oxidized G-actin-3NT; the blue arrow shows the higher frequency of 3-4 nm height values in the non-oxidized G-actin. 156

Figure 4. Comparison of the height profiles of the actin filaments treated by SIN-1 in the experimental and simulated HS-AFM images. **(a)** Diagram representing the peak height measurements along actin filament. The red points show the peaks (P) in the actin structure with the highest values as a cross-over of the double F-actin helix. **(b)** Representative HS-AFM images of control and SIN-1-treated actin filaments located on mica-supported lipid bilayer with corresponding Z-scales in nm. Scan area: 150 x 150 nm² (80 x 80 pixels²), scale bar: 35 nm. **(c, d)** Peak height and half-helical pitch measurements for the non-treated and SIN-1-treated F-actin. No differences were noted in half-helical pitch between control (n = 178) and SIN-1 filaments (n = 142, P = 0.3994), whereas peak height (d) was significantly lower in SIN-1 filaments (n = 207) compared to controls (n = 315, P = 0.006). All values shown as mean ± SD. 158

Figure 5. Global fitting of experimental (Exp) and simulated (Sim) HS-AFM images. **(a)** Best-fitted orientations of the simulated actin filaments with experimental HS-AFM images of the non-oxidized F-actin and the oxidized by SIN-1 F-actin used as a template. **(b)** An example of the cross-section analysis for the simulated F-actin structure (PDB 6BNO) with non-modified Tyr residues and oxidized Tyr-3NT residues. **(c)** Comparison of the height profiles of the actin filaments in the experimental and simulated HS-AFM images. 159

Figure 6. Oxidation-induced structural changes in HMM molecules and the HMM displacement. **(a)** The non-oxidized and SIN-1-treated skeletal HMM, a double-headed fragment of myosin, on the mica-APTES surface. Scan area: 150 × 75 nm², 80 × 40 pixels², temporal resolution: 5 frame per second, Scale bar: 30 nm. **(b)** The distance between two HMM heads measured over time: 8.9 nm ± 2.7 nm (SD) for SIN-1-treated HMM and 22.9 ± 4.6 nm (SD) for non-oxidized HMM. **(c, e)** HS-AFM images of skeletal HMM bound to the non-oxidized F-actin **(c)** and SIN-1 treated F-actin **(e)** in the presence of ATP. Scan area: 150 × 75 nm², 80 × 40 pixels², temporal resolution: 6.7 frame per second. Scale bar: 30 nm. Arrows with symbols, (↔), (↔): forward or backward head displacement between reference frame and subsequent frame; (↔): no

head displacements between reference frame and subsequent frame. **(d)** Histogram of the HMM displacements along the non-oxidized F-actin (blue) and SIN-1 treated F-actin (red). Data were fitted by two Gaussians: $r^2=0.99$, $r^2=0.90$ and $r^2=0.99$, 0.91 for Fa-HMM and SIN-1-Fa-HMM, respectively; $n=758$ events (Fa-HMM), $n=303$ events (SIN-1-Fa-HMM). The average displacements for Fa-HMM: $2.6 \text{ nm} \pm 0.5 \text{ nm}$ (1st peak) and $6.1 \text{ nm} \pm 0.8 \text{ nm}$ (2nd peak); for SIN-1-Fa-HMM: $1.7 \text{ nm} \pm 0.5 \text{ nm}$ and $4.0 \pm 0.5 \text{ nm}$ (2nd peak) **(f, g)** The force produced by myosin molecule in the Fa-HMM (blue) and in the SIN-1-Fa-HMM complex (red) calculated from myosin displacements over time **(f)** and plotted as a histogram **(g)**. The force values were calculated from the equation $F = k \times d$, where k is a stiffness of HMM equal to 2 pN/nm per head (Månsson, Ušaj, Moretto, & Rassier, 2018) and d is a displacement of myosin molecule along the actin filament observed in the present study. 165

Experimental Study 3 Supplementary Figures

Supplementary Figure 1. **Flowchart of the project.** 179

Supplementary Figure 2. **The successive x-axis rotation of the G-actin structures.** The non-oxidized G-actin **(a)** and the oxidized G-actin-3NT **(b)** structures with 45° step from initial position showed the local changes in the electrostatic potential energy around oxidized residues. The matched colored boxes for each orientation were magnified to show the charge differences more precisely. The map scale represents the electrostatic potential energy from -5.0 kBT (red) to 5.0 kBT (blue). 180

Supplementary Figure 3 **Correlation between pseudo-AFM G-actin image and G-actin structure using TensorFlow platform.** The pseudo-AFM images were obtained by BioAFM software (v.2.5) as described in the Methods using tip radii 2 nm . The mean squared error: 6.52×10^{-7} indicates the high correlation between pseudo-AFM image and G-actin atomic structure. 181

Supplementary Figure 4. **Simulated HS-AFM images captured with different tip radii and apex angles.** The images were captured at tip radii ranging from 0.5 to 4 nm and different apex angles from 0° to 15° , showcasing how the tip makes a contact with the surface. 182

Supplementary Figure 5. **Local height measurements by cross-sectional analysis in the simulated G-actin and G-actin-3NT HS-AFM images.** **(a-c)** The initial conformation of the G-

actin monomer structure (PDB: 2ZWH) rotated with 45° step around y-axis and corresponding simulated HS-AFM images obtained with BioAFM viewer with the tip radius 2 nm and the apex angle 5°. G-actin structures with non-oxidized Tyr and Tyr-3NT residues, indicating the x, y-axis used to obtain the local height values. **(d, e)** local height profiles for the G-actin structures with non-oxidized Tyr (blue) and Tyr-3NT (red) residues. 183

List of Tables

Literature Review Tables

Table 1. Oxidized amino acids in thick filament proteins. Chemical abbreviations: ROS: reactive oxygen species; HNO: Nitroxyl, the one electron reduced form of nitric oxide (NO); IASL: 4-(2-Iodoacetamido)-2,2,6,6-tetramethyl-1-piperidinyloxy; SNAP: S-nitroso-N-acetyl-d,l-penicillamine; NEM: N-ethylmaleimide; DTDP: 2,2'-dithiodipyridine; DHNBS: dimethyl (2-hydroxy-5-nitrobenzyl) sulphonium bromide; Bz2ATP: photoaffinity analogue 3'(2')-O-(4-benzoylbenzoyl) adenosine triphosphate; AS: Angeli salt; NCA:1-nitrosocyclohexyl acetate; GSSG : glutathionylation. α or β designate isoform if specified. 57

Table 2. Oxidized amino acids in thin filament proteins. Chemical abbreviations: ROS: reactive oxygen species; HNO: Nitroxyl, facilitates disulfide oxidation into disulfide bridges; IASL: 4-(2-Iodoacetamido)-2,2,6,6-tetramethyl-1-piperidinyloxy; SNAP: S-nitroso-N-acetyl-d,l-penicillamine; NEM: N-ethylmaleimide; DTDP: 2,2'-dithiodipyridine; DHNBS: dimethyl (2-hydroxy-5-nitrobenzyl) sulphonium bromide; Bz2ATP: photoaffinity analogue 3'(2')-O-(4-benzoylbenzoyl) adenosine triphosphate; AS: Angeli salt; NCA:1-nitrosocyclohexyl acetate; CT: Chloramine T (sodium N-chloro-p-toluene sulfonamide). 60

Supplementary Table 3. Comparison between bovine Cardiac(TPM1) tropomyosin (Q5KR49) and human cardiac tropomyosin (P09493). 143

Supplementary Table 4. Comparison between cardiac isoform (TNNT2) of troponin T in bovine (P13789) and human (P45379). 144

Supplementary Table 5. Comparison between cardiac troponin I (TNNI3) in bovine (P08057) and human (P19429). 144

Supplementary Table 6. Comparison between troponin C (TNNC1) in bovine (P63315) and human (P63316)..... 144

Study 2 Supplementary Tables

Supplementary Table 1. Data collected from mass spectrometry were analyzed in pinnacle. This yielded data as shown above. Peptide fragmentation spectra were listed, and the abundance in either reduced or oxidized samples could be qualitatively assessed. Oxidized residues listed as amino acid and either molecular weight associated with modification, or species name..... 142

Supplementary Table 2. Comparison between bovine cardiac actin (QZC07) and human cardiac actin (P68032) using BLAST alignment. Sequence match indicates an identical match between the actin sequences referenced in this study. 143

List of Abbreviations

1. 3-NT - 3-nitrotyrosine
2. ATP - Adenosine triphosphate
3. ATPase - Adenosine Triphosphatase
4. BSA - Bovine serum albumin
5. Cys- Cysteine
6. Ca²⁺ - Calcium ion
7. CATH - Class, Architecture, Topology, Homology
8. CBB - Coomassie Brilliant Blue
9. CFA – The arthric agent Complete Freund's Adjuvant
10. cTnC - Cardiac Troponin C
11. cTnI - Cardiac Troponin I
12. DAB - Diaminobenzidine
13. DED - DNase-I binding loop of domain 2
14. D/E – Region of troponin TnC
15. DMD - Duchenne Muscular Dystrophy
16. DMSO - Dimethyl sulfoxide
17. DTT - Dithiothreitol
18. EGTA - Ethylene glycol-bis(2-aminoethylether)-N,N,N',N'-tetraacetic acid
19. F-actin - Filamentous actin
20. G-actin - Globular actin
21. GSSG - Glutathione disulfide
22. HF - Heart Failure
23. HMM - Heavy Meromyosin
24. HNO - Nitroxyl
25. HS-AFM – High-Speed Atomic Force Microscope
26. HPLC - High-performance liquid chromatography
27. IVMA - In vitro motility assay
28. Lys - Lysine

29. KCl - Potassium chloride
30. LC-MS/MS - Liquid chromatography-tandem mass spectrometry
31. Met - Methionine
32. Mg²⁺-ATPase - Magnesium-activated adenosine triphosphatase
33. MHC - Myosin Heavy Chain
34. MLC 1 - Myosin Light Chain 1
35. MMP-2 - Matrix Metalloprotease-2
36. MS - Mass spectrometry
37. MyBP-C - Myosin Binding Protein C
38. NAC - N-acetylcysteine
39. nNOS - Neuronal Nitric Oxide Synthase
40. PAGE - Polyacrylamide gel electrophoresis
41. Pi - Inorganic phosphate
42. PIPES - Piperazine-N,N'-bis(2-ethanesulfonic acid)
43. PTMs - Post translational modifications
44. Arg - Arginine
45. ROS - Reactive Oxygen Species
46. RNS - Reactive Nitrogen Species
47. S1 - Myosin S1 fragment
48. SDS - Sodium dodecyl sulfate
49. SH1 - Reactive cysteine residue in myosin
50. SH2 - Reactive cysteine residue in myosin
51. SIN-1 - Hydrochloride, 3-morpholinopyridone
52. SNO-Cys - S-nitrosylated cysteine
53. SNP - Sodium nitroprusside
54. TBS - Tris-buffered saline
55. TEM - Transmission electron microscopy
56. TF - Thin filament
57. TFA - Trifluoroacetic acid
58. Tm - Tropomyosin
59. Tm-Tn - Tropomyosin-Troponin
60. TnC - Troponin C

61. TnI - Troponin I
62. TnI_f - Troponin I (fast isoform)
63. TnT - Troponin T
64. Tm - Tropomyosin
65. Tyr - Tyrosine

Introduction to Thesis

The central research problem that this thesis addresses is the investigation of the effects of oxidation on the fundamental components of muscle contraction: actin, myosin, and the thin filament proteins. While previous research has extensively studied these components in the context of whole and skinned muscles, or even as individual proteins, no studies to date have analyzed the contractile apparatus across the experimental spectrum employed in this thesis.

The novelty of our research lies in its comprehensive examination of oxidation, spanning from the assessment of amino acids via mass spectrometry (MS), through to the exploration of structural and dynamic changes measured with high-speed atomic force microscopy (HS-AFM), to *in vitro* studies evaluating velocity and force of actin-myosin interactions. Our study presents a perspective that is rarely articulated: the complexity of the oxidative landscape leaves us with a multitude of unanswered questions, yet it provides a foundational basis for a comprehensive survey of how contractile mechanics evolve as oxidative modifications accumulate.

Primary objectives of this research include the exploration of the effects of oxidation on the function of actin, myosin, and regulatory proteins. Understanding the changes in filament contractile mechanics as oxidative modifications accumulate is a critical component to this study. This thesis concludes with a discussion and summary of the findings, and finally the implications of such research.

The efforts undertaken herein are justified by the ambition of the scope; oxidative effects on muscle contraction components can provide a more holistic view of muscle function and dysfunction. Relating molecular changes with functional outcomes enables a clearer picture of how oxidative stress impacts muscle health and performance. This knowledge is crucial in aging populations and individuals with muscle-related diseases, where oxidative stress plays a significant role.

The insights garnered from this research will foremostly contribute to the mechanistic comprehension of muscle contraction. Moreover, broader implications of such studies deepen the understanding of muscular disorders, potentially paving the way for therapeutic interventions.

Literature Review

The following literature review was recently accepted for publication in the Journal of Muscle Research and Cell Motility. In this review, we delve more deeply into the wide range of oxidation studies, the effects of oxidation at the whole muscle level all the way to the molecular level. This review, while more comprehensive than traditional reviews, encompasses a whole field of work. While traditional oxidation studies span a limited range, usually on effects of disease and involvement in specific tissues or through restricted muscular preparations, we take a wider view. This was critical for formulating the direction for the thesis, and thus we believe the wider scope is justified and emulated by the scope of the experimental work which follows. This review also serves to compliment the work in study 1 and 2 nicely, first by referencing actin-myosin contraction directly, which was the primary and initial aim of the collection of studies, and second by providing a list of studies and oxidized residues within the literature as reference. We take this review further in study 3, where we assess the function and structure changes at a nearly atomic scope and supplement this review with work which was seldom done before- using molecular and dynamic simulations. Thus, not only has this review has acted as a guide for the study direction but it has proven a valuable reference for our experimental techniques. We hope that this review will act as a contextual reference for our readers so that they are not overwhelmed by the scope of the work attempted herein.

From Amino-acid to Disease: The Effects of Oxidation on Actin-Myosin Interactions in Muscle

Daren Elkrief¹, Oleg Matusovsky², Yu-Shu Cheng², Dilson E. Rassier³

1. McGill University, Department of Physiology, Montreal, Quebec, Canada
2. McGill University, Department of Kinesiology and Physical Education, Montreal, Quebec, Canada
3. Simon Fraser University, British Columbia, V5A 1S6, Canada

Accepted in: The Journal of Muscle Research and Cell Motility

Corresponding Author : Dr. Dilson Rassier (dilson.rassier@mcgill.ca)

Acknowledgements

This work was supported by Natural Sciences and Engineering Research Council of Canada (NSERC) Grant 2022-04770 (to D. E. Rassier).

Disclosures

No conflicts of interest, financial or otherwise, are declared by the authors.

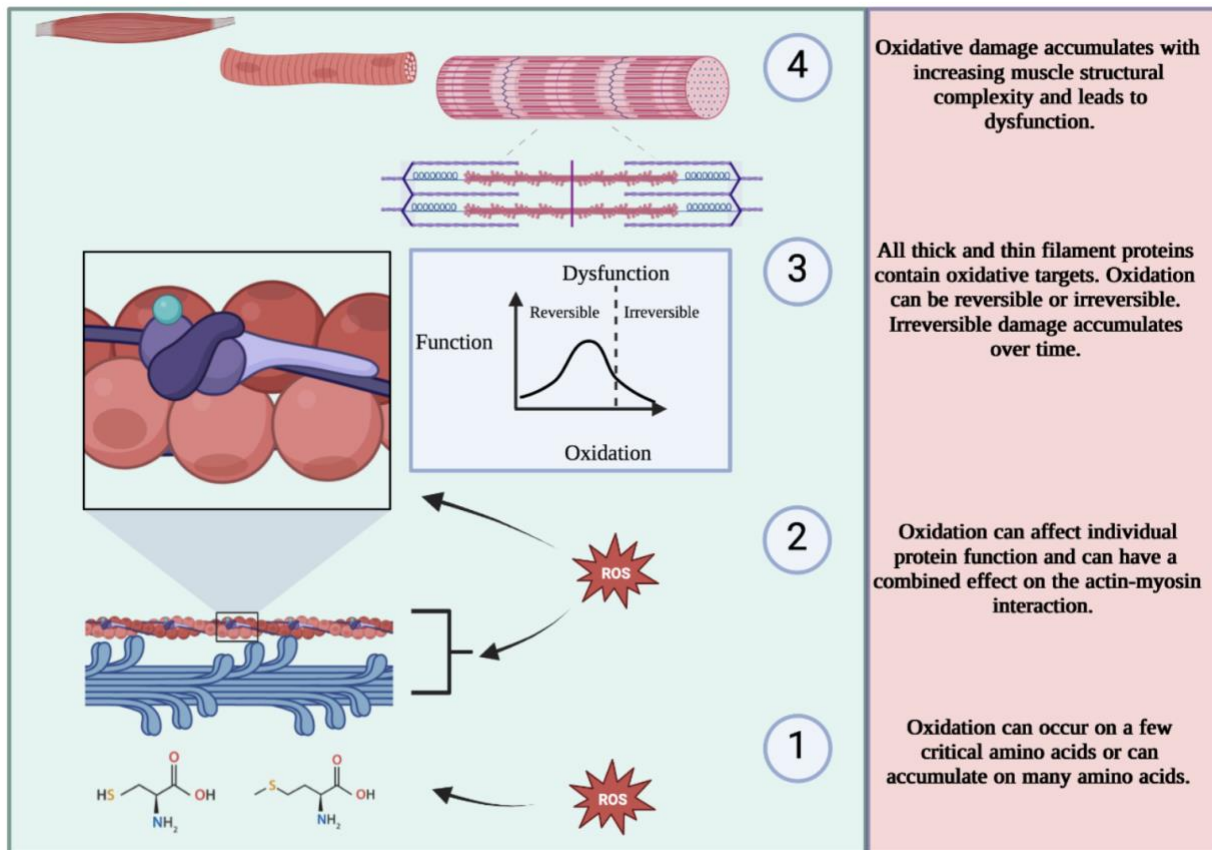
Author Contributions

D.E. and O.M conceived the manuscript; D.E. and Y.-S.C prepared figures; D.E. drafted manuscript; D.E. Y.S.C, O.M and D.R. edited and revised manuscript; D.E., Y.-S.C., O.M., and D.R. approved final version of manuscript.

Keywords

1. Actin-myosin Interaction, 2. Oxidation, 3. Skeletal & Cardiac Muscle, 4. Force Generation, 5. Myofibrillar Weakness, 6. Muscle Aging & Disease

Graphical Abstract



Abstract

Actin-myosin interactions form the basis of the force-producing contraction cycle within the sarcomere, serving as the primary mechanism for muscle contraction. Post-translational modifications, such as oxidation, have a considerable impact on the mechanics of these interactions. Considering their widespread occurrence, the explicit contributions of these modifications to muscle function remain an active field of research. In this review, we aim to provide a comprehensive overview of the basic mechanics of the actin-myosin complex and elucidate the extent to which oxidation influences the contractile cycle and various mechanical

characteristics of this complex at the single-molecule, myofibrillar, and whole-muscle levels. We place particular focus on amino acids shown to be vulnerable to oxidation in actin, myosin, and some of their binding partners. Additionally, we highlight the differences between *in vitro* environments, where oxidation is controlled and limited to actin and myosin, and myofibrillar or whole muscle environments, to foster a better understanding of oxidative modification in muscle. Thus, this review seeks to encompass a broad range of studies, aiming to lay out the multi layered effects of oxidation in *in vitro* and *in vivo* environments, with brief mention of clinical muscular disorders associated with oxidative stress.

Introduction

Muscle functionality is regulated by biochemical modifications, including arginylation, phosphorylation, and oxidation. These modifications fine tune protein stability, actin-myosin interactions, nucleotide affinity and other functions (Ferreira & Reid, 2008; Kobzik, Reid, Brecht, & Stamler, 1994; Nogueira et al., 2009; Reid, 2001; Terman & Kashina, 2013; Varland, Vandekerckhove, & Drazic, 2019). Muscle tissues are particularly susceptible to oxidation. Skeletal muscle susceptibility arises because muscle has a large amount of the total proteins in the body, accounting for 40% of body weight and 25% of total protein turnover (Otten, 1988; Schiaffino & Reggiani, 1996; Shishkin, Kovalyov, & Kovalyova, 2004), and the high metabolic rate of muscle leads to reactive oxygen and nitrogen species (ROS and RNS) production within muscle cells (E. Cadenas, 1989; T.-C. Chang, Chou, & Chang, 2000; Pfeilschifter, Eberhardt, & Huwiler, 2001; Stamler, Lamas, & Fang, 2001).

Skeletal muscle oxidation plays a significant role in regulating muscle contraction and has been shown to contribute to contractile dysfunction (Crowder & Cooke, 1984; G. D. Lamb & Posterino, 2003; Marechal & Gailly, 1999; Prochniewicz, Spakowicz, & Thomas, 2008; Reid, 2001; Maarten M Steinz et al., 2019; Supinski et al., 1999; Yamada et al., 2006). Over the past decade, studies have shown an increase in oxidative markers in diseases that are commonly associated with skeletal muscle weakness, such as rheumatoid arthritis (Yamada, Fedotovskaya, et al., 2015; Yamada et al., 2009), Duchenne muscle dystrophy (Matecki, Fauconnier, & Lacampagne, 2014), malignant hyperthermia (Durham et al., 2008), ageing (Capanni et al., 1998; Liguori et al., 2018; Prochniewicz, Thompson, & Thomas, 2007; Samengo et al., 2012) and in several cardiac diseases

(Digerness et al., 1999; Doroszko et al., 2009; Eaton, Byers, Leeds, Ward, & Shattock, 2002; Gao et al., 2012; Hong, Gokulrangan, & Schöneich, 2007; Kanski, Behring, Pelling, & Schoneich, 2005).

Oxidation affects many proteins in muscles, including actin, myosin, and their associated regulatory proteins, all of which are responsible for muscle contraction at the molecular level. Actin and myosin have a large number of residues susceptible to oxidative modification (Dean, Fu, Stocker, & Davies, 1997). There have been several studies exploring the effects of oxidation in skeletal muscle fibers and myofibrils (Callahan, She, & Nosek, 2001; Dutka, Mollica, & Lamb, 2011; Galler, Hilber, & Göbesberger, 1997; G. D. Lamb & Posterino, 2003; Marechal & Gailly, 1999; Prochniewicz, Lowe, et al., 2008; Supinski et al., 1999; Yamada et al., 2009). Some studies have assessed the individual and combined effects of oxidation on actin and myosin and the ensuing disruption on myofibrillar contractility (I. Dalle-Donne, Giustarini, Rossi, Colombo, & Milzani, 2003; I Dalle-Donne et al., 2002; I Dalle-Donne et al., 2001; Jeremy H Snook, Jiahui Li, Brian P Helmke, & William H Guilford, 2008; Teresa Tiago, Simao, Aureliano, Martín-Romero, & Gutiérrez-Merino, 2006). Oxidation of muscle cells is a complex phenomenon because of the high proportion of oxidizable amino acids in contractile and regulatory proteins (Dean et al., 1997). Additionally, varied timescales of ROS/RNS exposure can either regulate or damage skeletal muscle contractile function (Crowder & Cooke, 1984; G. D. Lamb & Posterino, 2003; Marechal & Gailly, 1999; Prochniewicz, Spakowicz, et al., 2008; Reid, 2001; Maarten M Steinz et al., 2019; Supinski et al., 1999; Yamada et al., 2006).

The type of ROS and RNS generated, the magnitude of the oxidant surge, the duration of this elevation—ranging from milliseconds to hours—and the precise intracellular location of ROS/RNS production all affect the oxidative environment in muscle (Droge, 2002; Merry & Ristow, 2016; Westerblad & Allen, 2011). Quantifying oxidant species load *in vivo* is a complex task, mainly due to the variable half-lives of these species. For instance, the half-life of peroxynitrite (ONOO⁻) is approximately 1.9 seconds. Due to such transient existence, detection often relies on measuring oxidative end products, such as nitrotyrosine, to estimate their impact on muscle physiology (Beckman, Beckman, Chen, Marshall, & Freeman, 1990; D. K. Polewicz, 2011). Furthermore, constant protein turnover and antioxidant presence result in a highly dynamic cellular environment which constantly affects macromolecules and organelles in the cell. Notably, the relationship between ROS/RNS adaptations and muscle physiology is non-linear. Moderate

levels of oxidation can induce beneficial adaptations, whereas extreme levels, whether high or low, can inflict cumulative damage (Merry & Ristow, 2016; Reid, 2001; Reid, Khawli, & Moody, 1993). This underscores the critical nature of maintaining an optimal level of oxidative activity within muscle cells.

Low level oxidation is reversible and may be beneficial for muscle contractility (Merry & Ristow, 2016), and includes thiolation and disulfide bond formation. Oxidation of cysteines and methionines can modulate structure, protein function, enzyme activity and contractile function while protecting proteins from irreversible oxidative damage (Barford, 2004; Cooper, Patel, Brookes, & Darley-USmar, 2002; Menon & Goswami, 2007; Morrison, Miller 3rd, & Reid, 1996). Modifications such as disulfides between cysteines and methionines can be enzymatically reversed (Berlett & Stadtman, 1997). However, when oxidant production exceeds scavenging, irreversible modifications may occur to muscle proteins, including carbonylation of lysine, arginine, and proline, formation of di-tyrosine cross-links, tryptophan oxidation and protein cross-linking (Stadtman & Levine, 2000; Uchida, 2003). These deleterious modifications result in loss of function, enzymatic degradation, structural damage, and protein aggregation (T.-C. Chang et al., 2000; Louie, Kapphahn, & Ferrington, 2002; Squier, 2001). The complexity owing to various response times, sources and reversibility make assessment of oxidative modifications challenging. This is further complicated by the fact that muscles proteins have multi-tiered function; actin and myosin have their own binding partners, such as troponin, tropomyosin (Tm) and myosin-binding protein C (MyBP-C), which could be affected by oxidation as well (Canton et al., 2011; Canton, Neverova, Menabò, Van Eyk, & Di Lisa, 2004; Maria Fedorova, Todorovsky, Kuleva, & Hoffmann, 2010). Moreover, non-contractile cellular components, such as the sarcoplasmic reticulum or ryanodine receptor may also be affected, in turn affecting overall muscle mechanics and confounding studies which involve Ca^{2+} regulation, which are controlled by both contractile proteins and non-contractile proteins (Durham et al., 2008). Thus, making the distinction between limited interactions in *in vitro* environments, where oxidation is controlled and limited to actin and myosin or myofilaments, and skinned myofiber, whole myofiber and whole muscle environments, is critical for understanding oxidative modification in muscle.

In this review, we aim to guide the reader through the smallest to the largest interactions in the muscle, starting with the oxidation targets at the amino acid and cross-bridge protein levels and

culminating in the whole muscle and disease model scenarios. Our objective is to outline a comprehensive landscape, hopefully enabling readers to appreciate the multifaceted complexity of the issue under consideration. This review will predominantly emphasize the oxidation of cardiac and skeletal muscle thick and thin filaments. As a foundation for navigating this complex issue, this review commences with a comprehensive summary of our present knowledge regarding actin-myosin interactions and the molecular processes that drive force production.

Actin-myosin interactions

Muscle contraction is the process where large ensembles of myosin molecules work in coordination to produce force. The force-generation step of myosin is a response to structural alterations within the molecule. A basic scheme of myosin-actin interactions, force generation and ATP hydrolysis has been defined over the years by biochemical, mechanical, and structural studies. It is generally accepted to cover the following sequence of events (Fig. 1): ATP binds to the myosin in the rigor actomyosin state (step 1, AM), which results in the A*M'T complex formation (step 2) and subsequent dissociation of myosin from actin (step 3, M'T). The recovery and ATP hydrolysis steps occur in the detached state (step 4, MT and MDP), where a configuration of myosin at the pre-power stroke is formed. Next, myosin rebinds to F-actin (step 5, A*M'DP), which causes the conformational changes in myosin motor domain (step 6, A*M'DP) and leads to the phosphate release step (step 7, A*M'D). The latter is coupled to the myosin lever arm swing (step 8, AMD) and followed by Mg^{2+} -ADP release (step 9, AM).

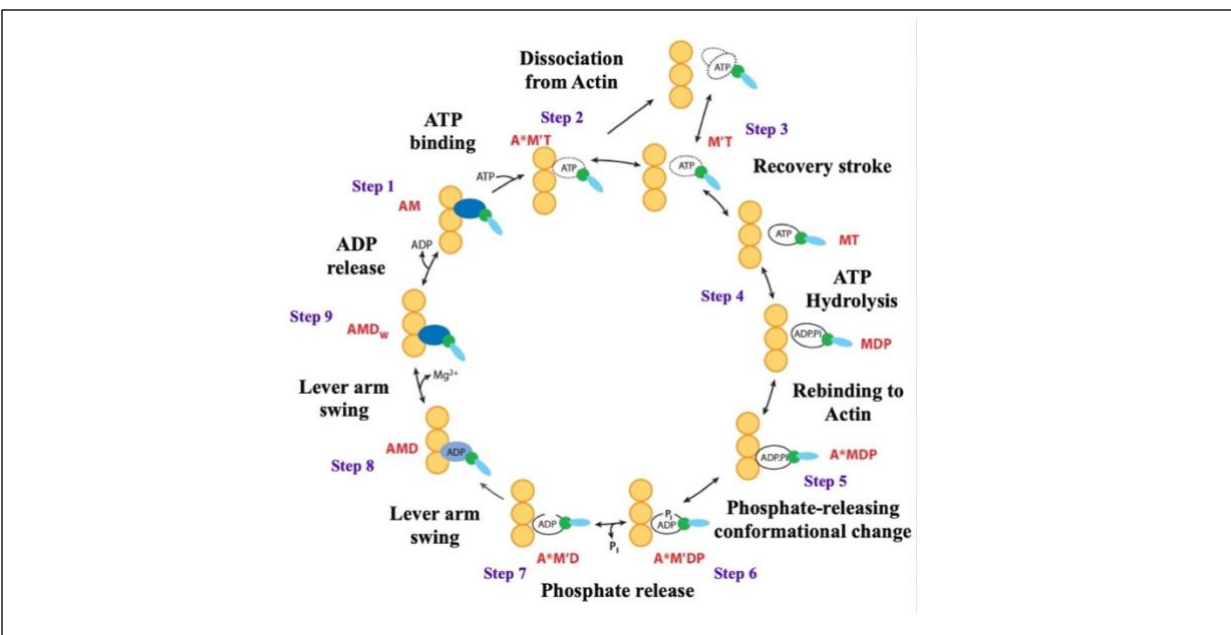


Figure 1. Myosin cross-bridge cycle. Circles represent actin monomers. A: Actin, M: Myosin, D: ADP (adenosine diphosphate), T: ATP (adenosine triphosphate), Pi: Inorganic phosphate.

The critical force-generating step in the scheme shown in Fig. 1 is the binding of the myosin head(s) to the actin filament (step 5), the initial formation of a non-stereospecific myosin-actin complex (Furch, Fujita-Becker, Geeves, Holmes, & Manstein, 1999) and movements of the heads and lever-arm domains of myosin (step 6) (Tsaturyan et al., 2005). Two events take place during this force-generating transition from $A^*M'DP$ – to $A^*M'D$: the swing of the lever arm and the release of P_i , resulting in the AMD state. The dissociation of P_i from the nucleotide pocket happens prior to the release of ADP, leading to the AM state. There are different proposed mechanisms for P_i release, including the existence of multiple high-energy intermediate states with the P_i binding to more than one site outside the active site of myosin II (Moretto et al., 2022). It's surmised that by releasing P_i in multiple steps, the myosin head could adopt different conformations, leading to changes in the rate of the power stroke and the force production, and possibly have a regulatory role in muscle physiology (Moretto et al., 2022). The transition from the weakly non-stereospecifically bound state to strong stereo-specifically bound state is coupled to P_i and ADP release (steps 7-9). The release of the hydrolysis products is linked to the rotation of the myosin lever arm (Dominguez, Freyzon, Trybus, & Cohen, 1998; Holmes, 1997; Houdusse, Szent-Györgyi, & Cohen, 2000; E. M. Ostap & Thomas, 1991). Structural states suggest a ~ 60 - 70° change in the angle of the lever arm between pre- and post-power stroke states relative to actin filaments, which varies by isoform (Gollub, Cremo, & Cooke, 1996). The swing in the lever arm causes the myosin to bind actin more tightly, triggering the filament to slide and the nucleotide pocket to close and enter the AMD state, resulting in the power stroke. If dissociation of P_i happens prior to the lever arm swing, both the ADP position and the lever arm position need to be maintained through these phases.

We used some of the structures available in the literature to create a simple qualitative model (Fig. 2), showing the myosin II states during the cross-bridge cycle and the force generating cycle. Consistent with the lever arm model, it has four distinct conformations: rigor state (PDB: 3I5G), post-rigor state (PDB:1SR6), pre-powerstroke state (PDB:1BR1) and post-powerstroke state (PDB:2MYS). These states illustrate that small conformational changes in the motor domain are coupled to large changes in the position of the lever arm. In the sections that follow, we will explore

how changes in conformation due to modifications such as oxidation may have profound effects on the force produced by myosin .

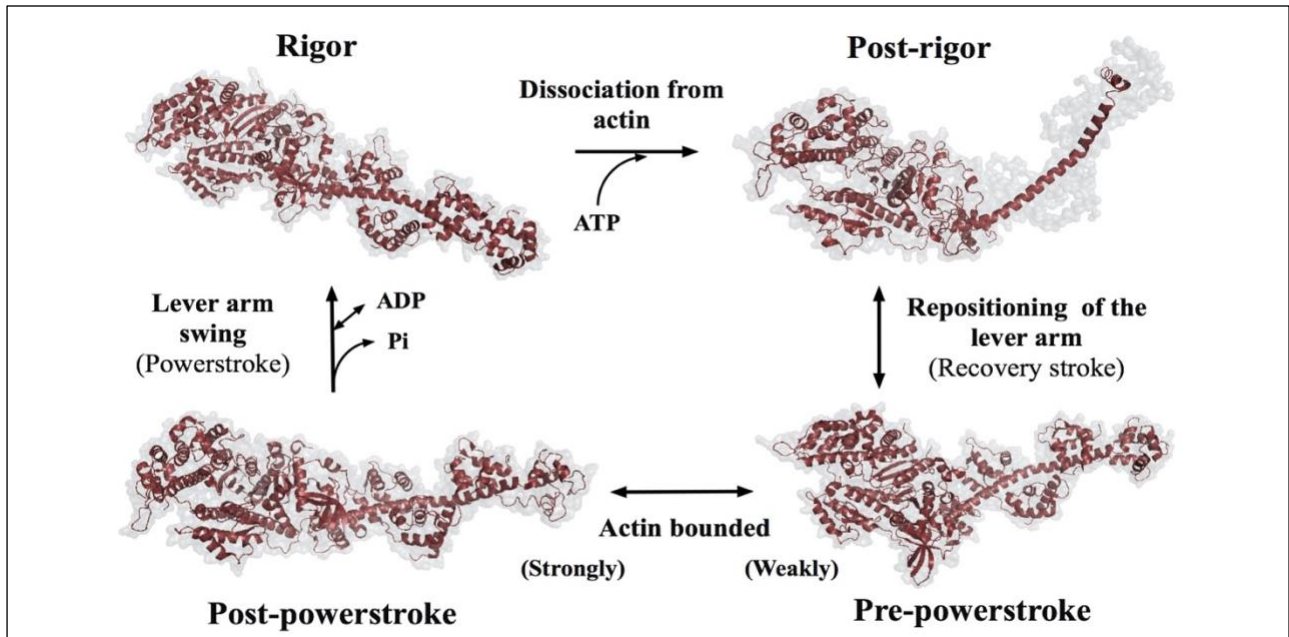


Figure 2. The ribbon diagram of the myosin II molecule in four structure states: rigor, post-rigor, pre-power stroke and post-power stroke. The lever arm position is controlled by the position of the converter, which swings relative to the rest of the motor domain. Model designed by Y.S. Cheng.

Major Sources of muscle oxidation

The muscle cell exhibits a large range of oxidant concentrations which fluctuate in response to different conditions. While there is a lack of data regarding redox states within muscle cells, some estimates have been made. Microdialysis studies of skeletal muscle indicate that interstitial hydrogen peroxide ranges from 10-15 μM (Vasilaki et al., 2006) with non-muscle cells exhibiting stress gene responses to similar concentrations (Khassaf et al., 2003). Muscle cells have shown adaptive stress responses at 100 μM cellular hydrogen peroxide and total loss of function at >1 mM (McArdle, Dillmann, Mestrl, Faulkner, & Jackson, 2004; F. McArdle et al., 2004). Interestingly, far higher 50 mM concentrations of hydrogen peroxide have been used to mimic the effects of muscle oxidation (Prochniewicz, Lowe, et al., 2008) with studies showing a seven fold drop across the membrane indicating that 2-15 μM intracellular hydrogen peroxide can elicit an adaptive response (Antunes & Cadenas, 2000). Of course, the range of oxidants and antioxidants

is beyond the scope of this paper and well researched reviews are recommended on the topic (Powers & Jackson, 2008; Reid, 2001).

During muscle contraction, reactive oxygen species (ROS), including superoxide radicals $O_2^{\cdot-}$, hydrogen peroxide H_2O_2 and hydroxyl radicals $\cdot OH$ can be formed by a 20-fold increase in mitochondria activity (Chance, Sies, & Boveris, 1979) and muscle contraction (Jackson, Edwards, & Symons, 1985; Silveira, Pereira-Da-Silva, Juel, & Hellsten, 2003). An increased (nearly 100-fold) production of reactive nitrogen species (RNS) such as nitric oxide ($\cdot NO$) along with its downstream derivatives, such as peroxynitrite, also occurs during contraction (Andrade, Reid, Allen, & Westerblad, 1998b; Kobzik et al., 1994; Morrison et al., 1996). $O_2^{\cdot-}$ is generated through either incomplete reduction of oxygen in the mitochondrial electron transport chain or as a specific product of enzymatic reactions. The half-life ($\sim 1 \mu s$) is sufficient to permit diffusion and interaction with several cellular targets (Winkler, Boulton, Gottsch, & Sternberg, 1999). Calculations in endothelial cells indicate that the steady-state cellular concentration of $O_2^{\cdot-}$ is in the pico- to nanomolar range (Carballal, Bartsaghi, & Radi, 2014; A. J. Cheng et al., 2016). Complexes I and III are the two major sites of $O_2^{\cdot-}$ production in the mitochondria (E. Cadenas, 1989; Enrique Cadenas & Boveris, 1980; M. P. Murphy, 2009; Quinlan, Treberg, Pervoshchikova, Orr, & Brand, 2012; Tahara, Navarete, & Kowaltowski, 2009; Turrens & Boveris, 1980). Enzymes that produce $O_2^{\cdot-}$ in skeletal muscle include NADPH oxidase (Pal, Thakur, Li, Minard, & Rodney, 2013), phospholipase A2 (Nethery et al., 2000), xanthine oxidase (Gomez-Cabrera et al., 2010) and uncoupled $\cdot NO$ synthase (NOS) (Santolini, Adak, Curran, & Stuehr, 2001). Dismutation of $O_2^{\cdot-}$, both spontaneous and catalyzed by superoxide dismutase (SOD), constitutes the major source of H_2O_2 in muscle cells ($2O_2^{\cdot-} + 2H^+ \rightarrow H_2O_2 + O_2$). Two out of three SOD isoforms are highly abundant ($\sim 10\text{--}20 \mu M$) within the skeletal muscle fibers: SOD1 requires copper–zinc as a cofactor and is located in the cytosol and in the mitochondrial intermembrane space; SOD2 uses manganese as a cofactor and is located in the mitochondrial matrix (Powers & Jackson, 2008). Of the total SOD activity in skeletal muscle fibers, $\sim 15\text{--}35\%$ is in the mitochondria and the remaining $65\text{--}85\%$ exist in the cytosol. Nitrogen based oxidants are also abundant and essential signaling molecules within muscle cells. $\cdot NO$ is a versatile biological signaling molecule that is generated via enzymatic reactions of nitric oxide synthase (NOS) and the production increases in muscle fibers during repeated contractions (A. J. Cheng, Bruton, Lanner, & Westerblad, 2015; Pye, Palomero, Kabayo, & Jackson, 2007). $\cdot NO$ can also be formed

from the inorganic anions nitrate (NO^{3-}) and nitrite (NO^{2-}) (Weitzberg, Hezel, & Lundberg, 2010). Skeletal muscle constitutively expresses neuronal and endothelial NOS (nNOS and eNOS, respectively), whereas inducible NOS (iNOS) is upregulated in response to acute inflammatory insults. NO is synthesized by NOS from L-arginine, NADPH and O_2 . nNOS and eNOS are activated by increases in the free cytosolic Ca^{2+} concentration $[\text{Ca}^{2+}]_i$ (Förstermann et al., 1994). In the sections that follow, we will pivot to outline a few of the oxidized residues in thick and thin filaments.

Oxidative alterations in thick filament proteins

The main component of the thick filament is the myosin II motor. Myosin is a protein that exerts its effects through both its enzymatic and biophysical components (Ait-Haddou & Herzog, 2003; Andrew F Huxley, 1957; Lombardi, Piazzesi, & Linari, 1992; Thomas, Prochniewicz, & Roopnarine, 2002). Modifications in myosin can affect either the enzymatic components of the ATPase or the power stroke and cross-bridge formation through conformational changes (Ait-Haddou & Herzog, 2003; Andrew F Huxley, 1957; Lombardi et al., 1992; Thomas et al., 2002). Studying the effects of thick filament oxidation poses a challenge in determining the effects on each myosin function, the effects of different oxidants, and the effect of oxidant concentration on cross-bridge state and myosin oxidation.

Under oxidative conditions several residues are affected, and varying types of oxidations have been observed with distinct functional consequences. There are a wide range of oxidants and targets, and thus we have made a list of oxidized residues in thick and thin filaments (Table 1, 2). Oxidation of skeletal muscle myosin is so common in fact that some of the studied residues are often modified before explicit oxidant treatment, although most oxidizable residues tend to exist in a reduced state at physiological pH. Out of 22 methionine residues found in myosin II catalytic domains; 9 residues are susceptible to oxidation. Among these 9 methionines, 4 residues had displayed oxidation even before being subjected to hydrogen peroxide treatment in *Dicteostelyum*, suggesting that there may be a baseline redox state where oxidized residues are common (Klein, Moen, Smith, Titus, & Thomas, 2011). Note that the cysteine residue is one of the most ROS-sensitive residues in the myosin molecule – we reviewed multiple cysteine residues oxidized by different agents, however myosin contains 40 cysteines in its sequence and the functional

outcomes of oxidation of the majority are not yet known and require specific study to determine (Table. 1). There are more cysteines and methionines in the whole molecule yet over 50% of both are in the catalytic domains, thus catalytic activity is highly susceptible to oxidation (Table 1). Therefore, oxidation occurring in the myosin S1 region is of the greatest interest, yet the functional outcomes of oxidation in this region have shown mixed results depending on the species of oxidant used and whether oxidation is administered in rigor or relaxed conformation. Myosin S1 has been shown to be susceptible to all products of SIN-1, an NO and $\text{O}_2^{\cdot-}$ donor that forms ONOO^- (Martin-Romero, Gutiérrez-Martin, Henao, & Gutiérrez-Merino, 2004), which resulted in partial denaturation of the protein as well as inhibition of ATPase activity (Teresa Tiago et al., 2006). The S1 region in fast myosin contains 10 cysteines, all of which have varying degrees of susceptibility to oxidation depending on their accessibility in either the rigor or relaxed conformation of the cross-bridge (Gross & Lehman, 2013). Among these cysteine residues, ventricular and fast twitch myofibrils have more exposed cysteines, which resulted in decreased ATPase activity upon oxidation by hydrogen peroxide. However, oxidation of less exposed cysteines in rigor instead show increased ATPase activity and Ca^{2+} sensitivity, but only in ventricular myofibrils, indicating that accessibility and muscle type can have different functional effects from the same oxidant (Gross & Lehman, 2013). Muscle in the lattice does not seem to oxidize reactive cysteines likely due to the protective effect of actin, whereas exposed myosin's reactive cysteines are oxidized (Duke, Takashi, Ue, & Morales, 1976). It should be noted that ATPase activity exhibited a steeper decrease in isolated myosin than in muscle fibers, suggesting that purified myosin may not accurately mimic muscle lattice myosin (Duke et al., 1976).

It is currently unknown whether the decreases in function in whole fiber oxidation, aging and disease are driven by a small number of key residue oxidation, or whether many oxidative events accumulate in otherwise structural amino acids to cause widespread dysfunction, a theme which will be revisited multiple times in this review. This concept is exemplified by the study of the myosin S1 and its reactive cysteines. Reactive cysteines are those adjacent to basic and aromatic residues which form anions susceptible to modification. Among the amino acids in myosin, perhaps the most significantly studied are reactive cysteines. Two out of 40 cysteines in the skeletal muscle myosin (Maita et al., 1991), sulfhydryl-1 SH1 (Cys-707) and SH2 (Cys-697) are considered highly reactive. These residues are linked to major functions in the S1, including ATPase function and force translocation as well as with actin binding (Prochniewicz et al., 2007).

Study of SH1 and SH2 oxidation have been of major interest, yet there is some debate on whether they are oxidized under physiological conditions. For instance, there are debates on what the effects are on the super reactive cysteines of Cys-696 and Cys-702 and whether it decreases the maximal force and results in deterioration of muscle contractility or even whether they are accessible at all under physiological conditions (Bobkov, Bobkova, Homsher, & Reisler, 1997; Passarelli et al., 2008; Prochniewicz, Lowe, et al., 2008; Teresa Tiago, Palma, Gutierrez-Merino, & Aureliano, 2010). In one study, high concentrations of 50 mM of ONOO⁻ in rat muscle fibers was not enough to oxidize the reactive cysteines SH1 or SH2, yet a number of other cysteines were oxidized. Permeabilized bundles were oxidized in rigor, possibly blocking the binding site's accessibility to oxidation (Prochniewicz, Lowe, et al., 2008). Thus, reductions in muscle function were related to the cumulative effect of oxidation, as shown by the mass-spectrometry (MS) data, rather than the site-specific major effects that would otherwise be produced by the oxidation of key residues such as SH1 and SH2 (Prochniewicz, Lowe, et al., 2008). The results of this study support that changes in myosin caused by oxidation are dependent on the concentration of oxidant (Prochniewicz, Lowe, et al., 2008). A low level of oxidation results in cooperative changes which indirectly alter the myosin head motor domain, while a high level of oxidation results in both indirect and direct changes to the myosin head motor domain (Prochniewicz, Lowe, et al., 2008). Therefore, the results are complicated by the fact that their effects are cumulative, resulting in modification which scales with increased oxidation (Andrade, Reid, Allen, & Westerblad, 1998a; Andrade, Reid, & Westerblad, 2001; G. D. Lamb & Posterino, 2003; Prochniewicz, Lowe, et al., 2008). Modifications are also allosteric, for instance where alterations in the essential light chain may induce distortions in other parts of the molecule (Klein et al., 2011). These studies show that cross-bridge status and oxidant concentration, which effectively sum to solvent access and likelihood of residue modification, matter for a globular shaped protein such as myosin.

Several residues affected by oxidation are located near the actin binding cleft or the ATP binding site, with likely effects on the communication between the different parts of the molecule. Oxidation of some critical functional residues display very clear effects whereas others lack conclusive evidence. For instance, Lys-84, a residue in the N-terminal subdomain, is located in the converter or lever arm region, which underlies mechanochemical energy transfer between ATP hydrolysis and the working stroke (Fisher et al., 1995b; Geeves & Holmes, 2005). Lys-84 is considered the most reactive lysine residue in the myosin head and is in the 25 kDa NH₂- terminal

tryptic fragment near the reactive cysteine SH1 (Fabian & Mühlrad, 1968; Hozumi & Mühlrad, 1981; Kubo, Tokura, & Tonomura, 1960; Mornet, Pantel, Bertrand, Audemard, & Kassab, 1980). Both these residues are in close proximity of the ATPase domain and Lys-84 carbonylation has been shown to result in a reduction of ATPase activity by about half (Teresa Tiago et al., 2010). However, there may be further effects of Lys-84 oxidation which require further investigation. Lys-84 binds with Arg-704, a residue in the converter domain, in an interaction critical in determining the steady state distribution of myosin heads in the up or down lever arm positions. This interaction is thus critical in determining the propensity for weak and strong binding states of the contractile cycle (Málnási-Csizmadia et al., 2007) and this transition is critical for force generation (Rayment et al., 1993; Thomas et al., 2002). When *Dictyostelium* myosin II Lys-84 was modified, the Lys-84 - Arg-704 bond and thus the recovery stroke were shown to be disrupted. The recovery stroke, *i.e.*, the process where ATP binds the myosin head and causes a large structural rearrangement which brings catalytic residues into place to enable ATP hydrolysis while simultaneously causing a swing of the myosin lever arm into a primed state. Given that the recovery stroke is coupled to ATP hydrolysis and P_i release, oxidative disruption of the recovery stroke, presumably changes the equilibrium between the normally high repulsion Lys-84 - Arg-704 in the down state and the high attraction in the up state. Thus we could expect that upon oxidation, ATPase and weak/strong equilibrium is perturbed, favoring weak binding or down states (Teresa Tiago et al., 2010; Teresa Tiago et al., 2006). This example illustrates the need for further inquiry into the effects of oxidation of residues which are responsible for mechanochemical transduction.

Other examples of single target functional effects include oxidation of Met-394, which is located at the upper domain of the myosin S1 fragment near the cardiomyopathy loop (CM-loop) in the actin binding interface, in *Dictyostelium* myosin II. The location of Met-394 residue suggests it may be responsible for the interaction with actin and initiation of the power stroke. Mammalian myosin isoforms containing cysteines in the same position shown to be glutathionylated, resulting in reduced activity of actin-bound myosin ATPase (Moen et al., 2014), most likely due to conformational changes in actin-binding cleft (Klein et al., 2011). The Met-394 residue in *Dictyostelium* myosin II is equivalent to Cys-402 in skeletal myosin and Cys-400 in cardiac myosin. More work must be done to determine the role that oxidation has on each amino acid given that some modifications have effects on either structure, ATPase rate or both, depending on

whether the amino acid or bond plays a role in translating energy. In light of oxidation's effect on multiple protein functions, we have provided a concise illustration of the prevalence of oxidation within the cross-bridge in Fig. 3.

Other thick filament proteins and domains other than the myosin catalytic head domain have also been shown to be targets of oxidation. In particular, the myosin light chain (MLC), which is thought to play a major structural role in the thick filament, exhibits significant effects when oxidized. Tyrosine nitration has been shown at Tyr-73 and Tyr-185 in MLC1, as well as Tyr-182 in MLC2, the two latter of which showed increased susceptibility to degradation by matrix metalloproteinase-2 (MMP-2), a major factor contributing to cardiac dysfunction after hypoxia-reoxygenation (Doroszkowski et al., 2010; D. Polewicz et al., 2011). MLC1 was also shown to contain oxidized sulfhydryls in cysteines and methionines, which led to a decrease in force of human cardiomyocytes (Hertelendi et al., 2008). Although most modifications have been shown to lead to negative consequences on contractility and increased degradation, oxidation in myosin head regulatory proteins were shown to result in hyper-contractility, a phenomenon we will also discuss among thin filament regulatory proteins. Nitroxyl (HNO), the one-electron-reduced form of nitric oxide, has been observed to induce redox modifications in the contractile machinery of the heart, thereby affecting cardiac contractility. This is achieved through the oxidation of cysteine residues in myofilament proteins, leading to the formation of disulfide bonds that result in structural changes in these proteins. Cross-linked myosin heavy chains (MHC) and MLC1 in cardiomyocytes treated with HNO was found to increase contractility (Gao et al., 2012). HNO-induced formation of dimers in myosin motor domain, involving Cys-81 in myosin light chains, enhanced the myofilament Ca^{2+} sensitivity possibly by enhancing myosin stiffness and therefore force generation (Gao et al., 2012). Interestingly, the effects of HNO seem to be donor dependent. For instance, while the HNO-donor, 1-nitrosocyclohexyl acetate, was found to both increase maximum force (F_{max}) and reduce the concentration of Ca^{2+} needed for 50% activation (Ca_{50}), another HNO donor, Angeli salt, primarily increased F_{max} without significantly affecting Ca_{50} . Furthermore, these HNO-induced effects are reversible, as reducing agents can revert the cysteine modifications and thus, the contractile properties of the cardiac muscle cells. The reversibility and donor-dependency of HNO provide an example of the complexity of redox functional modulation in the thick filament (Gao et al., 2012). This complexity is furthered when factoring in the thick filament sarcomere regulatory proteins. MyBP-C was shown to act as a redox sensor in normal

heart function (Balogh et al., 2014; Brennan et al., 2006). MyBP-C has been shown to be reversibly oxidized by glutathione (GSSG) at Cys-479, Cys-627, and Cys-655 and reduced by dithioereitol (DTT) (Patel, Wilder, & Solaro, 2013), where specific antioxidant function was shown to benefit diastolic dysfunction by countering GSSG in MyBP-C (Lovelock et al., 2012). These modifications were found to enhance myofilament Ca^{2+} sensitivity, yet persistent oxidation contributed to diastolic dysfunction (Lovelock et al., 2012; Patel et al., 2013). The specific effect of other thick filament protein oxidation will be explored further in disease sections.

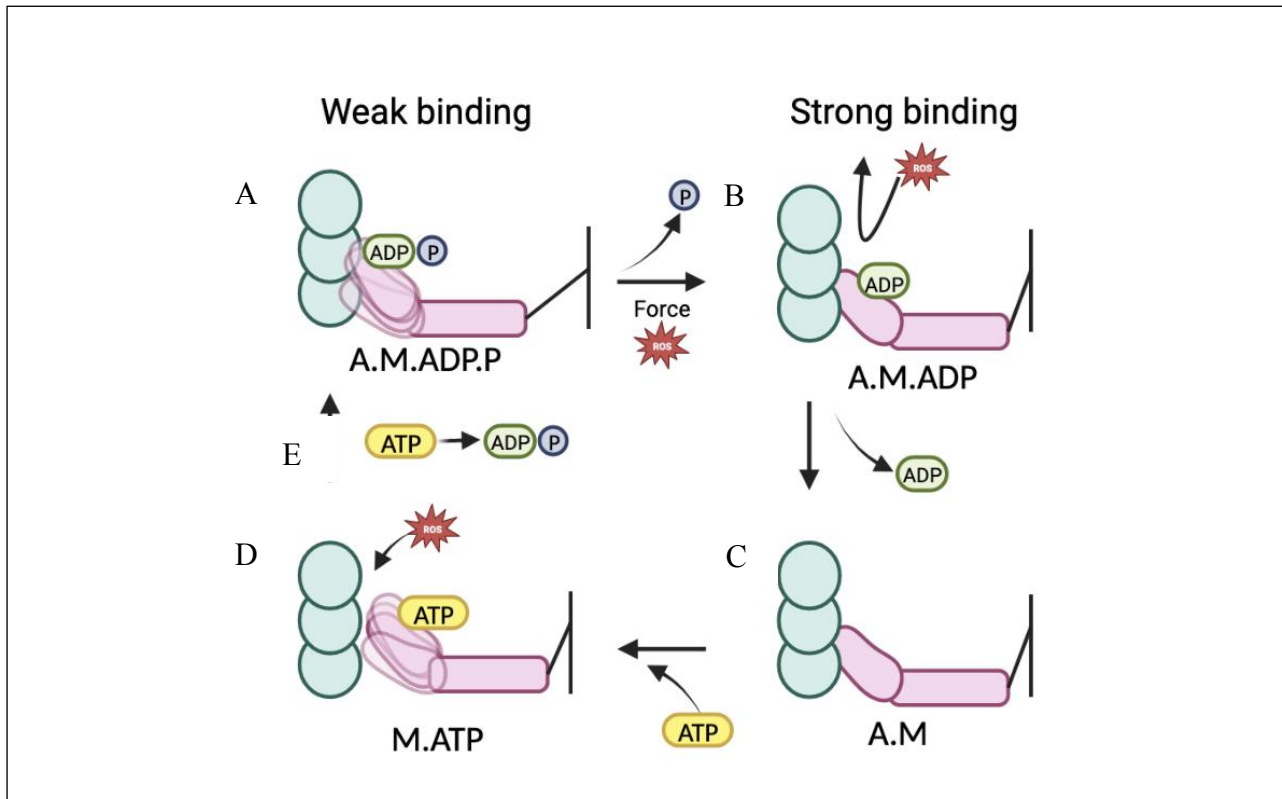


Figure 3. Oxidation of the actin-myosin cross-bridge. **a.** Oxidative PTMs have a preferential effect on the weak to strong transition, and thus reduction in force. A greater reduction in proportion of strong binding cross-bridges at steady state. Oxidation of MHC Cys-707 and Cys-697 may impair transition state. **b.** Decreased access of oxidizable residues in strong binding states in absence of ATP, when actin is blocking sensitive residues on the S1 may prevent oxidation of key cysteines. **c.** Nitrosylation of actin Cys-374 and Cys-285 increases the time which actin is bound to myosin or decreases the detachment rate. **d.** Oxidation can preferentially modify actin and myosin during the relaxing state because the actin myosin binding pockets are exposed. **e.** Multiple targets alter ATPase directly, such as Lys-84.

Oxidative alterations in thin filament proteins

Oxidation of thin filament components have been shown to result in significant effects both *in vitro* and in disease (Elkrief, Cheng, Matusovsky, & Rassier, 2022; Rayment et al., 1993; Maarten M Steinz et al., 2019). Using mass-spectrometry analysis, 3-NT nitrotyrosine (NO₂; +46 Da) and malonaldehyde MDA (C₃H₃O; +54 Da) were identified as consistently occurring modifications caused by SIN-1 in myofibril actin, and in purified skeletal muscle F-actin from arthritis induced-mice. There were several oxidized residues in all 4 subdomains (SD1-SD4) of G-actin with high amino acid position homology, called hotspots (Table 2). In SD1 of G-actin such hotspot included His-101-MDA, Tyr-362-NT, Glu-360-MDA that were shown to undergo modifications. It had previously been shown that Tyr-362 residue has a 2.2 fold greater protection from oxidation via synchrotron X-ray beam when bound to S1 of myosin, suggesting that this residue may be involved in actin-myosin interaction and is exposed to oxidation when unbound (Oztug Durer, Kamal, Benchaar, Chance, & Reisler, 2011). In SD2, oxidized residues in the purified F-, G- and myofibrillar actin included Tyr-53-NT, and His-40-MDA, Glu-41-MDA, Glu-49-MDA, Glu-59-MDA, that have been reported to involve flexing of the actin polypeptide chain upon ATP hydrolysis (Takashi Fujii, Iwane, Yanagida, & Namba, 2010) and actin polymerization (T. Fujii & Namba, 2017). The Tyr-53 residue has been shown to result in slower polymerization and impaired filament stability (Baek et al., 2008; X. Liu, Shu, Hong, Levine, & Korn, 2006; X. Liu, Shu, Hong, Yu, & Korn, 2010). In SD3, oxidized residues included His-40-MDA and Glu-41-MDA located in the DNase binding (D-loop), which is involved in intramolecular binding and bonding between SD1 and SD3. SD3 modifications common to all models included Tyr-294-3NT, Asn-296-MDA and Asn-297-MDA, indicating their general susceptibility to oxidation. Root-mean square fluctuation analysis measuring domain flexibility revealed decreased domain flexibility in both SD1 and SD3 of G-actin. SD4 has a region with high flexibility, including the oxidized Q246-MDA, which is known to interact with SD3 and contribute to filament stability. The authors observed the effect of side chain oxidation on intramolecular bonding by analyzing close contacts bonding, as defined as contacts of less than 4 Å between non-hydrogen atoms. His-101, His-275 and Tyr-218 residues were shown to be particularly heavily affected, losing hydrogen bonding with direct consequences on the internal stability of the molecule (Table 2). Furthermore, close

contact bonds within each of the 11 modified residues in rheumatoid arthritis patients were shown to be disrupted, likely decreasing intramolecular H-bonding and potential actin-myosin interactions (Maarten M Steinz et al., 2019).

In sum, 3-NT and MDA are thought to sterically hinder intramolecular hydrogen bonding and thus trigger conformational changes within actin structure (Oztug Durer et al., 2011; Maarten M Steinz et al., 2019; van der Veen & Roberts, 1999). It would be interesting to perform this analysis in attached actin-myosin interactions to determine whether oxidation influences contact between the two molecules. The few studies which have assessed the effects of actin oxidation on the cross-bridge cycle and actin-myosin interaction have revealed that often small modifications result in significant functional outcomes. Treatment of actin with increasing amounts of SNO-Cys lead to ~25% decrease in actin velocity at 50 μ M SNO-Cys (Bansbach & Guilford, 2016). The study failed to find an effect of SNO-Cys on actin-activated ATPase reaction rate (V_{max}) or K_m . Optical trap measurement of force between heavy meromyosin (HMM), the isolated double headed myosin fragment immobilized on a glass coverslip also failed to see a difference in stall forces in SNO-Cys treated actin when compared to a control interaction. In this study, 2 cysteines per actin monomer were determined to be nitrosylated: Cys-374 and Cys-285. Nitrosylation of these residues is thought to alter actin-myosin interactions directly and/or indirectly. Since Cys-374 is in subdomain 1 at the C-terminus near the myosin binding site (Miki & Remedios, 1988; Phillips, Separovic, Cornell, Barden, & dos Remedios, 1991; Sun, Rose, Ananthanarayanan, Jacobs, & Yengo, 2008), oxidation of this site caused multiple effects on the functional properties of actin, including decreased rate of actin polymerization *in vitro*, destabilization of actin filament structure *in vivo*, altered actin-myosin binding affinity and thus decreased muscle contractility (Passarelli et al., 2010; Maarten M Steinz et al., 2019). Additionally, it has been shown that copper oxidation of Cys-374 results in reduced actin motility in the *in vitro* motility assay (IVMA) (Vikhoreva et al., 2009), underlying the significance of actin oxidation on myosin-actin interactions. Importantly, some have noted that Cys-374, along with Cys-10, solvent accessibility, and therefore oxidation sensitivity, depend heavily on contractile state, and thus these residues are unlikely to be oxidized at all times in the contractile cycle (Duke et al., 1976; Gross & Lehman, 2013).

Actin has been shown to translate structural changes between its monomers and thus it is suspected that oxidative modifications, including nitrosylation may result in global changes to the actin

structure, secondarily impairing myosin binding and thus motility in the IVMA. Whether actin acts as an oxidant reservoir for S1 on the myosin head *in vivo* is unclear, although it has been proposed that actin may oxidize myosin *in vitro* and thus effects in ATPase could be due to protein cross-reactivity and thus support studies which have shown that actin oxidation is not sufficient to reduce myosin ATPase (Bansbach & Guilford, 2016). Using divalent cations to stabilize different forms of actin has been shown to alter the cooperative binding of actin to myosin (Orlova & Egelman, 1997). Similarly, phalloidin binding has been shown to increase actin stiffness and in turn alter the sliding velocity of actin in IVMA (Tokuraku, Uyeda, & Motility, 2001; Vikhorev, Vikhoreva, & Månsson, 2008). Electron paramagnetic resonance spectra of spin labels attached to Cys-374 showed that there were altered rotational dynamics of nitrosylated Cys-374 (I. Dalle-Donne et al., 2003). Given that rotations of actin parallel rotations of myosin heads during interaction (Borejdo et al., 2004), Cys-374 nitrosylation may cause coupled structural changes during actin-myosin association. Cys-285 is involved in the internal stability of skeletal actin (Khaitlina, 2001) and has also been shown to form a disulfide bond with Cys374 (Varland et al., 2019), a modification which reduces actin cytoskeleton dynamics (Farah, Sirotkin, Haarer, Kakhniashvili, & Amberg, 2011). In sum, depending on the oxidant species it appears that key residue oxidation plays a significant role in affecting actin stability and actin-myosin binding, yet oxidation of structural amino acids in other domains are also sufficient to induce widespread changes along the actin molecule.

In addition to actin, thin filament contractile regulatory proteins are well-known oxidation targets. Given the faster kinetics of troponin-tropomyosin regulation compared to crossbridge cycling, there's ongoing debate about whether oxidation of regulatory components significantly affects cross-bridge kinetics, as opposed to direct oxidation of the cross-bridge itself (MacFarlane & Miller, 1992). We have summarized some of the effects of thin filament oxidation in Fig. 4 and in table 2.

There are far fewer oxidizable components of the smaller thin filament proteins. For instance, there are only three oxidizable cysteine residues in TnI, only one of which Cys-133 is solvent accessible in mammals (Mollica et al., 2012). However, this may mean that oxidation of key cysteines in this case exhibit an even more significant effect. At rest, there is low intracellular Ca^{2+} and the C-terminal domain of TnI locks Tm in a myosin-blocking position, preventing the actin-myosin interaction (Galińska-Rakoczy et al., 2008). When the muscle fiber is depolarized, Ca^{2+} is released

from the sarcoplasmic reticulum and binds to TnC, releasing TnI inhibition off Tm allowing for actin-myosin binding (Geeves & Holmes, 2005; Kress, Huxley, Faruqi, & Hendrix, 1986). Perturbing the TnI-TnC interaction as shown through cTnI mutations in cardiomyopathy mutants, which have presented alterations in contraction and relaxation kinetics by indirectly altering cross-bridge kinetics. TnI-TnC alterations have shown delayed relaxation, and TnC oxidation by H₂O₂ was shown to increase its complex dissociation (Pinto, de Sousa, & Sorenson, 2011). Given thin filament regulatory protein function is inextricable from actin function, many of the modifications exhibit effects on interacting pairs, sometimes resulting in reduced cooperativity. However, some have reported increased interactions by dimerization. Glutathionylation of Cys-374 in actin has been shown to lead to decreased Tm-actin binding cooperativity as well as crosslinking with laterally adjacent actin Gln-41, leading to diminished filament force in permeabilized trabeculae (Chen & Ogut, 2006). Disulfide bridge formation of Tm as a result of Cys-190 oxidation in ischemic pig hearts was purported to directly impact Tm flexibility and Tm-thin filament interactions (Canton et al., 2006; Williams Jr & Swenson, 1982). Interestingly, heterodimerization between Cys-257 in actin and Cys-190 in tropomyosin due to HNO-induced disulfide formation was suggested to shift the tropomyosin strand to an open position, where actin-binding sites are more available for myosin binding, thereby increasing contractility (Gao et al., 2012; Murray et al., 2009; Steinberg, 2013). Tropomyosin cross-linking and overall ROS was also observed in dystrophic mdx mouse models (El-Shafey, Armstrong, Terrill, Grounds, & Arthur, 2011; Menazza et al., 2010) as well as increased nitration products in aging rat skeletal muscles (Kanski, Hong, & Schöneich, 2005). Cardiac troponin subunits cTnI and cTnC contain tyrosine residues which have been shown to be nitrated in aged rat hearts (Kanski, Behring, et al., 2005). S-glutathionylated TnI Cys-133 was found in fast-twitch skeletal muscle in both rats and humans, which was surprisingly shown to result in increased Ca²⁺ sensitivity (Mollica et al., 2012). The redox state of TnC has been shown to reversibly tune binding affinity (Pinto et al., 2011). Similarly, it was determined that phosphorylation of the homologous serine in cTnI impeded interaction with cTnC (Ward, Ashton, Trayer, & Trayer, 2001). Accordingly, Cys-133 oxidation in TnI is suspected to reduce interaction with TnC (Mollica et al., 2012). Hydrogen peroxide modification of Cys-98 in the D/E helix of TnC was shown to tune its binding affinity with the thin filament, where oxidation reduced affinity and modifications were reversible with DTT. In sum, in both skeletal and cardiac muscle, low levels of regulatory thin filament oxidation may increase contractility particularly in heart, while persistent oxidation reduces Ca²⁺ sensitivity and force production (Graham D Lamb &

Westerblad, 2011; Steinberg, 2013). Given the Tm-Tn complex's proximity to other thin filament proteins and their small individual subunit sizes, it appears that Tm-Tn oxidation results in relatively more intermolecular crosslinking compared to actin or myosin oxidation.

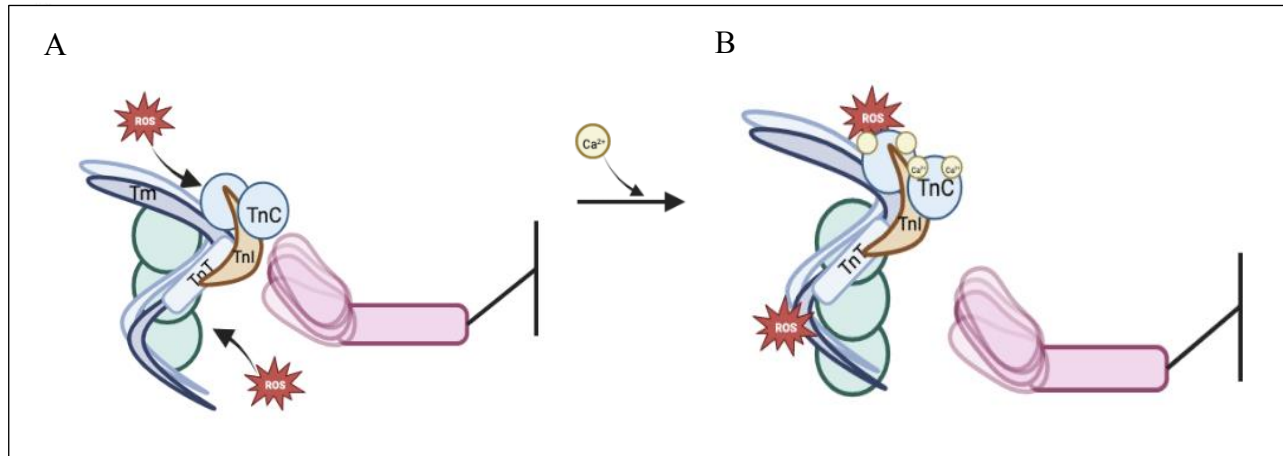


Figure 4. Oxidation in thin filament proteins. **a.** TnC binds Ca^{2+} and undergoes conformational change that exposes a hydrophobic region. there is no evidence that oxidation of TnC alters Ca^{2+} binding however, oxidation of TnC Cys-98 has been shown to reduce binding to TnI. Oxidation of TnI Cys-133 increases Ca^{2+} sensitivity. **b.** After Ca^{2+} binding, TnC-TnI dissociates from actin allowing Actin-myosin binding. TnT moves Tm to expose myosin binding site on actin. Oxidation of Tm Cys-190 increases Ca^{2+} sensitivity by crosslinking with actin Cys-257, biasing Tm to an open configuration.

Impacts of oxidation actin-myosin interactions

Understanding how oxidative modifications influence the contractile cycle is a complex task, given that numerous proteins work with and regulate each other. While numerous separate modifications might result in reduced force or velocity, it may be that the pathway to this common outcome is distinct for each molecule. (Bansbach & Guilford, 2016; Elkrief et al., 2022). For instance, myosin oxidation is likely to cause direct changes to the myosin head, impacting both its enzymatic and mechanical properties related to actin binding and step-size (Bansbach & Guilford, 2016; Stewart, Murthy, Dugan, & Baker, 2021). On the other hand, actin's oxidative modifications would predominantly affect myosin attachment and detachment as well as overall filament stability (Bansbach & Guilford, 2016; Maarten Michiel Steinz, 2020; Maarten M Steinz et al., 2019). While

myosin likely has a greater susceptibility to oxidation compared to actin, modification on binding partner results in impaired cross-bridge function in general. Nonetheless, it's important to note that excessive modification on either actin or myosin results in a common outcome, a loss of velocity or force due to a disruption of the cross-bridge, although the degree to which this occurs can vary depending on the species of oxidant and degree of oxidation. To understand how oxidation affects the cross-bridge it is beneficial to understand how oxidation affects proteins of the thick and thin filament individually.

As we first mentioned in section 3 there are two theories relating oxidation accumulation on amino acids and protein dysfunction. The first mechanism is that protein dysfunction is a result of accumulation of modifications on a wide range of residues with variable susceptibility to oxidation (LaDora V Thompson, 2009) driving force loss (Dos Santos et al., 2015; Oh-Ishi, Ueno, & Maeda, 2003; Snow, Fugere, & Thompson, 2007; L. V. Thompson, Durand, Fugere, & Ferrington, 2006; Watanabe, Ogasawara, Suzuki, Nishizawa, & Ambo, 1992). The second suggested mechanism is that dysfunction is driven by a small number of residues with high susceptibility to oxidation (I. Dalle-Donne et al., 2003; Prochniewicz et al., 2007), which have an outsized effect on the functionality of the molecule. This is exemplified by oxidation of SH1 and SH2 in the myosin S1 (Cheung et al., 1991; Kirshenbaum, Papp, & Highsmith, 1993), which may have a disproportionate effect on muscle contraction (Dutka et al., 2011; Gross & Lehman, 2013; Teresa Tiago et al., 2006). Simultaneous and cumulative effects of residue modification complicate the study of exactly what modification leads to which effect, and under what biochemical circumstances. For instance, Tiago et al. 2010 explored how peroxynitrite can enhance the intrinsic Mg^{2+} -ATPase activity while inhibiting the actin-stimulated Mg^{2+} -ATPase activity of S1 depending on reaction media (by changing nucleotide and phosphate presence) available (Teresa Tiago et al., 2010). Mechanistically, modifications of amino acids involved in the ATPase cycle, including SH1, have been shown to increase P_i dissociation rate and shift the rate limiting step to hydrolysis, thereby increasing basal Mg^{2+} -ATPase activity and reducing actin-activated ATPase activity (Muhlrad, 1983; E Michael Ostap, White, & Thomas, 1993; Reynoso, Bobkov, Muhlrad, & Reisler, 2001). It would be interesting to know whether oxidation sufficiently alters phosphate release during this transition state to affect force generation in whole muscle (Allingham, Smith, & Rayment, 2005; Kovács, Tóth, Hetényi, Málnási-Csizmadia, & Sellers, 2004; Offer & Ranatunga, 2020; Rahman, Ušaj, Rassier, & Månsson, 2018).

It was noted that at peroxyxynitrite concentrations where there was optimal ATPase activity, four cysteines were already oxidized, including SH1 and SH2. Only when SH1 was selectively modified did ATPase activity increase, which was neutralized when SH2 was also oxidized, thus emphasizing the combined role of other cysteines in increasing basal ATPase activity. Therefore, whether oxidation-induced damage is primarily determined by key residue oxidation or operates by a consortium of minor accumulated insults is likely determined by the type of oxidant and amino acid target, however there is evidence for effect of oxidation on general protein stability. Multi-target oxidants such as SIN-1 resulting in extensive cysteine oxidation (Teresa Tiago et al., 2006) in S1 were shown to impair the S1 intermediate conformation catalytic state $S1 \cdot Mg^{2+} \cdot ADP \cdot P_i$ and thus block the shift to the intermediate state needed to continue the catalytic cycle. SIN-1-oxidation likely caused a general and partially reversible protein unfolding indicated by enthalpy measurements and increased susceptibility to trypsin digestion (Teresa Tiago et al., 2006), which resulted in a diminished force production (Fisher et al., 1995a; Holmes, 1997; Rayment et al., 1993). Therefore, while oxidation of critical residues may affect critical transition steps of force generation, prolonged exposure results in widespread effects on the molecule which manifest in force changes as well.

Oxidation on actin may affect both intramolecular bonding (Maarten Michiel Steinz, 2020; Maarten M Steinz et al., 2019) as well as actin-myosin binding, which is sufficient to result in reduced cross-bridge cycling and force. Thus, it is likely that modifications in key residues as well as modifications among structural residues accumulate with increasing oxidation, resulting in widespread protein changes. Oxidation can lead to an increase in muscle stiffness and rigidity, making it difficult for the muscle to stretch and contract properly. This cumulative mechanism can make muscle function less effective, and accelerate muscle weakness, fatigability, and muscle wasting.

Oxidation of contractile proteins in disease and aging

Oxidative damage has been identified as a contributing factor in aging and several muscular diseases including muscular dystrophy, arthritis, and heart disease. Depending on the disease, oxidation can either be a primary factor or secondary disease marker, often resultant from

inflammation. Despite interest and efforts to employ antioxidant treatments, the widespread oxidation and the difficulty of maintaining a redox balance without disturbing normal physiology continue to be challenges (Lian, Chen, Wu, Deng, & Hu, 2022; Yamada, Abe, et al., 2015). Oxidation in disease has a range of impacts, including DNA damage, lipid oxidation, and cell death (Le Moal et al., 2017; Serra, Pinto, Prokić, Arsa, & Vasconsuelo, 2020). In the context of muscular damage, a reduction in specific force due to oxidation has been documented in rodent models of heart failure, cancer, and arthritis, suggesting that muscle weakness is a common condition across several diseases, regardless of whether oxidation is a primary cause or secondary marker of disease (Canton et al., 2011; Digerness et al., 1999; Höök, Sriramoju, & Larsson, 2001; Kanski, Behring, et al., 2005; Larsson, Li, & Frontera, 1997; M. Li et al., 2015; Liguori et al., 2018; Masuko, 2014; Menazza et al., 2015; Münzel et al., 2017; Prochniewicz et al., 2007; Maarten Michiel Steinz, 2020; L. V. Thompson et al., 2006; van der Pol, van Gilst, Voors, & van der Meer, 2019; Walsmith & Roubenoff, 2002; L. Wang, Lopaschuk, & Clanachan, 2008; Yamada, Fedotovskaya, et al., 2015). Contractile proteins seem to have an intrinsic susceptibility to oxidative post-translational modifications and have been noted in diseases as diverse as Alzheimer's, Friedrich's ataxia and inflammatory mouse models (Aksenov, Aksenova, Butterfield, Geddes, & Markesbery, 2001; Lu, Katano, Uta, Furue, & Ito, 2011; Pastore et al., 2003). Given the broad spectrum of oxidation, relief for muscle weakness would require site-specific therapeutics which are not aided by conventional immunosuppressants and glucocorticoids used to lower rheumatic activity (Maarten M Steinz et al., 2019). As such, a SOD2/catalase mimetic (EUK-134) has shown positive effects in treating muscle weakness in rats with arthritis (Yamada, Abe, et al., 2015) although there are no approved drugs with this specific mechanism of action. Therefore, it becomes crucial to deepen our understanding of the role of oxidation in disease processes. Filling this knowledge gap could potentially pave the way for targeted therapeutics that go beyond the conventional modes of treatment. Understanding the involvement of oxidation to contractile dysfunction is critical to this effort. Therefore, in the following sections we will compile instances where oxidative modifications have a direct effect on contraction in disease.

Arthritis

It has recently been shown that skeletal muscle protein oxidation contributes to a significant degree of contractile weakness in arthritis patients (Maarten Michiel Steinz, 2020; Maarten M Steinz et

al., 2019; Yamada, Abe, et al., 2015; Yamada, Fedotovskaya, et al., 2015; Yamada et al., 2009). Interestingly, oxidation of skeletal muscle actin has been shown to be sufficient to cause weakness in human patients. Studies linking rheumatoid arthritis and oxidation of actin filaments noted several changes in human subjects, rodent models, and isolated actin in *in vitro* experiments. 3-nitrotyrosine (3-NT) and malondialdehyde (MDA) modifications were found in similar oxidation hotspots across SIN-1 treated actin, arthritis-induced mice, and human arthritis patients. Oxidized actin showed dysregulated G-actin to F-actin polymerization as well as decreased force production in myofibers (Maarten M Steinz et al., 2019). Interestingly, there were no differences in muscle cross-sectional area or Ca^{2+} released by sarcoplasmic reticulum between arthritis muscles and controls, with differences in force due to an absolute loss in myofibrillar force (Maarten M Steinz et al., 2019). Further investigation into the cause of reduced myofibrillar force revealed a slower twitch contraction and decreased shortening velocity, which we corroborated in *in vitro* environments (Elkrief et al., 2022). An analysis of the force- Ca^{2+} relationship showed that while there was impaired force at maximal Ca^{2+} level, there was no reduction in force at 50% Ca^{2+} nor in the shape of the Ca^{2+} sensitivity curve, thus reductions in force were attributed to reduced cross-bridge force generation (Yamada et al., 2009). It should be noted that CFA-treated mouse Ca^{2+} -sensitivity was similar to that of untreated mice (Maarten M Steinz et al., 2019). A reduction of cycling rate of the cross-bridges was also observed, and given cycling rate is determined by ATPase activity, there was likely an oxidation-induced reduction in ATP hydrolysis, a result also shown to occur when NO is administered to skinned muscle fibers (Perkins, Han, & Sieck, 1997). Additionally, a small (7%) decrease in force attributed to collagen induced arthritic mice was attributed to a decrease in myosin heavy chains content (Yamada et al., 2009).

Heart disease

Heart disease and heart failure (HF) have several clinical presentations and is associated with substantial mortality and comorbidities. Reactive oxygen species are well-known contributors to HF (Giordano, 2005; Seddon, Looi, & Shah, 2007; Sheeran & Pepe, 2006) and thought to contribute to cardiac remodeling, chemo-mechanical uncoupling and altered Ca^{2+} sensitivity (Hool, 2009; Hutchinson, Stewart Jr, & Lucchesi, 2010; Zima & Blatter, 2006). There is an extensive literature covering the signaling role of oxidative modifications in other aspects of cardiac function, not covered in this review (D’Oria et al., 2020). Some have noted potentially

cardioprotective effects of oxidation which cause a reduced contractility in short term reversible environment which reduces metabolic demand in hyper contractile heart disease (Cuello, Wittig, Lorenz, & Eaton, 2018; Nag et al., 2017) and yet become damaging if the oxidative environment becomes chronic or reverses and the oxidation persists, leaving behind suboptimal contraction. As with other diseases, contractile dysfunction in heart disease can be attributed to ROS dependent modifications of contractile proteins independent of Ca^{2+} handling (Gao, Liu, & Marban, 1996; Luo, Xuan, Gu, & Prabhu, 2006; Schulz, Dodge, Lopaschuk, & Clanachan, 1997; Vaage et al., 1997; L. Wang et al., 2008). ROS-induced damage in heart disease, while serving protective functions at physiological levels, advances heart failure due to hormone dysregulation and hemodynamic factors (Burgoyne, Mongue-Din, Eaton, & Shah, 2012; Münzel et al., 2017). ONOO⁻ modifications of cysteines in heart disease are a common source of inquiry in hypoxia induced pig and rat models. Excesses in peroxidation were shown to cause modifications in Cys-138, facilitating degradation of myocardial protein caused by increased matrix metalloprotease-2 (MMP-2) activity, causing contractile dysfunction (Doroszko et al., 2009; Passarelli et al., 2008; D. K. Polewicz, 2011). Additionally, nitrated tyrosines (Tyr-114, Tyr-116, Tyr-134, and Tyr-142) detected in aging cardiac myosin heavy chain (Hong et al., 2007) and have been shown to directly contribute to reduced force generation in rat ventricular trabeculae (Michael J Mihm, Yu, Reiser, & Bauer, 2003). Actin and Tm have been shown to be major targets of oxidation during ischemia-reperfusion of the isolated rat heart (Canton et al., 2004). Researchers found that the increase in carbonylation in actin and Tm proteins were correlated with a poor survival outcome in biopsies from end-stage failing human donor hearts as compared to nonfailing donor hearts. Actin and Tm were particularly susceptible to oxidation and while actin was predominantly carbonylated, heart failure Tm showed an increase in carbonylation, disulfide cross-bridges as well as nitrosylated cysteines (Canton et al., 2011), indicating differing susceptibilities to oxidation. The myosin light chain (MLC 1) was also shown to contain oxidized sulfhydryls in cysteines and methionines, which were shown to cause a decrease in force of human cardiomyocytes (Hertelendi et al., 2008). Heart disease models have exhibited a general oxidative environment, with oxidation present in skeletal muscle as well. Increased myosin protein carbonylation was detected in soleus and diaphragm of induced heart failure rats, with concomitant decrease in the actin myosin interaction as shown in the in vitro motility assay (Coirault et al., 2007). The authors showed that there was an inverse relationship between increasing amount of ONOO⁻ and cardiac muscle protein motility in the IVMA (Coirault et al., 2007). While some oxidation in the heart is clearly deleterious, some

results in increased contractile function. Cys-37 oxidation, has been linked with improved Ca^{2+} sensitivity and oxidation (Gao et al., 2012). With respect to increasing force, there is an interesting interplay between amino acids of neighboring proteins. Increase in myofilament Ca^{2+} -sensitivity and increased cardiac force production after oxidation have been noted, by purported disulfide bonding between MLC-1 Cys-81 and MHC Cys-37, hypothesized to increase lever arm rigidity and swing force (D. K. Polewicz, 2011). At low levels GSSG oxidation of cardiac MHC Cys-400, Cys-695 and Cys-947 have shown optimal function compared to reduced and higher GSSG concentrations (Passarelli et al., 2008). A singular approach to treating oxidation as a pathology may have the unintended consequence of undermining the potentially adaptive role that oxidation plays in some conditions. Although antioxidant treatment of heart disease has largely been unsuccessful, it remains an area of interest for potential therapy (Thomson, Frenneaux, & Kaski, 2009; van der Pol et al., 2019). To improve outcomes, general approaches such as lifestyle and dietary changes (Nuttall, Kendall, & Martin, 1999), as well as more targeted approaches such as administering exogenous antioxidants only to those with low endogenous antioxidant reserves or specifically upregulating endogenous antioxidants such as GSH through NAC administration (Arstall, Yang, Stafford, Betts, & Horowitz, 1995; Mehra et al., 1994; Šochman & Peregrin, 1992; Šochman, Vrbská, Musilová, & Roček, 1996), have been implemented.

Muscular dystrophy

Muscular dystrophies are a group of 30 genetic disorders caused by a host of potential factors, which result in the loss of contractile force (Guellich, Negroni, Decostre, Demoule, & Coirault, 2014). Due to the complex etiology of muscular dystrophy, the exact source of oxidation, whether its inflammation or muscle disuse (Canton, Menazza, & Di Lisa, 2014) and how it contributes to force loss due to oxidation of the contractile proteins is still being explored. However, the contribution that oxidation plays in cell death and contractile dysfunction has been well-documented (Lawler, 2011; Menazza et al., 2010; Ragusa, Chow, & Porter, 1997; Rando, Disatnik, Yu, & Franco, 1998; Tidball & Wehling-Henricks, 2007). One of the ways oxidation is increased in Duchenne Muscular Dystrophy (DMD) is due to nNOS dissociation from the sarcolemma (Brenman, Chao, Xia, Aldape, & Brecht, 1995). During contraction, weakened sarcolemma dystrophin dissociates, taking its associated nNOS with it. NO from nNOS produced during contraction is known to be protective against oxidation (Wink et al., 1995), thus increasing the

susceptibility of oxidation damage in DMD muscle (Brenman et al., 1995; Disatnik et al., 1998; Haycock, Jones, Harris, & Mantle, 1996). Dystrophies may affect contraction by either reducing the number of active cross-bridges producing force, or by the force produced by each cross-bridge because of altered actin-myosin interactions or cross-bridge kinetics. As with arthritis, reduced specific force was exhibited in muscles from *mdx* mice, yet an increase in the ATPase cross-bridge cycling was observed (Coirault et al., 1999). Conversely, myosin taken from *mdx* mouse diaphragms has been shown to move actin at a slower velocity in the IVMA (Coirault, Lambert, Pourny, & Lecarpentier, 2002) and this difference was shown to be fiber type specific, while no changes in fiber type composition were observed (Canepari, Rossi, Pansarasa, Maffei, & Bottinelli, 2009). The authors concluded that the *mdx* mouse diaphragm has reduced ATPase efficiency to maintain overall force. Interestingly, the differences were not observed at the level of the single permeabilized cell, thus it was suggested that changes in actin-myosin interactions were likely attributable to changes in muscle protein structure due to oxidation (Bates et al., 2013). Furthermore, an increase in actin fragments due to oxidation-induced caspase-3 targeting of actin is also thought to contribute to reduced structural integrity and altered cross-bridge cycling in dystrophies and muscle wasting conditions (Du et al., 2004). Ultimately, altered contractile protein structure due to oxidative modifications and reduced protein content from oxidation-induced removal of actin result in long term energy inefficient contractile elements with reduced cross-bridge output (Guellich et al., 2014).

Aging

Previous studies have shown a decrease in contraction at both the muscle and motor protein level in aging muscle (Höök, Li, Sleep, Hughes, & Larsson, 1999; Höök et al., 2001; Larsson et al., 1997; M. Li et al., 2015; X. Li & Larsson, 1996). Studies have also shown increased glycation in aged rat muscles (Ramamurthy & Larsson, 2013). Mass spectrophotometry proteome of aging rat muscles revealed that overall protein carbonylation increased in aged group biopsies compared to the young group yet some areas showed reduced carbonylation (Dos Santos et al., 2015). Understanding the oxidative effects on Ca^{2+} handling is challenging across many diseases given the Ca^{2+} dependence at both the membrane and contractile protein level. The use of skinned muscle fibers, where the membrane proteins are removed mechanically or chemically, leaving contractile elements, and enabling direct control of Ca^{2+} and thus control over filament activation has been

critical for understanding contractile responses in fibers. By assessing the maximal isometric force at each Ca^{2+} concentration and superimposing this on the Hill curve, the pCa at half maximum force can help determine the myofibrillar Ca^{2+} sensitivity. Ca^{2+} sensitivity of aging myofibrils has been explored as a result of oxidative modifications (Lowe, Surek, Thomas, & Thompson, 2001; Powers & Jackson, 2008; Prochniewicz et al., 2007; Reid & Moylan, 2011) reporting a reduced sensitivity in aged human *vastus lateralis* in all fiber types, with type I fibers being preferentially affected (Straight, Ades, Toth, & Miller, 2018). This point is in contention, as others have reported that the degree of this effect seems to be minor or even neutral (Hvid, Ørtenblad, Aagaard, Kjaer, & Suetta, 2011; Hvid et al., 2013) whereas type II fibers were shown to be preferentially affected compared to type I fibers (Lamboley et al., 2015). Interestingly, S-glutathionylation of fast troponin I (TnI_f) has been shown to result in increased Ca^{2+} sensitivity and contribute to reduced fatiguability in exercise (Mollica et al., 2012). Administration of reduced glutathione was shown to increase Ca^{2+} sensitivity skinned muscle fibers although to a far lesser extent in aged fibers, indicating a reduced sensitivity of TnI to adaptive oxidative modifications (Lamboley et al., 2015). Furthermore, prolonged oxidation has been shown to irreversibly damage and inhibit the Ca^{2+} -sensitizing effects of glutathionylation (R. Murphy, Dutka, & Lamb, 2008) suggesting that critical residues on the regulatory thin filament are damaged in type II fibers during aging. Muscle contraction and structural proteins shown to have higher oxidation included myosin 7, troponin T and myosin binding protein C (MyBP-C). MyBP-C stabilizes thick filaments and is essential for actin-myosin thin and thick filament cross-bridge interaction (Ackermann & Kontogianni-Konstantopoulos, 2011; Van Dijk, Bezold, & Harris, 2014) and mutations in MyBP-C cause a host of myopathies (Ackermann et al., 2013; Bonne, Carrier, Richard, Hainque, & Schwartz, 1998; Harris, Lyons, & Bezold, 2011; Markus et al., 2012; Schlossarek, Mearini, & Carrier, 2011).

Increased oxidation of MyBPC along with the decrease in other myosin binding proteins and myosin itself has been proposed to reduce muscle fiber stability with age (D. Capitanio et al., 2009; Gannon, Doran, Kirwan, & Ohlendieck, 2009; Gelfi et al., 2006; L. V. Thompson et al., 2006). It was also found that oxidized troponin T (TnT) levels were increased in elderly biopsies (Dos Santos et al., 2015). TnT inhibits the actin-myosin interaction, which is only released upon Ca^{2+} attachment to Troponin C (TnC), whereby a conformational change in the TnT-TnC-TnI complex allows cross-bridge formation and ATP hydrolysis (Gomes, Potter, & Szczesna-Cordary, 2002; Wei & Jin, 2011). Given the importance of thin filaments for stability and contraction, oxidation

during aging of regulatory proteins may affect filament stability as well as thin filament contraction regulation. Other studies comparing the muscular properties between young and old rats show decreases in the actomyosin ATPase V_{\max} and half V_{\max} in old rats, attributing the reduction in ATPase activity to the number of oxidized cysteines in myosin as opposed to actin (Prochniewicz et al., 2007). Modifications of Cys-697 and Cys-707 in the catalytic domain of myosin have been implicated in diminished myofibrillar output in aging (Lowe et al., 2001; Lowe, Warren, Snow, Thompson, & Thomas, 2004; Zhong, Lowe, & Thompson, 2006). Modifications of these specific residues has been shown to have significant effects on the actin-myosin interaction thus causing dysfunction of the cross-bridges (Bobkova, Bobkov, Levitsky, & Reisler, 1999; Crowder & Cooke, 1984), where ATPase K_m and V_{\max} were lower in fluorescent and spin probe labeled Cys-707 (Bobkov et al., 1997). This damage was inducible in rabbit muscle fibers as shown after administering the •NO donor sodium nitroprusside (Perkins et al., 1997). Specifically, oxidative modifications in the catalytic domain have a direct effect on the cross-bridge in aging. Permeabilized fibers labeled at Cys-707 and analyzed by electron paramagnetic resonance spectroscopy determined that the fraction of the myosin heads in the strong-binding states during maximal contraction were reduced by 30% in aged rats and 27% reduced specific force in aging human fibers (Lowe et al., 2001). Thus, contractile dysfunction in age is associated with a reduction in the force per cross-bridge, a decrease in the number of force producing cross-bridges, and the oxidation of thick and thin filament regulatory proteins such as TnT and MLC-2 (Brocca et al., 2017).

Although by no means exhaustive, the above diseases showcase how oxidation plays a diverse role in the pathogenesis of many muscular diseases. Its contribution is multifaceted, making it challenging to establish causal relationships (Forman & Zhang, 2021). In some cases, as in ischemia reperfusion, heart failure (Peoples, Saraf, Ghazal, Pham, & Kwong, 2019), and rheumatoid arthritis (Persson, Steinz, Westerblad, Lanner, & Rassier, 2019; Maarten Michiel Steinz, 2020; Maarten M Steinz et al., 2019), oxidative stress is a known exacerbating factor and crucially damages muscle function. In other diseases with muscle involvement such as ALS, COPD, and aging, oxidation levels are elevated in proportion with disease progression (Liguori et al., 2018). This increase in oxidation often accompanies the rise of comorbidities and may be considered as progressing in tandem with the disease or as a secondary consequence of disease progression (Cunha-Oliveira et al., 2020; Kapchinsky et al., 2018; Zinellu, Zinellu, Fois, Carru, &

Pirina, 2016). Regardless of the disease, there has been a recognition that the effectiveness of antioxidant defenses can depend on where, when, and to what extent oxidative stress is a part of a disease. Oxidative insult represents an imbalance between oxidants, antioxidants, and enzymes. Current paradigms in medicine prefer to limit the mechanism of action to as restricted an effect as possible. This approach, however, has proven challenging when treating oxidation in disease. Accordingly, most antioxidant defense within cells is not provided by small molecules acting as scavengers, but by antioxidant enzymes using their specific substrates to reduce oxidants. As such, therapeutic opportunities may lie in preventing the production of oxidants that cause direct injury to macromolecules, inhibiting downstream signaling by oxidants that results in signaling for inflammation or cell death, and increasing both antioxidant enzymes and their substrate. This could lead to a more rational and successful approach to antioxidant therapies (Forman & Zhang, 2021). As evidenced in the supplementary tables, different oxidation events can either increase or decrease contractile and enzymatic properties, as is the case when the thin filament is oxidized (Table 2). Thus, it is critical to understand the multi-layered mechanisms on how oxidation affects protein interactions. As with disease, the question of whether systemic or specific oxidative imbalances drive dysfunction is recapitulated at the molecular level, as we have explored in previous sections. Ultimately, whether accumulation of modifications or specific key-residue modifications drive oxidant damage, and the degree to which oxidation is a cause or a reflection of disease state remains an active area of research. To further our understanding of these complex oxidative dynamics, transgenic animal models have proven invaluable. They allow for targeted manipulations of key enzymes and proteins, providing a robust understanding of the role these proteins play in normal and pathological conditions.

Transgenic models in redox regulation

While this review has surveyed many studies which have relied on the exogenous addition of oxidants to muscle tissues, the use of transgenic animal models complements studies with chemical modification. By enabling endogenous manipulation of the redox environment, researchers can provide insights that more closely align with physiological or pathological conditions. They allow for targeted manipulations of key enzymes and proteins, providing a robust understanding of the role these proteins play in normal and pathological conditions.

Transgenic models are well suited to understand heart disease, muscular dystrophy, and aging. Steinhorn et al., 2018 utilized a chemogenetic system to control intracellular H₂O₂ production in the heart. They found that chronic H₂O₂ generation in D-amino acid oxidase (DAAO)-expressing animals led to a significant decrease in left ventricular systolic pressures and dP/dt during isovolumetric contraction, indicative of systolic dysfunction (Steinhorn et al., 2018). These findings highlight the role of oxidative stress in inducing cardiac pathophysiology and contractile dysfunction. Transgenic studies have also proven valuable for understanding muscular dystrophy. Wehling et al., 2001 showed that dystrophin-deficient muscles exhibit reduced nitric oxide synthase (NOS) expression. By using a transgenic mdx mouse model maintaining normal muscle NO levels, they found that the normalization of NO production reduced muscle inflammation and fiber damage, further solidifying the importance of NO in muscular pathology (Wehling, Spencer, & Tidball, 2001). The role of antioxidants in age-related muscle dysfunction has been explored through transgenic models as well. Umanskaya et al., 2014, used a transgenic mouse model with targeted overexpression of the human catalase gene in mitochondria. Their findings demonstrate the crucial role of mitochondrial free radicals in promoting pathological intracellular Ca²⁺ leak, which underlies the age-dependent loss of skeletal muscle function. Aged mice with this genetic enhancement exhibited improved voluntary exercise, increased skeletal muscle specific force and Ca²⁺ transients, and decreased intracellular Ca²⁺ leak compared with age-matched controls. Furthermore, the ryanodine receptor 1 (RyR1), the sarcoplasmic reticulum Ca²⁺ release channel required for skeletal muscle contraction, was less oxidized, depleted of the channel stabilizing subunit, calstabin1, and displayed increased single channel open probability in these aged mice (Umanskaya et al., 2014). Taken together, these studies indicate that contractile and general cellular phenotypes can be manipulated using transgenic models. While transgenic models are insightful, they also have limitations, including potential compensatory mechanisms that could nullify expected changes, and the possible lack of specificity of the targeted protein to the process under investigation. The direct link between oxidation and contractile dysfunction at the actin-myosin interface or the thin filament regulatory mechanism is still difficult to interpret. More studies that can effectively assess contractile, velocity, ATPase function in the context of redox changes is needed. Overall, combining insights from studies using exogenously added oxidants and those employing transgenic models provides a comprehensive understanding of redox regulation of muscle contraction. Including recent studies using transgenic models, especially

those utilizing modern genetic methods for generating specific oxidants, paves the way for a more holistic approach to studying muscle contraction.

Conclusion

In this review we attempted to synthesize information on numerous specific instances where oxidation is present in disease and in specific oxidation models, contributing to the understanding of the complex role of oxidation in muscle contraction. The primary aim of this review was to outline known amino acid targets in muscle in various *in vitro*, animal, and human research. Despite the extensive catalog of amino acid targets that we have compiled, it is likely that we have missed some and that more remain to be discovered.

Typically, the redox state of muscle proteins transiently shifts to a greater oxidized state during exercise or due to other environmental factors. Furthermore, there appears to be a milieu where some modification is necessary for optimal force development and exercise response (Ferreira & Reid, 2008; Merry & Ristow, 2016; Otten, 1988; Powers & Jackson, 2008). This results in reversible oxidation of amino acids, up to a certain threshold (Merry & Ristow, 2016; Nogueira et al., 2009). However, in disease states, there is a disequilibrium in the cell's redox state, leading to an increased baseline oxidant load on proteins. This may result in an accumulation of oxidation on proteins, resulting in wide spread effects on whole protein structure (Maarten M Steinz et al., 2019) and/or specific oxidation on key residues, which have a significant effect on structure and function (Bobkova et al., 1999).

Given that actin and myosin are the major components of the contractile apparatus, we particularly focused on how oxidation affects each of these proteins and the contractile cycle. We noted the presence of a high number of oxidized residues in the motor domain of myosin, specifically in the myosin heavy chains at the actin binding interface, ATP binding interface, and to a lesser extent in the light chains. This distribution suggests that alterations to these residues may modulate actin-myosin interactions, leading to reversible changes at low levels of oxidation. However, irreversible oxidation can also occur, impairing actin-myosin binding and myosin's force-generating capacity at high levels (Moen et al., 2014; Pizarro & Ogut, 2009; D. K. Polewicz, 2011). Actin contains several residues known to be oxidized, impacting actin structure and function in both reversible (I.

Dalle-Donne et al., 2003; Farah et al., 2011; Moen et al., 2014; Terman & Kashina, 2013) and irreversible manners (Bansbach & Guilford, 2016; Maarten M Steinz et al., 2019; Terman & Kashina, 2013; Varland et al., 2019; Yamada, Fedotovskaya, et al., 2015; Yamada et al., 2009). Moreover, the sarcomere contains multiple other contractile proteins susceptible to oxidation, contributing to the cell's overall response to oxidative stress (Capanni et al., 1998; Durham et al., 2008; Hong et al., 2007; G. D. Lamb & Posterino, 2003; Prochniewicz et al., 2007; Samengo et al., 2012; Yamada et al., 2009). To further our understanding, we touched on studies utilizing genetic manipulations which, in conjunction with chemical and clinical studies, allow for a holistic understanding of the impacts of oxidation on muscle contraction (Steinhorn et al., 2018; Umanskaya et al., 2014; Wehling et al., 2001). The impact of oxidation on myosin binding, actin binding, and passive force element proteins, as well as large proteins like titin and the potential effect of oxidation on the three-dimensional lattice, were beyond the scope of this review but are well-deserving of further investigation. Additional investigation into building models which allow for adequate translation across *in vitro*, animal, and humans as well as accurate oxidative load quantification in different models is a valuable future line of inquiry.

As we strive to enhance our understanding of the redox regulation of muscle contraction, we must grapple with the challenges of translating findings across *in vitro*, animal, and human models, along with accurately quantifying oxidative loads in diverse models. These challenges are compounded by the complexities and redundancies of oxidant systems in the body. The current limitations of antioxidant treatments may indeed stem from our inadequate understanding of these intricate systems and an inability to manipulate them effectively, although we have mentioned some attempts at doing so via transgenic systems. Despite the hurdles, the vista that lies ahead is encouraging. An accumulating body of research is gradually unravelling the complexity of redox interactions within contractile proteins. The prospect of synthesizing these insights into a coherent and comprehensive understanding of muscle redox biology holds promise for future discoveries and potential therapeutics.

Residue	Type of Oxidation	Location	Muscle info	Purported Effect	Reference
Cys-37 α	NCA/AS	MHC	Rat cardiac muscle, intact and skinned.	Increased maximum force and increased Ca^{2+} sensitivity.	(Gao et al., 2012)
Cys-67 Cys-76	ONOO ⁻	MLC-1	Human cardiac muscle.	Unclear functional effect.	(D. K. Polewicz, 2011)
Cys-81	NCA, HNO	MLC-1	Rat cardiac muscle.	Increased myofilament Ca^{2+} -sensitivity and increased cardiac force production, possibly by increasing disulfide bonding with MHC Cys-37, thus increasing lever arm rigidity and swing force.	(Gao et al., 2012; D. K. Polewicz, 2011)
Cys-138 Tyr-141	Cys S-nitrosylation Tyr nitration, ONOO ⁻ from hypoxia-reoxygenation	MLC-1	Cardiac muscle in hypoxia-induced piglets as well as hypoxic rat.	Increased degradation of myocardial protein caused by increased matrix metalloproteinase-2 (MMP-2) activity and myocardial ONOO ⁻ production, causing contractile dysfunction.	(Doroszkowski et al., 2009; D. K. Polewicz, 2011)
Cys-697 (SH2) Cys-707 (SH1)	ONOO ⁻ , SIN-1	S1 MHC	Rabbit skeletal muscle.	Decreased maximal force resulting in deterioration of muscle contractility. Suspected decrease in ATPase activity shown when residues are modified (Bobkova et al., 1999; Seidel, 1969; Yamaguchi & Sekine, 1966). Oxidation of Cys-707 shown to increase Ca^{2+} ATPase, and additional Cys-697 oxidation inhibits all ATPase activity.	(Teresa Tiago et al., 2010; Teresa Tiago et al., 2006),
Cys-400 Cys-695 Cys-947	GSSG	MHC, cardiac β isoform	Rat cardiac muscle ventriculum.	GSSG at 0.1mM stimulates ATPase. GSSG greater than 1mM decreases ATPase.	(Passarelli et al., 2008)
Cys-541	SNAP NO donor, NEM and DTDP	Lower 50K domain	Rat skeletal EDL and cardiac muscle myofibrils.	Ventricular and fast twitch myofibrils, which had more exposed cysteines resulted in decreased ATPase, while oxidation of less exposed cysteines in rigor instead resulted in increased in ATPase and Ca^{2+} sensitivity	(Gross & Lehman, 2013)
Cys-699 Cys-709 Cys-796	SNAP NO donor, NEM and DTDP	MLC binding region			
Cys-817	SNAP NO donor, NEM and DTDP	Cys-817 in RLC binding region			

				(only in ventricular myofibrils).	
Cys-907	AS	MHC $\alpha\beta$	Rat cardiac muscle, permeabilized and skinned muscle fibers.	Increased fiber force without changing Ca^{2+} sensitivity.	(Gao et al., 2012)
Cys-947 β Cys-1750 $\alpha \beta$	NCA	MHC	Rat cardiac muscle, skinned and whole muscle fibers.	Increased fiber force and increase Ca^{2+} sensitivity.	(Gao et al., 2012)
Met-394	H ₂ O ₂	MHC. Actin binding cleft. Located in α helix of the cardiomyopathy loop in S1	Met-394 in <i>Dictyostelium</i> , equivalent to Cys-402 in human skeletal muscle.	Decreased actin-activated ATPase activity and decreased actin interaction by changing the structure and dynamics of the actin-binding cleft.	(Klein et al., 2011; Moen et al., 2014)
Met-100 Met-113 Met-189	H ₂ O ₂	ELC	Rabbit skeletal muscle.	Unclear functional effect.	(Prochniewicz, Lowe, et al., 2008)
Met-94 Met-166	H ₂ O ₂ ONOO ⁻	MHC 23 kDa	Rabbit skeletal muscle, Human cardiac muscle.	Unclear functional effect.	(Prochniewicz, Lowe, et al., 2008) (D. K. Polewicz, 2011)
Met-496 Met-542	H ₂ O ₂ ONOO ⁻	MHC 50 kDa	Rabbit skeletal muscle Human cardiac muscle.	Unclear functional effect.	(D. K. Polewicz, 2011; Prochniewicz, Lowe, et al., 2008)
Met-779	H ₂ O ₂ ONOO ⁻	MHC 20 kDa	Rabbit skeletal muscle Human cardiac muscle.	Unclear functional effect	(D. K. Polewicz, 2011; Prochniewicz, Lowe, et al., 2008)
Tyr-73 Tyr-185 Tyr 130	H ₂ O ₂ ONOO ⁻	MLC-1	Rabbit skeletal muscle Human cardiac muscle.	Unclear functional effect.	(D. K. Polewicz, 2011; Prochniewicz, Lowe, et al., 2008)
Tyr-182	H ₂ O ₂ ONOO ⁻	MLC-2	Rabbit skeletal muscle Human cardiac muscle.	Unclear functional effect.	(D. K. Polewicz, 2011; Prochniewicz, Lowe, et al., 2008)
Met-486	H ₂ O ₂	Located at a bend in the relay helix, a major path of	<i>Dictyostelium</i> Met-486 myosin equivalent to human Met-496 in skeletal muscle and	Structural impact with reduced conformational space and a large redistribution of existing structural	(Klein et al., 2011)

		communication between the nucleotide-binding site and the force-generating domain	to Cys-400 in cardiac muscle	states of the actin-binding cleft. Minimal functional impact.	
Tyr-78 Tyr-190	ONOO ⁻	MLC-1	Cardiac muscle in rat	Unclear functional effect.	(D. K. Polewicz, 2011)
Lys-84	Carbonylation, ONOO ⁻	The motor domain of the myosin head.	Skeletal muscle rabbit	Enhanced ATPase activity by possibly shifting rate limiting step of cross-bridge cycle from P _i dissociation to ATP hydrolysis. Lys-84 is situated in the NH ₂ -terminal tryptic fragment weighing 25 kDa. It is positioned at the boundary between the tryptic fragment weighing 20 kDa and resides within a fissure that stretches towards the reactive cysteine SH1	(Teresa Tiago et al., 2010)
Tyr-114 Tyr-116 Tyr-134 Tyr-142	Nitration as consequence of aging	MHC	Rat cardiac muscle, 5-month-old, or 34-month-old.	Potentially decreased contractile function.	(Hong et al., 2007)
Tyr-118 Tyr -152	ONOO ⁻ from hypoxia-reoxygenation	MLC-2	Human and pig cardiac muscle.	Increased degradation by MMP-2, leading to cardiac dysfunction.	(Doroszko et al., 2010)
Ser-180	UV irradiation, ATP photolabeling	S1 region near ATP binding site	Rabbit skeletal muscle.	Possible disruption of ATP binding. There are potential effects of oxidation on ATP binding, as Ser-180 has been shown to directly bind to the ATP gamma phosphate. It is unclear whether ser-180 oxidation would occur under physiological conditions.	(Cremo, Grammer, & Yount, 1989; Yount, Cremo, Grammer, & Kerwin, 1992)
Trp-130	ATP Photolabeling DHNBS	Near ATP binding site in S1 on 27 kDa	Rabbit skeletal muscle.	Unclear whether oxidized under physiological conditions, possibly only accessible during	(Peysers, Muhrad, & Werber, 1990; Yount et al., 1992)

		fragment of S1		transition. Little effect on ATPase activity when oxidized, although this has been contested and even shown to affect tension in skinned fibers (Pate, Nakamaye, Franks-Skiba, Yount, & Cooke, 1991).	
Ser-324	Bz2ATP trapped in binding pocket after UV radiation	ATP binding site of S1 near ATP ribose ring	Rabbit skeletal muscle.	Unclear functional effect.	(Mahmood, Elzinga, & Yount, 1989)
Ser-243	Photochemical oxidation	ATP phosphate binding site	Rabbit skeletal muscle.	There are several residues that have been shown to be susceptible to photo oxidation, yet unlikely to be accessible under physiological conditions. Unclear functional effect.	(Grammer & Yount, 1991)
Cys-475	NCA/AS	MyBP-C	Rat Cardiac muscle.	Increased fiber force and increase Ca ²⁺ sensitivity.	(Gao et al., 2012)
Cys-479 Cys-627 Cys-655	GSSG	MyBP-C	Mouse Cardiac muscle.	Enhanced myofilament Ca ²⁺ sensitivity, yet diastolic dysfunction.	(Patel et al., 2013)

Table 1. Oxidized amino acids in thick filament proteins. Chemical abbreviations: ROS: reactive oxygen species; HNO: Nitroxyl, the one electron reduced form of nitric oxide (NO); IASL: 4-(2-Iodoacetamido)-2,2,6,6-tetramethyl-1-piperidinyloxy; SNAP: S-nitroso-N-acetyl-d,l-penicillamine; NEM: N-ethylmaleimide; DTDP: 2,2'-dithiodipyridine; DHNBS: dimethyl (2-hydroxy-5-nitrobenzyl) sulphonium bromide; Bz2ATP: photoaffinity analogue 3'(2')-O-(4-benzoylbenzoyl) adenosine triphosphate; AS: Angeli salt; NCA:1-nitrosocyclohexyl acetate; GSSG : glutathionylation. α or β designate isoform if specified.

Residue	Oxidation	Location	Muscle type	Functional Effect	Reference
Cys-12 Cys-219	NCA/AS	Actin	Rat skeletal actin, permeabilized and whole cardiac muscle fibers.	Unclear functional effect.	(Gao et al., 2012)

Cys-374	DTDP, NEM, SNAP, GSSG	Actin C-terminal helix	Rat skeletal EDL and soleus, cardiac ventricular myofibrils.	Decreased myofibril contractile function, Tm-actin binding, ATPase activity, actin filament sliding velocity and F-actin polymerization.	(I. Dalle-Donne et al., 2003; Gross & Lehman, 2013; Milzani et al., 2000)
Cys-257	NCA, Nitroxyl	Actin SD 4	Rat skeletal actin, permeabilized and whole muscle cardiac fibers.	Increased contractile function, increased Ca ²⁺ sensitivity by shifting Tm from blocked state to open state while cross linking with Tm Cys-190.	(Gao et al., 2012)
Cys-285	DTDP, NEM, SNAP [3H]1,5-IAEDANS	Actin-myosin binding site	Rat Skeletal EDL and soleus, actin.	Decreased actin-myosin binding. Cys-10 and SH1 thiol on myosin have inverse reactivities when in a different contractile state (Duke et al., 1976), with myosin residues being more reactive and actin residues being less reactive in relaxing solution. The inverse occurs in rigor conditions.	(Gross & Lehman, 2013)
Cys-10	DTDP, NEM, SNAP	Actin C-terminal helix	Rat skeletal EDL and soleus, cardiac ventricular myofibrils.	Decreased actin-myosin binding. Cys-10 and SH1 thiol on myosin have inverse reactivities when in different contractile state (Duke et al., 1976), with myosin residues SH1 being more reactive and actin residues Cys-10 being less reactive in relaxing solution and the inverse being true in rigor solution.	(Duke et al., 1976; Gross & Lehman, 2013)
His-101 Gln-360 Tyr-362 His-87	SIN-1, Freund's adjuvant induced arthritis	Actin SD1	Mouse skeletal myofibrils, Human rheumatoid arthritis patients.	Examination of close contact hydrogen bonds show that His-101 has diminished bonding with neighbors.	(Maarten M Steinz et al., 2019)
His-40 Gln-41 Tyr-53	SIN-1, Freund's adjuvant,	Actin SD2	Mouse skeletal myofibrils,	Likely to affect the flexing of the polypeptide chain	(Maarten M Steinz et al., 2019)

Gln-59	Rheumatoid arthritis patient		Human rheumatoid arthritis patients.	proposed to occur upon ATP hydrolysis.	
Tyr-294 Asn-296 Asn-297 His-275	SIN-1, Freund's adjuvant, Rheumatoid arthritis patient	Actin SD3	Human and mouse purified skeletal α -actinin; skeletal G- actin; skeletal myofibrils.	Oxidation of His-275, Asn-297 and Tyr-294, all of which are near the D loop, may interfere with internal bonding. Close contact bond analysis of His-275 shows that oxidation caused loss of bonding.	(Maarten M Steinz et al., 2019)
Met-44 Met-47 Met-176 Met-190 Met-296 Met-355	H ₂ O ₂ , CT	All subdomains of actin	Rabbit skeletal actin.	Substantial increase in actin hydrophobicity, and conformation changes in SD1 and SD2 and decreased susceptibility to proteolysis. H ₂ O ₂ treatment induces structural alterations in helix 338–348 and in the loop 355–359 within subdomain 1 of the actin molecule. Complete inhibition of actin polymerization.	(I Dalle-Donne et al., 2002; Milzani et al., 2000)
Cys-190	NCA/AS	α -Tm	Rat skeletal actin, permeabilized and whole muscle cardiac fibers.	Increased contractile function, increased Ca ²⁺ sensitivity by shifting Tm from a blocked state to an open state while cross linking with actin Cys-257.	(Gao et al., 2012)
Cys-889	NCA/AS	α -actinin	Rat skeletal actin, permeabilized and whole muscle cardiac fibers.	Unclear functional effect.	(Gao et al., 2012)
Cys-35	NCA/AS	TnC	Rat skeletal actin, permeabilized and whole muscle cardiac fibers.	Unclear functional effect.	(Gao et al., 2012)
Cys-98	H ₂ O ₂	TnC, DE helix	Rat skeletal muscle psoas, skinned fiber.	Oxidation of TnC reduced binding affinity with TnI, which is rescued by DTT. Thus, oxidation reduced Cys-98	(Pinto et al., 2011)

				ability to anchor TnC to thin filament.	
Cys-133 Cys-38 or Cys-85 (non-mammalian)	GSSG	TnI _f	Rat cardiac muscle, chicken pectoralis major, toad iliofibrularis	Increased Ca ²⁺ sensitivity for mammalian Cys-133 only, by possibly loading steric effects Cys-133 of TnI toward TnC bound state so that interaction occurs at lower Ca ²⁺ .	(Mollica et al., 2012)

Table 2. Oxidized amino acids in thin filament proteins. Chemical abbreviations: ROS: reactive oxygen species; HNO: Nitroxyl, facilitates disulfide oxidation into disulfide bridges; IASL: 4-(2-Iodoacetamido)-2,2,6,6-tetramethyl-1-piperidinyloxy; SNAP: S-nitroso-N-acetyl-d,l-penicillamine; NEM: N-ethylmaleimide; DTDP: 2,2'-dithiodipyridine; DHNBS: dimethyl (2-hydroxy-5-nitrobenzyl) sulphonium bromide; Bz2ATP: photoaffinity analogue 3'(2')-O-(4-benzoylbenzoyl) adenosine triphosphate; AS: Angeli salt; NCA:1-nitrosocyclohexyl acetate; CT: Chloramine T (sodium N-chloro-p-toluene sulfonamide).

Bridging Text Between Literature Review and Experimental Studies

In the above review, we explored the impacts of oxidation from the actin-myosin complex to contractile dysfunction in disease. The foundational understanding provided by the review allows us to shift our focus to a more detailed exploration based on our empirical studies.

In our first study, we assessed the direct effects of oxidation on actin-myosin interactions. Much like the central topic of the above survey. In addition to *in vitro* functional assessment of cross bridge velocity and calcium sensitivity in study 2, our studies corroborated the effects of SIN-1 oxidation on the amino acids of contractile proteins using MS. This validation revealed a pervasive oxidation across all thin filament proteins, a finding that holds significant implications for muscle contraction mechanics.

In study 2, we aimed to characterize the effects of SIN-1 oxidation on regulated thin filament function and tabulated oxidation locations. Cross-referencing the tables above with the amino acid locations served to enrich our understanding of what putative effects of oxidation events could be. We also detected some oxidized residues not mentioned in our literature review which have yet to be challenged or validated. These results could guide researchers showing them that these residues have potential for oxidation, thus providing a starting point for future structure-function surveys.

Progressing to the G-actin and F-actin levels, and then to HMM, we detected alterations both in actual and simulated environments under the HS-AFM. Study 3 takes the information in the above review further, by presenting direct structure-function evidence that oxidation has an impact on contractile mechanics. This third study directly assessed the mechanisms of action at the structure-function level using computational models and AFM experiments for the first time.

By assessing both the specific effects of oxidation on *in vitro* function and surveying oxidation locations, we place the collection of studies presented below squarely within the purview of the above literature. We aim to help contextualize these seemingly disparate effects which, while apparent at individual amino acid levels, sum to a large effect as they accumulate on the contractile apparatus. The following studies will help contextualize the work for the reader and contribute to the knowledge base of the future.

Experimental Study 1

Oxidation alters myosin-actin interaction and force generation in skeletal muscle filaments

Daren Elkrif¹, Yu-Shu Cheng², Oleg S. Matusovsky², Dilson E. Rassier^{1,2*}

1. Department of Physiology, McGill University, Montreal, QC H3G 1Y6, Canada
2. Department of Kinesiology and Physical Education, McGill University, Montreal, QC H2W 1S4, Canada

Published in: “American Journal of Physiology - Cell Physiology”

July, 2022.

Abstract

The interaction between actin and myosin is the basis of contraction and force production in muscle fibers. Studies have shown that actin and myosin oxidation cause myofibrillar weakness in healthy and diseased muscles. The degree to which oxidation of each of these proteins contributes to an attenuated force in myofibrils is unclear. In this study, we show that exposure of actin and myosin to the chemical 5-amino-3-(4-morpholinyl)-1,2,3-oxadiazolium chloride (SIN-1), an NO and O₂⁻ donor, affected actin-myosin interactions, as shown by a decreased myosin-propelled actin velocity in the in vitro motility assay. We also observed that oxidation of actin and myosin resulted in a decrease in force generated by myosin and actin filaments, as determined by a system of microfabricated cantilevers. Although myosin is more sensitive to oxidative modifications than actin, as indicated by a steeper decrease in velocity and force by the filaments following oxidation, modifications on actin are sufficient to affect force and velocity of contraction, and also contribute to a decrease in contractile activity in muscles.

Introduction

Production of excess reactive oxygen species (ROS) and reactive nitrogen species (RNS) reduces the force produced by healthy skeletal muscles (Berlett & Stadtman, 1997; E. Cadenas, 1989; Dean et al., 1997; Persson et al., 2019; Maarten M Steinz et al., 2019), the force in skeletal muscles from animals and patients with rheumatoid arthritis (RA) (Maarten M Steinz et al., 2019; Yamada et al., 2009; Yamada, Steinz, Kenne, & Lanner, 2017), and the contractile function in conditions of heart disease (Durham et al., 2008; J. H. Snook, J. Li, B. P. Helmke, & W. H. Guilford, 2008; Yamada et al., 2009). Sources of ROS/RNS in skeletal muscle include nitric oxide synthase (NOS), NADPH oxidases (NOX), and mitochondria, with various amino acid targets (Ayala, Muñoz, & Argüelles, 2014; Radi, 2012; Maarten M Steinz et al., 2019) in both contractile and noncontractile proteins (Durham et al., 2008; J. H. Snook et al., 2008; Yamada, Fedotovskaya, et al., 2015).

Muscle contraction depends on the interaction between myosin and actin filaments (A. F. Huxley & Niedergerke, 1954; H. Huxley & Hanson, 1954). Given the complexities of actin-myosin arrangements within sarcomeres and muscle fibers, the specific contributions of actin and myosin oxidation on the cross-bridge cycle and, ultimately, force production remain unknown (Balta, Kramer, & Samstag, 2020; Prochniewicz, Spakowicz, et al., 2008). Myosin has been regarded as the primary target in force loss in aging and disease due to its catalytic activity (Coirault et al., 2007; Prochniewicz, Spakowicz, et al., 2008; L. V. Thompson et al., 2006; Yamada et al., 2006) and has been broadly studied, given the potential for therapeutics in cardiac disease (Eaton et al., 2002; Hong et al., 2007; Kanski, Behring, et al., 2005; Michael J Mihm et al., 2003; M. J. Mihm, Yu, Weinstein, Reiser, & Bauer, 2002). Exposure of purified myosin S1 to the chemical 5-amino-3-(4-morpholinyl)-1,2,3-oxadiazolium chloride (SIN-1), an NO and O₂⁻ donor, results in partial denaturation and inhibition of ATPase activity (Teresa Tiago et al., 2006). Furthermore, it has been shown that peroxynitrite treatment of rat cardiac myosin results in an up to 60% decrease in myosin-induced actin motility, indicating an impairment in actin-myosin interaction (J. H. Snook et al., 2008).

Actin also contributes to oxidation-induced impairment in contractility. We have recently observed that treatment with SIN-1 decreases actin polymerization rate and myofibrillar force in mice

(Maarten M Steinz et al., 2019). The key residues subjected to SIN-1 exposure decreased actin flexibility, intramolecular bonding, and stability (Maarten M Steinz et al., 2019), suggesting that changes in actin structure may be responsible for the decreased force production at the molecular level. In addition, *S*-nitrosocysteine modifications on smooth, skeletal, and nonmuscle actin showed a comparably reduced motility across conditions (Bansbach & Guilford, 2016). We also showed that both SIN-1 and peroxynitrite significantly reduce force production in single myofibrils (Persson et al., 2019).

In this study, we investigated the effects of actin and myosin oxidation on actin sliding and force produced by the myofilaments. We measured *I*) the F-actin sliding velocity over heavy meromyosin (HMM) using an in vitro motility assay (IVMA) and *II*) the force production by thick and thin filaments, using a cantilever-based filament force measurement system (FFMS) (Kalganov, Novinger, & Rassier, 2010; A. Kalganov et al., 2013). Assessing forces in filaments is of particular interest, as previous studies on oxidation have been done for the whole tissue or skinned muscle fibers (Dutka et al., 2011; G. D. Lamb & Posterino, 2003; Prochniewicz, Lowe, et al., 2008; Prochniewicz, Spakowicz, et al., 2008; Yamada et al., 2009) or single myosin molecules (Bansbach & Guilford, 2016; M. Fedorova, Kuleva, & Hoffmann, 2010; Greenberg & Moore, 2010; Passarelli et al., 2010; Passarelli et al., 2008; J. H. Snook et al., 2008), but never with an experimental system that allows force measurements with the motors working cooperatively, without the confounding effects of other sarcomeric components, essential for our understanding of myosin-actin interactions (Albet-Torres et al., 2009; Y.-S. Cheng, de Souza Leite, & Rassier, 2020; Y.-S. Cheng, Matusovskiy, & Rassier, 2019; Kalganov et al., 2010). We observed that the motile velocity of actin propelled by myosin decreased when each of these proteins was oxidized. Intriguingly, the combined decrease in velocity when both proteins were oxidized was greater than the sum of individual decreases from actin and myosin oxidation alone. We also observed that the filament forces were reduced when either thick or thin filaments were oxidized. Altogether, these results show that oxidation of both myosin and actin affects contractile events at the molecular levels, which may ultimately lead to a decrease in force generation in skeletal muscles.

Methods

The ethical protocol for use of animal material was approved by the Animal Care Committee at McGill University (Ref. No. MCGL-5227) and the Canadian Council on Animal Care.

Two different myosin filaments were used in this study: native thick filaments isolated from the anterior byssus retractor muscle (ABRM) of *Mytilus edulis* (mussel) and native thick filaments isolated from the psoas muscle from rabbits. They were isolated according to standard procedures performed in our laboratory (Cornachione et al., 2014; Kalganov et al., 2010; Albert Kalganov et al., 2013).

New Zealand white rabbits (female, 2.6–2.7 kg, 11–12 wk) were purchased from Charles River Laboratories (QC, Canada). On the day of sample collection, the animals were killed by barbiturate overdose. An incision of ~20 cm was made in the mid-section of the animals' belly using a sharp scalpel (No. 10 surgical blade equipped; FEATHER). The psoas was identified, and strips of the muscle (~3 mm in diameter and ~5 cm in length) were dissected using surgical tweezers (No. 5 fine-needle sharp; Sigma-Aldrich). The muscle strips were tied in 6" applicator sticks (Fisher) with black braided silk (2-0, SP118, LOOK) and stored on ice at -4°C in rigor solution. Approximately 6 h after extraction, the muscle samples were transferred to a mixed solution containing rigor/glycerol (50%/50%) and stored at -20°C. On the day of the experiment, the sample was defrosted at 4°C in rigor solution for 30 min. Then, the samples were left in a relaxing solution [100 mM KCl, 10 mM PIPES (pH 7.0), 10 mM MgCl₂, 2 mM EGTA, 10 mM ATP, and 2 mM DTT] for 1 h, before being diced into thin strips and homogenized on ice (SNMX 1092, OmniInc) at 2°C for 30 s, with 1-min intervals. The homogenate was centrifuged (5804 R, Eppendorf) at 4,500 g for 30 min to remove undamaged myofibrils and other contaminants.

Mussels (*Mytilus edulis*) were purchased from a local seafood market (Poissonnerie La Mer, QC) and brought to the laboratory on the day of filament extraction. They were dissected by using a scalpel (No. 10 surgical blade equipped; FEATHER) and washed with rigor solution [50 mM Tris, 100 mM KCl, 2 mM MgCl₂, and 1 mM EGTA (pH 7.0)]. The filaments were teased apart and isolated by using surgical tweezers (No. 5 fine-needle sharp; Sigma-Aldrich), and anterior byssus

retractor muscles (ABRMs) were isolated from fresh *Mytilus edulis* by cutting with micro-dissecting scissors (size 4, curved, sharp point stainless steel). After extraction, the samples were stored on ice at 4°C in rigor solution. After 24 h, these muscles were transferred to a mixed solution containing rigor/glycerol (50%/50%) and stored at -20°C.

Myosin and HMM Preparation for IVMA

Skeletal muscle myosin was isolated from the rabbit psoas samples using a known protocol (Margossian & Lowey, 1982). In summary, 5 g of muscle was homogenized in 15 mL of Hasselbalch–Schneider buffer (0.1 M KH₂PO₄/K₂HPO₄ at pH 6.4; 0.6 M KCl, 10 mM Na₄P₂O₇·10H₂O, 1 mM MgCl₂, and 20 mM ethylene glycol tetra-acetic acid) using an Omni mixer homogenizer (Omni International, Inc., GA). The solution was stirred at 4°C for 15 min, and the reaction was stopped with the addition of 20 mL of 4°C distilled water. The mixture was centrifuged at 3,000 g (5804 R, Eppendorf AG, Hamburg, Germany) for 10 min, and the myosin supernatant was passed through a 55-mm hardened circle filter paper (No. 54, GE Healthcare, IL). The filtrate was diluted with 4°C distilled water and centrifuged at 10,000 g for 15 min. The pellet was washed with buffer B [20 mM K₂HPO₄ at pH 7.2; 0.12 M KCl; 1 mM EDTA; and 1 mM dl-dithiothreitol (DTT)], resuspended in buffer C (50 mM sodium pyrophosphate and 1 mM DTT at pH 7.8), and centrifuged at 10,000 g for 10 min. The supernatant was filtered through No. 54 filter paper (Whatman, GE), and the myosin solution was either stored in a glycerol solution in a -80°C freezer or stored for HMM preparation (Salhotra et al., 2021).

An imidazole-based method for HMM preparation was adapted from previous studies (Kron, Toyoshima, Uyeda, & Spudich, 1991a; Okamoto & Sekine, 1985). Nine volumes of buffer solution (0.1 M imidazole hydrochloride, 0.1 mM EGTA, and 2 mM DTT added after setting to pH 7.0) was added to a centrifuge tube with 21 mg of stock myosin solution, mixed slowly to precipitate myosin filaments, and then left on ice for 10 min. The solution was centrifuged at 15,000 g for 60 min at 4°C. The pellet was dissolved in buffer (20 mM imidazole hydrochloride, 1 M KCl, 4 mM MgCl₂, and 10 mM DTT added as before) 2× to obtain a final concentration of 15 mg/mL myosin in buffer. The myosin solution was then incubated in a shaking water bath at 25°C for 5 min. Then, 1 mg/mL chymotrypsin was added to the myosin to a final concentration of 12.5 µg/mL, and this mixed solution was set in a water bath for 10 min at 25°C. Seven microliters of 0.2 M stock PMSF protease inhibitor and 12.6 mL of cold buffer were added to the solution and gently mixed. The

mixture was left on ice for up to 1 h and then centrifuged at 15,000 g for 60 min at 4°C. At this stage, the myosin was pelleted, and HMM was recovered from the supernatant. The HMM concentration was determined via the Bradford assay (Bradford, 1976)(Bio-Rad, CA). Sucrose was added to aliquots of HMM in Eppendorf tubes to a final concentration of 2 mg/mL, frozen in liquid nitrogen, and stored at -80°C.

Myosin Isolation for Force Measurements

For force measurements, fresh thick myosin filaments were isolated from the anterior byssus reactor muscle of *Mytilus edulis* (mussel) according to an established protocol (Kalganov et al., 2010). Briefly, pairs of byssus reactor muscles were quickly excised from fresh mussels and immediately placed in a thick filament buffer solution [10 mM PIPES (pH 7.0), 10 mM MgCl₂, 2 mM EGTA, 10 mM ATP, 2 mM DTT]. Muscle bundles were manually separated into thin strips, which were then homogenized (SNMX 1092, Omni Inc., GA) three times for 7 s, with 1-min intervals, and then placed on ice. The muscle homogenate was mixed with an equal volume of the thick filament buffer solution containing 0.1% Triton X-100 and left on ice for 15 min. The homogenate was precipitated in a centrifuge at 700 g for 5 min, and the pellet was discarded. The supernatant was further centrifuged at 4,500 g for 40 min, and pelleted filaments were resuspended in the thick filament buffer. Centrifugation steps were repeated, and thick filaments were resuspended in an ATP-free buffer solution.

F-actin Preparation

Actin was extracted from rabbit psoas and isolated according to a modified protocol (Pardee & Spudich, 1982). Briefly, actin was purified in 10 mL of fresh G-actin buffer (2 mM imidazole, 0.2 mM Na₂ATP, and 0.2 mM CaCl₂) per gram of acetone powder. The solution was stirred for 30 min on ice and filtered through four layers of cheesecloth. The liquid was further extracted with 10 mL of G-actin buffer per gram of acetone powder and stirred for 10 min at 0–0.5°C. Filtrates were centrifuged at 20,400 g for 20 min at 4°C and passed through a cheesecloth, and pellets were discarded. The supernatant was then dissolved in 50 mM MgCl₂, and actin filaments were polymerized with the addition of 0.2 mM ATP. The solution was left for 1 h at room temperature while KCl was slowly added to a final concentration of 0.8 M. The solution was stirred again for 10 min and then centrifuged at 12,000 g for 1 h at 4°C. The supernatant was discarded. Actin

concentration of 7 μM was determined using $E = 0.63 \text{ mL/mg} \times \text{cm}$, where E is the molar extinction coefficient. E is used to calculate the concentration of solute by measuring absorbance at 290 nm (Houk Jr & Ue, 1974). The product purity was determined using 10% SDS-PAGE. HMM and polymerized actin filaments (F-actin) were frozen in liquid nitrogen in the presence of 2 mg/mL sucrose and stored at -80°C , ideal conditions for long-time storage (Balaz & Månsson, 2005).

SIN Modification of F-actin and Myosin

F-actin was treated with SIN-1 and hydrochloride (Sigma-Aldrich, MO) according to a protocol outlined elsewhere (Maarten M Steinz et al., 2019). Briefly, 10 μM SIN-1 was added to tubes containing 7 μM F-actin and a labeling buffer (10 mM MOPS at pH 7.0, 0.1 mM EGTA, 3 mM NaN_3 , 60 mM KCl, and 2 mM MgCl_2) and allowed to react for 10 min. The solutions could be used immediately or stored at -80°C . Similarly, 920 $\mu\text{g/mL}$ HMM was combined with 10 μM SIN-1 for 10 min, and reactions were stopped with solution exchange, as done previously (Persson et al., 2019; Maarten M Steinz et al., 2019). For the IVMA, HMM was diluted to 120 $\mu\text{g/mL}$, and imaging was performed immediately after incubation of HMM with the oxidant to reduce variability across experiments. Our use of a MOPS buffer in conjunction with SIN-1 contributed to the formation of H_2O_2 , echoing the reactions observed with HEPES in the literature, which suggests that similar buffers can be oxidized by peroxynitrite to produce H_2O_2 (Kirsch, Lomonosova, Korth, Sustmann, & de Groot, 1998)

F-actin Labeling for IVMA and Filament Force Measurement System

F-actin (7 μM) was labeled with Alexa Fluor-488 phalloidin (A-488) (R415, Invitrogen) at 1:1 actin:A-488 in 10 mM 4-morpholinepropanesulfonic acid (MOPS) buffer at pH 7.0 [60 mM KCl, 2 mM MgCl_2 , 0.1 mM ethylene-bis (oxyethylenenitrilo) tetraacetic acid (EGTA), and 3 mM NaN_3]. The fluorophore was initially left to dry, allowing the methanol to evaporate to concentrate the fluorophore and remove impurities. After ~ 3 h, it was then redissolved in fresh methanol. Using a pipette with a scissor-cut end to reduce actin shear, F-actin was slowly added to a separate tube with labeling buffer to 20 μM and placed on ice. Labeling buffer was added to the fluorophores, vortexed, and centrifuged, and the concentrated F-actin in the labeling buffer was added to the tube with the fluorophore, resulting in a 2 μM final solution. The solution was left on ice in the dark for 6 h or overnight and could be stored for 2–4 wk.

In Vitro Motility Assay

Motility experiments were run at $\sim 23^{\circ}\text{C}$ and performed as described previously (Rahman, Salhotra, & Månsson, 2018). Glass coverslips ($60 \times 24 \text{ mm}^2$, No. 0, Menzel-Glaser, Braunschweig, Germany) were soaked in 70% EtOH overnight, dried, and coated with 1% nitrocellulose to create an isotropic and nonspecific binding surface for HMM attachment (Kron, Toyoshima, Uyeda, & Spudich, 1991b). Nitrocellulose was chosen because it can be easily applied manually on coverslips. Furthermore, varying amounts of nitrocellulose (0.25–2.1 μL) have been shown to have no effect on motility speed, motile fraction, or the quality of filament movement (Kron et al., 1991b; Sundberg et al., 2003). Flow cells were constructed using double-sided adhesive tape to build a fluid chamber between a nonfunctionalized small coverslip ($20 \times 20 \text{ mm}^2$) and a large coverslip ($60 \times 24 \text{ mm}^2$). During experiments, one coverslip was used for each condition and sampled at least five times in different regions on the coverslip. The in vitro motility assay was performed by slowly adding 60 μL volumes of the following solutions to the side of the flow chamber in the following order: 1) HMM (120 $\mu\text{g}/\text{mL}$) diluted to 60 $\mu\text{g}/\text{mL}$ in L65 solution [low ionic strength solution (LISS), composed of 1 mM MgCl_2 , 10 mM MOPS, 0.1 mM K2EGTA, pH 7.4, 1 M KCl, and 15 mM DTT], 2) bovine serum albumin (BSA, 1 mg/mL) in LISS, 3) L65, 4) fluorescently labeled actin diluted to 10 nM in L65, 5) L65, and 6) assay solution (15 mM LISS, 1 mM MgATP, 10 mM DTT, 0.64% methylcellulose, 130 mM KCl, 3 mg/mL glucose, 0.1 mg/mL glucose oxidase, 0.02 mg/mL catalase, 2.5 mM phosphocreatine, and 0.2 mg/mL creatine kinase). The coverslip and sliding actin filaments were imaged using an inverted darkfield fluorescent microscope, specifically an Axio Observer D1 by Zeiss (Jena, Germany) or an Eclipse TE300 by Nikon (Tokyo, Japan), equipped with a 100x plan-apochromat objective (1.4 N.A.) for high-resolution imaging. The resolution of the microscope using this 100x objective is approximately 185.36 nanometers, calculated based on the emission wavelength of the fluorescent dye used, Alexa Fluor 488, which has an emission peak at around 519 nanometers. Our specifications effectively limit our resolution to the standard resolution limit of 200 - 250 nanometers, demonstrating that we have the necessary resolution to distinguish between sliding, which are micrometers apart. Analyzed images were taken at $1,200 \times 1,200$ pixels and 110 nm/pixel using the 100x objective. Fluorescence microscopy was used to image actin filaments with a filter set for Alexa-488 (Exciter ET470/40x, Dichroic T495LP, Emitter ET525/50m; Chroma), corresponding to the excitation and emission wavelengths of the Alexa Fluor 488 dye. Images

were captured using a Prime 95B Scientific CMOS (sCMOS) with 95% QE, 11 μm x 11 μm pixel area (Teledyne, AZ, USA). The frame rate was 10 fps and exposure was 50 ms. MatLab software (MatLab R2017b; MathWorks, Natick, MA) (Ijpma, Balassy, & Lauzon, 2018) was used to obtain velocity of filament sliding. After a short \sim 1–2-min incubation, videos were acquired as quickly as possible, within 5 min of placing assay solution on the coverslip, to avoid increasing variance in motility over time. Immobile actin filaments as well as those with aberrant start and stop motion were excluded from analysis based on criteria as outlined elsewhere (Månsson & Tågerud, 2003; Rahman, Salhotra, et al., 2018). All filament velocities (\sim 50–100 filaments per frame) were averaged per frame. All frame averages were then compiled over the length of the video, which lasted \sim 45 sec, resulting in an n of the number of videos per treatment as opposed to other methods which rely on the number of filaments to derive sliding velocities.

We performed a series of experiments with antioxidant cocktails, in which we doubled the antioxidant concentration already used for the IVMA, namely 0.4 mg/mL catalase, to check for reversibility of oxidation.

Filament Force Measurement System

Myosin and Alexa-488-labeled actin filaments (Exciter ET470/ \times 40, Dichroic T495LP, Emitter ET525/50 m, Chroma) were visualized using darkfield microscopy (Kalganov et al., 2010). Images were captured with a Rolera-MGi Plus video camera (QImaging, Canada) and recorded using Streampix6 software (Norpix, Canada; pixel size: 120 nm; rate: 50 fps). Microfabricated cantilevers created from silicon nitride using a photolithography process were used to measure the force between actin and myosin filaments, as previously detailed (Kalganov et al., 2010). Cantilever tips were gold coated in a 50-nm layer to maximize optical contrast. Cantilevers were 550 μm long, 1.0 μm wide, and 0.6 μm thick, and stiffnesses were made to match forces produced by filaments. Cantilever stiffness was determined by the resonance frequency detection method (0.18 pN/nm) (Fauver, Dunaway, Lilienfeld, Craighead, & Pollack, 1998). Stiffnesses obtained with this method were averaged over the length of the cantilever. Cantilevers were glued to the bottoms of metal holders, which were connected to micromanipulators, allowing for three-dimensional movement within the experimental chamber.

Left and right cantilevers were driven through the experimental chamber using two separately controlled manual piezo motors and brought 10–15 mm apart under the view of a $\times 100$ objective. The right cantilever was placed in myosin buffer (75 mM KCl, 2 mM MgCl₂, 10 mM EGTA, 10 mM PIPES, 10 mM ATP, and 2 mM DTT, pH 7.0), allowing it to spontaneously attach myosin filaments, and the left cantilever was immersed in α -actinin solution (25 mM imidazole-HCl, pH 7.4, 25 mM KCl, 4 mM MgCl₂, 1 mM EGTA, and 1 mM DTT) and allowed to sit for 10 min. α -Actinin is an actin filament crosslinker and has a high affinity of binding to actin so it is used to anchor actin to the left cantilever (Luther, 2009). A constant flow of actin buffer/BSA/glucose oxidase/ATP solution (0.5 mg/mL BSA, 0.018 mg/mL catalase, 0.1 mg/mL glucose oxidase, 3 mg/mL glucose, 20 mM DTT, and 50 μ M ATP) was passed through a syringe pump (Pump 33, Harvard Apparatus) at 0.5 mL/min to wash away unbound α -actinin and myosin filaments. After incubation, cantilevers repositioned within micrometers to allow filament interaction.

Thick filaments from blue mussels were isolated 1–2 days before the experiments (A. Kalganov et al., 2013). Fluorescently labeled actin filaments (2 nM) from rabbit psoas used in IVMA experiments were injected into the flow chamber and allowed to passively attach to α -actinin on the left cantilever. Near-perpendicular attachment of actin to the cantilever was facilitated by constant chamber flow. Filaments attached near the tips of the cantilevers (<50 μ m) were brought near each other. Once near enough, filaments interacted, and thick filaments produced a force on the actin filaments and displaced the left cantilever. Displacement was tracked using ImageJ as previously described (Kalganov et al., 2010; A. Kalganov et al., 2013). Force (F) was calculated from $F = k \times \Delta d$, where k is the stiffness of the cantilever and Δd is its displacement. The full force was calculated from the vector components of force using the equation $F = F_x + F_y$, where F_x and F_y are the vectors as the horizontal force component and the vertical force component, respectively. Cantilever displacement videos were analyzed by contour tracking using ABSnake algorithm on ImageJ (Andrey & Boudier, 2006). Contours were used to determine object centroids, which would then allow for displacement calculations of the cantilevers.

Statistical Analysis

All results were analyzed, and graphs were generated using GraphPad Prism (version 8.0, GraphPad software, CA). Comparisons between groups were performed using one-way analysis

of variance (ANOVA). A significance level of $P < 0.05$ was regarded as significant in all analyses. All data are reported as means \pm standard error of the mean (SE).

Results

The IVMA was used to determine whether there were differences between the velocity of actin filaments sliding over HMM before and after treatment with SIN-1. HMM, F-actin, or both were treated with 10 μM SIN-1 for 10 min (Maarten M Steinz et al., 2019). We observed a decrease in motility when either actin or HMM was oxidized with SIN-1 (Fig. 1). There was an $\sim 10\%$ decrease in sliding velocity when actin was oxidized and an $\sim 16\%$ decrease in sliding velocity when HMM was oxidized. Interestingly, there was an $\sim 40\%$ decrease in sliding velocity when both HMM and actin were oxidized (Fig. 1, A, B). We also compared the relative motile fractions of actin filaments that were moved by the HMM molecules. The results were not statistically different among conditions (Fig. 1C), suggesting that oxidation does not affect the overall quality of the filament preparations in the IVMA. Thus, the decreased velocity of actin is a result of altered myosin-actin interactions. Sample videos collected during the experiments showing the myosin-driven motility of actin under all conditions can be seen in the Supplemental Materials.

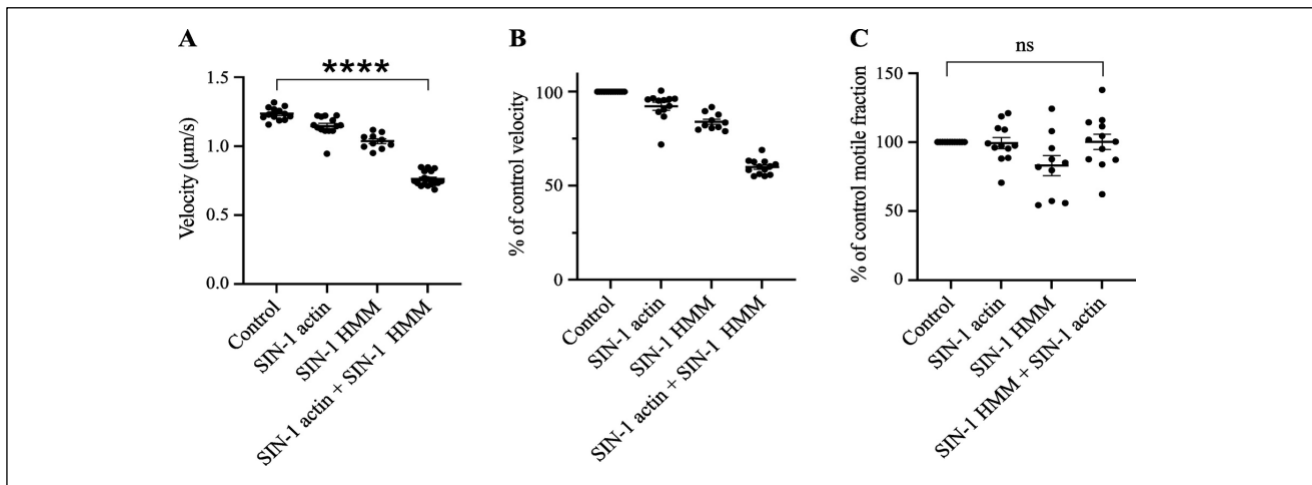


Figure 1. Myosin-propelled actin sliding velocities. A: comparison between control and SIN-1 oxidized actin filament and HMM in the IVMA. There was a significant decrease for SIN-1-treated actin ($n = 14$), SIN-1-treated HMM ($n = 10$), and SIN-1-treated actin + HMM ($n = 10$, videos) ($P < 0.01$) when compared with untreated filaments ($n = 13$, videos). B: relative decrease in motility velocity relative to control experiments. There was an $\sim 10\%$ decrease when actin was oxidized and a 15% decrease when HMM was oxidized. When both actin and HMM were oxidized, there was a 55% decrease in velocity. C: motile fractions were similar between control ($n = 12$, videos), SIN-1 actin ($n = 13$), SIN-1 HMM ($n = 10$), and SIN-1 actin + SIN-1 HMM ($n = 17$) ($P = 0.09$). All values are shown as means \pm SE. HMM, heavy meromyosin; IVMA, in vitro motility assay; SIN-1, 5-amino-3-(4-morpholinyl)-1,2,3-oxadiazolium chloride.

To check whether the preparations were affected by oxidation in a reversible manner, we performed some additional experiments to verify if the motility returned to the base level with antioxidant treatment. In fact, when we introduced catalase to the experimental chamber, the velocity returned to control levels (Fig. 2). It should be noted that photooxidative damage may also contribute to velocity decrease over time. Assuming that photooxidative damage was the primary driver for the decreased motility, we would expect to see a decrease in motility in control filaments over time. In our experiments, the filament velocity decreased by ~24% over 15 min. However, with the addition of SIN-1, there was a greater relative loss of ~42% after the same period of 15 min. When excess catalase was added, in both cases, the loss of motility was prevented, indicating that, although sources of oxidation are indistinguishable, about half of the scavenged radicals are from SIN-induced oxidation.

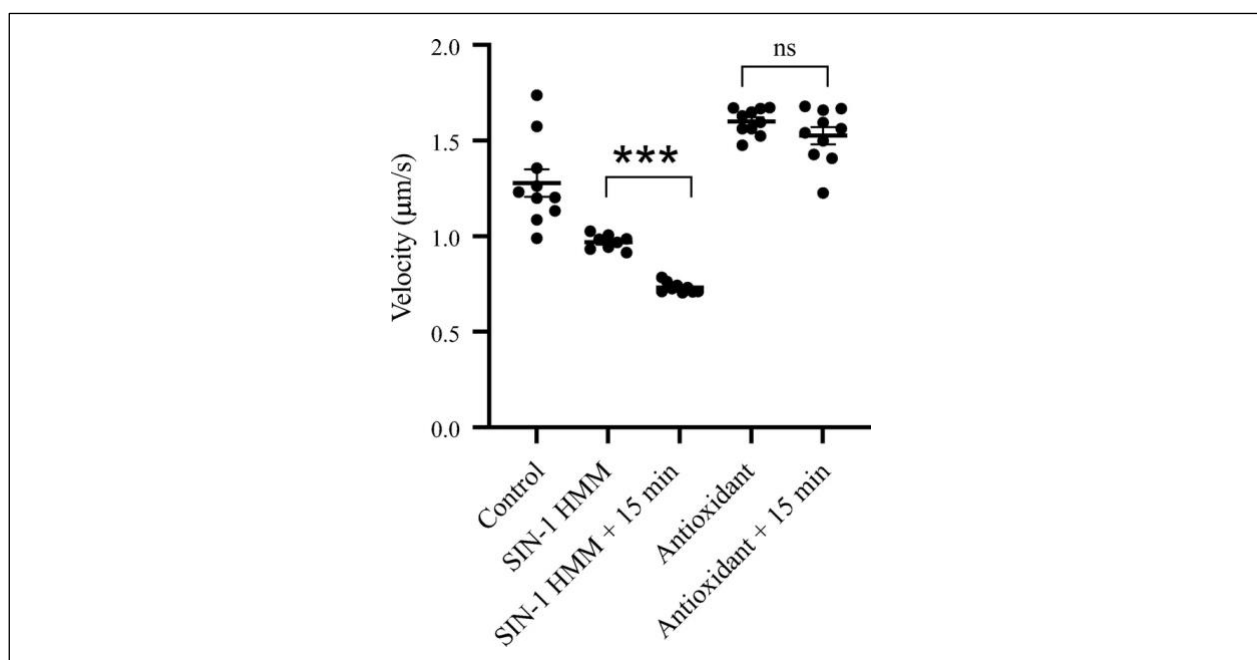


Figure 2. The effects of antioxidant in the myosin-propelled actin sliding. HMM was incubated with SIN-1 ($n = 10$). After initial imaging, the proteins were left on the coverslip in the dark for 15 min and the velocity decreased ($P < 0.001$). Catalase was added, and videos were taken 15 min later. At this point, velocity of actin motility was restored with values that were not statistically different from control ($P = 0.02$). Another 15-min period did not change the results ($P = 0.152$), and the velocity remained similar to control levels. All values are shown as means \pm SE. HMM, heavy meromyosin; SIN-1, 5-amino-3-(4-morpholinyl)-1,2,3-oxadiazolium chloride.

The FFMS developed in our laboratory (Kalganov et al., 2010; A. Kalganov et al., 2013) was used to investigate the force generated between actin and myosin filaments under oxidizing conditions (Fig. 3). The system uses microfabricated cantilevers of known stiffness that allow the simultaneous measurement of forces and the visualization of filaments (Fig. 3A) (A. Kalganov et al., 2013). Filaments on parallel cantilevers were brought together by a piezo manual control (Kalganov et al., 2010; A. Kalganov et al., 2013), and as filaments interacted, the displacement of the cantilevers was measured (Fig. 3A). SIN-1-treated actin filaments developed forces that were

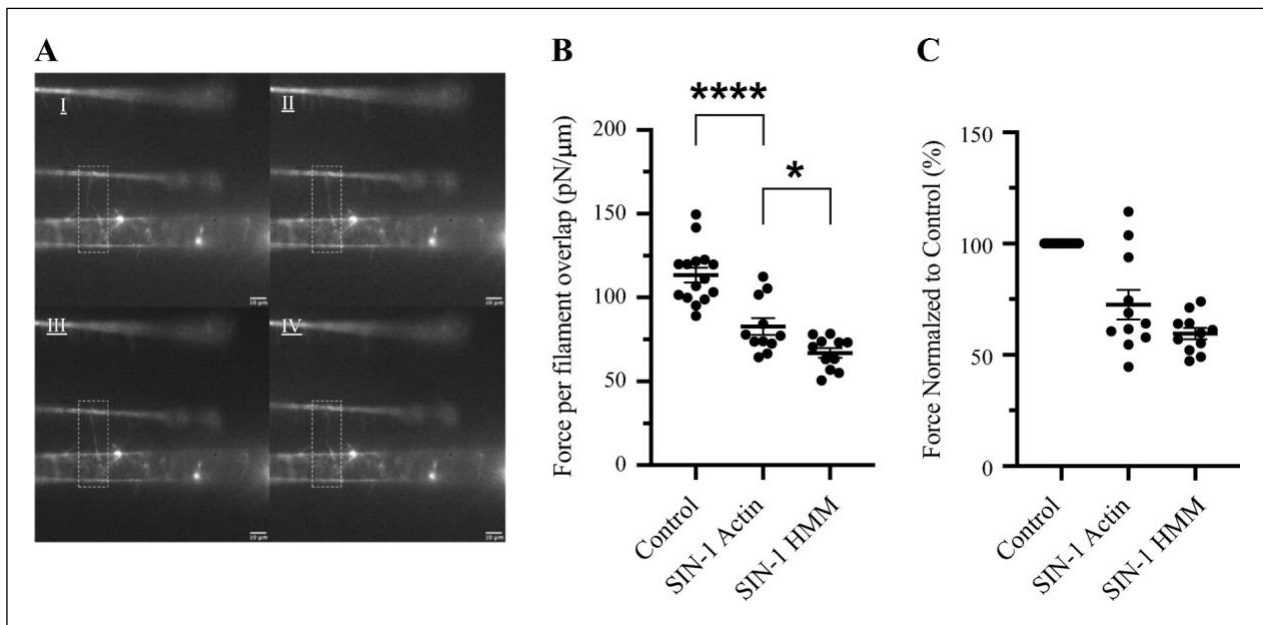


Figure 3. Filament force measurement in control and SIN-1-treated filaments. A: representative images of thick and thin filaments attached to the cantilevers. I) filaments are separated before actin-myosin interaction (boxed area). II): cantilevers are brought closer together, and actin and myosin interact. III): myosin filaments exert force on actin filaments, bending the cantilever. IV): actin-myosin interaction is disrupted when the filaments detach. B: there was a decrease in force observed in SIN-1-treated actin filaments (82.75 pN/μm, n = 11) and SIN-1-treated thick filaments (66.98 pN/μm, n = 11) when compared with control filaments (113.4 pN/μm, n = 15) (P = 0.0001). Scale bars: 10 μm. All values are shown as means ± SE. SIN-1, 5-amino-3-(4-morpholinyl)-1,2,3-oxadiazolium chloride.

~27% lower than control filaments when interacting with myosin filaments. SIN-1-treated thick filaments developed forces that were ~40% lower than the force produced by control thick filaments (Fig. 3B).

Sample videos collected during the experiments showing the myosin-actin interaction and force developed by the filament in all conditions can be seen in the Supplemental Materials.

Discussion

In this study, we observed that SIN-1 treatment of actin and HMM led to a decreased myosin-propelled sliding velocity of actin and a decreased force generation during interactions between myosin and actin filaments. These results show that oxidation is an important modulator of myosin-actin interactions, and, consequently, force generation in skeletal muscles, supporting a growing body of literature indicating that oxidative modification causes a significant impact on striated muscles (Bansbach & Guilford, 2016; J. H. Snook et al., 2008; Maarten M Steinz et al., 2019; Yamada, Fedotovskaya, et al., 2015; Yamada et al., 2009).

A previous study has shown that oxidation of actin does not affect the force produced by individual myosin molecules, investigated in the laser trap assay (Bansbach & Guilford, 2016). In our study, we instead used a system in which myosin molecules work in filaments, mimicking what happens at the sarcomere level (Y.-S. Cheng et al., 2020). When only actin was oxidized, the average forces produced during myosin interactions with control and oxidized actin filaments were 113.4 pN/ μm and 82.75 pN/ μm of filament overlap, respectively, or 0.11 pN/nm and 0.083 pN/nm. Assuming that there is one myosin cross bridge per 14.5 nm of thick/thin filament overlap (Gordon, Homsher, & Regnier, 2000), the filaments would have produced ~1.62 pN and ~1.18 pN per myosin bound to actin, respectively, if all cross bridges were attached to actin. Given that ~30% of cross bridges between filaments contribute to force production at a given time (Linari, Caremani, Piperio, Brandt, & Lombardi, 2007), we recorded a value of ~5.4 pN of force produced per myosin when interacting with untreated actin, a value that is within results observed in laser trap experiments, which report values between 5 and 7 pN (Finer, Simmons, & Spudich, 1994; Molloy, Burns, Kendrick-Jones, Tregear, & White, 1995). As the force produced per cross bridge in our

experiments is likely unaffected by actin oxidation, a decrease in force to ~ 3.59 pN when myosin interacted with oxidized actin filaments suggests that few myosin cross bridges are bound to actin at a given time during force generation. This could be obtained by a reduced number of transitions from cross bridges from the weak to the strong attachment states (Bansbach & Guilford, 2016; Y.-S. Cheng et al., 2019; Wulf et al., 2016). In the case where myosin is oxidized, the average force obtained by the filaments was 66.98 pN/ μm or 0.067 pN/nm. Maintaining the aforementioned assumptions, this value would result in a force of 3.19 pN per myosin molecule bound to actin. We have previously observed that oxidation of whole myofibrils resulted in a 50% decrease in isometric force independent of the number of cross bridges attached to actin, suggesting a possibly different mechanism when myosin is the sole target of oxidation (Persson et al., 2019). Thus, the exact mechanism of force loss when myosin is oxidized needs further investigation.

We previously suggested that the force loss induced by SIN-1 in skeletal muscle myofibrils was accompanied by an increase in the rate of the linear relaxation phase upon deactivation, which reflects the transition from force-generating to non-force-generating cross bridges (Persson et al., 2019). The velocity of actin in the IVMA is described by $V_{actin} = d * t_{on}$, where the actin velocity (V) depends on the distance actin moves in a single myosin step (d) and is inversely related to the time myosin is attached to actin (t_{on}). The increase in cross-bridge detachment rate in myofibrils would imply a decrease in t_{on} in the IVMA and thus an increased sliding velocity. Yet, we observed a decrease in sliding velocity when either actin or myosin was oxidized. The reason these results are not easily accommodated is not clear, but the difference is likely due to the different preparations and experimental conditions. There are difficulties in translating results across single molecules in vitro and in filamentous assemblies of myosin and actin. For instance, cooperative effects play a role in speeding up ADP release and increase the actin translocation depending on the number of myosin molecules bound per actin (Stewart et al., 2021; Walcott, Warshaw, & Debold, 2012). Furthermore, it is known that a residue's susceptibility to oxidation depends on its exposure, where deeper residues with brief exposure are less likely to become oxidized than surface residues (I. Dalle-Donne et al., 2003; I. Dalle-Donne et al., 2002; Maarten M Steinz et al., 2019). For example, a study showed that S-nitrosylation of cardiac myosin and rat skeletal myosin in fact increased the force of single myosin molecules (Evangelista et al., 2010), although this effect may be a unique response to endogenous NO donors, suggesting that different sources of oxidation have different effects on contractility. Even if studies performed at different levels of

analyses do not yet provide a full picture of the effects of oxidation in skeletal muscles, the reductionist approach that we used in this study is important, as it shows that oxidation of the molecular components—myosin and actin—may cause contractile dysfunction.

It has been suggested that a small number of residues with high susceptibility to oxidation can cause force loss (Prochniewicz et al., 2007). For example, it has been shown that inhibition of the subfragment 1 (S1) ATPase in human muscles is primarily caused by oxidation of critical myosin sulfhydryl groups, Cys-707 SH1 and Cys-697 SH2 (Dutka et al., 2011; Gross & Lehman, 2013; Teresa Tiago et al., 2006). These residues are located near each other in the S1 catalytic domain of myosin, which undergoes significant structural change during ATP hydrolysis (Cheung et al., 1991; Kirshenbaum et al., 1993). SH1 and SH2 stabilities in forming a complex with MgATP have been shown to be critical for regulating ATPase function. Actin has been shown to activate this ATPase complex by binding at the SH1 site, disrupting the cyclic SH1 SH2 MgATP complex, and releasing inhibition of ATP hydrolysis. When SH1 and SH2 are altered, actin becomes nonmotile in the IVMA (Bobkova et al., 1999), and SH2 modification was shown to directly alter cross-bridge kinetics (Bell, Matta, Thomas, & Goldman, 1995). Oxidation of Cys-707 and Cys-697 may interfere with shifts in the catalytic intermediate $S1 \cdot Mg^{2+} \cdot ADP \cdot Pi$ state during the cross-bridge cycle. In another study, concentrations of $\geq 100 \mu M$ SIN-1 or a flux of $1 \mu M/min$ SIN-1 was shown to partially unfold S1 at physiological temperatures (Teresa Tiago et al., 2006). SIN-1 oxidation can also cause conformational changes in the myosin lever arm that are critical for force generation during myosin-actin interactions (Fisher et al., 1995a; Holmes, 1997; Rayment et al., 1993). Therefore, there are different mechanisms by which oxidation of myosin can affect force production and determining the relationship between *in vitro* oxidation on myosin and *in vivo* whole muscle impairment is difficult, given the high number of amino acid modifications (Kirsch et al., 1998; Tien, Berlett, Levine, Chock, & Stadtman, 1999). Nevertheless, our study shows that oxidation of actin and myosin has significant implications for contractile activity, as they affect the myosin-actin interactions at the molecular level with a highly significant disruption when there is oxidation of both myosin and actin.

SUPPLEMENTAL DATA

Supplemental Video 1: <https://doi.org/10.6084/m9.figshare.20304075.v1>

Supplemental Video 2: <https://doi.org/10.6084/m9.figshare.20304354.v1>

Supplemental Video 3: <https://doi.org/10.6084/m9.figshare.20304372.v1>

Supplemental Video 4: <https://doi.org/10.6084/m9.figshare.20304378.v1>

Supplemental Video 5: <https://doi.org/10.6084/m9.figshare.20304402.v1>

Supplemental Video 6: <https://doi.org/10.6084/m9.figshare.20304408.v1>

Supplemental Video 7: <https://doi.org/10.6084/m9.figshare.20304411.v1>.

Grants

This work was supported by Natural Sciences and Engineering Research Council of Canada (NSERC) Grant 2022-04770 (to D. E. Rassier).

Disclosures

No conflicts of interest, financial or otherwise, are declared by the authors.

Author contributions

D.E. and Y.-S.C. conceived and designed research; D.E. and O.S.M. performed experiments; D.E., Y.-S.C., and O.S.M. analyzed data; D.E., Y.-S.C., O.S.M., and D.E.R. interpreted results of experiments; D.E. prepared figures; D.E. drafted manuscript; D.E. and D.E.R. edited and revised manuscript; D.E., Y.-S.C., O.S.M., and D.E.R. approved final version of manuscript.

ACKNOWLEDGMENTS

The authors thank Dr. Malin Persson, Dr. Alf Mansson, and Dr. Gijs Ipjma for technical assistance during data collection and analysis of this article. The authors thank Chelsea Eng for assistance during initial data collection.

References

- Persson, M., et al., *Force generated by myosin cross-bridges is reduced in myofibrils exposed to ROS/RNS*. American Journal of Physiology-Cell Physiology, 2019. **317**(6): p. C1304-C1312.
- Steinz, M.M., et al., *Oxidative hotspots on actin promote skeletal muscle weakness in rheumatoid arthritis*. JCI insight, 2019. **4**(9).
- Dean, R.T., et al., *Biochemistry and pathology of radical-mediated protein oxidation*. Biochemical Journal, 1997. **324**(1): p. 1-18.
- Berlett, B.S. and E.R. Stadtman, *Protein oxidation in aging, disease, and oxidative stress*. Journal of Biological Chemistry, 1997. **272**(33): p. 20313-20316.
- Cadenas, E., *Biochemistry of oxygen toxicity*. Annu Rev Biochem, 1989. **58**: p. 79-110.
- Yamada, T., et al., *Impaired myofibrillar function in the soleus muscle of mice with collagen-induced arthritis*. Arthritis Rheum, 2009. **60**(11): p. 3280-9.
- Yamada, T., et al., *Muscle Weakness in Rheumatoid Arthritis: The Role of Ca(2+) and Free Radical Signaling*. EBioMedicine, 2017. **23**: p. 12-19.
- Durham, W.J., et al., *RyR1 S-nitrosylation underlies environmental heat stroke and sudden death in Y522S RyR1 knockin mice*. Cell, 2008. **133**(1): p. 53-65.
- Snook, J.H., et al., *Peroxynitrite inhibits myofibrillar protein function in an in vitro assay of motility*. Free Radic Biol Med, 2008. **44**(1): p. 14-23.
- Radi, R., *Protein tyrosine nitration: biochemical mechanisms and structural basis of functional effects*. Accounts of chemical research, 2012. **46**(2): p. 550-559.
- Ayala, A., M.F. Muñoz, and S. Argüelles, *Lipid peroxidation: production, metabolism, and signaling mechanisms of malondialdehyde and 4-hydroxy-2-nonenal*. Oxidative medicine and cellular longevity, 2014. **2014**.
- Yamada, T., et al., *Nitrosative modifications of the Ca²⁺ release complex and actin underlie arthritis-induced muscle weakness*. Annals of the rheumatic diseases, 2015. **74**(10): p. 1907-1914.
- Huxley, A.F. and R. Niedergerke, *Structural Changes in Muscle During Contraction: Interference Microscopy of Living Muscle Fibres*. Nature, 1954. **173**(4412): p. 971-973.

- Huxley, H. and J. Hanson, *Changes in the Cross-Striations of Muscle during Contraction and Stretch and their Structural Interpretation*. Nature, 1954. **173**(4412): p. 973-976.
- Prochniewicz, E., D. Spakowicz, and D.D. Thomas, *Changes in actin structural transitions associated with oxidative inhibition of muscle contraction*. Biochemistry, 2008. **47**(45): p. 11811-11817.
- Balta, E., J. Kramer, and Y. Samstag, *Redox Regulation of the Actin Cytoskeleton in Cell Migration and Adhesion: On the Way to a Spatiotemporal View*. Frontiers in Cell and Developmental Biology, 2020. **8**.
- Yamada, T., et al., *Oxidation of myosin heavy chain and reduction in force production in hyperthyroid rat soleus*. J Appl Physiol (1985), 2006. **100**(5): p. 1520-6.
- Thompson, L.V., et al., *Myosin and actin expression and oxidation in aging muscle*. J Appl Physiol (1985), 2006. **101**(6): p. 1581-7.
- Coirault, C., et al., *Oxidative stress of myosin contributes to skeletal muscle dysfunction in rats with chronic heart failure*. American Journal of Physiology-Heart and Circulatory Physiology, 2007. **292**(2): p. H1009-H1017.
- Eaton, P., et al., *Detection, quantitation, purification, and identification of cardiac proteins S-thiolated during ischemia and reperfusion*. Journal of Biological Chemistry, 2002. **277**(12): p. 9806-9811.
- Mihm, M.J., et al., *Effects of peroxynitrite on isolated cardiac trabeculae: selective impact on myofibrillar energetic controllers*. Biochimie, 2003. **85**(6): p. 587-596.
- Mihm, M.J., et al., *Intracellular distribution of peroxynitrite during doxorubicin cardiomyopathy: evidence for selective impairment of myofibrillar creatine kinase*. Br J Pharmacol, 2002. **135**(3): p. 581-8.
- Kanski, J., et al., *Proteomic identification of 3-nitrotyrosine-containing rat cardiac proteins: effects of biological aging*. American Journal of Physiology-Heart and Circulatory Physiology, 2005. **288**(1): p. H371-H381.
- Hong, S.J., G. Gokulrangan, and C. Schöneich, *Proteomic analysis of age dependent nitration of rat cardiac proteins by solution isoelectric focusing coupled to nanoHPLC tandem mass spectrometry*. Experimental gerontology, 2007. **42**(7): p. 639-651.
- Tiago, T., et al., *Inhibition of skeletal muscle S1-myosin ATPase by peroxynitrite*. Biochemistry, 2006. **45**(11): p. 3794-3804.

- Bansbach, H.M. and W.H. Guilford, *Actin nitrosylation and its effect on myosin driven motility*. AIMS Molecular Science, 2016. **3**(3): p. 426-438.
- Kalaganov, A., et al., *Forces measured with micro-fabricated cantilevers during actomyosin interactions produced by filaments containing different myosin isoforms and loop 1 structures*. Biochim Biophys Acta, 2013. **1830**(3): p. 2710-9.
- Lamb, G.D. and G.S. Posterino, *Effects of oxidation and reduction on contractile function in skeletal muscle fibres of the rat*. J Physiol, 2003. **546**(Pt 1): p. 149-63.
- Prochniewicz, E., et al., *Functional, structural, and chemical changes in myosin associated with hydrogen peroxide treatment of skeletal muscle fibers*. American Journal of Physiology-Cell Physiology, 2008. **294**(2): p. C613-C626.
- Dutka, T.L., J.P. Mollica, and G.D. Lamb, *Differential effects of peroxynitrite on contractile protein properties in fast- and slow-twitch skeletal muscle fibers of rat*. Journal of Applied Physiology, 2011. **110**(3): p. 705-716.
- Fedorova, M., N. Kuleva, and R. Hoffmann, *Identification of cysteine, methionine and tryptophan residues of actin oxidized in vivo during oxidative stress*. J Proteome Res, 2010. **9**(3): p. 1598-609.
- Greenberg, M.J. and J.R. Moore, *The molecular basis of frictional loads in the in vitro motility assay with applications to the study of the loaded mechanochemistry of molecular motors*. Cytoskeleton, 2010. **67**(5): p. 273-285.
- Passarelli, C., et al., *Myosin as a potential redox-sensor: an in vitro study*. Journal of muscle research and cell motility, 2008. **29**(2-5): p. 119-126.
- Passarelli, C., et al., *Susceptibility of isolated myofibrils to in vitro glutathionylation: potential relevance to muscle functions*. Cytoskeleton, 2010. **67**(2): p. 81-89.
- Albet-Torres, N., et al., *Drug effect unveils inter-head cooperativity and strain-dependent ADP release in fast skeletal actomyosin*. Journal of Biological Chemistry, 2009. **284**(34): p. 22926-22937.
- Cheng, Y.-S., O.S. Matusovskiy, and D.E. Rassier, *Cleavage of loops 1 and 2 in skeletal muscle heavy meromyosin (HMM) leads to a decreased function*. Archives of Biochemistry and Biophysics, 2019. **661**: p. 168-177.
- Cheng, Y.-S., F. de Souza Leite, and D.E. Rassier, *The load dependence and the force-velocity relation in intact myosin filaments from skeletal and smooth muscles*. American Journal of Physiology-Cell Physiology, 2020. **318**(1): p. C103-C110.

- Kalaganov, A., R. Novinger, and D.E. Rassier, *A technique for simultaneous measurement of force and overlap between single muscle filaments of myosin and actin*. Biochemical and biophysical research communications, 2010. **403**(3-4): p. 351-356.
- Cornachione, A. S., Leite, F. S., Wang, J., Leu, N. A., Kalaganov, A., Volgin, D., . . . Yates III, J. R. (2014). Arginylation of myosin heavy chain regulates skeletal muscle strength. *Cell reports*, *8*(2), 470-476.
- Margossian, S.S. and S. Lowey, [7] *Preparation of myosin and its subfragments from rabbit skeletal muscle*. Methods in enzymology, 1982. **85**: p. 55-71
- Salhotra, A., et al., *Prolonged function and optimization of actomyosin motility for upscaled network-based biocomputation*. New Journal of Physics, 2021. **23**(8): p. 085005.
- Kron, S.J., et al., [33] *Assays for actin sliding movement over myosin-coated surfaces*, in *Methods in enzymology*. 1991, Elsevier. p. 399-416.
- Okamoto, Y. and T. Sekine, *A streamlined method of subfragment one preparation from myosin*. The Journal of Biochemistry, 1985. **98**(4): p. 1143-1145.
- Bradford, M.M., *A rapid and sensitive method for the quantitation of microgram quantities of protein utilizing the principle of protein-dye binding*. Analytical biochemistry, 1976. **72**(1-2): p. 248-254.
- Pardee, J.D. and J. Spudich, [18] *Purification of muscle actin*. Methods in enzymology, 1982. **85**: p. 164-181.
- Houk Jr, T.W. and K. Ue, *The measurement of actin concentration in solution: a comparison of methods*. Analytical biochemistry, 1974. **62**(1): p. 66-74.
- Balaz, M. and A. Månsson, *Detection of small differences in actomyosin function using actin labeled with different phalloidin conjugates*. Analytical biochemistry, 2005. **338**(2): p. 224-236.
- Rahman, M.A., A. Salhotra, and A. Månsson, *Comparative analysis of widely used methods to remove nonfunctional myosin heads for the in vitro motility assay*. Journal of muscle research and cell motility, 2018. **39**(5): p. 175-187.
- Sundberg, M., Rosengren, J. P., Bunk, R., Lindahl, J., Nicholls, I. A., Tågerud, S., . . . Månsson, A. (2003). *Silanized surfaces for in vitro studies of actomyosin function and nanotechnology applications*. Anal Biochem, *323*(1), 127-138.
- Månsson, A. and S. Tågerud, *Multivariate statistics in analysis of data from the in vitro motility assay*. Analytical biochemistry, 2003. **314**(2): p. 281-293.

- Fauver, M.E., et al., *Microfabricated cantilevers for measurement of subcellular and molecular forces*. IEEE transactions on biomedical engineering, 1998. **45**(7): p. 891-898.
- Luther, P.K., *The vertebrate muscle Z-disc: sarcomere anchor for structure and signalling*. Journal of muscle research and cell motility, 2009. **30**(5-6): p. 171-185.
- Andrey, P. and T. Boudier, *Adaptive active contours (snakes) for the segmentation of complex structures in biological images*. Centre de Recherche Public Henri Tudor Copyright Notice, 2006. **181**.
- Yamada, T., Abe, M., Lee, J., Tatebayashi, D., Himori, K., Kanzaki, K., . . . Lanner, J. T. (2015). *Muscle dysfunction associated with adjuvant-induced arthritis is prevented by antioxidant treatment*. Skeletal muscle, 5(1), 1-10.
- Gordon, A.M., E. Homsher, and M. Regnier, *Regulation of contraction in striated muscle*. Physiological reviews, 2000. **80**(2): p. 853-924.
- Linari, M., et al., *Stiffness and fraction of myosin motors responsible for active force in permeabilized muscle fibers from rabbit psoas*. Biophysical journal, 2007. **92**(7): p. 2476-2490.
- Finer, J.T., R.M. Simmons, and J.A. Spudich, *Single myosin molecule mechanics: piconewton forces and nanometre steps*. Nature, 1994. **368**(6467): p. 113-119.
- Molloy, J., et al., *Movement and force produced by a single myosin head*. Nature, 1995. **378**(6553): p. 209-212.
- Wulf, S.F., et al., *Force-producing ADP state of myosin bound to actin*. Proceedings of the National Academy of Sciences, 2016. **113**(13): p. E1844-E1852.
- Walcott, S., D.M. Warshaw, and E.P. Debold, *Mechanical coupling between myosin molecules causes differences between ensemble and single-molecule measurements*. Biophysical journal, 2012. **103**(3): p. 501-510.
- Stewart, T.J., et al., *Velocity of myosin-based actin sliding depends on attachment and detachment kinetics and reaches a maximum when myosin-binding sites on actin saturate*. Journal of Biological Chemistry, 2021. **297**(5).
- Dalle-Donne, I., et al., *Methionine oxidation as a major cause of the functional impairment of oxidized actin*. Free Radic Biol Med, 2002. **32**(9): p. 927-37.
- Dalle-Donne, I., et al., *Reversible S-glutathionylation of Cys 374 regulates actin filament formation by inducing structural changes in the actin molecule*. Free Radic Biol Med, 2003. **34**(1): p. 23-32.

- Evangelista, A.M., et al., *Direct regulation of striated muscle myosins by nitric oxide and endogenous nitrosothiols*. PLoS one, 2010. **5**(6): p. e11209.
- Prochniewicz, E., Thompson, L. V., & Thomas, D. D. (2007). Age-related decline in actomyosin structure and function. *Experimental gerontology*, *42*(10), 931-938.
- Gross, S.M. and S.L. Lehman, *Accessibility of myofilament cysteines and effects on ATPase depend on the activation state during exposure to oxidants*. PLoS One, 2013. **8**(7).
- Cheung, H.C., et al., *Conformational flexibility of the Cys 697-Cys 707 segment of myosin subfragment-1: distance distributions by frequency-domain fluorometry*. Biophysical chemistry, 1991. **40**(1): p. 1-17.
- Kirshenbaum, K., S. Papp, and S. Highsmith, *Cross-linking myosin subfragment 1 Cys-697 and Cys-707 modifies ATP and actin binding site interactions*. Biophysical journal, 1993. **65**(3): p. 1121-1129.
- Bobkova, Elena A, Andrey A Bobkov, Dmitrii I Levitsky, and Emil Reisler. 1999. 'Effects of SH1 and SH2 modifications on myosin similarities and differences', *Biophysical journal*, *76*: 1001-07.
- Bell, M., Matta, J., Thomas, D., & Goldman, Y. (1995). Changes in cross-bridge kinetics induced by SH-1 modification in rabbit psoas fibers. *Biophysical journal*, *68*(4 Suppl), 360s.
- Holmes, K.C., *The swinging lever-arm hypothesis of muscle contraction*. Current Biology, 1997. **7**(2): p. R112-R118.
- Rayment, I., et al., *Structure of the actin-myosin complex and its implications for muscle contraction*. Science, 1993. **261**(5117): p. 58-65.
- Fisher, A.J., et al., *Structural studies of myosin: nucleotide complexes: a revised model for the molecular basis of muscle contraction*. Biophysical Journal, 1995. **68**(4 Suppl): p. 19S.
- Tien, M., et al., *Peroxynitrite-mediated modification of proteins at physiological carbon dioxide concentration: pH dependence of carbonyl formation, tyrosine nitration, and methionine oxidation*. Proceedings of the National Academy of Sciences, 1999. **96**(14): p. 7809-7814.
- Kirsch, M., et al., *Hydrogen Peroxide Formation by Reaction of Peroxynitrite with HEPES and Related Tertiary Amines IMPLICATIONS FOR A GENERAL MECHANISM*. Journal of Biological Chemistry, 1998. **273**(21): p. 12716-12724.

Bridging text between study 1 and study 2

Having examined the impact of oxidation on actin and myosin interactions and the subsequent effects on muscle contractile activity in Study 1, we turn our attention to the thin filament regulatory proteins in Study 2. Our initial findings showed a significant effect of oxidation on actin-myosin interactions and force generation, emphasizing the importance of oxidation in the major components of the thick and thin filaments.

Far less research has been done on the impacts of oxidation on the thin filament regulatory components. *In vitro* studies have shown that oxidation on troponin proteins results in complex dissociation (Pinto et al., 2011). Interestingly, while some have shown reduced contractility and calcium sensitivity, others have shown the inverse or unknown effects (Gao et al., 2012; D. Polewicz et al., 2011; Prochniewicz, Spakowicz, et al., 2008). Furthermore, research has shown that redox state of regulatory components is an important marker of disease (Scott et al., 2003). Thus, understanding thin filament regulation using a similar *in vitro assay* as was done in study 1 would help contextualize the effects of thin filament oxidation.

Study 2 builds upon the insights from study 1, investigating the role of oxidation in modifying the interactions and function of thin filament proteins. These proteins also interact with myosin and are crucial for muscle contraction and thus oxidation on regulatory components is thought to have effects on cross bridging itself. Study 2 broadens the scope of this thesis by assessing oxidation sites using mass spectrometry. This holistic perspective allows us to explore potential changes in the calcium handling properties of the thin filament while assessing oxidation sites across the contractile apparatus. In conjunction with study 1, the following study offers a more nuanced understanding of how oxidation affects muscle contraction.

Experimental Study 2

Oxidation of striated muscle thin filaments

Daren Elkrief¹, Yu-Shu Cheng², Oleg S. Matusovsky², Dilson E. Rassier^{1,2}

1. Department of Physiology, McGill University, Montreal, QC H3G 1Y6, Canada
2. Department of Kinesiology and Physical Education, McGill University, Montreal, QC H2W 1S4, Canada

August, 2023.

Abstract

Muscle contraction is governed by thick and thin filament interactions at the molecular level. These filaments are composed mostly by myosin, actin, and regulatory proteins. Studies have shown that excessive oxidation of myosin and actin cause myofibrillar weakness in healthy and diseased muscles. However, the degree to which oxidation of each of these proteins contributes to an attenuated force in myofibrils is unclear. We had previously shown that oxidation using the chemical 5-amino-3-(4-morpholinyl)-1,2,3-oxadiazolium chloride (SIN-1) of actin and myosin was sufficient to alter sliding velocity in the *in vitro* motility assay (IVMA). In the current study, we explore how oxidation affects the function of thin filament regulatory proteins, called the troponin-tropomyosin complex. We analyzed the mass spectrometry data of oxidized thin filaments and confirmed that several residues were oxidized by SIN-1. We show that exposure of the thin filament to SIN-1 was sufficient to alter thin filament interaction with myosin, as shown by a decreased myosin-propelled actin velocity in the IVMA. The results suggest that oxidation plays a critical role in force regulation at the molecular level.

Introduction

Muscle cells are composed of interlacing thick and thin filament proteins, which interact as they slide past each other to contract the sarcomeres. Thin filament regulatory proteins are crucial for translating excitation signals to muscular contraction. Following the release of calcium from the sarcoplasmic reticulum, calcium binding with regulatory proteins enables interactions between the thick and thin filaments, called actin-myosin cross-bridges. The contraction process is primarily regulated by Ca^{2+} binding to Troponin C (TnC), which interacts with other thin filament proteins such as Troponin I (TnI), Troponin T (TnT), and Tropomyosin (Tm), which are collectively called either TM-Tn or the thin filament (TF) regulatory complex. Ca^{2+} binding releases the TM-Tn inhibition on actin-myosin interactions, allowing for cross-bridging to occur (Gordon et al., 2000; Kobayashi, Jin, & de Tombe, 2008; Kobayashi & Solaro, 2005). Upon Ca^{2+} dissociation from TnC, the thin filament protein Tm resumes obstruction of the actin-myosin binding site. This action inhibits the actin-myosin interaction, allowing the sarcomere to return to a state of relaxation.

In a previous study, we investigated the effects of actin and myosin oxidation on actin sliding and force produced by the myofilaments, noting that filament force and in vitro motility were reduced following SIN-1 oxidation (Elkrief et al., 2022). To expand on this line of inquiry, in the present study we measured the effects of oxidation on thin filaments, containing all regulatory proteins. Our objectives were to assess (i) the F-actin sliding velocity over heavy meromyosin (HMM) using an in-vitro motility assay and (ii) to assess whether oxidation occurs in thin filament proteins, as analyzed by mass spectrometry (MS). We noted that the motile velocity of regulated actin, propelled by myosin, diminished in the presence of oxidation. Concurrently, changes were identified in both calcium sensitivity and velocity at all tested calcium concentrations. Further analysis using mass spectrometry to assess thin filament proteins confirmed SIN-1-induced oxidation. Oxidized residues were detected in all thin filament proteins, with a particularly significant presence in the actin derived from reconstituted bovine cardiac thin filament complexes. Taken together, these findings indicate a significant influence of oxidation on the performance of thin filament proteins, which likely interferes with the finely tuned process of muscle contraction. This novel insight sets the stage for more focused investigations into the role of oxidation in muscle function and pathology.

Methods

Ethics and Animals

The ethical protocol for use of animal material was approved by the Animal Care Committee at McGill University (reference# MCGL-5227) and the Canadian Council on Animal Care. Native thick filaments were isolated from the psoas muscle from the rabbit, according to standard procedures performed in our laboratory (Cornachione et al., 2014; Kalganov et al., 2010; Albert Kalganov et al., 2013).

New Zealand White rabbits (female, 2.6–2.7 kg, 11–12 weeks) were purchased from Charles River Laboratories (QC, Canada). On the day of sample collection, the animals were killed by barbiturate overdose. An incision of approximately 20cm was made in the mid-section of the animals' belly using a sharp scalpel (No.10 surgical blade equipped, FEATHER®). The psoas was identified, and stripes of the muscle (~3 mm in diameter, ~5 cm long) were dissected using surgical tweezers (No.5 fine-needle-sharp Sigma-Aldrich). The muscle strips were tied in 6" applicator sticks (Fisher®) with black braided silk (2-0, SP118, LOOK™) and stored in ice at -4°C in Rigor solution. Approximately 6 hours after extraction, the muscle samples were transferred to a mixed solution containing rigor/glycerol (50%/50%) and stored at -20°C. In the day of the experiment, the sample was defrosted at 4°C in Rigor solution for 30 minutes. Then, they were then left in a relaxing solution (100 mM KCl, 10 mM PIPES (pH 7.0), 10 mM MgCl₂, 2 mM EGTA, 10 mM ATP, 2 mM DTT) for 1 h, before being diced into thin strips and homogenized on ice (SNMX 1092, OmniInc) at 2° C for 30 s, with 1 min intervals. The homogenate was centrifuged (5804R, Eppendorf) at 4500 g for 30 minutes to remove undamaged myofibrils and other contaminants.

Protein preparation for IVMA

Skeletal muscle myosin was isolated from the rabbit psoas samples using a known protocol (Margossian & Lowey, 1982). In summary, 5 g of muscle was homogenized in 15 ml of Hasselbalch-Schneider buffer (0.1 M KH₂PO₄/K₂HPO₄ at pH 6.4; 0.6 M KCl, 10 mM Na₄P₂O₇·10H₂O, 1 mM MgCl₂ and 20 mM ethylene glycol tetra-acetic acid) using an Omni mixer

homogenizer (Omni International, Inc., Georgia, USA). The solution was stirred at 4°C for 15 min and stopped with the addition of 20 ml of 4°C distilled water. The mixture was centrifuged at 3000 x g (5804R, Eppendorf AG, Hamburg, Germany) for 10 min and the myosin supernatant was passed through a 55 mm hardened circle filter paper (No.54, GE Healthcare, IL, USA). The filtrate was diluted with 4°C distilled water and centrifuged at 10,000 × g for 15 min. The pellet was washed with buffer B (20 mM K₂HPO₄ at pH 7.2; 0.12 M KCl; 1 mM EDTA and 1 mM DL-Dithioereitol (DTT)) and re-suspended in buffer C (50 mM sodium pyrophosphate and 1 mM DTT at pH 7.8), and centrifuged at 10,000 × g for 10 min. Supernatant was filtered through No.54 filter paper (WHATMAN™, GE, USA) and the myosin solution was either stored in a -80°C freezer in a glycerol solution, or stored for HMM preparation (Salhotra et al., 2021).

An imidazole based method for HMM preparation was adapted from previous studies (Kron et al., 1991a; Okamoto & Sekine, 1985). Nine volumes of IED solution (0.1 M imidazole hydrochloride, 0.1 mM EGTA, 2 mM DTT added after setting to pH 7.0) was added to a centrifuge tube with 21 mg of stock myosin solution, mixed slowly to precipitate myosin filaments and then left on ice for 10 min. The solution was centrifuged at 15,000 x g for 60 min at 4°C. The pellet was dissolved in CHB (20 mM imidazole hydrochloride, 1 M KCl, 4 mM MgCl₂, 10 mM DTT added as before) 2x to obtain a final concentration of 15 mg/ml myosin in CHB. The myosin solution was then incubated in a shaking water bath at 25°C for 5 min. 1 mg/ml chymotrypsin was added to the myosin to final concentration of 12.5 µg/ml and set in a water bath for 10 min at 25°C. 7 µl of 0.2 M stock PMSF protease inhibitor and 12.6 ml cold BED were added to the solution and gently mixed. The mixture was left on ice for up to one hour and then centrifuged at 15,000 × g for 60 min at 4°C. At this stage the myosin was pelleted and HMM was recovered from the supernatant. The HMM concentration was determined via Bradford assay (Bradford, 1976) (Bio-Rad, CA, USA). Sucrose was added to aliquots of HMM in Eppendorf tubes to a final concentration of 2 mg/ml, frozen in liquid nitrogen, and stored at -80°C.

Bovine thin filament (troponin-tropomyosin complex) was purchased from Cytoskeleton (Cytoskeleton Inc. CO, USA). For control experiments, actin was extracted in-lab. Actin was extracted from rabbit psoas, and isolated according to a modified protocol (Pardee & Spudich, 1982). Briefly, actin was purified in 10 ml fresh G-actin buffer (2 mM Imidazole, 0.2 mM Na₂ATP, 0.2 mM CaCl₂) per g of acetone powder. The solution was stirred for 30 min on ice and filtered through 4 layers of cheesecloth. The liquid was further extracted with 10 ml G-actin buffer per

gram of acetone powder and stirred for 10 min at 0 – 0.5°C. Filtrates were centrifuged at 20,400 × g for 20 min at 4°C and passed through a cheesecloth and pellets were discarded. The supernatant was then dissolved in 50 mM MgCl₂, and actin filaments polymerized with the addition of 0.2 mM ATP. The solution was left for 1 hr at room temperature while KCl was slowly added to a final concentration of 0.8 M. The solution was stirred again for 10 min and then centrifuged at 12,000 × g for 1 hr at 4°C. The supernatant was discarded. Actin concentration of 7 μM was determined using absorbance measurement at 290 nm using E=0.63 ml/mg x cm as described elsewhere (Houk Jr & Ue, 1974). The product purity was determined using 10% SDS-PAGE. HMM and polymerized actin filaments (F-actin) were frozen in liquid nitrogen in the presence of 2 mg/ml sucrose and stored at – 80 °C which could be kept for years (Balaz & Månsson, 2005).

SIN modification of F-actin and HMM

F-actin was treated with SIN-1, hydrochloride (Sigma-Aldrich, MO, USA) according to a protocol outlined elsewhere (Maarten M Steinz et al., 2019). Briefly, 10 μM SIN-1 was added to tubes containing 7 μM F-actin and a labeling buffer (10 mM MOPS at pH 7.0, 0.1 mM EGTA, 3 mM NaN₃, 60 mM KCl, 2 mM MgCl₂), and allowed to react for 10 min. The solutions could be used immediately or stored at – 80°C. Similarly, 920 ug/ml HMM was combined with 10 μM SIN-1 for 10 minutes, and reactions were stopped with solution exchange, as done previously (Persson et al., 2019; Maarten M Steinz et al., 2019). For the IVMA, HMM was diluted to 120 ug/ml and imaging was performed immediately after incubation of HMM with the oxidant to reduce variability across experiments. In SDS PAGE gels, proteins were separated into reduced and oxidized groups, both groups were set to rest, and oxidized groups were treated with SIN-1 for one hour to ensure maximum effect.

In-vitro motility assay

Motility experiments were run at ~23 °C, and performed as described previously (Rahman, Salhotra, et al., 2018). Glass coverslips (60 × 24 mm², #0, Menzel-Glaser, Braunschweig, Germany) were soaked in 70% EtOH overnight, dried, and coated with 1% nitrocellulose to create an isotropic and non-specific binding surface for HMM attachment (Kron et al., 1991b). We used #0 coverslips, which have a thickness ranging from 0.085 to 0.13 mm. While coverslip thickness can influence the working distance in high-resolution microscopy, our mechanical-based imaging

system is less sensitive to these variations, and the chosen coverslips provided consistent and reliable results for our in vitro motility assays. Nitrocellulose was chosen because it is easily applied manually as a film on coverslips. Furthermore, varying amounts (0.25 μL – 2.1 μL) have been shown to have no effect on motility speed, motile fraction, or quality of filament movement (Kron et al., 1991b; Sundberg et al., 2003). Flow cells were constructed using double-sided adhesive tape to build a fluid chamber between a non-functionalized small coverslip (20 \times 20 mm^2) and a large coverslip (60 \times 24 mm^2). During experiments, one coverslip was used for each condition and sampled at 3 - 5 times in different areas on the coverslip. The in vitro motility assay was performed by slowly adding 60 μL volumes of the following solutions to the side of the flow chamber in the following order: 1. HMM (120 $\mu\text{g}/\text{mL}$) diluted to 60 $\mu\text{g}/\text{mL}$ in L65 solution (low ionic strength solution (LISS), comprised of 1 mM MgCl_2 , 10 mM MOPS, variable K2EGTA, pH 7.4, 1 M KCl, 15 ml DTT, or without EGTA and Ca^{2+} for experiments to activate thin filaments), 2. Bovine serum albumin (BSA, 1 mg/ml) in LISS, 3. L65, 4. Fluorescently labeled actin diluted to 10 nM in L65, 5. L65, 6. Assay solution (15 mM LISS, 1 mM MgATP, 10mM DTT, 0.64% methylcellulose, 130mM KCl, 3 mg/ml glucose, 0.1 mg/ml glucose oxidase, 0.02 mg/ml catalase, 2.5 mM phosphocreatine, 0.2 mg/ml creatine kinase). The coverslip and sliding actin filaments were then imaged under an inverted darkfield fluorescent microscope (Axio Observer D1, Zeiss, Jena, Germany or Eclipse TE300, Nikon, Tokyo, Japan) using a 100 X objective (Zeiss: 1.4 N.A. 63 \times plan-apochromat or 0.6 N.A 40 \times plan-neofluar; Nikon: 1.4 N. A. 100 X plan-apochromat objective). Images were 1200 \times 1200 pixels, and 110 nm/pixel for the 100 X objective. Fluorescence microscopy was used to image actin filaments with a filter set for Alexa-488 (Exciter ET470/40x, Dichroic T495LP, Emitter ET525/50m; Chroma). Images were captured using a Prime 95B Scientific CMOS (sCMOS) with 95% QE, 11 μm \times 11 μm pixel area (Teledyne, AZ, USA). The frame rate was 10 fps and exposure was set between 20 to 100 ms for seeking and then imaging. The frame rate was 10 fps. MatLab software (MatLab R2017b; MathWorks, Natick, MA) was used to obtain velocity of filament sliding. After a short \sim 1-2-minute incubation, videos were acquired as quickly as possible, within 5 minutes of placing assay solution on the coverslip to avoid increasing variance in motility over time. Immobile actin filaments as well as those with aberrant start and stop motion were excluded from analysis based on criteria as outlined elsewhere (Månsson & Tågerud, 2003; Rahman, Salhotra, et al., 2018). All filament velocities (\sim 50-100 filaments per frame) were averaged per frame. All frame averages were then compiled over the length of the video, which lasted \sim 45 sec, resulting in an n of the

number of videos per treatment as opposed to other methods which rely on the number of filaments to derive sliding velocities.

Free calcium concentration was calculated using the Maxchelator program (<https://somapp.ucdmc.ucdavis.edu/pharmacology/bers/maxchelator/CaEGTA-TS.htm>) based on the constants in Shoenmaker's Chelator (Schoenmakers, Visser, Flik, & Theuvenet, 1992). The Maxchelator program is a web-based tool that calculates the concentrations of free and bound species in solutions containing various mixtures of ligands and metal ions. In our experiments, we used the program to determine the exact amount of calcium chloride to add to our solutions to achieve the desired free calcium concentrations (ranging from pCa4 to pCa7). We used the Hill equation to analyze the relationship between velocity and calcium concentration and used this to assess calcium sensitivity in the *in vitro* assay (Fraser & Marston, 1995; Gordon, LaMadrid, Chen, Luo, & Chase, 1997; Kellermayer & Granzier, 1996).

Labelling F-actin

F-actin (7 μM) was labeled with Alexa fluor-488 phalloidin (A-488) (R415, Invitrogen, USA) at 1:1 actin: A-488 in 10 mM 4-morpholinepropanesulfonic acid (MOPS) buffer at pH 7.4 (60 mM KCl, 2 mM MgCl_2 , 0.1 mM ethylene-bis (oxyethylenenitrilo) tetraacetic acid (EGTA) and 3 mM NaN_3). The methanol in the fluorophore was allowed to evaporate and then the protein was re-dissolved in methanol. Using a pipette with a scissor-cut end to reduce actin shear, actin F-actin was slowly added to a separate tube with labelling buffer to 20 μM and placed on ice. Labeling buffer was added to the fluorophores, vortexed and centrifuged, and the concentrated F-actin in labeling buffer was added to the tube with the fluorophore, resulting in a 2 μM final solution. The solution was left on ice in the dark for 6 hr or overnight and could be stored for 2-4 weeks.

Gel electrophoresis

Sodium dodecyl sulfate (SDS) polyacrylamide gel electrophoresis (PAGE) was conducted on 0.75 mm thick gels (Mini Protein $\text{\textcircled{R}}$ electrophoresis system from BioRad, USA) to separate out proteins of the thin filament prior to mass spectroscopy analysis. We used a 10% acrylamide resolving gel and a 4% bis/acrylamide stacking gel. These gels were treated with SimpltBlueTM Safe Stain

(Invitrogen, Carlsbad, CA) and refrigerated at 4 degrees Celsius overnight. The molecular mass determinations of the proteins were accomplished using SeeBlue™ Plus2 Pre-stained Protein Standard (Thermo Fisher Scientific, Canada) as the benchmark. Thin filament was concentrated in varying amounts depending on the experiment, ranging from 5 µg/µl to 8.4 µg/µl, where actin was concentrated in sufficient amounts at lower concentrations and troponins required higher concentration to be detected on gels. The concentrations of Actin and HMM were ascertained through a Bradford Protein Assay kit (Quick Start – BioRad, CA, USA), with the readings taken on an iMark Microplate Absorbance Reader (Bio Rad, USA). To ensure non-oxidized proteins were minimally impacted, SIN-oxidized gels were run separately from those which were reduced. Proteins were minimally exposed to air. Saturating concentrations of antioxidant (15% sodium metabisulfite, 10% DMF) were added to gel running buffer. Gel bands were then selected based on expected protein weights.

Mass Spectrometry

Each gel band was reduced with DTT, alkylated with iodoacetic acid and digested with trypsin. Extracted peptides were re-solubilized in 0.1% aqueous formic acid and loaded onto a Thermo Acclaim Pepmap (Thermo, 75µM ID X 2cm C18 3µM beads) precolumn and then onto an Acclaim Pepmap Easyspray (Thermo, 75µM X 15cm with 2µM C18 beads) analytical column separation using a Dionex Ultimate 3000 uHPLC at 250 nl/min with a gradient of 2-35% organic (0.1% formic acid in acetonitrile) over 2 hours . Peptides were analyzed using a Thermo Orbitrap Fusion mass spectrometer operating at 120,000 resolutions for MS1 with HCD sequencing at top speed (15,000 resolutions) for all peptides with a charge of 2+ or greater. The raw data were converted into .mgf format (Mascot generic format) for searching using the Mascot 2.5.1 search engine (Matrix Science) against bovine protein sequences (Uniprot). The database search results were loaded onto Scaffold Q+ Scaffold 5.1 (Proteome Sciences) for statistical treatment and data visualization. Pinnacle (Optys Tech) was used to quantify all detected peptides using a MS1 quantification workflow (Targeted Quantification: Label Free DDA) wherein the peptide specific XICs from the raw mass spec data (.raw) were used to directly compare all identified peptide (*.dat) amounts across all experiments using precursor ion integrals (in counts).

Protein visualization

In the InterPro database, the actin domain structure was examined, specifically focusing on the predicted domains section. The predicted domains are generated by Genome 3D, a collaborative project that uses computational methods to predict the three-dimensional structure of proteins. Several computational algorithms were used to compile domain structure and listed via Genome3D. While we analyzed Bos Taurus (Uniprot accession number P68138) proteins initially, insufficient data was available to adequately characterize the amino acid sequence. Thus, we show subdomain designation for well characterized human actin (P68133) based on the predicted domains listed in the InterPro Skeletal muscle actin section. The domains predicted by these methods were highlighted in alpha fold to visualize their locations within the protein structure. To address the discrepancies in domain assignments for bovine cardiac actin across various protein databases, we utilized sequence homology to infer the domain structure of bovine actin from a well-characterized homolog, human cardiac actin. We performed a sequence alignment between human cardiac actin (UniProt accession number P68032) and bovine cardiac actin (UniProt accession number QZC07) using the Basic Local Alignment Search Tool (BLAST) provided by the National Center for Biotechnology Information (NCBI). The BLAST alignment revealed a 100% sequence identity between human and bovine cardiac actin, with a score of 789 bits and an Expect value of 0.0, indicating a highly significant alignment. This perfect match suggests a high degree of conservation between human and bovine cardiac actin, supporting the use of human actin domain assignments for bovine actin. Based on this alignment, we assigned the domain structures to bovine cardiac actin in Fig. 2.

Statistical analysis

All results were analyzed, and graphs were generated using Graphpad Prism (version 8.0, Graphpad software, CA, USA). Comparisons between groups were performed using a one-way analysis of variance (ANOVA) or t-test where appropriate. A significance level of $P < 0.05$ was regarded as significant in all analyses. Data all reported as mean \pm S.E.M (Standard Error of the Mean).

Acknowledgements

The authors thank Lorne Taylor and Amy Wong of the Proteomics and Molecular Analysis Platform, RIMUHC, McGill for critical assistance with the mass spectrometry and analyses. The authors thank Dr. Malin Persson, Dr. Alf Mansson, and Dr. Gijs Ipjma for programs used for analysis during data collection.

Results

In the *in vitro* motility assay experiments, we measured the velocity of unloaded sliding of both actin filaments and regulated actin filaments. At a saturating calcium concentration (pCa 4.5), the velocity of regulated thin filament was $0.95 \pm 0.045 \mu\text{m/s}$ (mean \pm standard error mean), and $0.65 \pm 0.039 \mu\text{m/s}$ for the unregulated actin filaments (Fig. 1). In regulated oxidized filaments, the mean was $0.62 \pm 0.20 \mu\text{m/s}$ pCa 4.5, and $0.58 \pm 0.10 \mu\text{m/s}$ in oxidized unregulated actin filaments. Thus, the velocity of an unoxidized regulated thin filament exceeds the velocity of an unregulated thin filament by 46% ($P < 0.001$). For SIN-1-oxidized filaments, the velocity of regulated thin filament exceeds that of an unregulated thin filament by 7% yet was not statistically significant ($P = 0.29$)

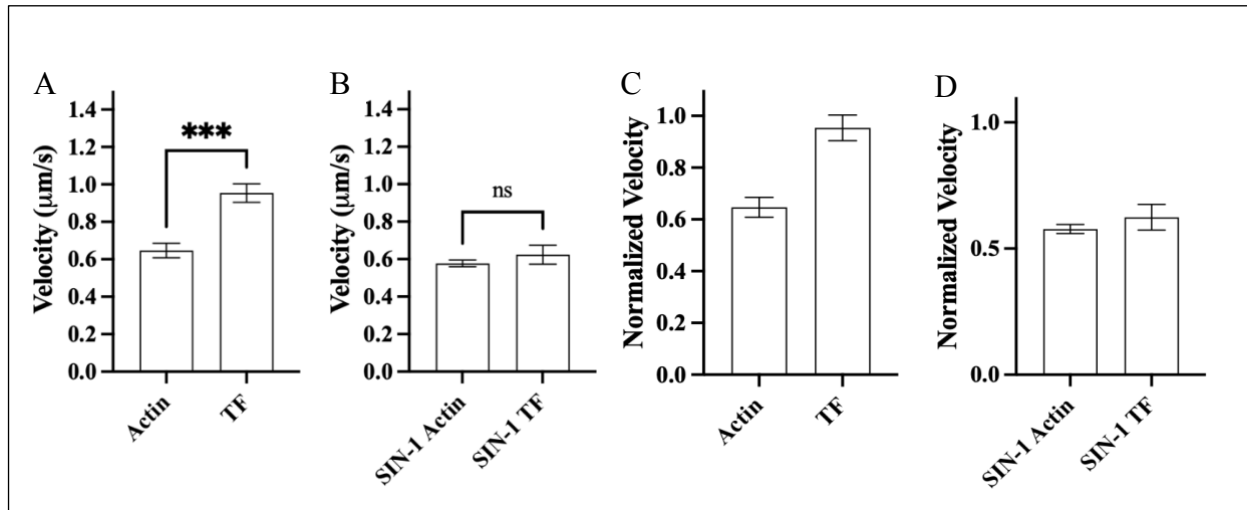


Figure 1 Velocity comparison between (A) unregulated (Actin) and regulated thin filaments (TF) in non-oxidized (A) and oxidized (B) (SIN-1) conditions. Velocities were normalized to actin filaments in non-oxidized (C) and oxidized (D) conditions. Data presented as mean \pm S.E.M.

Utilizing the data from the experiments, we generated the velocity versus pCa curves across a range of calcium concentrations (pCa 4.5–6.5) (Fig. 2). For all calcium concentrations tested, there was a decrease in velocity in SIN-1-oxidized thin filaments compared to control thin filaments ($P < 0.001$, two-way ANOVA). The data were fitted by a sigmoid regression curve in accordance

with a modified Hill equation $V = V_{min} + \frac{(V_{max}-V_{min})K_h[Ca]^h}{1+K_h[Ca]^h}$. In this equation, V_{max} signifies the maximal velocity of a thin filament at a saturating calcium concentration, which was found to be $1.29 \mu\text{m/s}$ for the control and $0.94 \mu\text{m/s}$ for the SIN-1-oxidized filaments. V_{min} was the lowest speed found in the assay, below which reliable movement was not assessed by our program. K_h is 5.43 , a value indicating the calcium concentration at which the velocity is half maximal, for the control and 5.16 for the SIN-1-oxidized filaments. The Hill coefficient h , representing the steepness of the curve, is 1.23 for the control and 0.43 for the SIN-1-oxidized filaments. The lower Hill coefficient for the SIN-1-oxidized filaments suggests a blunted response to calcium, which could be due to alterations in the regulatory proteins or the actin itself, affecting the cooperative binding of calcium and subsequent filament movement.

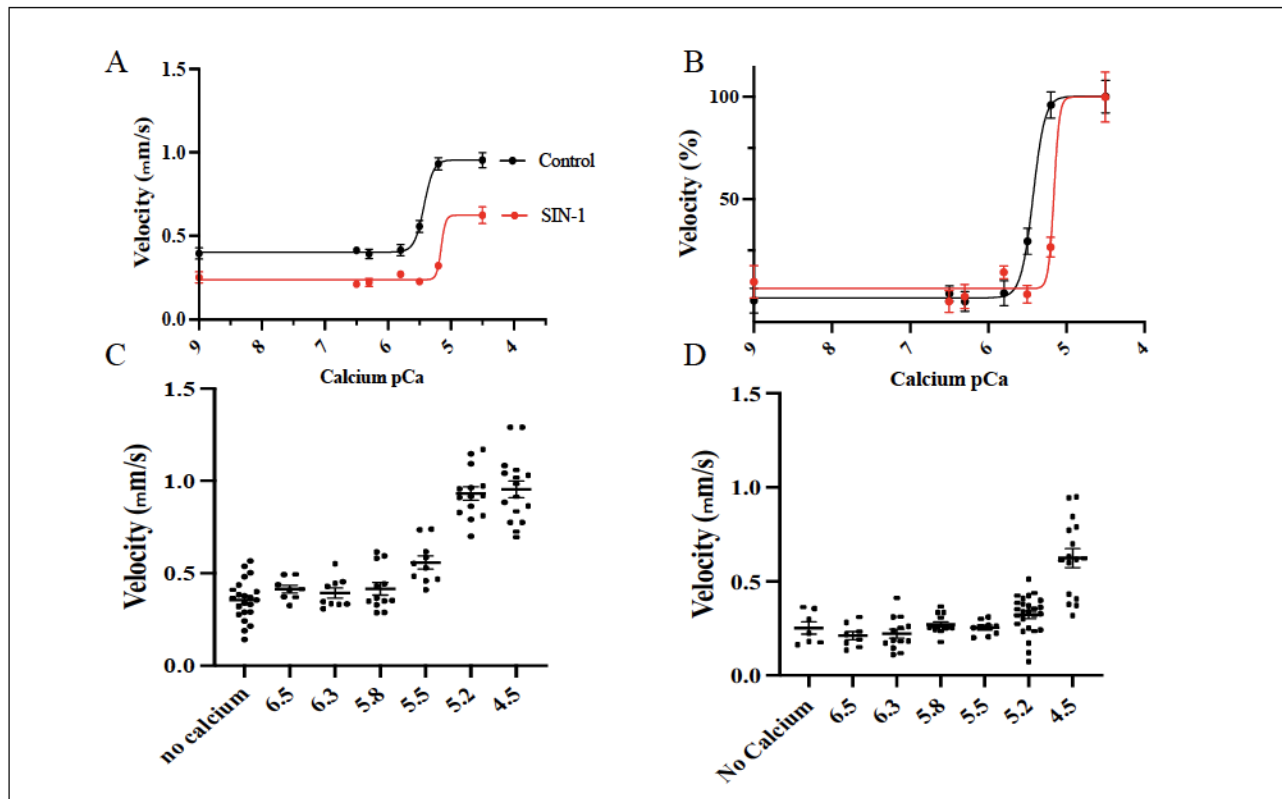


Figure 2. Semi log plot of the velocity of regulated thin filament as a function of the free calcium concentration for (A) control and SIN-1-treated thin filaments. (B) Plots were normalized to their respective V_{max} . Average frame filament velocities are shown for control (C) and oxidized (D) thin filaments. Each point represents an entire frame from the video, and all velocities are averaged for each frame. Data was fitted to the Hill equation. Data presented as mean \pm S.E.M.

filaments. Altogether, these results suggest that oxidation of proteins can alter contractile properties of skeletal muscles.

Regulated actin filaments sliding in the *in vitro* motility assay have been shown to move more quickly than unregulated filaments (Kopylova, Katsnelson, Ovsyannikov, Bershitsky, & Nikitina, 2006) (Fig. 1). In oxidized conditions there was no statistical increase in the velocity between oxidized actin and regulated oxidized actin (Fig. 1). This could be due to several factors. Firstly, SIN-1 oxidation is not restricted to regulatory proteins, and actin oxidation, which has previously shown to be sufficient to reduce sliding velocity (Elkrief et al., 2022; Heather & William, 2016; J. H. Snook et al., 2008), may be a primary contributor to reduced motility. Secondly, the potential velocity increase from adding thin filament may be insufficient to outweigh the direct impairment of the actin-myosin interaction. Lastly, oxidation may cause some dissociation of the thin filament regulatory components (Pinto et al., 2011), reducing the difference in velocity of cross bridge cycling across these groups.

These findings beg a deeper exploration of the regulatory mechanisms of striated muscle contraction, which are driven by cooperativity between contractile and regulatory proteins. We assessed calcium response in regulated actin filaments, a measure of the cooperativity in the regulated thin filaments. The most notable effect was a decrease in velocity at all tested calcium concentrations in oxidized conditions (Fig. 2). Accordingly, 10 μM ONOO⁻ treatment of thin filaments resulted in a decrease in velocity at saturating calcium conditions (J. H. Snook et al., 2008). It is unknown whether solely oxidizing the thin filament would reduce velocity, as specifically targeting actin has been shown to be sufficient to reduce sliding velocity (Elkrief et al., 2022; Heather & William, 2016; J. H. Snook et al., 2008). As mentioned above, it is more intuitive that oxidation proximal to the crossbridge would have a preferential impact on sliding velocity compared to oxidation in the regulatory component. Because adding regulatory components to actin are sufficient to increase sliding velocity (Fig. 1), it is conceivable that oxidizing the thin filament would reduce velocity by reducing the number of cross bridges (Homsher, Lee, Morris, Pavlov, & Tobacman, 2000) or by increasing regulatory complex dissociation (Pinto et al., 2011; Pinto, Veltri, & Sorenson, 2008). TnC has been shown to be susceptible to dissociation from the regulatory complex during oxidation (Pinto et al., 2011; Pinto et al., 2008). Furthermore, -SH protection from oxidation was shown to be critical for full-complex

precipitation, suggesting oxidation may disrupt Tm-Tn intermolecular stability (Yasui, Fuchs, & Briggs, 1968). In this respect, oxidation would make the thin filament behave as if it were less regulated and it is conceivable that solely oxidizing thin filament components could compromise crossbridge efficiency by promoting complex dissociation, although direct exploration of this question would be required.

Our *in vitro* studies provided insights into the behavior of thin filament function under different conditions. A key point of interest was the variation in half-maximal effective concentration, a measure that reflects the sensitivity of thin filaments to calcium, essentially indicating at what calcium concentration the thin filament velocity reaches half of its maximum potential. In our findings, oxidized thin filaments showed a comparatively lower half-maximal effective concentration, indicating an increased sensitivity to calcium fluctuations relative to the control filaments. We also observed discrepancies in the h factor, an aspect of the Hill equation that represents the cooperativity of the system. Interestingly in oxidized filaments, cooperativity was reduced.

Our findings were intriguing; oxidized thin filaments demonstrated enhanced sensitivity to calcium changes while exhibiting decreased cooperativity. Several mechanisms may account for this observation. Firstly, oxidative modifications in the troponin complex, particularly TnC, could have increased its calcium-binding affinity, thereby enhancing calcium sensitivity. However, these alterations may simultaneously affect the structural transitions crucial for cooperativity, introducing rigidity into TnC-TnI-TnT interactions and hindering the propagation of cooperative conformational changes along the thin filament. Secondly, oxidative changes could distort the structure or flexibility of tropomyosin, facilitating its transition from the 'off' to the 'on' state in response to calcium binding, yet impeding the coordinated movements of tropomyosin along the filament, thus decreasing cooperativity. Thirdly, oxidative modifications could impact the interactions between thin filament components and other proteins. Increasing thin filament-actin rigidity could bias the complex to an open state (Gao et al., 2012). A combination of these factors likely plays a role, warranting further investigation.

Mass Spectrometry

Oxidation of thin filament proteins by SIN-1 elicits a variety of functional alterations *in vitro*, ranging from dissociation of F-actin, reduced ATPase activity, dampened motility, and diminished filament force (Elkrief et al., 2022; Maarten M Steinz et al., 2019; T. Tiago, Ramos, Aureliano, & Gutierrez-Merino, 2006). The wide range of functional effects by oxidation may be due to the non-specific nature of oxidation. SIN-1 decomposes to produce NO and O₂⁻, which subsequently react to form ONOO⁻. Although SIN-1 is primarily used as a peroxide or NO donor, under certain conditions, it can preferentially donate NO (Singh, Hogg, Joseph, Konorev, & Kalyanaraman, 1999; Maarten M Steinz et al., 2019). As such, there were many potential oxidation products indicated in the mass spectroscopy results on all thin filament proteins. It is therefore unlikely that functional outcomes are driven by individual modifications. Rather, an assortment of oxidized amino acids likely contributes to these effects. Consequently, understanding the exact sites of modifications is essential. Our study employed mass spectrometry to probe the products of SIN-1 oxidation as previously done in other studies (M. Fedorova et al., 2010; Hong et al., 2007; Kanski, Hong, et al., 2005; Oh-Ishi et al., 2003). While we cannot infer direct relationships, this approach has paved the way to a comprehensive understanding of potential oxidation sites and their functional implications.

Actin

Actin is particularly susceptible to oxidation, given its mass abundance in both muscle and non-muscle cells, its proximity to oxidant sources and its number of oxidizable amino acids (Otten, 1988; Schiaffino & Reggiani, 1996; Shishkin et al., 2004). Structural and functional effects of SIN-1 oxidation, specifically on actin, have been extensively explored (Maarten M Steinz et al., 2019). Several specific modifications have been correlated with functional alterations. For example, Met-46 and Met-49 in the DNase-I binding loop of subdomain 2 have been shown to be oxidized by MICALs, and to promote filament depolarization and dissociation, being proximal to proteolytic cleavage sites (I. Dalle-Donne et al., 2003; Lee et al., 2013). Our results showed a large range of oxidized residues interspersed throughout the molecule (Supplementary table 1), likely contributing to the wide range of functional effects we have noted in this study and in the past (Elkrief et al., 2022). It should be noted that correlating our residue locations with those in the literature is difficult because differences in species sequences and canonical sequences have changed over time as databases have improved. Nonetheless, some analogous domain-specific

modifications can be inferred. We noted Cys-259 in our data set, correlated to Cys-259 in rat skeletal muscle sub domain 4 (Gao et al., 2012). Interestingly, increased Ca^{2+} sensitivity has been noted, likely by shifting Tm from a blocked state to open state while cross linking with Tm Cys-190, which we also observed. Cys-285 was oxidized in our set, a known oxidation product said to reduce actin-myosin binding, although shown to be highly dependent on contractile state for solvent access (Duke et al., 1976; Gross & Lehman, 2013). We noted arginine nitrosylation, which has been observed as an undesirable meat processing by-product (R. Liu, Warner, Zhou, & Zhang, 2018; Taldone et al., 2005). We observed oxidation in Met-46, Met-49, Met-178, Met-192, which were correlated to oxidation sites found in the literature. Methionine oxidation in actin has been shown to substantially increase actin hydrophobicity, and conformation changes in SD1 and SD2 as well as decreased susceptibility to proteolysis (I Dalle-Donne et al., 2002; Milzani et al., 2000). Oxidation of N terminal methionines by H_2O_2 , particularly Met-296 and Met-355 in rabbit actin have been shown to lead to structural alterations in helix 338–348 and in the loop 355–359 within subdomain 1 of the actin molecule and complete inhibition of actin polymerization (I Dalle-Donne et al., 2002; Milzani et al., 2000). Therefore, oxidation throughout the molecule has been known to exhibit a wide range of functional and structural effects. It should be noted that due to incomplete protein coverage, we lacked a number of residues shown to be oxidized in the literature (Verrastro, Pasha, Tveen Jensen, Pitt, & Spickett, 2015). Despite the high number of tyrosines in actin, we only noted one instance of oxidation supported by the literature. Tyr-296 near the D-loop, which is thought to alter actin internal stability (Maarten M Steinz et al., 2019). Given actin's high number of oxidizable residues, it follows that this protein bore the highest number of targets.

Tropomyosin

Crosslinking between actin and tropomyosin and the exposed residues along the length of Tm make it a well-known target of oxidation. While we noted that it is the next-most oxidized protein after actin, there was far less total oxidation in Tm than in actin. In striated muscle cells, Tm plays a pivotal role in mediating the interactions between the troponin complex and actin (Wolska & Wieczorek, 2003). Tropomyosins are oriented parallel to each other and contain regions of repeats along the molecule, which bind to actin along these regional repeats (Bai, Wang, & Kawai, 2013; Lewis & Smillie, 1980; Muthuchamy, Pajak, Howles, Doetschman, & Wieczorek, 1993). Notably, Tm does not have distinct locations where it interacts with actin, it instead relies on weak

electrostatic interactions to cover the binding site. Thus, it is likely that coils carry structural information along the molecule, which is critical for cooperativity. This is exemplified by Tm's 7-fold pattern of charged and hydrophobic surface residues, which act as weak actin binding sites (Hitchcock-DeGregori & Barua, 2017). Therefore, while localizing amino acid to function disruptions is difficult, oxidation among a dispersed range of residues could conceivably alter binding propensity. Actin-Tm interaction residues were detected in our data, including Lys-168 near the Arg-167 actin interaction site, and residues Met-327 and Lys-328 on actin, which interact with Tm. In contrast to potential disruptions to generalized charge-hydrophobic interactions, Tm Cys-190 has been specifically noted to be oxidized in the literature. Interestingly, Cys-190 modification by nitroxyl (HNO) resulted in cross-linking with actin Cys-257 may result in increased Ca^{2+} sensitivity by shifting Tm from a blocked state to an open state (Gao et al., 2012).

Troponin T

Along with tropomyosin, the troponins play a critical role in regulating muscle activity. Interestingly, Tn addition to actin was shown to have a greater effect on sliding velocity increase than Tm (Homsher et al., 2000). TnT inhibits the actin-myosin interaction, a process that is only released upon Ca^{2+} attachment to Troponin C (TnC), leading to a conformational change in the troponin complex that allows cross-bridge formation (Gomes et al., 2002; Wei & Jin, 2011).

While the troponin proteins showed the least number of modifications in our data, redox status of these proteins are critical to disease. For instance, TnT nitration has been suggested to contribute to cardiac dysfunction after MDMA administration in rodents (Shenouda, Lord, McIlwain, Lucchesi, & Varner, 2008). Oxidized troponin assays have been of particular interest, as circulating TnT levels have been used as a measure of myocardial infarction (Mair, Dienstl, & Puschendorf, 1992). Additionally, TnT oxidation has been noted in post-stroke and utilized as an exercise intensity marker (De Palma et al., 2014; Ferreira & Reid, 2008; Merry & Ristow, 2016; Powers & Jackson, 2008). Furthermore, the lipid-oxidation adduct MDA-TnT has been used as a marker of cardiac stress (Scott et al., 2003). Finally, elevated levels of oxidized TnT have also been observed in elderly biopsies (Dos Santos et al., 2015).

Despite this evidence, there are few reports of amino-acid specific oxidation events of cardiac or skeletal TnT in the literature. In our data we detected oxidized lysines (Lys-90, Lys-112, Lys-113) in the central helical domain which could not be localized to specific functionalities. The effects of TnT oxidation on thin filament function are unclear. As with actin, introductions of bulky covalent modifications to Lys and Arg would conceivably induce wider structural alterations, sterically hindering close-contact bonds (Maarten M Steinz et al., 2019). One clear effect of TnT oxidation is complex instability, where both TnI and TnT have been noted in increasing concentrations in the blood of patients after acute myocardial infarction (Wu et al., 1998).

Troponin I

As with TnT, the oxidation state of TnI plays a significant role in the assembly of the troponin complex. When a mixture containing oxidized TnI, TnT, and TnC was exposed to an oxidant and then reconstituted with the reducing agent DTT, the reconstituted complex calcium sensitivity of actomyosin ATPase activity was restored (Horwitz, Bullard, & Mercola, 1979). TnI is critical for stabilizing the Tm-Tn complex and for inhibiting the actin-myosin interaction prior to calcium entry (Bowman & Lindert, 2019; Galińska-Rakoczy et al., 2008; Mollica et al., 2012). Oxidation of TnI has been shown to be present following myocardial insult, and as with TnT, increase in circulation (La Vecchia et al., 2000; Missov & Mair, 1999). While TnI and TnT nearly always dissociate from the thin filament together (Korff, Katus, & Giannitsis, 2006) there are biochemical differences between the two. TnI is more unstable than TnT and is thought to have a higher propensity for fragmentation or oxidation (Korff et al., 2006). Furthermore, there are a wide array of assays used for detecting its circulation in clinical and laboratory settings, underscoring its importance as a marker for disease (Apple, Sandoval, Jaffe, & Ordonez-Llanos, 2017). Interestingly, glutathionylation of rat Cys-133 TnI in fast twitch muscle was linked to increased Ca²⁺ sensitivity, possibly by sterically hindering the TnI-TnC interaction, biasing the complex toward an open conformation (Mollica et al., 2012). This was interestingly shown to reduce fatigability during exercise, implying that low level reversible oxidation may allow the muscle to adapt contractility. In our data set, we noted oxidation of residues Met-155 and Arg-164 in the beta coil regions, which are thought to confer intermolecular stability (Takeda, Yamashita, Maeda, & Maéda, 2003). Met-156 and Met-157 in the regulatory domain, which interact with TnC, showed oxidation as well (Vassylyev, Takeda, Wakatsuki, Maeda, & Maéda, 1998). Similarly, the

oxidation of Met-203, Arg-206, and Lys-207 in the N terminal region, thought to be involved in actin binding and binding inhibition, could potentially alter the hydrophobic and electrostatic landscapes, affecting the protein's interaction with actin and its regulatory function (Takeda, Kobayashi, Taniguchi, Hayashi, & Maéda, 1997; Takeda et al., 2003; Vassilyev et al., 1998). These findings suggest that oxidative modifications could have significant implications for the function and stability of the troponin complex, warranting further investigation.

Troponin C

Among the troponins, TnC has the lowest molecular mass and few oxidizable residues. Yet as we have seen with the other troponins, redox state on this protein seems to influence complex integrity as well. Cys-133 oxidation in TnI is suspected to reduce interaction with TnC (Mollica et al., 2012; Ward et al., 2001). TnC is composed of two globular lobes connected via a flexible link domain (Kabsch, Mannherz, Suck, Pai, & Holmes, 1990; Slupsky & Sykes, 1995; Sundaralingam et al., 1985). In muscle cells, the C lobe of TnC interacts with the N-terminal amphiphilic α -helix of TnI. This interaction plays a crucial structural role by anchoring TnC to the rest of the troponin complex (Gasmi-Seabrook et al., 1999; Vassilyev et al., 1998). The N lobe of TnC interacts with other components of the troponin complex, and oxidation in this region, (Met-157 and Lys-158) could perturb these interactions. The redox state of troponin C has been shown to reversibly tune binding affinity with other thin filament proteins (Pinto et al., 2011). While TnC only has two cysteines, both have been shown to be oxidized in different conditions. Cys-35 in rat thin filaments by 1-nitrosocyclohexyl acetate (NCA) (Gao et al., 2012) and H₂O₂ oxidation rat psoas yielded oxidation of Cys-98. Oxidation of TnC Cys-98 was ascribed responsibility for reduced binding affinity with TnI, which was reversible upon DTT administration (Pinto et al., 2011). Another critical component to TnC function, the D/E helix, which links the N and C terminal domains of TnC, allows for high intramolecular flexibility. Changes in the stiffness of the D/E helix, potentially induced by oxidation, could alter TnC activation by calcium (Babu, Rao, Su, & Gulati, 1993; Ramakrishnan & Hitchcock-DeGregori, 1995). Further studies are needed to explore the functional implications of these oxidative modifications.

Conclusion

The assumptions of cross bridge cycling are subject to re-examination when oxidative modifications are introduced. For instance, while binding of calcium to TnC is understood as a unidirectional process leading to thin-filament activation, communication along this pathway can occur in both directions (Pinto et al., 2008). Conformational changes at one end of TnC can influence the other end and changing Tm-Tn composition affects the seemingly-distal actin-myosin interactions (Homsher et al., 2000). Interestingly, the number and strength of cross-bridge attachments to the thin filament can significantly alter the binding of the TnC C-domain (Pinto et al., 2008). When cross-bridges are attached to the thin filament, calcium binds more tightly to the N-domain, indicating that signal transmission from actin through the C-domain and the central helix to the N-domain is required (Potter, Seidel, Leavis, Lehrer, & Gergely, 1976). Any loosening of the attachment at the TnC–TnI junction could potentially impact the kinetics of this process. Thus, thin filament instability caused by oxidation or a reduction in the number of strongly bound cross bridges would serve to both reduce the calcium sensitivity and velocity. Additionally, oxidation on any one of the troponins promotes complex dissociation, while tropomyosin's loose binding to the complex is subject to frequent perturbations. This is further complicated by the finding that intermolecular cross bridging can transiently increase calcium sensitivity, while eventually diminishing it. Finally, events occurring at the cross bridge, while distal to the events in the regulatory complex, cannot be divorced from regulatory function. While it is evident that the kinetics of cross bridge function are rate-limited by the attachment and detachment rates of cross-bridges, rather than by the faster events occurring in the thin-filament regulatory proteins (Pinto et al., 2011; Stehle, Solzin, Iorga, & Poggesi, 2009), evidence from several cardiomyopathy mutants of cTnI suggests that abnormal TnI–TnC interactions can indirectly affect cross-bridge cycling and alter contraction and relaxation kinetics. These abnormalities can cause a delay in the onset of relaxation, and similar effects have been observed in skeletal myofibrils with TnC mutants. These findings underscore the complex interplay between the various components involved in muscle contraction and relaxation (Stehle et al., 2009). Our study indicates that broad spectra of oxidation result in myriad effects on calcium sensitivity and a multitude of oxidation sites. Such studies, tying broad scope surveys to specific functional effects are critical for understanding the range of outcomes from such a ubiquitous modification.

References

- Ackermann, Maegen A, and Aikaterini Kontrogianni-Konstantopoulos. 2011. 'Myosin binding protein-C: a regulator of actomyosin interaction in striated muscle', *Journal of Biomedicine and Biotechnology*, 2011.
- Ackermann, Maegen A, Puja D Patel, Jane Valenti, Yasuharu Takagi, Earl Homsher, James R Sellers, and Aikaterini Kontrogianni-Konstantopoulos. 2013. 'Loss of actomyosin regulation in distal arthrogryposis myopathy due to mutant myosin binding protein-C slow', *The FASEB Journal*, 27: 3217.
- Ait-Haddou, Rachid, and Walter Herzog. 2003. 'Brownian ratchet models of molecular motors', *Cell biochemistry and biophysics*, 38: 191-213.
- Aksenov, MY, MV Aksenova, DA Butterfield, JW Geddes, and WR Markesbery. 2001. 'Protein oxidation in the brain in Alzheimer's disease', *Neuroscience*, 103: 373-83.
- Allingham, John S, Robert Smith, and Ivan Rayment. 2005. 'The structural basis of blebbistatin inhibition and specificity for myosin II', *Nature Structural & Molecular Biology*, 12: 378-79.
- Andrade, Francisco H, Michael B Reid, David G Allen, and Håkan Westerblad. 1998a. 'Effect of hydrogen peroxide and dithiothreitol on contractile function of single skeletal muscle fibres from the mouse', *The Journal of Physiology*, 509: 565.
- . 1998b. 'Effect of nitric oxide on single skeletal muscle fibres from the mouse', *The Journal of Physiology*, 509: 577-86.
- Andrade, Francisco H, Michael B Reid, and Håkan Westerblad. 2001. 'Contractile response to low peroxide concentrations: myofibrillar calcium sensitivity as a likely target for redox-modulation of skeletal muscle function', *The FASEB Journal*, 15: 309-11.
- Antunes, Fernando, and Enrique Cadenas. 2000. 'Estimation of H₂O₂ gradients across biomembranes', *FEBS letters*, 475: 121-26.

- Arstall, Margaret A, Jeifu Yang, Irene Stafford, W Henry Betts, and John D Horowitz. 1995. 'N-acetylcysteine in combination with nitroglycerin and streptokinase for the treatment of evolving acute myocardial infarction: safety and biochemical effects', *Circulation*, 92: 2855-62.
- Baek, Kyuwon, Xiong Liu, François Ferron, Shi Shu, Edward D Korn, and Roberto Dominguez. 2008. 'Modulation of actin structure and function by phosphorylation of Tyr-53 and profilin binding', *Proceedings of the National Academy of Sciences*, 105: 11748-53.
- Balogh, Ágnes, David Santer, Enikő T Pásztor, Attila Tóth, Dániel Czuriga, Bruno K Podesser, Karola Trescher, Kornelia Jaquet, Ferenc Erdődi, and István Édes. 2014. 'Myofilament protein carbonylation contributes to the contractile dysfunction in the infarcted LV region of mouse hearts', *Cardiovascular research*, 101: 108-19.
- Bansbach, Heather M, and William H Guilford. 2016. 'Actin nitrosylation and its effect on myosin driven motility', *AIMS Molecular Science*, 3: 426-38.
- Barford, David. 2004. 'The role of cysteine residues as redox-sensitive regulatory switches', *Current opinion in structural biology*, 14: 679-86.
- Bates, Genevieve, Sara Sigurdardottir, Linda Kachmar, Nedjma B Zitouni, Andrea Benedetti, Basil J Petrof, Dilson Rassier, and Anne-Marie Lauzon. 2013. 'Molecular, cellular, and muscle strip mechanics of the mdx mouse diaphragm', *American Journal of Physiology-Cell Physiology*, 304: C873-C80.
- Beckman, Joseph S, Tanya W Beckman, Jun Chen, Patricia A Marshall, and Bruce A Freeman. 1990. 'Apparent hydroxyl radical production by peroxynitrite: implications for endothelial injury from nitric oxide and superoxide', *Proceedings of the National Academy of Sciences*, 87: 1620-24.
- Berlett, Barbara S, and Earl R Stadtman. 1997. 'Protein oxidation in aging, disease, and oxidative stress', *Journal of Biological Chemistry*, 272: 20313-16.
- Bobkov, Andrey A, Elena A Bobkova, Earl Homsher, and Emil Reisler. 1997. 'Activation of regulated actin by SH1-modified myosin subfragment 1', *Biochemistry*, 36: 7733-38.
- Bobkova, Elena A, Andrey A Bobkov, Dmitrii I Levitsky, and Emil Reisler. 1999. 'Effects of SH1 and SH2 modifications on myosin similarities and differences', *Biophysical journal*, 76: 1001-07.

- Bonne, Gisele, Lucie Carrier, Pascale Richard, Bernard Hainque, and Ketty Schwartz. 1998. 'Familial hypertrophic cardiomyopathy: from mutations to functional defects', *Circulation research*, 83: 580-93.
- Borejdo, J., A. Shepard, D. Dumka, I. Akopova, J. Talent, A. Malka, and T. P. Burghardt. 2004. 'Changes in orientation of actin during contraction of muscle', *Biophysical journal*, 86: 2308-17.
- Brandt, Philip W, David Roemer, and Fredrick H Schachat. 1990. 'Co-operative activation of skeletal muscle thin filaments by rigor crossbridges: The effect of troponin C extraction', *Journal of molecular biology*, 212: 473-80.
- Brenman, Jay E, Daniel S Chao, Houhui Xia, Ken Aldape, and David S Bredt. 1995. 'Nitric oxide synthase complexed with dystrophin and absent from skeletal muscle sarcolemma in Duchenne muscular dystrophy', *Cell*, 82: 743-52.
- Brennan, Jonathan P, Jonathan IA Miller, William Fuller, Robin Wait, Shajna Begum, Michael J Dunn, and Philip Eaton. 2006. 'The utility of N, N-biotinyl glutathione disulfide in the study of protein S-glutathiolation', *Molecular & Cellular Proteomics*, 5: 215-25.
- Brocca, Lorenza, Jamie S McPhee, Emanuela Longa, Monica Canepari, Olivier Seynnes, Giuseppe De Vito, Maria Antonietta Pellegrino, Marco Narici, and Roberto Bottinelli. 2017. 'Structure and function of human muscle fibres and muscle proteome in physically active older men', *The Journal of Physiology*, 595: 4823-44.
- Brunello, Elisabetta, Luca Fusi, Andrea Ghisleni, So-Jin Park-Holohan, Jesus G Ovejero, Theyencheri Narayanan, and Malcolm Irving. 2020. 'Myosin filament-based regulation of the dynamics of contraction in heart muscle', *Proceedings of the National Academy of Sciences*, 117: 8177-86.
- Burgoyne, Joseph R, Héloïse Mongue-Din, Philip Eaton, and Ajay M Shah. 2012. 'Redox signaling in cardiac physiology and pathology', *Circulation research*, 111: 1091-106.
- Cadenas, E. 1989. 'Biochemistry of oxygen toxicity', *Annu Rev Biochem*, 58: 79-110.
- Cadenas, Enrique, and Alberto Boveris. 1980. 'Enhancement of hydrogen peroxide formation by protophores and ionophores in antimycin-supplemented mitochondria', *Biochemical Journal*, 188: 31-37.
- Callahan, L. A., Z. W. She, and T. M. Nosek. 2001. 'Superoxide, hydroxyl radical, and hydrogen peroxide effects on single-diaphragm fiber contractile apparatus', *J Appl Physiol (1985)*, 90: 45-54.

- Canepari, Monica, Rosetta Rossi, Orietta Pansarasa, Manuela Maffei, and Roberto Bottinelli. 2009. 'Actin sliding velocity on pure myosin isoforms from dystrophic mouse muscles', *Muscle & Nerve: Official Journal of the American Association of Electrodiagnostic Medicine*, 40: 249-56.
- Canton, Marcella, Sara Menazza, and Fabio Di Lisa. 2014. 'Oxidative stress in muscular dystrophy: from generic evidence to specific sources and targets', *Journal of muscle research and cell motility*, 35: 23-36.
- Canton, Marcella, Sara Menazza, Freya L Sheeran, Patrizia Polverino de Laureto, Fabio Di Lisa, and Salvatore Pepe. 2011. 'Oxidation of myofibrillar proteins in human heart failure', *Journal of the American College of Cardiology*, 57: 300-09.
- Canton, Marcella, Irina Neverova, Roberta Menabò, Jennifer Van Eyk, and Fabio Di Lisa. 2004. 'Evidence of myofibrillar protein oxidation induced by postischemic reperfusion in isolated rat hearts', *American Journal of Physiology-Heart and Circulatory Physiology*, 286: H870-H77.
- Canton, Marcella, Andreas Skyschally, Roberta Menabo, Kerstin Boengler, Petra Gres, Rainer Schulz, Michael Haude, Raimund Erbel, Fabio Di Lisa, and Gerd Heusch. 2006. 'Oxidative modification of tropomyosin and myocardial dysfunction following coronary microembolization', *European Heart Journal*, 27: 875-81.
- Capanni, Cristina, Stefano Squarzone, Stefania Petrini, Marcello Villanova, Claudio Muscari, Nadir Mario Maraldi, Carlo Guarnieri, and Claudio Marcello Caldarera. 1998. 'Increase of neuronal nitric oxide synthase in rat skeletal muscle during ageing', *Biochemical and biophysical research communications*, 245: 216-19.
- Capitanio, Daniele, Michele Vasso, Chiara Fania, Manuela Moriggi, Agnese Viganò, Patrizia Procacci, Valerio Magnaghi, and Cecilia Gelfi. 2009. 'Comparative proteomic profile of rat sciatic nerve and gastrocnemius muscle tissues in ageing by 2-D DIGE', *Proteomics*, 9: 2004-20.
- Carballal, Sebastián, Silvina Bartesaghi, and Rafael Radi. 2014. 'Kinetic and mechanistic considerations to assess the biological fate of peroxynitrite', *Biochimica et Biophysica Acta (BBA)-General Subjects*, 1840: 768-80.
- Chance, Britton, Helmut Sies, and Alberto Boveris. 1979. 'Hydroperoxide metabolism in mammalian organs', *Physiological reviews*, 59: 527-605.

- Chang, Tsu-Chung, Wei-Yuan Chou, and Gu-Gang Chang. 2000. 'Protein oxidation and turnover', *Journal of biomedical science*, 7: 357-63.
- Chen, Frank C, and Ozgur Ogut. 2006. 'Decline of contractility during ischemia-reperfusion injury: actin glutathionylation and its effect on allosteric interaction with tropomyosin', *American Journal of Physiology-Cell Physiology*, 290: C719-C727.
- Cheng, Arthur J, Joseph D Bruton, Johanna T Lanner, and Håkan Westerblad. 2015. 'Antioxidant treatments do not improve force recovery after fatiguing stimulation of mouse skeletal muscle fibres', *The Journal of physiology*, 593: 457-72.
- Cheng, Arthur J, Takashi Yamada, Dilson E Rassier, Daniel C Andersson, Håkan Westerblad, and Johanna T Lanner. 2016. 'Reactive oxygen/nitrogen species and contractile function in skeletal muscle during fatigue and recovery', *The Journal of Physiology*, 594: 5149-60.
- Cheung, Herbert C, Ignacy Gryczynski, Henryk Malak, Wieslaw Wiczak, Michael L Johnson, and Joseph R Lakowicz. 1991. 'Conformational flexibility of the Cys 697-Cys 707 segment of myosin subfragment-1: distance distributions by frequency-domain fluorometry', *Biophysical chemistry*, 40: 1-17.
- Coirault, Catherine, Aziz Guellich, Thomas Barbry, Jane Lise Samuel, Bruno Riou, and Yves Lecarpentier. 2007. 'Oxidative stress of myosin contributes to skeletal muscle dysfunction in rats with chronic heart failure', *American Journal of Physiology-Heart and Circulatory Physiology*, 292: H1009-H117.
- Coirault, Catherine, Francine Lambert, Sylvain Marchand-Adam, Pierre Attal, Denis Chemla, and Yves Lecarpentier. 1999. 'Myosin molecular motor dysfunction in dystrophic mouse diaphragm', *American Journal of Physiology-Cell Physiology*, 277: C1170-C76.
- Coirault, Catherine, Francine Lambert, Jean-Claude Pourny, and Yves Lecarpentier. 2002. 'Velocity of actomyosin sliding in vitro is reduced in dystrophic mouse diaphragm', *American Journal of Respiratory and Critical Care Medicine*, 165: 250-53.
- Cooper, Chris E, Rakesh P Patel, Paul S Brookes, and Victor M Darley-Usmar. 2002. 'Nanotransducers in cellular redox signaling: modification of thiols by reactive oxygen and nitrogen species', *Trends Biochem Sci*, 27: 489-92.
- Cremon, CR, JC Grammer, and RG Yount. 1989. 'Direct chemical evidence that serine 180 in the glycine-rich loop of myosin binds to ATP', *Journal of Biological Chemistry*, 264: 6608-11.

- Crowder, MS, and R Cooke. 1984. 'The effect of myosin sulphhydryl modification on the mechanics of fibre contraction', *Journal of Muscle Research & Cell Motility*, 5: 131-46.
- Cuello, Friederike, Ilka Wittig, Kristina Lorenz, and Philip Eaton. 2018. 'Oxidation of cardiac myofilament proteins: Priming for dysfunction?', *Molecular Aspects of Medicine*, 63: 47-58.
- Cunha-Oliveira, Teresa, Liliana Montezinho, Catarina Mendes, Omidreza Firuzi, Luciano Saso, Paulo J Oliveira, and Filomena SG Silva. 2020. 'Oxidative stress in amyotrophic lateral sclerosis: pathophysiology and opportunities for pharmacological intervention', *Oxidative medicine and cellular longevity*, 2020.
- D'Oria, Rossella, Rossella Schipani, Anna Leonardini, Annalisa Natalicchio, Sebastio Perrini, Angelo Cignarelli, Luigi Laviola, and Francesco Giorgino. 2020. 'The role of oxidative stress in cardiac disease: from physiological response to injury factor', *Oxidative medicine and cellular longevity*, 2020.
- Dalle-Donne, I, R Rossi, D Giustarini, N Gagliano, P Di Simplicio, R Colombo, and A Milzani. 2002. 'Methionine oxidation as a major cause of the functional impairment of oxidized actin', *Free Radical Biology and Medicine*, 32: 927-37.
- Dalle-Donne, I, R Rossi, D Giustarini, N Gagliano, L Lusini, A Milzani, P Di Simplicio, and R Colombo. 2001. 'Actin carbonylation: from a simple marker of protein oxidation to relevant signs of severe functional impairment', *Free Radical Biology and Medicine*, 31: 1075-83.
- Dalle-Donne, I., D. Giustarini, R. Rossi, R. Colombo, and A. Milzani. 2003. 'Reversible S-glutathionylation of Cys 374 regulates actin filament formation by inducing structural changes in the actin molecule', *Free Radic Biol Med*, 34: 23-32.
- Dean, Roger T, Shanlin FU, Roland Stocker, and Michael J Davies. 1997. 'Biochemistry and pathology of radical-mediated protein oxidation', *Biochemical Journal*, 324: 1-18.
- Digerness, S. B., K. D. Harris, J. W. Kirklin, F. Urthaler, L. Viera, J. S. Beckman, and V. Darley-Usmar. 1999. 'Peroxyntirite irreversibly decreases diastolic and systolic function in cardiac muscle', *Free Radic Biol Med*, 27: 1386-92.
- Disatnik, Marie-Helene, Jyotsna Dhawan, Yip Yu, M Flint Beal, Michelle M Whirl, Alexa A Franco, and Thomas A Rando. 1998. 'Evidence of oxidative stress in mdx mouse muscle: studies of the pre-necrotic state', *Journal of the neurological Sciences*, 161: 77-84.

- Dominguez, Roberto, Yelena Freyzon, Kathleen M Trybus, and Carolyn Cohen. 1998. 'Crystal structure of a vertebrate smooth muscle myosin motor domain and its complex with the essential light chain: Visualization of the pre-power stroke state', *Cell*, 94: 559-71.
- Doroszko, Adrian, Dorota Polewicz, Virgilio JJ Cadete, Jolanta Sawicka, Michelle Jones, Danuta Szczesna-Cordary, Po-Yin Cheung, and Grzegorz Sawicki. 2010. 'Neonatal asphyxia induces the nitration of cardiac myosin light chain 2 (MLC2) which is associated with cardiac systolic dysfunction', *Shock (Augusta, Ga.)*, 34: 592.
- Doroszko, Adrian, Dorota Polewicz, Jolanta Sawicka, J Steven Richardson, Po-Yin Cheung, and Grzegorz Sawicki. 2009. 'Cardiac dysfunction in an animal model of neonatal asphyxia is associated with increased degradation of MLC1 by MMP-2', *Basic research in cardiology*, 104: 669.
- Dos Santos, Sofia Lourenço, Martin A Baraibar, Staffan Lundberg, Orvar Eeg-Olofsson, Lars Larsson, and Bertrand Friguet. 2015. 'Oxidative proteome alterations during skeletal muscle ageing', *Redox biology*, 5: 267-74.
- Droge, Wulf. 2002. 'Free radicals in the physiological control of cell function', *Physiological reviews*, 82: 47-95.
- Du, Jie, Xiaonan Wang, Christiane Miereles, James L Bailey, Richard Debigare, Bin Zheng, S Russ Price, and William E Mitch. 2004. 'Activation of caspase-3 is an initial step triggering accelerated muscle proteolysis in catabolic conditions', *The Journal of clinical investigation*, 113: 115-23.
- Duke, J, R Takashi, K Ue, and MF Morales. 1976. 'Reciprocal reactivities of specific thiols when actin binds to myosin', *Proceedings of the National Academy of Sciences*, 73: 302-06.
- Durham, W. J., P. Aracena-Parks, C. Long, A. E. Rossi, S. A. Goonasekera, S. Boncompagni, D. L. Galvan, C. P. Gilman, M. R. Baker, N. Shirokova, F. Protasi, R. Dirksen, and S. L. Hamilton. 2008. 'RyR1 S-nitrosylation underlies environmental heat stroke and sudden death in Y522S RyR1 knockin mice', *Cell*, 133: 53-65.
- Dutka, T. L., J. P. Mollica, and G. D. Lamb. 2011. 'Differential effects of peroxynitrite on contractile protein properties in fast- and slow-twitch skeletal muscle fibers of rat', *Journal of Applied Physiology*, 110: 705-16.
- Eaton, Philip, Helen L Byers, Nicola Leeds, Malcolm A Ward, and Michael J Shattock. 2002. 'Detection, quantitation, purification, and identification of cardiac proteins S-thiolated during ischemia and reperfusion', *Journal of Biological Chemistry*, 277: 9806-11.

- Eisenberg, Evan, and Terrell L Hill. 1985. 'Muscle contraction and free energy transduction in biological systems', *Science*, 227: 999-1006.
- El-Shafey, Ahmed F, Alexander E Armstrong, Jessica R Terrill, Miranda D Grounds, and Peter G Arthur. 2011. 'Screening for increased protein thiol oxidation in oxidatively stressed muscle tissue', *Free Radical Research*, 45: 991-99.
- Elkrief, Daren, Yu-Shu Cheng, Oleg S Matusovsky, and Dilson E Rassier. 2022. 'Oxidation alters myosin-actin interaction and force generation in skeletal muscle filaments', *American Journal of Physiology-Cell Physiology*, 323: C1206-C14.
- Fabian, F, and A Mühlrad. 1968. 'Effect of trinitrophenylation on myosin ATPase', *Biochimica et Biophysica Acta (BBA)-Bioenergetics*, 162: 596-603.
- Farah, Michelle E., Vladimir Sirotkin, Brian Haarer, David Kakhniashvili, and David C. Amberg. 2011. 'Diverse protective roles of the actin cytoskeleton during oxidative stress', *Cytoskeleton (Hoboken, N.J.)*, 68: 340-54.
- Fedorova, Maria, Toni Todorovsky, Nadezda Kuleva, and Ralf Hoffmann. 2010. 'Quantitative evaluation of tryptophan oxidation in actin and troponin I from skeletal muscles using a rat model of acute oxidative stress', *Proteomics*, 10: 2692-700.
- Ferreira, L. F., and M. B. Reid. 2008. 'Muscle-derived ROS and thiol regulation in muscle fatigue', *J Appl Physiol (1985)*, 104: 853-60.
- Fisher, Andrew J, Clyde A Smith, James Thoden, Robert Smith, Kazuo Sutoh, Hazel M Holden, and Ivan Rayment. 1995a. 'Structural studies of myosin: nucleotide complexes: a revised model for the molecular basis of muscle contraction', *Biophysical journal*, 68: 19S.
- . 1995b. 'X-ray structures of the myosin motor domain of dictyostelium discoideum complexed with MgADP. cntdot. BeFx and MgADP. cntdot. AlF4', *Biochemistry*, 34: 8960-72.
- Forman, Henry Jay, and Hongqiao Zhang. 2021. 'Targeting oxidative stress in disease: Promise and limitations of antioxidant therapy', *Nature Reviews Drug Discovery*, 20: 689-709.
- Förstermann, U, Ellen I Closs, Jennifer S Pollock, Masaki Nakane, Petra Schwarz, Ingo Gath, and Hartmut Kleinert. 1994. 'Nitric oxide synthase isozymes. Characterization, purification, molecular cloning, and functions', *Hypertension*, 23: 1121-31.
- Fujii, T., and K. Namba. 2017. 'Structure of actomyosin rigour complex at 5.2 Å resolution and insights into the ATPase cycle mechanism', *Nat Commun*, 8: 13969.

- Fujii, Takashi, Atsuko H. Iwane, Toshio Yanagida, and Keiichi Namba. 2010. 'Direct visualization of secondary structures of F-actin by electron cryomicroscopy', *Nature*, 467: 724-28.
- Furch, Marcus, Setsuko Fujita-Becker, Michael A Geeves, Kenneth C Holmes, and Dietmar J Manstein. 1999. 'Role of the salt-bridge between switch-1 and switch-2 of Dictyostelium myosin', *Journal of molecular biology*, 290: 797-809.
- Galińska-Rakoczy, Agnieszka, Patti Engel, Chen Xu, HyunSuk Jung, Roger Craig, Larry S Tobacman, and William Lehman. 2008. 'Structural basis for the regulation of muscle contraction by troponin and tropomyosin', *Journal of molecular biology*, 379: 929-35.
- Galler, S, Karlheinz Hilber, and Alfred Göbesberger. 1997. 'Effects of nitric oxide on force-generating proteins of skeletal muscle', *Pflügers Archiv*, 434: 242-45.
- Gannon, Joan, Philip Doran, Anne Kirwan, and Kay Ohlendieck. 2009. 'Drastic increase of myosin light chain MLC-2 in senescent skeletal muscle indicates fast-to-slow fibre transition in sarcopenia of old age', *European journal of cell biology*, 88: 685-700.
- Gao, Wei Dong, Yongge Liu, and Eduardo Marban. 1996. 'Selective effects of oxygen free radicals on excitation-contraction coupling in ventricular muscle: implications for the mechanism of stunned myocardium', *Circulation*, 94: 2597-604.
- Gao, Wei Dong, Christopher I Murray, Ye Tian, Xin Zhong, Jenna F DuMond, Xiaoxu Shen, Brian A Stanley, D Brian Foster, David A Wink, and S Bruce King. 2012. 'Nitroxyl-mediated disulfide bond formation between cardiac myofilament cysteines enhances contractile function', *Circulation research*, 111: 1002-11.
- Geeves, Michael A, and Kenneth C Holmes. 2005. 'The molecular mechanism of muscle contraction', *Advances in protein chemistry*, 71: 161-93.
- Gelfi, Cecilia, Agnese Viganò, Marilena Ripamonti, Alessandro Pontoglio, Shajna Begum, Maria Antonietta Pellegrino, Bruno Grassi, Roberto Bottinelli, Robin Wait, and Paolo Cerretelli. 2006. 'The human muscle proteome in aging', *J Proteome Res*, 5: 1344-53.
- Giordano, Frank J. 2005. 'Oxygen, oxidative stress, hypoxia, and heart failure', *The Journal of clinical investigation*, 115: 500-08.
- Gollub, Jeremy, Christine R Cremo, and Roger Cooke. 1996. 'ADP release produces a rotation of the neck region of smooth myosin but not skeletal myosin', *Nature structural biology*, 3: 796-802.
- Gomes, Aldrin V, James D Potter, and Danuta Szczesna-Cordary. 2002. 'The role of troponins in muscle contraction', *IUBMB life*, 54: 323-33.

- Gomez-Cabrera, Mari Carmen, Graeme L Close, A Kayani, Anne McArdle, Jose Vina, and Malcolm J Jackson. 2010. 'Effect of xanthine oxidase-generated extracellular superoxide on skeletal muscle force generation', *American Journal of Physiology-Regulatory, Integrative and Comparative Physiology*, 298: R2-R8.
- Grammer, JC, and RG Yount. 1991. 'Photochemical evidence that Ser-243 of myosin's heavy chain is near the phosphate binding site for ATP', *Biophys. J*, 59: 226a.
- Gross, Sean M, and Steven L Lehman. 2013. 'Accessibility of myofilament cysteines and effects on ATPase depend on the activation state during exposure to oxidants', *PLoS One*, 8.
- Guellich, Aziz, Elisa Negroni, Valérie Decostre, Alexandre Demoule, and Catherine Coirault. 2014. 'Altered cross-bridge properties in skeletal muscle dystrophies', *Frontiers in physiology*, 5: 393.
- Harris, Samantha P, Ross G Lyons, and Kristina L Bezold. 2011. 'In the thick of it: HCM-causing mutations in myosin binding proteins of the thick filament', *Circulation research*, 108: 751-64.
- Haycock, John W, Peter Jones, John B Harris, and David Mantle. 1996. 'Differential susceptibility of human skeletal muscle proteins to free radical induced oxidative damage: a histochemical, immunocytochemical and electron microscopical study in vitro', *Acta neuropathologica*, 92: 331-40.
- Hertelendi, Zita, Attila Toth, Attila Borbely, Zoltan Galajda, Jolanda Van Der Velden, Ger JM Stienen, Istvan Edes, and Zoltan Papp. 2008. 'Oxidation of myofilament protein sulfhydryl groups reduces the contractile force and its Ca²⁺ sensitivity in human cardiomyocytes', *Antioxid Redox Signal*, 10: 1175-84.
- Holmes, Kenneth C. 1997. 'The swinging lever-arm hypothesis of muscle contraction', *Current Biology*, 7: R112-R18.
- Hong, Sung Jung, Giridharan Gokulrangan, and Christian Schöneich. 2007. 'Proteomic analysis of age dependent nitration of rat cardiac proteins by solution isoelectric focusing coupled to nanoHPLC tandem mass spectrometry', *Experimental gerontology*, 42: 639-51.
- Höök, Peter, Xiaopeng Li, John Sleep, Simon Hughes, and Lars Larsson. 1999. 'In vitro motility speed of slow myosin extracted from single soleus fibres from young and old rats', *The Journal of Physiology*, 520: 463-71.

- Höök, Peter, Vidyasagar Sriramoju, and Lars Larsson. 2001. 'Effects of aging on actin sliding speed on myosin from single skeletal muscle cells of mice, rats, and humans', *American Journal of Physiology-Cell Physiology*, 280: C782-C88.
- Hool, Livia C. 2009. 'The L-type Ca²⁺ channel as a potential mediator of pathology during alterations in cellular redox state', *Heart, Lung and Circulation*, 18: 3-10.
- Houdusse, A, Andrew G Szent-Györgyi, and Carolyn Cohen. 2000. 'Three conformational states of scallop myosin S1', *Proceedings of the National Academy of Sciences*, 97: 11238-43.
- Hozumi, Tetsu, and Andras Muhlrád. 1981. 'Reactive lysyl of myosin subfragment 1: location on the 27K fragment and labeling properties', *Biochemistry*, 20: 2945-50.
- Hutchinson, Kirk R, James A Stewart Jr, and Pamela A Lucchesi. 2010. 'Extracellular matrix remodeling during the progression of volume overload-induced heart failure', *Journal of molecular and cellular cardiology*, 48: 564-69.
- Huxley, Andrew F. 1957. 'Muscle structure and theories of contraction', *Prog. Biophys. Biophys. Chem*, 7: 255-318.
- Hvid, Lars G, Niels Ørtenblad, Per Aagaard, Michael Kjaer, and Charlotte Suetta. 2011. 'Effects of ageing on single muscle fibre contractile function following short-term immobilisation', *The Journal of Physiology*, 589: 4745-57.
- Hvid, Lars G, Charlotte Suetta, Per Aagaard, Michael Kjaer, Ulrik Frandsen, and Niels Ørtenblad. 2013. 'Four days of muscle disuse impairs single fiber contractile function in young and old healthy men', *Experimental gerontology*, 48: 154-61.
- Jackson, MJ, RHT Edwards, and MCR Symons. 1985. 'Electron spin resonance studies of intact mammalian skeletal muscle', *Biochimica et Biophysica Acta (BBA)-Molecular Cell Research*, 847: 185-90.
- Kanski, Jaroslaw, Antje Behring, Jill Pelling, and Christian Schoneich. 2005. 'Proteomic identification of 3-nitrotyrosine-containing rat cardiac proteins: effects of biological aging', *American Journal of Physiology-Heart and Circulatory Physiology*, 288: H371-H81.
- Kanski, Jaroslaw, Sung J Hong, and Christian Schöneich. 2005. 'Proteomic analysis of protein nitration in aging skeletal muscle and identification of nitrotyrosine-containing sequences in vivo by nanoelectrospray ionization tandem mass spectrometry', *Journal of Biological Chemistry*, 280: 24261-66.
- Kapchinsky, S., M. Vuda, K. Miguez, D. Elkrief, A. R. de Souza, C. J. Baglole, S. Aare, N. J. MacMillan, J. Baril, P. Rozakis, V. Sonjak, C. Pion, M. Aubertin-Leheudre, J. A. Morais,

- R. T. Jagoe, J. Bourbeau, T. Taivassalo, and R. T. Hepple. 2018. 'Smoke-induced neuromuscular junction degeneration precedes the fibre type shift and atrophy in chronic obstructive pulmonary disease', *J Physiol*, 596: 2865-81.
- Khassaf, M, A McArdle, C Esanu, A Vasilaki, F McArdle, RD Griffiths, DA Brodie, and MJ Jackson. 2003. 'Effect of vitamin C supplements on antioxidant defence and stress proteins in human lymphocytes and skeletal muscle', *The Journal of Physiology*, 549: 645-52.
- Kirshenbaum, Kent, Sandor Papp, and Stefan Highsmith. 1993. 'Cross-linking myosin subfragment 1 Cys-697 and Cys-707 modifies ATP and actin binding site interactions', *Biophysical journal*, 65: 1121-29.
- Klein, Jennifer C, Rebecca J Moen, Evan A Smith, Margaret A Titus, and David D Thomas. 2011. 'Structural and functional impact of site-directed methionine oxidation in myosin', *Biochemistry*, 50: 10318-27.
- Kobzik, Lester, Michael B Reid, David S Bredt, and Jonathan S Stamler. 1994. 'Nitric oxide in skeletal muscle', *Nature*, 372: 546-48.
- Kovács, Mihály, Judit Tóth, Csaba Hetényi, András Málnási-Csizmadia, and James R Sellers. 2004. 'Mechanism of blebbistatin inhibition of myosin II', *Journal of Biological Chemistry*, 279: 35557-63.
- Kress, M, HE Huxley, AR Faruqi, and J Hendrix. 1986. 'Structural changes during activation of frog muscle studied by time-resolved X-ray diffraction', *Journal of molecular biology*, 188: 325-42.
- Kubo, Shuichiro, Seiichi Tokura, and Yuji Tonomura. 1960. 'On the active site of myosin A-adenosine triphosphatase I. Reaction of the enzyme with trinitrobenzenesulfonate', *Journal of Biological Chemistry*, 235: 2835-39.
- Lamb, G. D., and G. S. Posterino. 2003. 'Effects of oxidation and reduction on contractile function in skeletal muscle fibres of the rat', *J Physiol*, 546: 149-63.
- Lamb, Graham D, and Håkan Westerblad. 2011. 'Acute effects of reactive oxygen and nitrogen species on the contractile function of skeletal muscle', *The Journal of physiology*, 589: 2119-27.
- Lamboley, CR, VL Wyckelsma, TL Dutka, MJ McKenna, RM Murphy, and GD Lamb. 2015. 'Contractile properties and sarcoplasmic reticulum calcium content in type I and type II skeletal muscle fibres in active aged humans', *The Journal of Physiology*, 593: 2499-514.

- Larsson, Lars, Xiaopeng Li, and WR Frontera. 1997. 'Effects of aging on shortening velocity and myosin isoform composition in single human skeletal muscle cells', *American Journal of Physiology-Cell Physiology*, 272: C638-C49.
- Lawler, John M. 2011. 'Exacerbation of pathology by oxidative stress in respiratory and locomotor muscles with Duchenne muscular dystrophy', *The Journal of Physiology*, 589: 2161-70.
- Le Moal, Emmeran, Vincent Pialoux, Gaëtan Juban, Carole Groussard, Hassane Zouhal, Bénédicte Chazaud, and Rémi Mounier. 2017. 'Redox control of skeletal muscle regeneration', *Antioxid Redox Signal*, 27: 276-310.
- Li, Meishan, Hannah Ogilvie, Julien Ochala, Konstantin Artemenko, Hiroyuki Iwamoto, Naoto Yagi, Jonas Bergquist, and Lars Larsson. 2015. 'Aberrant post-translational modifications compromise human myosin motor function in old age', *Aging cell*, 14: 228-35.
- Li, XIAOPENG, and LARS Larsson. 1996. 'Maximum shortening velocity and myosin isoforms in single muscle fibers from young and old rats', *American Journal of Physiology-Cell Physiology*, 270: C352-C60.
- Lian, Di, Ming-Ming Chen, Hanyu Wu, Shoulong Deng, and Xiaoxiang Hu. 2022. 'The Role of Oxidative Stress in Skeletal Muscle Myogenesis and Muscle Disease', *Antioxidants*, 11: 755.
- Liguori, Ilaria, Gennaro Russo, Francesco Curcio, Giulia Bulli, Luisa Aran, David Della-Morte, Gaetano Gargiulo, Gianluca Testa, Francesco Cacciatore, Domenico Bonaduce, and Pasquale Abete. 2018. 'Oxidative stress, aging, and diseases', *Clinical interventions in aging*, 13: 757-72.
- Liu, Xiong, Shi Shu, Myoung-Soon S Hong, Rodney L Levine, and Edward D Korn. 2006. 'Phosphorylation of actin Tyr-53 inhibits filament nucleation and elongation and destabilizes filaments', *Proceedings of the National Academy of Sciences*, 103: 13694-99.
- Liu, Xiong, Shi Shu, Myoung-Soon S Hong, Bin Yu, and Edward D Korn. 2010. 'Mutation of actin Tyr-53 alters the conformations of the DNase I-binding loop and the nucleotide-binding cleft', *Journal of Biological Chemistry*, 285: 9729-39.
- Lombardi, Vincenzo, Gabriella Piazzesi, and Marco Linari. 1992. 'Rapid regeneration of the actin-myosin power stroke in contracting muscle', *Nature*, 355: 638-41.
- Louie, Jennifer L, Rebecca J Kappahn, and Deborah A Ferrington. 2002. 'Proteasome function and protein oxidation in the aged retina', *Experimental eye research*, 75: 271-84.

- Lovelock, Joshua D, Michelle M Monasky, Euy-Myoung Jeong, Harvey A Lardin, Hong Liu, Bindhya G Patel, Domenico M Taglieri, Lianzhi Gu, Praveen Kumar, and Narayan Pokhrel. 2012. 'Ranolazine improves cardiac diastolic dysfunction through modulation of myofilament calcium sensitivity', *Circulation research*, 110: 841-50.
- Lowe, Dawn A, Jack T Surek, David D Thomas, and LaDora V Thompson. 2001. 'Electron paramagnetic resonance reveals age-related myosin structural changes in rat skeletal muscle fibers', *American Journal of Physiology-Cell Physiology*, 280: C540-C47.
- Lowe, Dawn A, Gordon L Warren, LeAnn M Snow, LaDora V Thompson, and David D Thomas. 2004. 'Muscle activity and aging affect myosin structural distribution and force generation in rat fibers', *Journal of applied physiology*, 96: 498-506.
- Lu, Jingshan, Tayo Katano, Daisuke Uta, Hidemasa Furue, and Seiji Ito. 2011. 'Rapid S-nitrosylation of actin by NO-generating donors and in inflammatory pain model mice', *Molecular pain*, 7: 1744-8069-7-101.
- Luo, Jianzhu, Yu-Ting Xuan, Yan Gu, and Sumanth D Prabhu. 2006. 'Prolonged oxidative stress inverts the cardiac force–frequency relation: role of altered calcium handling and myofilament calcium responsiveness', *Journal of molecular and cellular cardiology*, 40: 64-75.
- MacFarlane, NG, and DJ Miller. 1992. 'Depression of peak force without altering calcium sensitivity by the superoxide anion in chemically skinned cardiac muscle of rat', *Circulation research*, 70: 1217-24.
- Mahmood, Riaz, Marshall Elzinga, and Ralph G Yount. 1989. 'Serine-324 of myosin's heavy chain is photoaffinity-labeled by 3'(2')-O-(4-benzoylbenzoyl) adenosine triphosphate', *Biochemistry*, 28: 3989-95.
- Maita, Tetsuo, Eiko Yajima, Shuichi Nagata, Takayuki Miyanishi, Susumu Nakayama, and Genji Matsuda. 1991. 'The primary structure of skeletal muscle myosin heavy chain: IV. Sequence of the rod, and the complete 1,938-residue sequence of the heavy chain', *The Journal of Biochemistry*, 110: 75-87.
- Málnási-Csizmadia, András, Judit Tóth, David S Pearson, Csaba Hetényi, László Nyitray, Michael A Geeves, Clive R Bagshaw, and Mihály Kovács. 2007. 'Selective perturbation of the myosin recovery stroke by point mutations at the base of the lever arm affects ATP hydrolysis and phosphate release', *Journal of Biological Chemistry*, 282: 17658-64.

- Marechal, G., and P. Gailly. 1999. 'Effects of nitric oxide on the contraction of skeletal muscle', *Cell Mol Life Sci*, 55: 1088-102.
- Markus, Barak, Ginat Narkis, Daniella Landau, Ruth Z Birk, Idan Cohen, and Ohad S Birk. 2012. 'Autosomal recessive lethal congenital contractural syndrome type 4 (LCCS4) caused by a mutation in MYBPC1', *Human mutation*, 33: 1435-38.
- Martin-Romero, Francisco Javier, Yolanda Gutiérrez-Martin, Fernando Henao, and Carlos Gutiérrez-Merino. 2004. 'Fluorescence measurements of steady state peroxynitrite production upon SIN-1 decomposition: NADH versus dihydrodichlorofluorescein and dihydrorhodamine 123', *Journal of fluorescence*, 14: 17-23.
- Masuko, Kayo. 2014. 'Rheumatoid cachexia revisited: a metabolic co-morbidity in rheumatoid arthritis', *Frontiers in nutrition*, 1: 20-20.
- Matecki, S, J Fauconnier, and A Lacampagne. 2014. "Reactive oxygen species and muscular dystrophy." In, 3055-79. Springer: Berlin Heidelberg.
- McArdle, Anne, Wolfgang H Dillmann, Ruben Mestril, John Faulkner, and Malcolm J Jackson. 2004. 'Overexpression of HSP70 in mouse skeletal muscle protects against muscle damage and age-related muscle dysfunction'.
- McArdle, F, S Spiers, H Aldemir, A Vasilaki, A Beaver, L Iwanejko, A McArdle, and MJ Jackson. 2004. 'Preconditioning of skeletal muscle against contraction-induced damage: the role of adaptations to oxidants in mice', *The Journal of Physiology*, 561: 233-44.
- Mehra, Anilkumar, Avraham Shotan, Enrique Ostrzega, Willa Hsueh, Janet Vasquez-Johnson, and Uri Elkayam. 1994. 'Potentiation of isosorbide dinitrate effects with N-acetylcysteine in patients with chronic heart failure', *Circulation*, 89: 2595-600.
- Menazza, Sara, Angel Aponte, Junhui Sun, Marjan Gucek, Charles Steenbergen, and Elizabeth Murphy. 2015. 'Molecular signature of nitroso-redox balance in idiopathic dilated cardiomyopathies', *Journal of the American Heart Association*, 4: e002251.
- Menazza, Sara, Bert Blaauw, Tania Tiepolo, Luana Toniolo, Paola Braghetta, Barbara Spolaore, Carlo Reggiani, Fabio Di Lisa, Paolo Bonaldo, and Marcella Canton. 2010. 'Oxidative stress by monoamine oxidases is causally involved in myofiber damage in muscular dystrophy', *Human molecular genetics*, 19: 4207-15.
- Menon, SG, and PC Goswami. 2007. 'A redox cycle within the cell cycle: ring in the old with the new', *Oncogene*, 26: 1101-09.

- Merry, Troy L, and Michael Ristow. 2016. 'Do antioxidant supplements interfere with skeletal muscle adaptation to exercise training?', *The Journal of physiology*, 594: 5135-47.
- Metzger, Joseph M. 1995. 'Myosin binding-induced cooperative activation of the thin filament in cardiac myocytes and skeletal muscle fibers', *Biophysical journal*, 68: 1430-42.
- Mihm, Michael J, Fushun Yu, Peter J Reiser, and John Anthony Bauer. 2003. 'Effects of peroxynitrite on isolated cardiac trabeculae: selective impact on myofibrillar energetic controllers', *Biochimie*, 85: 587-96.
- Miki, Masao, and Cristobal G dos %J The Journal of Biochemistry Remedios. 1988. 'Fluorescence quenching studies of fluorescein attached to Lys-61 or Cys-374 in actin: effects of polymerization, myosin subfragment-1 binding, and tropomyosin-troponin binding', 104: 232-35.
- Milzani, A., R. Rossi, P. Di Simplicio, D. Giustarini, R. Colombo, and I. DalleDonne. 2000. 'The oxidation produced by hydrogen peroxide on Ca-ATP-G-actin', *Protein science : a publication of the Protein Society*, 9: 1774-82.
- Moen, Rebecca J, Sinziana Cornea, Daniel E Oseid, Benjamin P Binder, Jennifer C Klein, and David D Thomas. 2014. 'Redox-sensitive residue in the actin-binding interface of myosin', *Biochemical and biophysical research communications*, 453: 345-49.
- Mollica, JP, TL Dutka, TL Merry, Cedric R Lamboley, GK McConell, Michael J McKenna, Robyn Maree Murphy, and GD Lamb. 2012. 'S-Glutathionylation of troponin I (fast) increases contractile apparatus Ca²⁺ sensitivity in fast-twitch muscle fibres of rats and humans', *The Journal of Physiology*, 590: 1443-63.
- Moretto, Luisa, Marko Ušaj, Oleg Matusovsky, Dilson E Rassier, Ran Friedman, and Alf Månsson. 2022. 'Multistep orthophosphate release tunes actomyosin energy transduction', *Nature communications*, 13: 4575.
- Mornet, D, P Pantel, R Bertrand, E Audemard, and R Kassab. 1980. 'Localization of the reactive trinitrophenylated lysyl residue of myosin ATPase site in the NH₂-terminal (27 k domain) of S1 heavy chain', *FEBS letters*, 117: 183-88.
- Morrison, RJ, CC Miller 3rd, and Michael B Reid. 1996. 'Nitric oxide effects on shortening velocity and power production in the rat diaphragm', *Journal of applied physiology*, 80: 1065-69.
- Muhlrad, Andras. 1983. 'Mechanism of adenosine triphosphatase activity of trinitrophenylated myosin subfragment 1', *Biochemistry*, 22: 3653-60.

- Münzel, Thomas, Giovanni G Camici, Christoph Maack, Nicole R Bonetti, Valentin Fuster, and Jason C Kovacic. 2017. 'Impact of oxidative stress on the heart and vasculature: part 2 of a 3-part series', *Journal of the American College of Cardiology*, 70: 212-29.
- Murphy, Michael P. 2009. 'How mitochondria produce reactive oxygen species', *Biochemical Journal*, 417: 1-13.
- Murphy, RM, TL Dutka, and GD Lamb. 2008. 'Hydroxyl radical and glutathione interactions alter calcium sensitivity and maximum force of the contractile apparatus in rat skeletal muscle fibres', *The Journal of Physiology*, 586: 2203-16.
- Murray, Christopher I, Wei Dong Gao, Xin Zhong, Brian A Stanley, D Brain Foster, S Bruce King, David A Wink, Jennifer E Van Eyk, and Nazareno Paolucci. 2009. "HNO Induces a Disulfide Bond Between Cysteine Residues on Actin (Cys 257) and Tropomyosin (Cys 190) Increasing Cardiac Force Development: A Novel, Redox-based Mechanism for Contractile Regulation." In.: Am Heart Assoc.
- Nag, Suman, Darshan V Trivedi, Saswata S Sarkar, Arjun S Adhikari, Margaret S Sunitha, Shirley Sutton, Kathleen M Ruppel, and James A Spudich. 2017. 'The myosin mesa and the basis of hypercontractility caused by hypertrophic cardiomyopathy mutations', *Nature Structural & Molecular Biology*, 24: 525-33.
- Nagashima, Hajime, and Sho Asakura. 1982. 'Studies on co-operative properties of tropomyosin-actin and tropomyosin-troponin-actin complexes by the use of N-ethylmaleimide-treated and untreated species of myosin subfragment 1', *Journal of molecular biology*, 155: 409-28.
- Nethery, D, LA Callahan, D Stofan, R Mattera, A DiMarco, and G Supinski. 2000. 'PLA2 dependence of diaphragm mitochondrial formation of reactive oxygen species', *Journal of applied physiology*, 89: 72-80.
- Nogueira, L., C. Figueiredo-Freitas, G. Casimiro-Lopes, M. H. Magdesian, J. Assreuy, and M. M. Sorenson. 2009. 'Myosin is reversibly inhibited by S-nitrosylation', *Biochem J*, 424: 221-31.
- Nuttall, SL, MJ Kendall, and U Martin. 1999. 'Antioxidant therapy for the prevention of cardiovascular disease', *QJM*, 92: 239-44.
- Offer, Gerald, and KW Ranatunga. 2020. 'The Location and Rate of the Phosphate Release Step in the Muscle Cross-Bridge Cycle', *Biophysical journal*, 119: 1501-12.

- Oh-Ishi, M., T. Ueno, and T. Maeda. 2003. 'Proteomic method detects oxidatively induced protein carbonyls in muscles of a diabetes model Otsuka Long-Evans Tokushima Fatty (OLETF) rat', *Free Radic Biol Med*, 34: 11-22.
- Orlova, A., and E. H. Egelman. 1997. 'Cooperative rigor binding of myosin to actin is a function of F-actin structure', *Journal of molecular biology*, 265: 469-74.
- Ostap, E Michael, Howard D White, and David D Thomas. 1993. 'Transient detection of spin-labeled myosin subfragment 1 conformational states during ATP hydrolysis', *Biochemistry*, 32: 6712-20.
- Ostap, E. M., and D. D. Thomas. 1991. 'Rotational dynamics of spin-labeled F-actin during activation of myosin S1 ATPase using caged ATP', *Biophys J*, 59: 1235-41.
- Otten, Egbert. 1988. 'Concepts and models of functional architecture in skeletal muscle', *Exercise and sport sciences reviews*, 16: 89-138.
- Oztug Durer, Zeynep A., J. K. Amisha Kamal, Sabrina Benchaar, Mark R. Chance, and Emil Reisler. 2011. 'Myosin binding surface on actin probed by hydroxyl radical footprinting and site-directed labels', *Journal of molecular biology*, 414: 204-16.
- Pal, Rituraj, Poulami Basu Thakur, Shumin Li, Charles Minard, and George G Rodney. 2013. 'Real-time imaging of NADPH oxidase activity in living cells using a novel fluorescent protein reporter', *PloS one*, 8: e63989.
- Passarelli, Chiara, Almerinda Di Venere, Nicoletta Piroddi, Anna Pastore, Beatrice Scellini, Chiara Tesi, Stefania Petrini, Patrizio Sale, Enrico Bertini, and Corrado Poggesi. 2010. 'Susceptibility of isolated myofibrils to in vitro glutathionylation: potential relevance to muscle functions', *Cytoskeleton*, 67: 81-89.
- Passarelli, Chiara, Stefania Petrini, Anna Pastore, Valentina Bonetto, Patrizio Sale, Laura M Gaeta, Giulia Tozzi, Enrico Bertini, Monica Canepari, and Rosetta Rossi. 2008. 'Myosin as a potential redox-sensor: an in vitro study', *Journal of muscle research and cell motility*, 29: 119-26.
- Pastore, Anna, Giulia Tozzi, Laura Maria Gaeta, Enrico Bertini, Valentina Serafini, Silvia Di Cesare, Valentina Bonetto, Filippo Casoni, Rosalba Carrozzo, and Giorgio Federici. 2003. 'Actin glutathionylation increases in fibroblasts of patients with Friedreich's ataxia: a potential role in the pathogenesis of the disease', *Journal of Biological Chemistry*, 278: 42588-95.

- Pate, E, KL Nakamaye, K Franks-Skiba, RG Yount, and R Cooke. 1991. 'Mechanics of glycerinated muscle fibers using nonnucleoside triphosphate substrates', *Biophysical journal*, 59: 598-605.
- Patel, Bindiya G, Tanganyika Wilder, and R John Solaro. 2013. 'Novel control of cardiac myofilament response to calcium by S-glutathionylation at specific sites of myosin binding protein C', *Frontiers in physiology*, 4: 336.
- Peoples, Jessica N, Anita Saraf, Nasab Ghazal, Tyler T Pham, and Jennifer Q Kwong. 2019. 'Mitochondrial dysfunction and oxidative stress in heart disease', *Experimental & molecular medicine*, 51: 1-13.
- Perkins, William J, Young-Soo Han, and Gary C Sieck. 1997. 'Skeletal muscle force and actomyosin ATPase activity reduced by nitric oxide donor', *Journal of applied physiology*, 83: 1326-32.
- Persson, Malin, Maarten M Steinz, Håkan Westerblad, Johanna T Lanner, and Dilson E Rassier. 2019. 'Force generated by myosin cross-bridges is reduced in myofibrils exposed to ROS/RNS', *American Journal of Physiology-Cell Physiology*, 317: C1304-C12.
- Peyster, Y Michael, Andras Muhrad, and Moshe M Werber. 1990. 'Tryptophan-130 is the most reactive tryptophan residue in rabbit skeletal myosin subfragment-1', *FEBS letters*, 259: 346-48.
- Pfeilschifter, J., W. Eberhardt, and A. Huwiler. 2001. 'Nitric oxide and mechanisms of redox signalling: matrix and matrix-metabolizing enzymes as prime nitric oxide targets', *Eur J Pharmacol*, 429: 279-86.
- Phillips, L., F. Separovic, B. A. Cornell, J. A. Barden, and C. G. dos Remedios. 1991. 'Actin dynamics studied by solid-state NMR spectroscopy', *European Biophysics Journal*, 19: 147-55.
- Pinto, José Renato, Valeria Pereira de Sousa, and Martha M Sorenson. 2011. 'Redox state of troponin C cysteine in the D/E helix alters the C-domain affinity for the thin filament of vertebrate striated muscle', *Biochimica et Biophysica Acta (BBA)-General Subjects*, 1810: 391-97.
- Pizarro, Gresin O, and Ozgur Ogut. 2009. 'Impact of actin glutathionylation on the actomyosin-S1 ATPase', *Biochemistry*, 48: 7533-38.
- Polewicz, Dorota, Virgilio JJ Cadete, Adrian Doroszko, Beth E Hunter, Jolanta Sawicka, Danuta Szczesna-Cordary, Peter E Light, and Grzegorz Sawicki. 2011. 'Ischemia induced

- peroxynitrite dependent modifications of cardiomyocyte MLC1 increases its degradation by MMP-2 leading to contractile dysfunction', *Journal of cellular and molecular medicine*, 15: 1136-47.
- Polewicz, Dorota Katarzyna. 2011. 'Oxidative stress-induced, peroxynitrite-dependent, modifications of myosin light chain 1 lead to its increased degradation by matrix metalloproteinase-2', Citeseer.
- Powers, Scott K, and Malcolm J Jackson. 2008. 'Exercise-induced oxidative stress: cellular mechanisms and impact on muscle force production', *Physiological reviews*, 88: 1243-76.
- Powers, Scott K, Li Li Ji, Andreas N Kavazis, and Malcolm J Jackson. 2011. 'Reactive oxygen species: impact on skeletal muscle', *Comprehensive Physiology*, 1: 941-69.
- Prochniewicz, Ewa, Dawn A Lowe, Daniel J Spakowicz, LeeAnn Higgins, Kate O'Connor, LaDora V Thompson, Deborah A Ferrington, and David D Thomas. 2008. 'Functional, structural, and chemical changes in myosin associated with hydrogen peroxide treatment of skeletal muscle fibers', *American Journal of Physiology-Cell Physiology*, 294: C613-C26.
- Prochniewicz, Ewa, Daniel Spakowicz, and David D. Thomas. 2008. 'Changes in actin structural transitions associated with oxidative inhibition of muscle contraction', *Biochemistry*, 47: 11811-17.
- Prochniewicz, Ewa, LaDora V. Thompson, and David D. Thomas. 2007. 'Age-related decline in actomyosin structure and function', *Experimental gerontology*, 42: 931-38.
- Pye, Deborah, Jesus Palomero, Tabitha Kabayo, and Malcolm J Jackson. 2007. 'Real-time measurement of nitric oxide in single mature mouse skeletal muscle fibres during contractions', *The Journal of physiology*, 581: 309-18.
- Quinlan, Casey L, Jason R Treberg, Irina V Perevoshchikova, Adam L Orr, and Martin D Brand. 2012. 'Native rates of superoxide production from multiple sites in isolated mitochondria measured using endogenous reporters', *Free Radical Biology and Medicine*, 53: 1807-17.
- Ragusa, Robert J, Ching K Chow, and John D Porter. 1997. 'Oxidative stress as a potential pathogenic mechanism in an animal model of Duchenne muscular dystrophy', *Neuromuscular disorders*, 7: 379-86.
- Rahman, Mohammad A, Marko Ušaj, Dilson E Rassier, and Alf Månsson. 2018. 'Blebbistatin effects expose hidden secrets in the force-generating cycle of actin and myosin', *Biophysical journal*, 115: 386-97.

- Ramamurthy, B, and Lars Larsson. 2013. 'Detection of an aging-related increase in advanced glycation end products in fast-and slow-twitch skeletal muscles in the rat', *Biogerontology*, 14: 293-301.
- Rando, Thomas A, Marie-Helene Disatnik, Yip Yu, and Alexa Franco. 1998. 'Muscle cells from mdx mice have an increased susceptibility to oxidative stress', *Neuromuscular disorders*, 8: 14-21.
- Rayment, Ivan, Hazel M Holden, Michael Whittaker, Christopher B Yohn, Michael Lorenz, Kenneth C Holmes, and Ronald A Milligan. 1993. 'Structure of the actin-myosin complex and its implications for muscle contraction', *Science*, 261: 58-65.
- Reid, Michael B. 2001. 'Invited Review: redox modulation of skeletal muscle contraction: what we know and what we don't', *Journal of applied physiology*, 90: 724-31.
- Reid, MICHAEL B, FA Khawli, and MELANIE R Moody. 1993. 'Reactive oxygen in skeletal muscle. III. Contractility of unfatigued muscle', *Journal of applied physiology*, 75: 1081-87.
- Reid, Michael B, and Jennifer S Moylan. 2011. 'Beyond atrophy: redox mechanisms of muscle dysfunction in chronic inflammatory disease', *The Journal of Physiology*, 589: 2171-79.
- Reynoso, Juan, Andrey Bobkov, Andras Muhrad, and Emil Reisler. 2001. 'Solution properties of full length and truncated forms of myosin subfragment 1 from Dictyostelium discoideum', *Journal of Muscle Research & Cell Motility*, 22: 657-64.
- Samengo, G., A. Avik, B. Fedor, D. Whittaker, K. H. Myung, M. Wehling-Henricks, and J. G. Tidball. 2012. 'Age-related loss of nitric oxide synthase in skeletal muscle causes reductions in calpain S-nitrosylation that increase myofibril degradation and sarcopenia', *Aging cell*, 11: 1036-45.
- Santolini, Jérôme, Subrata Adak, Christine ML Curran, and Dennis J Stuehr. 2001. 'A kinetic simulation model that describes catalysis and regulation in nitric-oxide synthase', *Journal of Biological Chemistry*, 276: 1233-43.
- Schiaffino, Stefano, and Carlo Reggiani. 1996. 'Molecular diversity of myofibrillar proteins: gene regulation and functional significance', *Physiological reviews*, 76: 371-423.
- Schlossarek, Saskia, Giulia Mearini, and Lucie Carrier. 2011. 'Cardiac myosin-binding protein C in hypertrophic cardiomyopathy: mechanisms and therapeutic opportunities', *Journal of molecular and cellular cardiology*, 50: 613-20.

- Schulz, RICHARD, KAREN L Dodge, GARY D Lopaschuk, and ALEXANDER S Clanachan. 1997. 'Peroxynitrite impairs cardiac contractile function by decreasing cardiac efficiency', *American Journal of Physiology-Heart and Circulatory Physiology*, 272: H1212-H119.
- Seddon, Mike, Yee H Looi, and Ajay M Shah. 2007. 'Oxidative stress and redox signalling in cardiac hypertrophy and heart failure', *Heart*, 93: 903-07.
- Seidel, JC. 1969. 'Similar effects on enzymic activity due to chemical modification of either of two sulfhydryl groups of myosin', *Biochimica et Biophysica Acta (BBA)-Bioenergetics*, 180: 216-19.
- Serra, Andrey Jorge, José Renato Pinto, Marko D Prokić, Gisela Arsa, and Andrea Vasconsuelo. 2020. "Oxidative stress in muscle diseases: current and future therapy 2019." In.: Hindawi.
- Sheeran, Freya L, and Salvatore Pepe. 2006. 'Energy deficiency in the failing heart: linking increased reactive oxygen species and disruption of oxidative phosphorylation rate', *Biochimica et Biophysica Acta (BBA)-Bioenergetics*, 1757: 543-52.
- Shishkin, SS, LI Kovalyov, and MA Kovalyova. 2004. 'Proteomic studies of human and other vertebrate muscle proteins', *Biochemistry (Moscow)*, 69: 1283-98.
- Silveira, Leonardo R, Lucia Pereira-Da-Silva, Carsten Juel, and Ylva Hellsten. 2003. 'Formation of hydrogen peroxide and nitric oxide in rat skeletal muscle cells during contractions', *Free Radical Biology and Medicine*, 35: 455-64.
- Snook, Jeremy H, Jiahui Li, Brian P Helmke, and William H Guilford. 2008. 'Peroxynitrite inhibits myofibrillar protein function in an in vitro assay of motility', *Free Radical Biology and Medicine*, 44: 14-23.
- Snow, LeAnn M, Nicole A Fugere, and LaDora V Thompson. 2007. 'Advanced glycation end-product accumulation and associated protein modification in type II skeletal muscle with aging', *The Journals of Gerontology Series A: Biological Sciences and Medical Sciences*, 62: 1204-10.
- Šochman, Jan, and Jan H Peregrin. 1992. 'Total recovery of left ventricular function after acute myocardial infarction: comprehensive therapy with streptokinase, N-acetylcysteine and percutaneous transluminal coronary angioplasty', *Int J Cardiol*, 35: 116-18.
- Šochman, Jan, Jana Vrbská, Blanka Musilová, and Miroslav Roček. 1996. 'Infarct size limitation: acute N-acetylcysteine defense (ISLAND trial): preliminary analysis and report after the first 30 patients', *Clinical cardiology*, 19: 94-100.

- Squier, Thomas C. 2001. 'Oxidative stress and protein aggregation during biological aging', *Experimental gerontology*, 36: 1539-50.
- Stadtman, Earl R, and Rodney L Levine. 2000. 'Protein oxidation', *Annals of the New York Academy of Sciences*, 899: 191-208.
- Stamler, J. S., S. Lamas, and F. C. Fang. 2001. 'Nitrosylation. the prototypic redox-based signaling mechanism', *Cell*, 106: 675-83.
- Steinberg, Susan F. 2013. 'Oxidative stress and sarcomeric proteins', *Circulation research*, 112: 393-405.
- Steinhorn, Benjamin, Andrea Sorrentino, Sachin Badole, Yulia Bogdanova, Vsevolod Belousov, and Thomas Michel. 2018. 'Chemogenetic generation of hydrogen peroxide in the heart induces severe cardiac dysfunction', *Nature communications*, 9: 4044.
- Steinz, Maarten M, Malin Persson, Bejan Aresh, Karl Olsson, Arthur J Cheng, Emma Ahlstrand, Mats Lilja, Tommy R Lundberg, Eric Rullman, and Kristina Ängeby Möller. 2019. 'Oxidative hotspots on actin promote skeletal muscle weakness in rheumatoid arthritis', *JCI insight*, 4.
- Steinz, Maarten Michiel. 2020. 'Oxidative stress and muscle weakness associated with rheumatoid arthritis'.
- Stewart, Travis J, Vidya Murthy, Sam P Dugan, and Josh E Baker. 2021. 'Velocity of myosin-based actin sliding depends on attachment and detachment kinetics and reaches a maximum when myosin-binding sites on actin saturate', *Journal of Biological Chemistry*, 297.
- Straight, Chad R, Philip A Ades, Michael J Toth, and Mark S Miller. 2018. 'Age-related reduction in single muscle fiber calcium sensitivity is associated with decreased muscle power in men and women', *Experimental gerontology*, 102: 84-92.
- Sun, Mingxuan, Michael B Rose, Shobana K Ananthanarayanan, Donald J Jacobs, and Christopher M Yengo. *J Proceedings of the National Academy of Sciences*. 2008. 'Characterization of the pre-force-generation state in the actomyosin cross-bridge cycle', 105: 8631-36.
- Supinski, G., D. Stofan, L. A. Callahan, D. Nethery, T. M. Nosek, and A. DiMarco. 1999. 'Peroxyntirite induces contractile dysfunction and lipid peroxidation in the diaphragm', *J Appl Physiol (1985)*, 87: 783-91.
- Tahara, Erich B, Felipe DT Navarete, and Alicia J Kowaltowski. 2009. 'Tissue-, substrate-, and site-specific characteristics of mitochondrial reactive oxygen species generation', *Free Radical Biology and Medicine*, 46: 1283-97.

- Terman, J. R., and A. Kashina. 2013. 'Post-translational modification and regulation of actin', *Curr Opin Cell Biol*, 25: 30-8.
- Thomas, David D, Ewa Prochniewicz, and Osha Roopnarine. 2002. 'Changes in actin and myosin structural dynamics due to their weak and strong interactions.' in, *Molecular Interactions of Actin* (Springer).
- Thompson, L. V., D. Durand, N. A. Fugere, and D. A. Ferrington. 2006. 'Myosin and actin expression and oxidation in aging muscle', *J Appl Physiol (1985)*, 101: 1581-7.
- Thompson, LaDora V. 2009. 'Age-related muscle dysfunction', *Experimental gerontology*, 44: 106-11.
- Thomson, Mandy J, Michael P Frenneaux, and JC Kaski. 2009. 'Antioxidant treatment for heart failure: friend or foe?', *QJM: An International Journal of Medicine*, 102: 305-10.
- Tiago, Teresa, Pedro S Palma, Carlos Gutierrez-Merino, and Manuel Aureliano. 2010. 'Peroxynitrite-mediated oxidative modifications of myosin and implications on structure and function', *Free Radical Research*, 44: 1317-27.
- Tiago, Teresa, Sónia Simao, Manuel Aureliano, Francisco Javier Martín-Romero, and Carlos Gutiérrez-Merino. 2006. 'Inhibition of skeletal muscle S1-myosin ATPase by peroxynitrite', *Biochemistry*, 45: 3794-804.
- Tidball, James G, and Michelle Wehling-Henricks. 2007. 'The role of free radicals in the pathophysiology of muscular dystrophy', *Journal of applied physiology*, 102: 1677-86.
- Tokuraku, Kiyotaka, Taro Q. P. %J Journal of Muscle Research Uyeda, and Cell Motility. 2001. 'Phalloidin affects the myosin-dependent sliding velocities of actin filaments in a bound-divalent cation dependent manner', 22: 371-78.
- Tsaturyan, Andrey K, Natalia Koubassova, Michael A Ferenczi, Theyencheri Narayanan, Manfred Roessle, and Sergey Y Bershtitsky. 2005. 'Strong binding of myosin heads stretches and twists the actin helix', *Biophysical journal*, 88: 1902-10.
- Turrens, Julio F, and Alberto Boveris. 1980. 'Generation of superoxide anion by the NADH dehydrogenase of bovine heart mitochondria', *Biochemical Journal*, 191: 421-27.
- Uchida, K. 2003. 'Histidine and lysine as targets of oxidative modification', *Amino acids*, 25: 249-57.
- Umanskaya, Alisa, Gaetano Santulli, Wenjun Xie, Daniel C Andersson, Steven R Reiken, and Andrew R Marks. 2014. 'Genetically enhancing mitochondrial antioxidant activity

- improves muscle function in aging', *Proceedings of the National Academy of Sciences*, 111: 15250-55.
- Vaage, Jarle, Massimo Antonelli, Maurizio Bufi, Öivind Irtun, Roberto Alberto DeBlasi, Giacomo G Corbucci, Alessandro Gasparetto, and Anne G Semb. 1997. 'Exogenous reactive oxygen species deplete the isolated rat heart of antioxidants', *Free Radical Biology and Medicine*, 22: 85-92.
- van der Pol, Atze, Wiek H van Gilst, Adriaan A Voors, and Peter van der Meer. 2019. 'Treating oxidative stress in heart failure: past, present and future', *European Journal of Heart Failure*, 21: 425-35.
- van der Veen, R. C., and L. J. Roberts. 1999. 'Contrasting roles for nitric oxide and peroxynitrite in the peroxidation of myelin lipids', *J Neuroimmunol*, 95: 1-7.
- Van Dijk, Sabine J, Kristina L Bezold, and Samantha P Harris. 2014. 'Earning stripes: myosin binding protein-C interactions with actin', *Pflügers Archiv-European Journal of Physiology*, 466: 445-50.
- Varland, S., J. Vandekerckhove, and A. Drazic. 2019. 'Actin Post-translational Modifications: The Cinderella of Cytoskeletal Control', *Trends Biochem Sci*.
- Vasilaki, Aphrodite, A Mansouri, Holly Van Remmen, JH Van Der Meulen, L Larkin, Arlan G Richardson, Anne McArdle, JA Faulkner, and Malcolm J Jackson. 2006. 'Free radical generation by skeletal muscle of adult and old mice: effect of contractile activity', *Aging cell*, 5: 109-17.
- Vikhorev, Petr G., Natalia N. Vikhoreva, and Alf Månsson. 2008. 'Bending flexibility of actin filaments during motor-induced sliding', *Biophysical journal*, 95: 5809-19.
- Vikhoreva, Natalia N, Petr G Vikhorev, Maria A Fedorova, Ralf Hoffmann, Alf Månsson, and Nadezda V Kuleva. 2009. 'The in vitro motility assay parameters of actin filaments from *Mytilus edulis* exposed in vivo to copper ions', *Archives of biochemistry and biophysics*, 491: 32-38.
- Walsmith, J., and R. Roubenoff. 2002. 'Cachexia in rheumatoid arthritis', *Int J Cardiol*, 85: 89-99.
- Wang, Lianguo, Gary D Lopaschuk, and Alexander S Clanachan. 2008. 'H₂O₂-induced left ventricular dysfunction in isolated working rat hearts is independent of calcium accumulation', *Journal of molecular and cellular cardiology*, 45: 787-95.
- Ward, Douglas G, Peter R Ashton, Hylary R Trayer, and Ian P Trayer. 2001. 'Additional PKA phosphorylation sites in human cardiac troponin I', *Eur J Biochem*, 268: 179-85.

- Watanabe, Hiroyuki, Mami Ogasawara, Noriko Suzuki, Naoyuki Nishizawa, and Kaichi Ambo. 1992. 'Glycation of myofibrillar protein in aged rats and mice', *Bioscience, biotechnology, and biochemistry*, 56: 1109-12.
- Wehling, Michelle, Melissa J Spencer, and James G Tidball. 2001. 'A nitric oxide synthase transgene ameliorates muscular dystrophy in mdx mice', *The Journal of cell biology*, 155: 123-32.
- Wei, Bin, and J-P Jin. 2011. 'Troponin T isoforms and posttranscriptional modifications: Evolution, regulation and function', *Archives of biochemistry and biophysics*, 505: 144-54.
- Weitzberg, Eddie, Michael Hezel, and Jon O Lundberg. 2010. 'Nitrate-nitrite-nitric oxide Pathway Implications for anesthesiology and intensive care', *Anesthesiology: The Journal of the American Society of Anesthesiologists*, 113: 1460-75.
- Westerblad, Håkan, and David G Allen. 2011. 'Emerging roles of ROS/RNS in muscle function and fatigue', *Antioxidants & redox signaling*, 15: 2487-99.
- Williams Jr, David L, and Charles A Swenson. 1982. 'Disulfide bridges in tropomyosin: effect on ATPase activity of actomyosin', *Eur J Biochem*, 127: 495-99.
- Wink, David A, John A Cook, Roberto Pacelli, James Liebmann, Murali C Krishna, and James B Mitchell. 1995. 'Nitric oxide (NO) protects against cellular damage by reactive oxygen species', *Toxicology letters*, 82: 221-26.
- Winkler, Barry S, Michael E Boulton, John D Gottsch, and Paul Sternberg. 1999. 'Oxidative damage and age-related macular degeneration', *Molecular vision*, 5: 32.
- Yamada, T., T. Mishima, M. Sakamoto, M. Sugiyama, S. Matsunaga, and M. Wada. 2006. 'Oxidation of myosin heavy chain and reduction in force production in hyperthyroid rat soleus', *J Appl Physiol (1985)*, 100: 1520-6.
- Yamada, T., N. Place, N. Kosterina, T. Ostberg, S. J. Zhang, C. Grundtman, H. Erlandsson-Harris, I. E. Lundberg, B. Glenmark, J. D. Bruton, and H. Westerblad. 2009. 'Impaired myofibrillar function in the soleus muscle of mice with collagen-induced arthritis', *Arthritis Rheum*, 60: 3280-9.
- Yamada, Takashi, Masami Abe, Jaesik Lee, Daisuke Tatebayashi, Koichi Himori, Keita Kanzaki, Masanobu Wada, Joseph D Bruton, Håkan Westerblad, and Johanna T Lanner. 2015. 'Muscle dysfunction associated with adjuvant-induced arthritis is prevented by antioxidant treatment', *Skeletal muscle*, 5: 1-10.

- Yamada, Takashi, Olga Fedotovskaya, Arthur J. Cheng, Anabelle S. Cornachione, Fabio C. Minozzo, Cecilia Aulin, Cecilia Fridén, Carl Turesson, Daniel C. Andersson, Birgitta Glenmark, Ingrid E. Lundberg, Dilson E. Rassier, Håkan Westerblad, and Johanna T. Lanner. 2015. 'Nitrosative modifications of the Ca²⁺ release complex and actin underlie arthritis-induced muscle weakness', *Annals of the rheumatic diseases*, 74: 1907-14.
- Yamaguchi, Masahiro, and Takamitsu Sekine. 1966. 'Sulfhydryl groups involved in the active site of myosin A adenosine triphosphatase', *The Journal of Biochemistry*, 59: 24-33.
- Yount, Ralph G, Christine R Cremo, Jean C Grammer, and Bruce A Kerwin. 1992. 'Photochemical mapping of the active site of myosin', *Philosophical Transactions of the Royal Society of London. Series B: Biological Sciences*, 336: 55-61.
- Zhong, Sheng, Dawn A Lowe, and LaDora V Thompson. 2006. 'Effects of hindlimb unweighting and aging on rat semimembranosus muscle and myosin', *Journal of applied physiology*, 101: 873-80.
- Zima, Aleksey V, and Lothar A Blatter. 2006. 'Redox regulation of cardiac calcium channels and transporters', *Cardiovascular research*, 71: 310-21.
- Zinellu, Elisabetta, Angelo Zinellu, Alessandro Giuseppe Fois, Ciriaco Carru, and Pietro Pirina. 2016. 'Circulating biomarkers of oxidative stress in chronic obstructive pulmonary disease: a systematic review', *Respiratory research*, 17: 1-11.

Supplementary Figures

	Name	Reduced	Oxidized
Protein	ACTA_BOVIN	5.976E+11	1.395E+12
Peptide	AGFAGDDAPR	7.682E+07	1.346E+11
Peptide	AGFAGDDAPR[15.995]	4.993E+05	5.148E+07
Peptide	AVFPSIVGRPR	1.885E+10	2.894E+10
Peptide	HQGVM[Oxid]VGM[Oxid]GQK	2.397E+09	6.935E+07
Peptide	HQGVMVGMGQK	2.019E+09	2.010E+09
Peptide	HQGVM[Oxid]VGMGQK	4.080E+08	9.438E+08
Peptide	HQGVMVGM[Oxid]GQK	4.080E+08	9.438E+08
Peptide	HQGVM[Oxid]VGM[Oxid]GQKDSYVGDEAQS	8.005E+06	3.278E+07
Peptide	HQGVM[Oxid]VGMGQK[Hydroxyl]	1.024E+09	5.319E+09
Peptide	HQGVMVGM[Oxid]GQK[Hydroxyl]	1.372E+09	6.999E+09
Peptide	DSYVGDEAQS	4.713E+10	8.991E+10
Peptide	DSYVGDEAQS	1.558E+09	2.637E+09
Peptide	DSYVGDEAQS[Hydroxyl]R	0.000E+00	1.337E+06
Peptide	RGILTLK	1.135E+08	4.987E+07
Peptide	C[Carboxymethyl]DIDIRK	3.309E+08	2.495E+08

Peptide	C[Carboxymethyl]PETLFQPSFIGM[Oxid]ESAGIHETTYNSIM[Oxid]K	3.169E+08	1.253E+09
Peptide	C[Carboxymethyl]PETLFQPSFIGM[Oxid]ESAGIHETTYNSIMK	3.956E+08	6.868E+08
Peptide	C[Carboxymethyl]PETLFQPSFIGM[Oxid]ESAGIHETTYNSIMK[Hydroxyl]	3.169E+08	1.253E+09
Peptide	C[Carboxymethyl]PETLFQPSFIGMESAGIHETTYNSIM[Oxid]K	3.956E+08	6.868E+08
Peptide	C[Carboxymethyl]PETLFQPSFIGMESAGIHETTYNSIMK	1.555E+08	1.524E+08
Peptide	DLY[28.990]ANNVLSGGTTM[Oxid]YPGIADR	1.591E+08	4.195E+08
Peptide	DLYANNVLSGGTTM[Oxid]Y[28.990]PGIADR	1.591E+08	3.561E+08
Peptide	DLYANNVLSGGTTM[Oxid]YPGIADR	1.050E+10	3.181E+10
Peptide	DLYANNVLSGGTTM[Oxid]YPGIADR[15.995]	6.364E+07	9.068E+08
Peptide	DLYANNVLSGGTTMYPGIADR	7.469E+09	1.029E+10
Peptide	DLTDYLM[Oxid]K	8.716E+09	3.940E+10
Peptide	DLTDYLMK	7.107E+09	1.047E+10
Peptide	DLTDYLM[Oxid]KILTER	3.537E+06	2.058E+07
Peptide	DLTDYLM[Oxid]K[Hydroxyl]	9.534E+07	5.753E+08
Peptide	DLTDYLMK[Hydroxyl]	8.716E+09	3.940E+10
Peptide	EK[Hydroxyl]LC[Carboxymethyl]YVALDFENEM[Oxid]ATAASSSSLEK	1.206E+07	1.191E+07
Peptide	EK[Hydroxyl]LC[DoubleOxid]YVALDFENEM[Oxid]ATAASSSSLEK	0.000E+00	1.219E+08
Peptide	EK[Hydroxyl]LC[DoubleOxid]YVALDFENEMATAASSSSLEK	2.472E+06	1.234E+07
Peptide	EKLC[Carboxymethyl]YVALDFENEM[Oxid]ATAASSSSLEK	1.184E+09	2.682E+09
Peptide	EKLC[Carboxymethyl]YVALDFENEMATAASSSSLEK	3.362E+08	2.631E+08
Peptide	FRC[Carboxymethyl]PETLFQPSFIGM[Oxid]ESAGIHETTYNSIM[Oxid]K	1.755E+08	9.440E+08
Peptide	FRC[Carboxymethyl]PETLFQPSFIGM[Oxid]ESAGIHETTYNSIMK[Hydroxyl]	1.755E+08	9.440E+08
Peptide	FRC[Carboxymethyl]PETLFQPSFIGMESAGIHETTYNSIM[Oxid]K	7.460E+07	3.070E+08
Peptide	SYELPDGQVITIGNER	1.161E+11	2.312E+11
Peptide	SY[28.990]ELPDGQVITIGNER	2.237E+09	1.954E+09
Peptide	SYELPDGQVITIGNER[15.995]	1.180E+06	3.223E+07
Peptide	GYSFVTTAER	2.134E+08	2.630E+08
Peptide	M[Oxid]QKEITALAPSTM[Oxid]K	4.769E+05	1.382E+07
Peptide	MQK[Hydroxyl]EITALAPSTM[Oxid]K	4.769E+05	1.382E+07
Peptide	EITALAPSTMK	1.199E+10	1.520E+10
Peptide	EITALAPSTM[Oxid]K	2.323E+08	2.052E+08
Peptide	EITALAPSTMK[Hydroxyl]	1.681E+10	6.340E+10
Peptide	EITALAPSTMKIK	2.587E+06	5.264E+06
Peptide	EITALAPSTM[Oxid]K[Hydroxyl]	2.175E+08	2.197E+09
Peptide	ILTERGYSFVTTAER	1.181E+07	1.498E+07
Peptide	IIAPPER	2.744E+10	4.484E+10
Peptide	IIAPPERK	1.739E+08	4.784E+08
Peptide	IWHHSFYNELR	5.589E+07	1.191E+08
Peptide	K[Hydroxyl]DLYANNVLSGGTTM[Oxid]YPGIADR	4.664E+07	3.156E+08
Peptide	K[Hydroxyl]DLYANNVLSGGTTMYPGIADR	4.869E+09	1.810E+10
Peptide	KDLY[28.990]ANNVLSGGTTM[Oxid]YPGIADR	9.221E+07	3.697E+08
Peptide	KDLYANNVLSGGTTM[Oxid]Y[28.990]PGIADR	8.912E+07	4.876E+07
Peptide	KDLYANNVLSGGTTM[Oxid]YPGIADR	1.858E+08	1.921E+10
Peptide	KDLYANNVLSGGTTM[Oxid]YPGIADR[15.995]	4.711E+07	3.156E+08
Peptide	KDLYANNVLSGGTTMYPGIADR	4.533E+09	5.905E+09
Peptide	LC[Carboxymethyl]YVALDFENEM[Oxid]ATAASSSSLEK	1.610E+09	1.514E+08
Peptide	LC[Carboxymethyl]YVALDFENEMATAASSSSLEK	3.353E+08	3.318E+08
Peptide	QEYDEAGPSIVHR	4.059E+10	9.298E+10
Peptide	QEYDEAGPSIVHRK	2.193E+06	0.000E+00
Peptide	TTGIVLDSGDGVTHNVPIYEGY[28.990]ALPHAIM[Oxid]R	8.182E+08	1.986E+09

Peptide	TTGIVLDSGDGVTHNVPIYEGYALPHAIM[Oxid]R	1.382E+10	6.933E+10
Peptide	TTGIVLDSGDGVTHNVPIYEGYALPHAIM[Oxid]R[15.995]	9.503E+07	9.317E+08
Peptide	TTGIVLDSGDGVTHNVPIYEGYALPHAIMR	1.502E+10	2.497E+10
Peptide	VAPEEHPTLLTEAPLNPK	2.176E+11	3.838E+11
Peptide	Y[28.990]PIEHGIITNWDDM[Oxid]EK	1.593E+08	3.920E+08
Peptide	YPIEHGIITNWDDM[Oxid]EK	1.153E+07	8.667E+07
Peptide	YPIEHGIITNWDDMEK	1.485E+07	1.301E+08
Peptide	YPIEHGIITNWDDMEK[Hydroxyl]	9.672E+06	8.198E+07

	Name	Reduced	Oxidized
peptide	TPM1_BOVIN	3.446E+11	9.487E+10
peptide	AADESER	1.488E+08	6.988E+05
peptide	AELSEGK[Hydroxyl]C[DoubleOxid]AELEEEELK	1.673E+06	2.966E+07
peptide	AELSEGKC[Carboxymethyl]AELEEEELK	0.000E+00	4.048E+06
peptide	AEQAEADK	7.415E+06	6.648E+04
peptide	AEQAEADKK	7.459E+07	2.178E+04
peptide	AEQAEADKKAEDR	9.815E+04	1.345E+06
peptide	AISEELDHALNDM[Oxid]TSI	6.955E+07	1.532E+09
peptide	AISEELDHALNDMTSI	1.600E+08	1.402E+07
peptide	AQK[Hydroxyl]DEEKMEIQEIQLKEAK	0.000E+00	7.190E+02
peptide	AQKDEEK	7.179E+06	0.000E+00
peptide	AQKDEEK[Hydroxyl]M[Oxid]EIQEIQLK	1.211E+08	5.535E+07
peptide	AQKDEEKM[Oxid]EIQEIQLK	1.284E+10	5.368E+09
peptide	AQKDEEKM[Oxid]EIQEIQLKEAK	2.353E+07	0.000E+00
peptide	AQKDEEKMEIQEIQLK	8.678E+08	7.412E+07
peptide	ATDAEADVASLNR	2.322E+10	6.795E+09
peptide	ATDAEADVASLNRR	1.432E+09	5.677E+08
peptide	ATEDELDK	6.636E+08	4.709E+08
peptide	ATEDELDKYSEALK	4.860E+07	3.185E+07
peptide	ATEDELDKYSEALKDAQEK	2.448E+10	4.683E+09
peptide	C[Carboxymethyl]AELEEEELK	9.031E+09	2.249E+09
peptide	CAELEEEELK	3.631E+06	1.303E+06
peptide	DAQEKLELAEK	3.294E+05	3.066E+08
peptide	DEEK[Hydroxyl]M[Oxid]EIQEIQLK	2.677E+07	1.375E+07
peptide	DEEK[Hydroxyl]MEIQEIQLK	2.637E+09	1.376E+09
peptide	DEEKM[Oxid]EIQEIQLK	3.522E+09	1.841E+09
peptide	DEEKMEIQEIQLK	5.605E+08	4.552E+07
peptide	EDKYEEEIK	7.326E+09	3.132E+09
peptide	GM[Oxid]KVIESR	0.000E+00	0.000E+00
peptide	HIAEDADR	1.527E+10	3.423E+07
peptide	HIAEDADRK	0.000E+00	1.528E+07
peptide	HIAEDADRKYEEVAR	5.691E+05	1.966E+07
peptide	IQLVEEELDR	4.990E+10	1.264E+10
peptide	IQLVEEELDRAQER	1.924E+08	7.982E+07
peptide	K[Hydroxyl]ATDAEADVASLNR	0.000E+00	3.554E+06
peptide	K[Hydroxyl]LVIIESDLER	0.000E+00	1.714E+04
peptide	KATDAEADVASLNR	2.144E+10	5.560E+09
peptide	KATDAEADVASLNRR	5.877E+08	2.407E+08

peptide	KLVIIESDLER	1.198E+07	7.234E+07
peptide	KLVIIESDLERAEEER	3.801E+06	0.000E+00
peptide	KYEEVAR	1.705E+10	5.485E+09
peptide	LATALQKLEEAEEK	2.885E+07	4.462E+07
peptide	LATALQKLEEAEEKAADESER	1.228E+07	7.213E+06
peptide	LEEAEEKAADESER	0.000E+00	1.690E+07
peptide	LELAEEK	3.403E+05	1.835E+07
peptide	LKATEDELDK	0.000E+00	7.532E+07
peptide	LKATEDELDKYSEALK	1.328E+09	5.394E+08
peptide	LKATEDELDKYSEALKDAQEK	3.749E+06	7.131E+08
peptide	LKEAETR	2.913E+04	0.000E+00
peptide	LVIIIESDLER	2.214E+10	5.761E+09
peptide	LVIIIESDLERAEEER	0.000E+00	9.376E+06
peptide	M[Oxid]EIQEIQLK	1.222E+09	1.326E+09
peptide	MEIQEIQLK	4.631E+09	6.320E+08
peptide	MEIQEIQLKEAK	0.000E+00	0.000E+00
peptide	QLEDELVSLQK	3.756E+10	8.338E+09
peptide	QLEDELVSLQKK	0.000E+00	9.848E+06
peptide	R[15.995]IQLVEEELDR	6.707E+05	0.000E+00
peptide	RIQLVEEELDR	1.725E+07	2.079E+07
peptide	SIDDLEDELYAQK	3.942E+10	8.830E+09
peptide	SIDDLEDELYAQK[Hydroxyl]	1.788E+08	2.376E+05
peptide	SIDDLEDELYAQKCLK	2.857E+07	0.000E+00
peptide	SIDDLEDELYAQKCLKYK	0.000E+00	0.000E+00
peptide	SKQLEDELVSLQK	5.114E+09	1.584E+09
peptide	SKQLEDELVSLQKK	0.000E+00	1.321E+07
peptide	SLEAQAEEK	1.729E+10	6.429E+09
peptide	SVTKLEK	6.001E+05	0.000E+00
peptide	TVTNNLK	6.227E+08	2.474E+07
peptide	TVTNNLKSLEAQAEEK	2.192E+07	0.000E+00
peptide	VLSDKLK	0.000E+00	6.009E+06
peptide	Y[28.990]SQKEDKYEEEEIK	7.393E+07	2.791E+07
peptide	YSEALKDAQEK	0.000E+00	2.825E+08
peptide	YSEALKDAQEKLELAEEK	1.159E+08	4.004E+07
peptide	YSQKEDK	6.456E+06	0.000E+00
peptide	YSQKEDKY[28.990]EEEEIK	8.450E+06	0.000E+00
peptide	YSQKEDKYEEEEIK	2.308E+10	7.370E+09

	Name	Reduced	Oxidized
Protein	TNNT2_BOVIN	6.321E+09	6.103E+10
Peptide	ALSNM[Oxid]M[Oxid]HFGGYIQK	5.014E+08	5.147E+07
Peptide	ALSNMM[Oxid]HFGGYIQK	0.000E+00	5.790E+06
Peptide	ALSNMMHFGGYIQK	8.189E+07	8.622E+04
Peptide	ARREEESR	0.000E+00	5.186E+05
Peptide	DLNELQTLIEAHFENR	5.980E+08	4.346E+07
Peptide	EEEELVSLK	1.070E+07	2.018E+08
Peptide	EEEELVSLKDR	0.000E+00	4.962E+07
Peptide	EEEEESRR	1.714E+04	2.315E+07
Peptide	IPDGERVDFDDIHR	3.275E+08	4.597E+09

Peptide	K[Hydroxyl]K[Hydroxyl]EEEELVSLK	0.000E+00	7.051E+06
Peptide	KAEDEAR	0.000E+00	1.960E+07
Peptide	KALSNM[Oxid]M[Oxid]HFGGYIQK	1.223E+04	9.091E+07
Peptide	KEEEELVSLK	6.026E+06	9.938E+07
Peptide	KEEEELVSLKDR	0.000E+00	1.522E+07
Peptide	KK[Hydroxyl]EEEELVSLK	3.983E+06	1.503E+05
Peptide	KK[Hydroxyl]EEEELVSLKDR	5.973E+04	1.286E+06
Peptide	KKEEEELVSLK	1.165E+09	1.512E+10
Peptide	KKEEEELVSLKDR	7.367E+07	2.407E+09
Peptide	KVLAIIDLHNLNEDQLR	2.197E+08	3.009E+09
Peptide	NRINDNQKVS	0.000E+00	0.000E+00
Peptide	QKYEINVL	0.000E+00	4.435E+06
Peptide	REEEESR	1.714E+04	2.894E+07
Peptide	VDFDDIHR	1.383E+08	1.740E+09
Peptide	VDFDDIHR[15.995]	1.266E+05	1.305E+06
Peptide	VDFDDIHRK	8.221E+07	3.982E+08
Peptide	VLAIDLHNLNEDQLR	1.905E+09	1.978E+10
Peptide	VLAIDLHNLNEDQLREK	0.000E+00	9.422E+06
Peptide	YEINVL	1.207E+09	1.331E+10

	Name	Reduced	Oxidized
Protein	TNNC1_BOVIN	1.120E+10	1.475E+10
Peptide	AAVEQLTEEQK	1.707E+09	2.664E+09
Peptide	AAVEQLTEEQK[Hydroxyl]NEFK	4.319E+05	5.598E+06
Peptide	AAVEQLTEEQKNEFK	7.013E+09	1.093E+10
Peptide	GKSEEELSDLFR	5.750E+08	2.489E+08
Peptide	IDYDEFLEFM[Oxid]K	9.288E+07	3.820E+06
Peptide	IDYDEFLEFMK[Hydroxyl]	9.288E+07	3.820E+06
Peptide	NADGYIDLEELK	1.124E+09	5.027E+08
Peptide	SEEELSDLFR	5.899E+08	3.888E+08

Supplementary Table 1. Data collected from mass spectrometry were analyzed in pinnacle. This yielded data as shown above. Peptide fragmentation spectra were listed, and the abundance in either reduced or oxidized samples could be qualitatively assessed. Oxidized residues listed as amino acid and either molecular weight associated with modification, or species name.

Score	Expect	Method	Identities	Positives	Gaps
789 bits(2038)	0.0	Compositional matrix adjust.	377/377(100%)	377/377(100%)	0/377(0%)
Query 1		MCDDEETALVCDNGSGLVKAGFAGDDAPRAVFP			60
Sbjct 1		MCDDEETALVCDNGSGLVKAGFAGDDAPRAVFP			60
Query 61		QSKRGILTLKYP			120
Sbjct 61		QSKRGILTLKYP			120
Query 121		MTQIMFETFNVP			180
Sbjct 121		MTQIMFETFNVP			180
Query 181		DLAGRDLTDYLMKIL			240
Sbjct 181		DLAGRDLTDYLMKIL			240
Query 241		SYELPDGQVITIGNER			300
Sbjct 241		SYELPDGQVITIGNER			300
Query 301		LSGGTTMYPGIADRMQKEIT			360
Sbjct 301		LSGGTTMYPGIADRMQKEIT			360
Query 361		KQEYDEAGPSIVHRKCF	377		
Sbjct 361		KQEYDEAGPSIVHRKCF	377		

Supplementary Table 2. Comparison between bovine cardiac actin (QZC07) and human cardiac actin (P68032) using BLAST alignment. Sequence match indicates an identical match between the actin sequences referenced in this study.

Score	Expect	Method	Identities	Positives	Gaps
523 bits(1348)	0.0	Compositional matrix adjust.	282/284(99%)	283/284(99%)	0/284(0%)
Query 1		MDAIAKKKMQMLKLDKENALDRAEQAEADKKA			60
Sbjct 1		MDAIAKKKMQMLKLDKENALDRAEQAEADKKA			60
Query 61		SEALKDAQEKLELA			120
Sbjct 61		SEALKDAQEKLELA			120
Query 121		DESERGMKVIESRAQ			180
Sbjct 121		DESERGMKVIESRAQ			180
Query 181		ERAELSEGKCAELE			240
Sbjct 181		ERAELSEGKCAELE			240
Query 241		FAERSVTKLEKS			284
Sbjct 241		FAERSVTKLEKS			284

Supplementary Table 3. Comparison between bovine Cardiac(TPM1) tropomyosin (Q5KR49) and human cardiac tropomyosin (P09493).

Score	Expect	Method	Identities	Positives	Gaps
372 bits(956)	2e-135	Compositional matrix adjust.	220/231(95%)	224/231(96%)	1/231(0%)
Query 56		GPVEEFKPKRPFMPNLVPPKIPDGERVDFDDIHRKRMEKDLNELQTLIEAHFENRKKEE			115
Sbjct 68		GP+EE KPKPR FMPNLVPPKIPDGERVDFDDIHRKRMEKDLNELQ LIEAHFENRKKEE			127
Query 116		EELVSLKDRIEKRAERAEEQQRIRAEREKERQTRLAEEERARREEEESRRKAEDARKKKA			175
Sbjct 128		EELVSLKDRIE+RRAERAEEQQRIR EREKERQ RLAEERARREEE+RRKAEDARKKKA			187
Query 176		LSNMMHFGGYIQK-AQTERKSGKRQTEREKKKKILAERRKVLADHNLNEDQLREKAKELW			234
Sbjct 188		LSNMMHFGGYIQK AQTERKSGKRQTEREKKKKILAERRKVLADHNLNEDQLREKAKELW			247
Query 235		QMIYDLAEKFDLQEKFKQKQYEINVLRRNRINDNQKVSCTRKGAKVTGRWK			285
Sbjct 248		QSIYNLEAEKFDLQEKFKQKQYEINVLRRNRINDNQKVSCTRKGAKVTGRWK			298

Supplementary Table 4. Comparison between cardiac isoform (TNNT2) of troponin T in bovine (P13789) and human (P45379).

Score	Expect	Method	Identities	Positives	Gaps
337 bits(865)	3e-124	Compositional matrix adjust.	195/212(92%)	201/212(94%)	2/212(0%)
Query 1		MADRSGGSTAGDTPAPPPVRRSSANYRAYATEPHAKKSKISASRKLQLKTLMLQIAK			60
Sbjct 1		MAD S + A + PAP P+RRRSS NYRAYATEPHAKKSKISASRKLQLKTL+LQIAK			58
Query 61		QELERAEERRGEKGRALSTRCPLELAGLGAELQDLCRQLHARVDKVEERYDVEAKV			120
Sbjct 59		QELERAEERRGEKGRALSTRCPLELAGLGAELQDLCRQLHARVDKVEERYD+EAKV			118
Query 121		TKNITEIADLNQKIFDLRGKFKRPTLRRVRISADAMMQALLGARAKETLDLRAHLKQVKK			180
Sbjct 119		TKNITEIADL QKIFDLRGKFKRPTLRRVRISADAMMQALLGARAKE+LDLRAHLKQVKK			178
Query 181		EDTEKENREVGDRKNIDALSGMEGRKKKFEG		212	
Sbjct 179		EDTEKENREVGDRKNIDALSGMEGRKKKFE		210	

Supplementary Table 5. Comparison between cardiac troponin I (TNNI3) in bovine (P08057) and human (P19429).

Score	Expect	Method	Identities	Positives	Gaps
315 bits(808)	2e-117	Compositional matrix adjust.	160/161(99%)	161/161(100%)	0/161(0%)
Query 1		MDDIYKAAVEQLTEEQKNEFKAAFDIFVLGAEDGCISTKELGKVMRMLGQNPTPEELQEM			60
Sbjct 1		MDDIYKAAVEQLTEEQKNEFKAAFDIFVLGAEDGCISTKELGKVMRMLGQNPTPEELQEM			60
Query 61		IDEVDEDESGTVDDEFVMMVRCMKDDSKGKSEELSDLFRMFDKNADGYIDLEELKIM			120
Sbjct 61		IDEVDEDESGTVDDEFVMMVRCMKDDSKGKSEELSDLFRMFDKNADGYIDL+ELKIM			120
Query 121		LQATGETITEDDIEELMKDGDKNNDGRIDYDEFLEFMKGVE		161	
Sbjct 121		LQATGETITEDDIEELMKDGDKNNDGRIDYDEFLEFMKGVE		161	

Supplementary Table 6. Comparison between troponin C (TNNC1) in bovine (P63315) and human (P63316).

Bridging text between study 2 and 3

The results until now indicate that oxidation has profound effects in actin-myosin interactions and calcium handling in the IVMA. Initial study identified the major components of the thick and thin filaments, and second study assessed regulatory components and identified various oxidized residues, which hinted at potential mechanisms behind these functional alterations. To delve deeper into the implications of these alterations, the focus of our research in Study 3 turns to the structural changes induced by oxidation.

We had previously shown that detailed structural and dynamic information could be garnered using the HS-AFM on thin filament regulatory proteins (Matusovsky, Mansson, Persson, Cheng, & Rassier, 2019). HS-AFM was deemed a valid tool to assess myosin II structure and dynamics despite the difficulty in assessing its non-processive, or transient, dynamics (Matusovsky et al., 2020; Matusovsky, Månsson, & Rassier, 2023).

In Study 3, we employ the HS-AFM and molecular dynamics simulations, to focus on how oxidation may induce changes in the structure of actin and myosin, affecting their displacement at the single-molecule level and, ultimately, the force generation by myosin motors.

Each of these studies adds a unique perspective to our understanding of the role of oxidation in muscle contraction. As we move from the microscopic interactions of actin and myosin in Study 1, to the broader network of thin filament proteins in Study 2, and finally, to the specific structural alterations induced by oxidation in Study 3, we gain a comprehensive understanding of how oxidation affects muscle function at multiple levels. This progression illustrates how the findings of each study contribute to and inform the next, together weaving a detailed and nuanced understanding of how oxidation influences striated muscle function.

Experimental Study 3

Oxidation-induced structural changes in actin and myosin evaluated by computational simulation and high-speed AFM

Oleg S. Matusovsky^{1*}, Daren Elkrif^{2*}, Yu-Shu Cheng¹, Dilson E. Rassier^{1,3}

1. Department of Physiology, McGill University, Montreal, QC H3G 1Y6, Canada
2. Department of Kinesiology and Physical Education, McGill University, Canada
3. Simon Fraser University, British Columbia, V5A 1S6, Canada

Submitted to: The Proceedings of National Academy of Sciences

August, 2023.

Abstract

The generation of reactive oxygen species during oxidative stress in muscles is induced by various oxidative modifications of muscle proteins and can lead to the development of various muscle diseases. To better understand the mechanism behind a reduced myosin force generation under oxidizing conditions, we analyzed the structural and functional changes in the actin and actin-myosin complex using high-speed atomic force microscopy (HS-AFM), structural analysis of simulated HS-AFM images, and molecular dynamics (MD) simulation. Computational oxidative nitration of tyrosine residues demonstrated instability in the molecular structure of G-actin. Cross-section analysis of the simulated HS-AFM images revealed a shift in the height values (~ 0.2 - 1.5 nm in magnitude) between the non-oxidized and oxidized actin, which correspond to the height differences observed in HS-AFM experiments with *in vitro* oxidized F-actin. The oxidation-induced structural alterations in actin impact myosin molecule displacement on the single-molecule level. The displacements of myosin heads on the F-actin, when ATP is present, indicates that the power stroke is occurring that can be described as binding the myosin molecule to the F-actin, rotation of the myosin lever arm that trigger Pi release, detachment of the myosin from the F-actin and re-binding to the new binding site on the F-actin. The formation of the SIN-1-treated F-actin-myosin complex in the presence of ATP resulted in a change in myosin head displacement size, with a significant decrease in the frequency of long displacements (≥ 4 nm). These results suggest that oxidation decreases the pool of the weak bound myosin molecules and shortens the long displacements related to the Pi release step, reducing the force generation by myosin motors.

Significance Statement

The generation of force in muscle contraction occurs when myosin II molecules attach to actin filaments. The purpose of this study is to identify the myosin force generation steps under oxidation conditions at the single-molecule level. We tested the idea that the actin-myosin interaction is disrupted due to oxidation-induced structural changes in actin filaments caused by the accumulation of the oxidative nitration of tyrosine residues (Tyr-3NT). The molecular dynamics simulation revealed that computational Tyr-3NT modifications caused instability in the molecular structure of G-actin. Furthermore, the oxidation-induced structural alterations in F-actin impact

the size of myosin head displacement in the presence of ATP. Thus, the capacity of the myosin molecule to generate force could also be affected.

Introduction

Oxidation is the result of an imbalance between production of reactive oxygen / nitrogen species (RONS) and an elaborate antioxidant defense system. The process causes an “oxidative damage” to different cell systems, including muscle, leading to various pathological conditions: muscular dystrophy (Tidball & Wehling-Henricks, 2007), muscle weakness in rheumatoid arthritis (Maarten M Steinz et al., 2019), sarcopenia or age-related muscle loss (Lowe et al., 2001; Prochniewicz et al., 2007; Reid & Durham, 2002), skeletal, cardiac myopathies and heart failure (Coirault et al., 2007; Maack et al., 2003; Takimoto & Kass, 2007).

In skeletal muscle, RONS such as hydrogen peroxide (H_2O_2), nitrogen oxide (NO^\bullet), peroxynitrite ($ONOO^\bullet$) or hydroxyl radical ($^\bullet OH$) have been shown to directly alter contractile function. The exact mechanism of the impaired contractility upon oxidation is still not clear. A broad range of manifestations due to protein oxidation has been observed *in vitro*: reducing motility of actin filaments in the *in-vitro* motility assays (Bansbach & Guilford, 2016; Elkrief et al., 2022), inhibition of the rate of polymerization of actin (Maarten M Steinz et al., 2019) and the myosin ATPase activity (Kirshenbaum et al., 1993), reducing force generation in the muscle fibers, myofibrils and myosin filaments (Bagni et al., 2019; Elkrief et al., 2022; Persson et al., 2019). It was suggested that oxidation may lead to a reduction in the number of myosin cross-bridges and thus a decrease in force generation (Persson et al., 2019) or increase in the rate of myosin head detachment from actin, further reducing muscle force. However, the underlying mechanism of the impaired ability of cross-bridges to generate force is still poorly understood with multiple factors yet to be identified.

The purpose of this study is to identify the myosin force generation steps under oxidation conditions at the single-molecule level. We tested the idea that the actin-myosin interaction is disrupted due to structural changes caused by the accumulation of the oxidative nitration of

tyrosine residues (Tyr-3NT). Tyrosine nitration is a post-translational modification that contributes to the development of protein dysfunction (Radi, 2004) having an impact on muscle contractile function as demonstrated with *in vitro* studies (Callahan et al., 2001; L. V. Thompson et al., 2006) and various pathological conditions, including neurodegenerative (Nakamura et al., 2015), cardiovascular (Michael J Mihm, Coyle, Schanbacher, Weinstein, & Bauer, 2001) and autoimmune diseases, such as rheumatoid arthritis (Ahmed, Anwar, Savage, Thornalley, & Rabbani, 2016). Therefore, understanding the role of oxidative nitration in muscle function and pathology can provide potential targets for therapeutic interventions aimed at preventing or slowing muscle dysfunction.

In this study we used computational simulation in combination with high-speed Atomic Force Microscopy (HS-AFM) to evaluate the impact of oxidative nitration on the structure-function relationship of the actin-myosin complex (see Flowchart in Fig. S1). The computational analysis included molecular dynamics (MD) simulation and HS-AFM simulation. MD simulation showed that the oxidative nitration of tyrosine residues in G-actin contributes to the instability of the system by affecting a root-mean-square deviation (RMSD). The peak height distribution near the oxidized sites in the simulated HS-AFM images of the G-actin and F-actin structures were changed in the magnitude of 0.2-1.5 nm in comparison to non-oxidized structure.

Along with the computational data, oxidation of the actin filaments by 5-amino-3-(4-morpholinyl)-1,2,3-oxadiazolium chloride (SIN-1) *in vitro* changed the heights of actin filaments captured by HS-AFM. Previously, observation of the actin topology under the HS-AFM has revealed changes at actin structure in response to binding partners such as Ca^{2+} binding to the thin filaments (Matusovsky et al., 2019), cofilin binding to the actin filaments (Ngo, Kodera, Katayama, Ando, & Uyeda, 2015), myosin binding to actin filaments (Matusovsky et al., 2020; Matusovsky et al., 2023) or actin-binding domain (Hayakawa et al., 2023). The analyses of actin structure included the assessment of peak heights, the highest points of the actin helix where two strands of actin filament are aligned atop each other, and the half-helical pitch, the distance between each peak.

There was a change in the size of myosin head displacement when the SIN-1-treated F-actin-myosin complex was formed in the presence of ATP. The displacements of the myosin heads on the F-actin in the presence of ATP suggests that the power stroke is occurring in a series of steps:

(i) the myosin molecule binds to the F-actin (M.ADP.Pi); (ii) the myosin lever arm rotates, inducing Pi release (M.ADP); (iii) the myosin molecule detaches from the F-actin (M.ATP), and (iv) the myosin molecule re-binds to the next binding site on the F-actin (M.ADP.Pi). The myosin heads were able to produce short (<1 nm), moderate (2-3 nm), and long (>4 nm) displacements on the non-oxidized F-actin, but the frequency of long displacements was significantly decreased in the presence of SIN-1-treated F-actin. According to numerous studies, the long displacements are related to the step of lever arm rotation and Pi release (Kaya & Higuchi, 2010; Moretto et al., 2022; Y. Wang, Ajtai, & Burghardt, 2014). The observed results suggest that oxidative nitration decreases the pool of the weak bound myosin molecules and shortens the long displacements related to the Pi release step, thus reducing the force generation by myosin motors.

Results and Discussion

Computational analysis of the non-treated and oxidized G-actin structures

We attempted to predict the impact of oxidation on the actin molecular structure by molecular dynamics (MD) and HS-AFM simulation before performing experiments of actin structure and actin-myosin interaction under oxidation conditions using HS-AFM. To initiate computational assessment and to make a connection with experimental data, certain tyrosine residues (Tyr) in the G-actin (PDB 2ZWH, 3.3 Å) or F-actin (PDB 6BNO, 5.5 Å) structures were subjected to the oxidative nitration (3NT) in the PyMOL environment (v.2.3.3, Schrodinger LLC) by adding the NO₂ group to the phenyl ring of the tyrosine. The Tyr residues that we modified were identified by mass-spectrometry analysis in actin filaments of patients with rheumatoid arthritis (Maarten M Steinz et al., 2019). The *in-vitro* treatment of purified skeletal G-actin and myofibril F-actin with 5-amino-3-(4-morpholinyl)-1,2,3-oxadiazolium chloride (SIN-1) caused an oxidation of similar Tyr residues (Maarten M Steinz et al., 2019). SIN-1 can generate both nitric oxide (NO) and superoxide (O₂⁻) in aqueous solutions. These two species can then react to form peroxynitrite (ONOO⁻), a potent oxidant and nitrating agent. Therefore, SIN-1 is often used to study the effects of oxidative nitration (3NT) on biological systems. The following residues in the G-actin subdomains (SD) were modified: Tyr 91, Tyr 362 (SD1); Tyr 53 (SD2); Tyr 166, Tyr 169, Tyr 294, Tyr 296, Tyr 297, Tyr 306 (SD3); Tyr 188, Tyr 198, Tyr 218, Tyr 240 (SD4) (Fig.1).

The comparison of the G-actin electrostatic maps revealed that total charge of the G-actin molecule was not affected by the presence of the residues modified by the oxidative nitration: -12.99 for both G-actin and G-actin-3NT. Similarly, the electrostatic potential (U) between two arbitrary charges q_1 , q_2 separated by distance r was calculated as the sum of the potential energy of all pairs of atoms in the structure divided by the distance between the charged atoms, according to Coulomb's law: $U = q_1 * q_2 / r^2$, was not different in both structures. However, the successive rotation of the structures around y-axis (Fig. 1) or x-axis (Fig. S1, Movie S3) revealed several spots affected by oxidative nitration between the non-oxidized and the oxidized structures. According to the electrostatic map, the spots were recognized as a change of the positive / negative charges (blue and red colors, respectively) in the non-oxidized structure to the neutral charge in the oxidized structure (Fig. 1c, Fig. S2,).

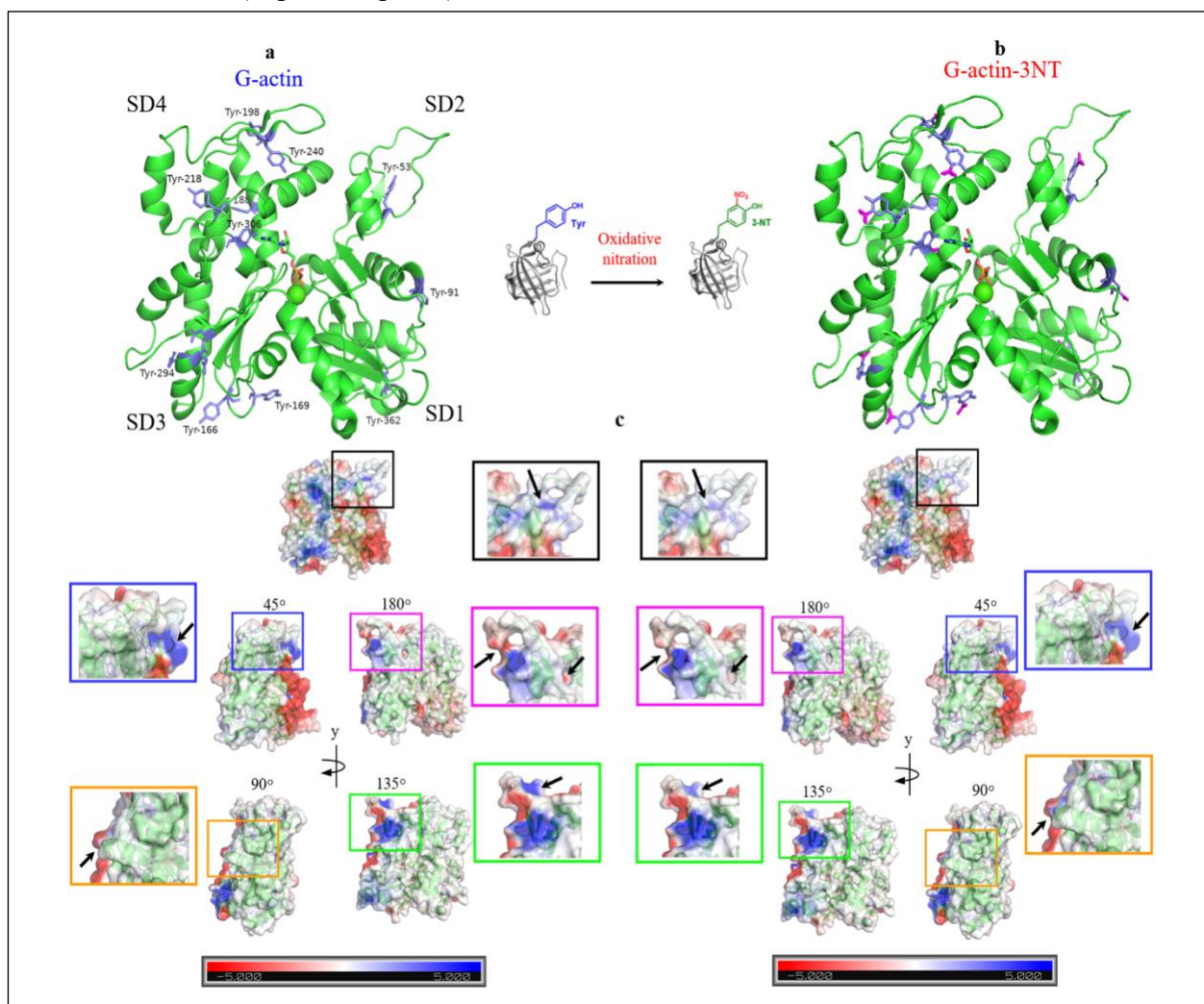


Figure. 1. **Computational oxidative nitration of the G-actin.** (a) The non-oxidized and (b) computationally oxidized G-actin (PDB 2ZWH). The modified residues shown as blue sticks with the phenyl ring in each subdomain (SD1-SD4). Oxidative modifications were performed in the pyMOL using pyTM plugin (v.1.2) (Warnecke, Sandalova, Achour, & Harris, 2014). The oxidized atoms in the residues highlighted by pink color. (c) The successive y-axis rotation of the non-oxidized and oxidized G-actin structures with 45° step from initial position showed the local changes in the electrostatic potential energy around oxidized residues. The matched colored boxes for each orientation were magnified to show the charge differences more precisely. The map scale represents the electrostatic potential energy from -5.0 k_BT (red) to 5.0 k_BT (blue).

To test whether the observed local changes in the electrostatic charges around Tyr-3NT residues affect the protein conformational dynamics *in silico*, we performed the molecular dynamics (MD) simulation of G-actin monomer with non-oxidized and Tyr-3NT oxidized residues. The details for MD simulation are described in the Methods. The custom Python code with OpenMM package (Eastman et al., 2017) used for MD simulation and to create the trajectory files can be found on GitHub (https://github.com/matusoff/Molecular_dynamics/blob/main/OpenMM_simulation.py) and in the Supplementary Data. Running the MD simulation for 100 ns at the temperature of 300 K revealed that the equilibration of G-actin structure, as judged by a root-mean-square deviation (RMSD), happened ~20 ns into the simulation.

Therefore, this conformation of the G-actin monomer can be used as the favoured conformation at the pH 7.0, 300 K and ionic strength 0.15 M (Movie S4, Movie S5). In the text below, this conformation will be titled as the initial conformation. In contrast, G-actin structure with Tyr-3NT residues, showed a less stable behaviour with areas of increasing RMSD, approximately every 10 ns (Fig. 2c). Thus, MD simulation demonstrated that 3-NT oxidative nitration of the tyrosine residues in G-actin contributes to the instability of the system.

HS-AFM simulation of the G-actin and G-actin-3NT

To further study the conformational changes in the area around oxidized residues we simulated HS-AFM image with a BioAFM viewer (v.2.5, Kanazawa University), a recently developed open-source software (Amyot & Flechsig, 2020; Amyot, Marchesi, Franz, Casuso, & Flechsig, 2022) that is able to simulate HS-AFM images from the PDB files of the atomic structure with high correlation (Fig. S3). The PDB files with the non-oxidized Tyr and the oxidized Tyr-3NT residues were used to simulate the HS-AFM images of the non-oxidized and the oxidized G-actin structures

in the initial and rotated conformations (Fig. 1, Fig. S2.). The BioAFM viewer allowed to change the apex angle and tip radius to be changed in order to obtain HS-AFM simulated images that were comparable to experimental conditions (Fig. S4).

The simulated HS-AFM images were used to gain the height profile using cross-section analysis. We measured the height values in the x, y directions in the area around Tyr-3NT residues (Fig. 3b, Fig. S5) as well as for the entire surface of the G-actin monomer in the initial conformation, collecting each of the three pixels along the x-direction (Fig. 3c). A cross-section analysis around oxidized and non-oxidized Tyr residues in the simulated HS-AFM images of G-actin monomers revealed a difference in the height values from ~0.2-0.6 nm in magnitude between two G-actin structures, one with non-modified Tyr residues and one with Tyr-3NT residues, respectively (Fig. 3b, lower panel). Rotation of these two structures with 45° step around x-axis or y-axis revealed similar magnitude in differences (Fig.S5).

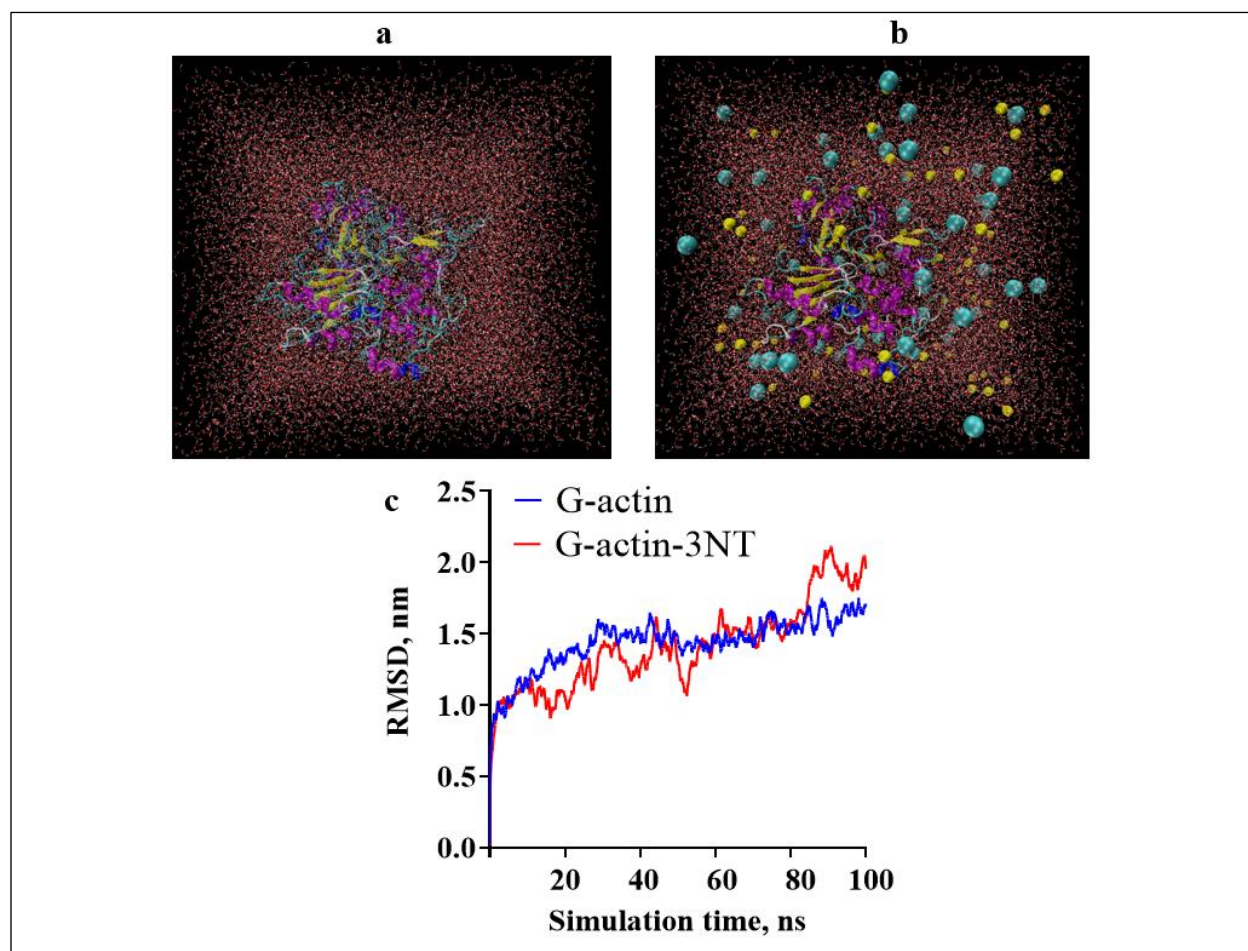


Figure 3. **Molecular dynamics (MD) simulation of the G-actin structure with non-oxidized and Tyr-3NT oxidized residues.** An example of solvation (a) and ionization (b) of the G-actin structure. The structure was placed in a rectangular box filled with water molecules. The cyan and yellow spheres represent Na^{2+} and Cl^- ions, respectively. (c) The

The entire surface scan of the simulated HS-AFM image of the G-actin monomer in the initial position (Fig. 3e) showed an interesting trend in the height distribution. Despite a similar mean value of $3.3 \text{ nm} \pm 0.66 \text{ nm}$ (G-actin) and $3.3 \text{ nm} \pm 0.70 \text{ nm}$ (G-actin-3NT), the height frequency comparison revealed that G-actin-3NT had a greater occurrence of low height values ($\sim 1.8\text{-}2.2 \text{ nm}$) compared to G-actin, which showed a higher frequency of values ranging from $3.5\text{-}4.0 \text{ nm}$ (Fig.3e, the height distribution panel). Thus, according to the computational analysis, the 3-NT oxidative nitration of the Tyr residues contributes to the instability of the system (Fig. 2) that can be evaluated in HS-AFM experiments by the height distributions analysis. Our next goal was to scale the observed differences on the F-actin structure using computational and experimental approaches.

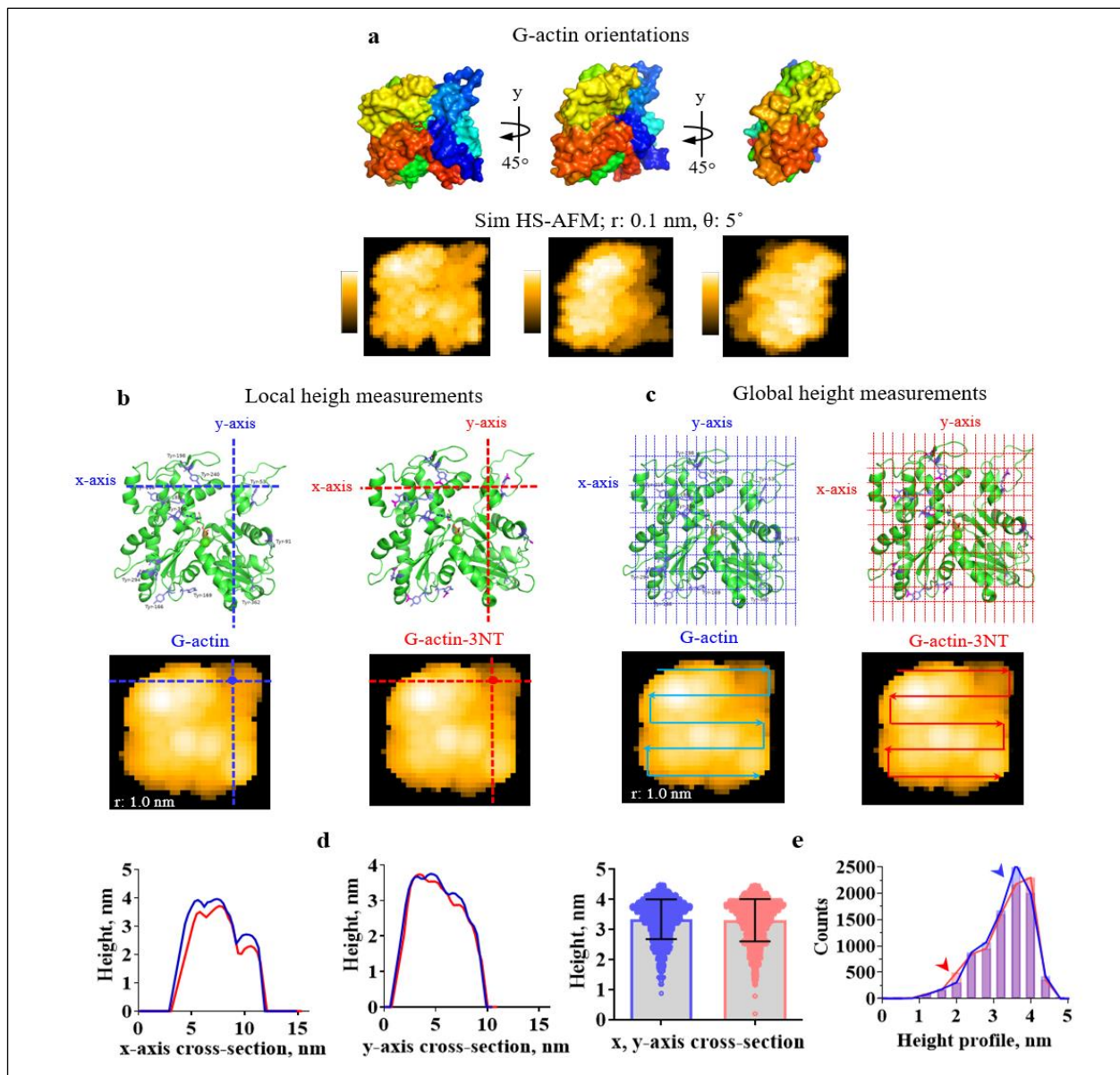


Figure 4. **Cross-sectional analysis in the simulated G-actin and G-actin-3NT HS-AFM images.** (a) The initial conformation of the G-actin monomer structure (PDB: 2ZWH) rotated with 45° step around y-axis and corresponding simulated HS-AFM images (Sim HS-AFM) obtained with BioAFM viewer with the tip radius 0.1 nm and the apex angle 5°. (b, c) G-actin structures with non-oxidized Tyr and Tyr-3NT residues, indicating the x, y-axis used to obtain the local height values (b) and global height values (c) with corresponding simulated HS-AFM images of the G-actin structures with tip radius 1.0 nm with schematic directions of the scanned surfaces. (d, e) local and global height profiles for the G-actin structures with non-oxidized Tyr (blue) and Tyr-3NT (red) residues with the frequency analysis of the height values from entire surface. The red arrow shows a higher frequency of 1.8-2.2 nm height values in the oxidized G-actin-3NT; the blue arrow shows the higher frequency of 3-4 nm height values in the non-oxidized G-actin.

Global fitting of experimental data for simulation of HS-AFM images

As discussed above, the molecular orientation of G-actin structure for cross-sectional analysis was selected from the molecular dynamics (MD) simulation (Fig. 2). To validate the conformations of the actin filaments in an experimental situation, tyrosine residues were modified by 3-NT oxidation and incorporated into the F-actin structure (Fig. 4). This F-actin structure (PDB 6BNO) contains four G-actin monomers for each actin helix, corresponding to ~22 nm in the length of the actin filament. To compare HS-AFM simulations of the non-oxidized and oxidized F-actin with experimental images, we conducted HS-AFM experiments on both untreated and SIN-1-treated skeletal F-actin. The SIN-1 treatment was performed according to our previous studies (Elkrief et al., 2022) and briefly described in the Methods. The imaging of the non-oxidized F-actin and the oxidized by SIN-1 F-actin attached to the mica-supported lipid bilayer surface (SLB) was performed by the same cantilever to avoid any difference caused by tip cantilever collision during HS-AFM scanning (Fig. 4b). There were no differences observed for the half helical pitch distances between the non-treated and SIN-1-treated F-actin (Fig. 4c). Conversely, the height distributions measurements of the highest points of the peak at the cross-over of the double F-actin helix, revealed significant difference between the non-treated and SIN-1-treated F-actin: $8.5 \text{ nm} \pm 2.9 \text{ nm (SD)}$ and $7.0 \text{ nm} \pm 1.2 \text{ nm (SD)}$ ($P=0.006$), respectively (Fig. 4d).

Validation of the structural difference between non-treated and treated HS-AFM simulated F-actin

The experimental HS-AFM images of the non-treated and SIN-1-treated F-actin were used as a template to gain the best-fitted orientations of simulated F-actin (PDB 6BNO) using global fitting approach available in BioAFM software (see Methods). The resulted best-fitted orientations of the non-oxidized and the oxidized F-actin shown in Figure 5: up to 5-7 different best-fitted orientations were considered to obtain the height profiles of the simulated images. The best-fitted orientations for each experimental HS-AFM datasets were obtained and used for cross-sectional analysis (Fig. 5).

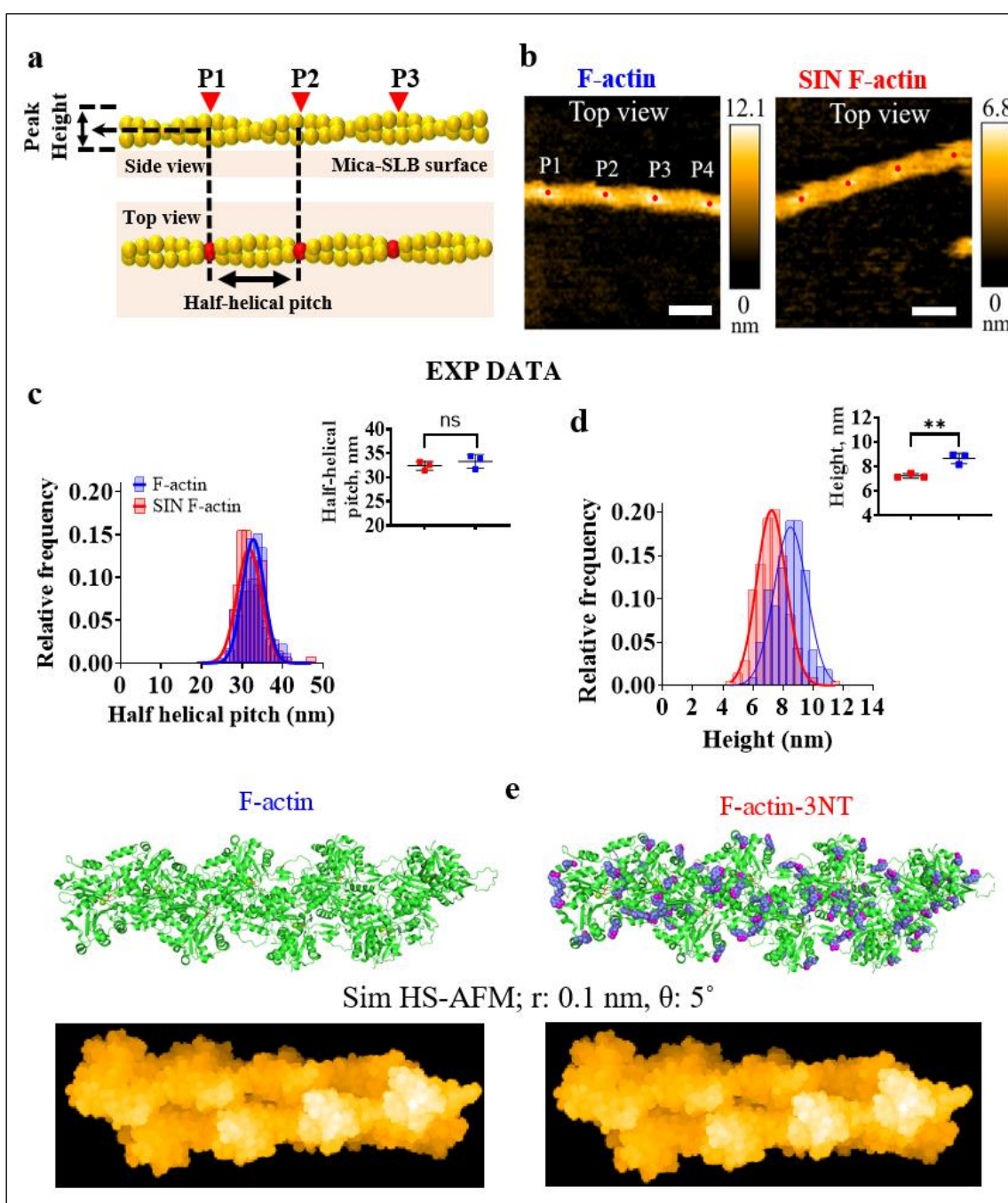


Figure 6. Comparison of the height profiles of the actin filaments treated by SIN-1 in the experimental and simulated HS-AFM images. (a) Diagram representing the peak height measurements along actin filament. The red points show the peaks (P) in the actin structure with the highest values as a cross-over of the double F-actin helix. (b) Representative HS-AFM images of control and SIN-1-treated actin filaments located on

The data for each best-fitted orientation were merged and plotted (Fig. 5c, right). The height profile from simulated HS-AFM images showed very similar height distribution in comparison to the experimental height distributions: $8.5 \text{ nm} \pm 1.1 \text{ nm}$ (SD) for non-treated F-actin and $7.2 \text{ nm} \pm 0.97 \text{ nm}$ (SD) for SIN-1 oxidized F-actin. The similarity between values measured in the experiments and in the simulated best-fitted orientations validates our computational approach to study conformational features of the biomolecules modified by oxidation conditions. Despite the fact that only one type of oxidized residue, tyrosine, is present in our computational model, it does not weaken the model and comparison with experimental data. Instead, it enables us to examine various oxidative agents and targets.

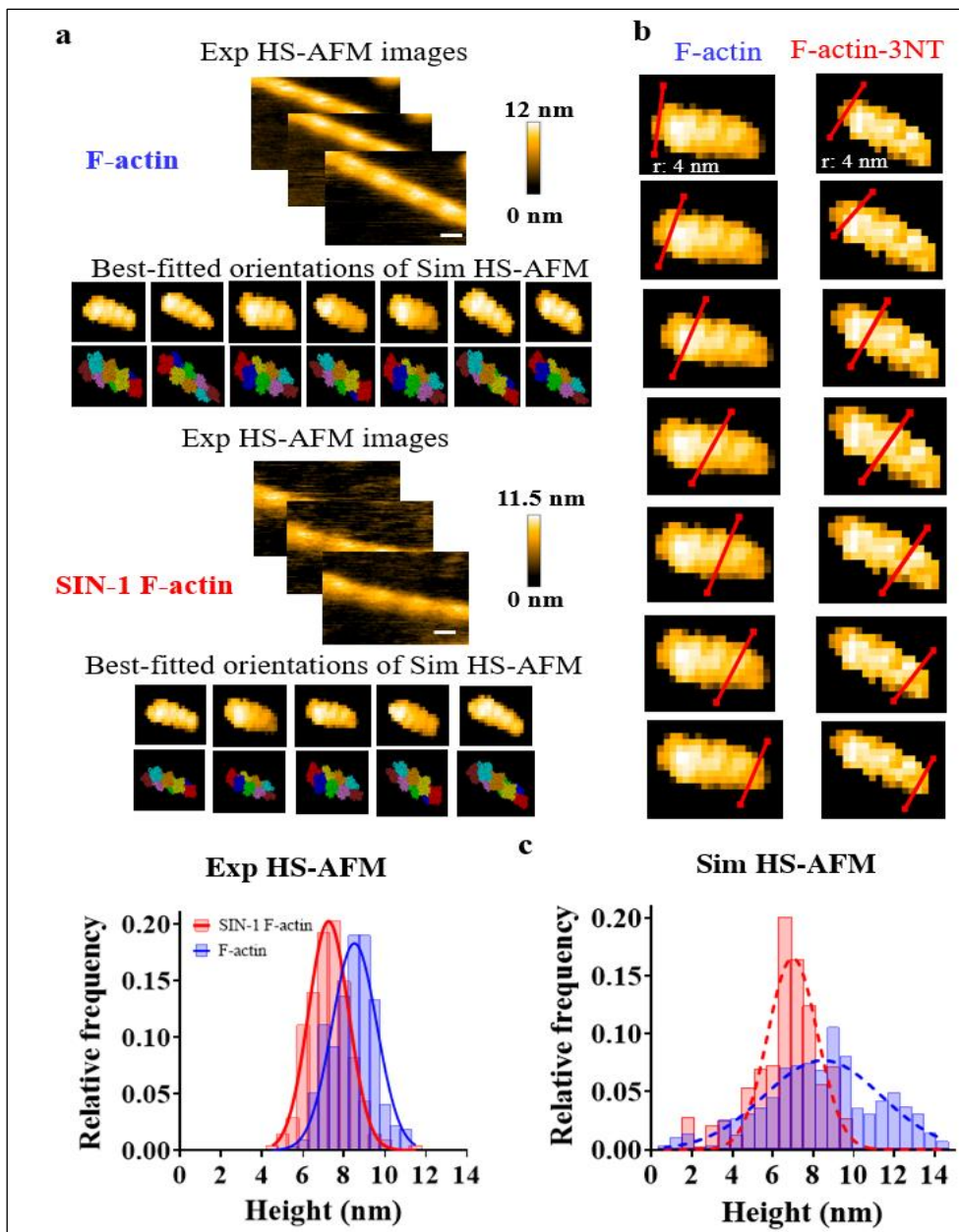


Figure 7. **Global fitting of experimental (Exp) and simulated (Sim) HS-AFM images.** (a) Best-fitted orientations of the simulated actin filaments with experimental HS-AFM images of the non-oxidized F-actin and the oxidized by SIN-1 F-actin used as a template. (b) An example of the cross-section analysis for the simulated F-actin structure (PDB 6BNO) with non-modified Tyr residues and oxidized Tyr-3NT residues. (c) Comparison of the height profiles of the actin filaments in the experimental and simulated HS-AFM images.

Evaluation of the myosin displacements under oxidation conditions

To evaluate the myosin displacements in the actin-myosin complex under oxidation conditions, we first tested the situation when the myosin HMM, a double-headed proteolytic fragment of

myosin, is oxidized by SIN-1. However, in our HS-AFM experiments the rate of success for the interaction of the single-molecule SIN-1-treated HMM and F-actin attached to mica-SBL surface was very low. One of the possible reasons for this issue can be explained by investigating the structure of SIN-1 oxidized HMM molecules in dynamics. As can be seen in Figure 6a, the oxidized SIN-1 HMM molecules exhibited a significant difference in the spatial orientation of the myosin heads from the non-oxidized HMM molecules. The heads of the oxidized HMM molecules appeared to be interlinked with the progression of the linkage over time. Indeed, the distance between two myosin heads within one molecule of the SIN-1-treated HMM was significantly reduced as can be observed from the Gaussian distributions (Fig. 6b).

Thus, to study the effect of SIN-1 oxidation on myosin power stroke at the single-molecule level in dynamics, we used SIN-1 treated F-actin attached to the mica-SLB surface, as shown on Fig. 4b, and added myosin HMM molecules to form actin-myosin complex in the presence of ATP. During the power strokes, the HMM molecules interact with either non-oxidized or SIN-1 oxidized F-actin and move myosin heads forward or backward along the actin filament. The analysis of the myosin displacements is detailed in our previously published studies (Matusovsky et al., 2020; Matusovsky et al., 2023) and briefly outlined in the Material and Methods.

The HMM heads displaced on the actin filaments as a consequence of the force-generation steps and cycling interaction with actin filaments in the presence of ATP. In terms of myosin cycling and the power stroke we defined the changing of the HMM position through a detachment and reattachment to the new binding site along F-actin as a transition from the weak to the strong-binding states that occurred within one or a few frames. In the presence of ATP, myosin heads detach from the actin filament and re-attach to the same or a new binding site, allowing us to determine the displacement by the evaluating the change in the averaged center of mass of the myosin heads between the reference frame and the next frame in HS-AFM successive images. For instance, if a myosin head binding to F-actin in one frame was observed in a different position in the next frame, it was considered as being detached and reattached to a new binding site. On the other hand, if the myosin head remained in the same position on F-actin for several frames without any change in its center of mass, it was assumed there were no displacement.

Typically, under our experimental conditions (low ionic strength with 25-100 mM KCl, 2-4 mM MgCl₂, 1 mM EGTA and neutral pH 7.0), the displacement distribution of the myosin heads bound to the non-oxidized F-actin showed three common sizes: short displacements (<1 nm), moderate displacements (1-3 nm) and long displacements (>4 nm). According to various experimental data, the long displacements ranged from 3-4 nm and over with averaged values ~4-6 nm, as in our study, represent the Pi release step. The short displacements ranged from 0.2-2.9 nm with averaged values ~1.7-2.6 nm represent the ADP release step (M. Capitano et al., 2006; Kaya & Higuchi, 2010; Uyeda, Kron, & Spudich, 1990; Veigel, Molloy, Schmitz, & Kendrick-Jones, 2003). This pattern of displacement distribution was also observed in our previous studies, where non-oxidized actin-myosin complex was used (Matusovsky et al., 2020; Matusovsky et al., 2023) and showed similar displacement size with experimental data for cardiac and skeletal myosins (Uyeda et al., 1990; Y. Wang, Yuan, Kazmierczak, Szczesna-Cordary, & Burghardt, 2018). Comparably to the previous published data, the displacement distribution of HMM heads along the non-oxidized F-actin was best fitted by the sum of two Gaussian functions and showed two main peaks with the mean averaged values indicated in the legend of the Figure 6. The displacement distribution of the HMM molecules complexed with SIN-1-treated F-actin revealed the shift to shorter displacements, suggesting that the frequency of long displacement events was significantly decreased by the oxidation (Fig. 6d). According to our previously published data (Matusovsky et al., 2020), the long displacements related to the phosphate (Pi) release step and lever arm movements responsible for force-generating step.

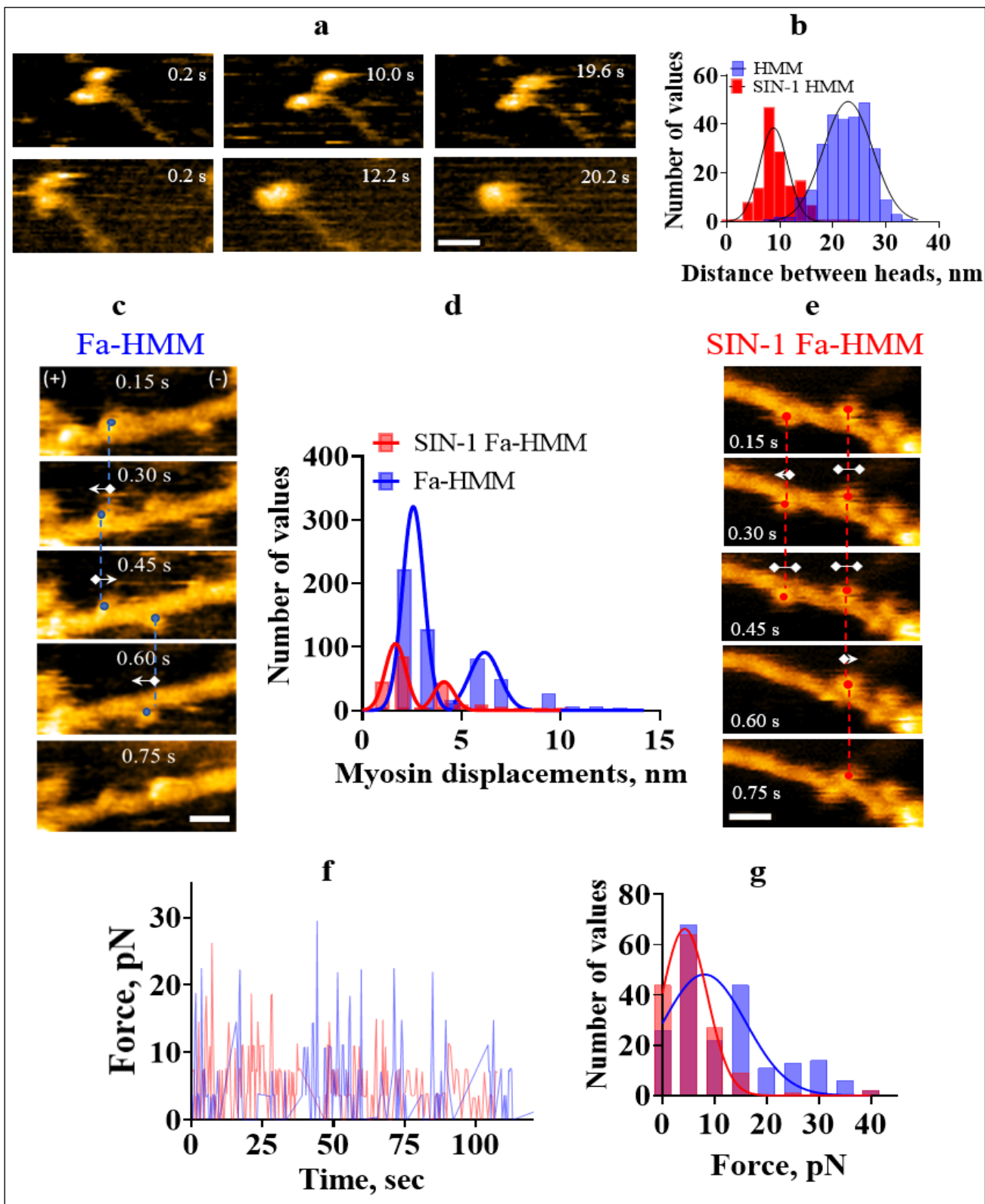


Figure 8. Oxidation-induced structural changes in HMM molecules and the HMM displacement. **(a)** The non-oxidized and SIN-1-treated skeletal HMM, a double-headed fragment of myosin, on the mica-APTES surface. Scan area: $150 \times 75 \text{ nm}^2$, $80 \times 40 \text{ pixels}^2$, temporal resolution: 5 frame per second, Scale bar: 30 nm. **(b)** The distance between two HMM heads measured over time: $8.9 \text{ nm} \pm 2.7 \text{ nm}$ (SD) for SIN-1-treated HMM and $22.9 \pm 4.6 \text{ nm}$ (SD) for non-oxidized HMM. **(c, e)** HS-AFM images of skeletal HMM bound to the non-oxidized F-actin **(c)** and SIN-1 treated F-actin **(e)** in the presence of ATP. Scan area: $150 \times 75 \text{ nm}^2$, $80 \times 40 \text{ pixels}^2$, temporal resolution: 6.7 frame per second. Scale bar: 30 nm. Arrows with symbols, (\leftrightarrow , $\leftarrow\rightarrow$): forward or backward head displacement between reference frame and subsequent frame; (\leftrightarrow): no head displacements between reference frame and subsequent frame. **(d)** Histogram of the HMM displacements along the non-oxidized F-actin (blue) and SIN-1 treated F-actin (red). Data were fitted by two Gaussians: $r^2=0.99$, $r^2=0.90$ and $r^2=0.99$, 0.91 for Fa-HMM and SIN-1-Fa-HMM, respectively; $n=758$ events (Fa-HMM), $n=303$ events (SIN-1-Fa-HMM). The average displacements for Fa-HMM: $2.6 \text{ nm} \pm 0.5 \text{ nm}$ (1st peak) and $6.1 \text{ nm} \pm 0.8 \text{ nm}$ (2nd peak); for SIN-1-Fa-HMM: $1.7 \text{ nm} \pm 0.5 \text{ nm}$ and $4.0 \pm 0.5 \text{ nm}$ (2nd peak) **(f, g)** The force produced by myosin molecule in the Fa-HMM (blue) and in the SIN-1-Fa-HMM complex (red) calculated from myosin displacements over time **(f)** and plotted as a histogram **(g)**. The force values were calculated from the equation $F = k \times d$, where k is a stiffness of HMM equal to 2 pN/nm per head (Månsson, Ušaj, Moretto, & Rassier, 2018) and d is a displacement of myosin molecule along the actin filament observed in the present study.

Conclusion

In our study, we observed that targeted tyrosine residues in G-actin and F-actin structures undergo oxidative modification destabilized the protein system. Simulated HS-AFM images of actin were analyzed to test structural modifications that occurred due to the oxidation of Tyr residues, by examining the peak heights distribution for the non-oxidized and oxidized proteins. The obtained results revealed a decrease of the height distribution in the oxidized G-actin/F-actin. Comparing our simulated results with experimental data confirmed observed difference in height distribution. Furthermore, we observed a reduction in the displacement size of myosin HMM molecules interacted with the oxidized actin filaments in the presence of ATP. There are several potential explanations for these findings: (i) alterations in the conformation of G-actin monomers through

3-NT oxidation impact the structure of actin filaments and ability of myosin binding, and (ii) the formation of cross-links between G-actin monomers through oxidation can impact the flexibility and polymerization rate of actin filaments (Maarten M Steinz et al., 2019), ultimately reducing the number of active myosin heads capable of producing force (Bagni et al., 2019; Elkrief et al., 2022; Persson et al., 2019). Therefore, the number of transitions from weak to strong attachment states of myosin heads is decreased. This can also result in a decrease in myosin attachment rate by rate limiting ADP release step, thus increasing myosin detachment rate. Thus, the capacity of the myosin molecule to generate force and its lifetime attachment to actin filaments could also be affected.

Methods

Proteins: Skeletal muscle HMM and F-actin were purified and tested for their functional activity by in-vitro motility assays, as described (Matusovsky et al., 2019). In some experiments skeletal HMM from Cytoskeleton Inc. (USA) was used.

3NT-oxidation of the tyrosine residues

The G-actin (PDB 2ZWH) and F-actin (PDB 6BNO) were used as non-oxidized molecular structures. The computational oxidative nitration (3NT) of the Tyr residues was implemented in a PyMOL software (v.2.3.3, Schrodinger LLC), using PyTMs plugin (Warnecke et al., 2014). The selection of the Tyr residues was based on the mass-spectrometry analysis of F-actin from patients with rheumatoid arthritis in our previous study (Maarten M Steinz et al., 2019). The analysis showed the hotspots of oxidized residues in each of the subdomain of G-actin.

Molecular dynamics simulations

The initial atomic coordinates were obtained from the 3.3 Å X-ray structure for skeletal G-actin (PDB 2ZWH). The atomic spatial coordinates of the non-modified G-actin and G-actin-3NT with oxidized Tyr residues were used to obtain trajectory from Molecular Dynamics (MD) simulations to evaluate the electrostatic potential energy and root-mean-square deviation (RMSD). MD simulations were carried out by our custom Python code (GitHub: https://github.com/matusoff/Molecular_dynamics/blob/main/OpenMM_simulation.py) using OpenMM package (<http://docs.openmm.org/latest/api-python/>) (Eastman et al., 2017) installed in the conda environment in Python. The TIP3P water model ('tip3p.xml') and the AMBER forcefield ('amber99sbildn.xml') from OpenMM module were used.

The non-oxidized G-actin and oxidized G-actin-3NT structures contain 5894 atoms and 5960 atoms, respectively. To pre-process the PDB files before MD simulations (add missing residues, add missing atoms, remove hydrogens, fix positions, get topology) we used PDBFixer.py script, based on OpenMM package, which is available on GitHub: (https://github.com/matusoff/Molecular_dynamics/blob/main/PDBFixer.py). The non-oxidized G-actin or oxidized G-actin-3NT structures were placed in a rectangular box, filled with water

molecules using VMD software (v.1.9.3)(Humphrey, Dalke, & Schulten, 1996). The size of the box defined by VMD software based on molecular dimensions of the protein structure: G-actin: 58.4 Å × 64.0 Å × 71.5 Å, G-actin-3NT: 83.2 Å × 88.8 Å × 96.5 Å. The protein atoms to its boundaries were at least 1.5 nm, and periodic conditions were set at the borders. Na⁺ and Cl⁻ ions were added to ensure the electrical neutrality of the system and the ionic strength was adjusted to 0.15 M. The charge of G-actin and G-actin-3NT before ionization was negative (-12.99); after ionization the charge was neutral (~4.3-4.5e⁻⁶).

Energy minimization was carried out using the OpenMM module using force groups defined by the LangevinIntegrator class. The process included finding a local minimum of the potential energy of a molecular system to optimize the initial structure. After energy minimization, the system was equilibrated in the NVT (constant number of particles, volume, and temperature) and NPT (constant number of particles, pressure, and temperature) ensembles. The system is balanced to a temperature of 300 K. The duration of the MD trajectories was adjusted up to 100 ns with a step of 1 ps. Following constants for the MD simulations were used: Boltzmann constant in kcal/mol/K: $k = 1.987e-3$; temperature in Kelvin: 300.0, number of MD steps to run:100000. The root-mean-square deviation (RMSD) was calculated in the VMD software with obtained during MD simulation trajectory dcd file.

Simulation of the HS-AFM images

Simulation of the HS-AFM images was done in BioAFM viewer (v.2.5, Kanazawa University). The following protocol was used: (i) Load PDB file with the non-modified Tyr residues or PDB file with the Tyr residues modified by oxidative nitration. The initial position of the atomic structure for G-actin was as shown in Fig. 1, where all four G-actin subdomains are visible. To ensure similar orientation of the two loaded structures, the correlation error was calculated by the custom Python script available in Supplementary Data; (ii) Rotation of the structure from the initial position by the step of 45° degree around y-axis or around x-axis; (iii) Cross-sectional analysis of the area around non-modified residues and residues modified by oxidative nitration (horizontal and vertical cross-sections).

As soon the initial position is adjusted, we save the initial position coordinates for further use. To obtain different structural orientation the rotation around x or y-axis was performed at 45° degree

step. The structural orientations shown in Figures 1 and S1. To compare the simulated non-oxidized and oxidized HS-AFM images correctly, the rotation of each image must be done to the exact degree step from the initial position. The spots around the non-oxidized and the oxidized Tyr residues were analyzed in the simulated HS-AFM images for the peak height distributions and cross-section analysis.

SIN-1 treatment of the skeletal F-actin and myosin HMM molecules

The SIN-1 treatment of F-actin and myosin HMM was performed according to our previously published paper (Elkrief et al., 2022). Briefly, freshly prepared SIN-1 was incubated at room temperature for 15 min and added to 7 μM F-actin in a buffer 60 mM KCl, 0.1 mM EGTA, 3 mM NaN_3 , 2 mM MgCl_2 , 10 mM MOPS at pH 7.0. and allowed to react for 10 min. The SIN-1-treated F-actin was stored at -80 C before use in the HS-AFM experiments. The HMM molecules were treated by SIN-1 in the following conditions: freshly prepared SIN-1 was incubated at room temperature for 15 min and added to 4 nM HMM (Cytoskeleton, USA). The final concentration of SIN-1 was 60 μM .

Myosin displacement analysis and force calculation

The definition of the power stroke during the HS-AFM acquisition of the actin-myosin complex and the approach to measure the myosin displacements described in detail in our previous works (Matusovsky et al., 2020; Moretto et al., 2022). Here, we compared the myosin HMM displacements along the non-oxidize and the oxidized actin filaments attached to the mica-SLB surface in the presence of 2 μM ATP. The myosin HMM displacement was calculated as the distance between the averaged center of mass (COM) position of HMM heads bound to F-actin in the reference frame and in the next frames, in successive HS-AFM images. The COM of the HMM head was calculated by the x, y, and z coordinates of the HS-AFM images. The x and y data correspond to the lateral coordinates, while the z coordinates described the height of the highest point in the HMM heads. The polarity of actin filament defined by the orientation of bound HMM head as described (Moretto et al., 2022).

The force estimation of the HMM heads bound to non-treated or SIN-1-treated F-actin was done with following equation:

$F = k * \Delta d$, where d is the displacement of HMM heads on actin filaments measured in the present study and k is a stiffness of myosin molecule (2 pN/nm), calculated based on experimental data and computational modelling of the free energy profiles of the attached cross-bridges (see (Månsson, 2016)).

HS-AFM and cantilevers: The experiments were performed on a tapping-mode HS-AFM system (RIBM) (Ando et al., 2001) by using small Olympus BL-AC10DS-A2 cantilevers with the following parameters: spring constant: 0.08-0.15 N/m, quality factor in water: \sim 1.4-1.6, resonant frequency in water: 06-1.2 MHz. The probe tip was fabricated on the tip of a cantilever by electron-beam deposition and sharpened by plasma etcher with a \sim 4 nm tip apex. A tip-sample loading force can be modulated by the free oscillation peak-to-peak amplitude (A_0) of the cantilever set to \sim 2.0 nm and the amplitude set point adjusted to more than 0.9 A_0 .

HS-AFM sample preparation: The lipid composition used for HS-AFM imaging contained 1,2-Dipalmitoyl-*sn*-glycero-3-phosphocholine (DPPC, Avanti Polar Lipids), 1,2-Dipalmitoyl-3-trimethylammonium-propane (DPTAP, Avanti Polar Lipids) and 1,2-dipalmitoyl-*sn*-glycero-3-phosphoethanolamine-*N*-(cap biotinyl) (biotin-cap-DPPE, Avanti Polar Lipids). DPPC: DPTAP: biotin-cap-DPPE were mixed in a weight ratio of 89:10:1. The preparation of lipid bilayer vesicles and deposition on mica substrate has been previously described (Matusovsky et al., 2020).

HS-AFM imaging: In order to assess possible structural changes in F-actin after exposure to SIN-1 modification, HS-AFM experiments were conducted with immobilized F-actin on a mica-supported lipid bilayer substrate (mica-SLB), containing a mixture of negatively (DPPC) and positively (DPTAP) charged lipids with small fraction of biotin-cap DPPE (ratio: 89:10:1). This lipid substrate allowed actin to attach to the surface, while maintaining some freedom of movement (Matusovsky et al., 2020; Matusovsky et al., 2019; Uchihashi, Kodera, & Ando, 2012) which was essential for the analysis of actin structure and oxidation-induced structural changes.

After rinsing the substrate with attachment buffer (25 mM KCl, 2 mM MgCl₂, 1 mM EGTA, 25 mM Imidazole-HCl, pH 7.0), 3.0 μ l of 7 μ M non-treated or SIN-1-treated actin filaments diluted in attachment buffer was deposited on the mica-SLB substrate and incubated for 10 minutes in a wet chamber. The unbounded actin filaments were washed by the same solution, and 3 μ l of 8 nM

HMM diluted in attachment buffer was placed on top of the bound to the substrate actin filaments and incubated for an additional 5 minutes. The actin-HMM complex in nucleotide-free conditions was rinsed by 20 μ l of attachment buffer, containing 2 μ M ATP dissolved in attachment buffer.

The sample stage with the mica-SLB substrate, containing actin-HMM complex was immersed into the AFM liquid cell chamber (volume \sim 120 μ l) filled with the solutions matching the experimental conditions. HS-AFM observations were performed at 5-10 frame per second (fps) with a typical scan area of 150 nm in x-direction and pixel resolutions of 80 x 40 pixels². The specific pixel resolutions and scan area range are indicated in the figure and movies legends. All experiments were performed at room temperature (25°C).

Data analysis and processing of HS-AFM images: The HS-AFM images were analyzed by Kodex software (4.4.7.39)(Ngo et al., 2015) and FIJI/ImageJ, with a low-pass filtering to remove spike noise in the image and to make the *xy*-plane flat. To simplify the analysis, we chose actin filaments located approximately in parallel to the x-direction. HMM heads bound to actin were visualized as a globular sphere of \sim 20 nm in diameter with the neck part, containing the \sim 8-12 nm lever-arm region. Statistical analysis (student t-test, correlation), Gaussian distributions and fitting were performed in GraphPad Prism software (v.9.3.0). Values are reported as mean \pm Standard Error Mean. A level of significance of $P \leq 0.05$ was set for all analyses.

Data availability

All data required for evaluation of the conclusions in the paper are present in the main body of the paper and/or in the Supporting Information. Additional data are available related to this paper may be requested from the authors.

Acknowledgments

This work was supported by the Natural Science and Engineering Research Council of Canada (to D.E.R). D.E.R. is a Canada Research Chair in Muscle Biophysics.

Author contributions

O.S.M. and D.E.R. designed research; O.S.M. performed HS-AFM experiments and created custom Python codes to pre-process files before MD simulations and Python codes to perform MD

simulations using OpenMM environment. D.E, Y.S.C, O.S.M were involved in analysis and interpretation of the data. O.S.M., D.E.R. wrote the paper and all authors approved the final version of the manuscript.

Ethics declarations

Competing interests

The authors declare no competing interests.

References

- Tidball, J. G., and Wehling-Henricks, M. The role of free radicals in the pathophysiology of muscular dystrophy. *J. Appl. Physiol.* 102, 1677–1686 (2007).
- Steinz, M. M, Persson, M., Aresh, B., Olsson, K., Cheng A. J. et al. Oxidative hotspots on actin promote skeletal muscle weakness in rheumatoid arthritis, *JCI insight* 4 (2019).
- Lowe, D. A., Surek, J. T., Thomas, D. D., and Thompson, L. V. Electron paramagnetic resonance reveals age-related myosin structural changes in rat skeletal muscle fibers. *Am. J. Physiol. Cell Physiol.* 280, C540–547 (2001).
- Reid, M. B., and Durham, W. J. Generation of reactive oxygen and nitrogen species in contracting skeletal muscle: potential impact on aging. *Ann. N.Y. Acad. Sci.* 959, 108–116 (2002).
- Prochniewicz, E., Thompson, L. V., and Thomas, D. D. Age-related decline in actomyosin structure and function. *Exp. Gerontol.* 42, 931–938 (2007).
- Coirault, C., Guellich, A., Barbry, T., Samuel, J. L., Riou, B., Lecar-pentier Y. Oxidative stress of myosin contributes to skeletal muscle dysfunction in rats with chronic heart failure. *Am. J. Physiol. Heart Circ. Physiol.* 292, H1009–H1017 (2007).
- Takimoto, E., and Kass, D. A. Role of Oxidative Stress in Cardiac Hypertrophy and Remodeling. *Hypertension* 49, 241–248 (2007).
- Maack, C., Kartes, T., Kilter, H., Schafers, H. J., Nickenig, G., Bohm, M., and Laufs, U. Oxygen free radical release in human failing myocardium is associated with increased activity of rac1-GTPase and represents a target for statin treatment. *Circulation* 108, 1567–1574 (2003).

- Ochala J, Gustafson AM, Diez ML, Renaud G, Li M. et al. Preferential skeletal muscle myosin loss in response to mechanical silencing in a novel rat intensive care unit model: underlying mechanisms. *J. Physiol.* 589, 2007–2026 (2011).
- Bansbach, H. M., Guilford, W. H. Actin nitrosylation and its effect on myosin driven motility. *AIMS Mol. Sci.* 3, 426–438 (2016).
- Elkrief, D., Cheng, Y. S., Matusovsky, O. S., Rassier, D. E. Oxidation alters myosin-actin interaction and force generation in skeletal muscle filaments. *Am. J. Physiol. Cell Physiol.* 323, C1206–C1214 (2022).
- Kirshenbaum, K., S. Papp, and S. Highsmith, Cross-linking myosin subfragment 1 Cys-697 and Cys-707 modifies ATP and actin binding site interactions. *Biophys. J.* 65 1121–1129 (1993).
- Bagni, M. A., Colombini, B., Nocella, M, Pregno, C., Cornachione, A. S., Rassier, D. E. The effects of fatigue and oxidation on contractile function of intact muscle fibers and myofibrils isolated from the mouse diaphragm. *Sci. Rep.* 9, 4422 (2019).
- Persson, M., Steinz, M. M., Westerblad, H., Lanner, J. T., Rassier, D. E. Force generated by myosin cross-bridges is reduced in myofibrils exposed to ROS/RNS. *Am. J. Physiol. Cell Physiol.* 317, C1304–C1312 (2019).
- Radi, R. Nitric oxide, oxidants, and protein tyrosine nitration. *Proc. Natl. Acad. Sci. USA* 101, 4003-4008 (2004).
- Callahan, L. A., She, Z. W., Nosek, T. M. Superoxide, hydroxyl radical, and hydrogen peroxide effects on single-diaphragm fiber contractile apparatus. *J. Appl. Physiol.* (1985) 90, 45–54 (2001).
- Thompson, L. V., Durand, D., Fugere, N. A., Ferrington, D. A. Myosin and actin expression and oxidation in aging muscle. *J. Appl. Physiol.* (1985) 101,1581–1587 (2006).
- Nakamura, T., Prikhodko, O. A., Pirie, E., Nagar, S., Akhtar, M. W. et al. Aberrant protein S-nitrosylation contributes to the pathophysiology of neurodegenerative diseases. *Neurobiol. Dis.* 84, 99–108 (2015).
- Mihm, M. J., Coyle, C. M., Schanbacher, B. L., Weinstein, D. M., Bauer, J. A. Peroxynitrite induced nitration and inactivation of myofibrillar creatine kinase in experimental heart failure. *Cardiovasc. Res.* 49, 798–807 (2001).
- Ahmed, U., Anwar, A., Savage, R.S., Thornalley, P. J., Rabbani, N. Protein oxidation, nitration and glycation biomarkers for early-stage diagnosis of osteoarthritis of the knee and typing and progression of arthritic disease. *Arthritis Res. Ther.* 18, 250 (2016).

- Matusovsky, O. S., Månsson, A., Persson, M., Cheng, Y. S., Rassier, D. E. High-speed AFM reveals subsecond dynamics of cardiac thin filaments upon Ca²⁺ activation and heavy meromyosin binding. *Proc. Natl. Acad. Sci. USA* 116, 16384–16393 (2019).
- Ngo, K. X., Kodera, N., Katayama, E., Ando, T., Uyeda, T. Q. Cofilin-induced unidirectional cooperative conformational changes in actin filaments revealed by high-speed atomic force microscopy. *Elife* 4, e04806 (2015).
- Matusovsky, O. S., Kodera, N., MacEachen, C., Ando, T., Cheng, Y. S., Rassier, D. E. Millisecond conformational dynamics of skeletal myosin II power stroke studied by high-speed atomic force microscopy. *ACS Nano* 15, 2229–2239 (2021).
- Matusovsky, O. S., Månsson, A., Rassier, D. E. Cooperativity of myosin II motors in the non-regulated and regulated thin filaments investigated with high-speed AFM. *J Gen Physiol.* 155, e202213190 (2023).
- Hayakawa, Y., Takaine, M., Ngo, K. X., Imai, T., Yamada, M. D., Behjat, A. B. et al. Actin-binding domain of Rng2 sparsely bound on F-actin strongly inhibits actin movement on myosin II. *Life Sci. Alliance* 6, e202201469 (2022).
- Kaya, M., Higuchi, H. Nonlinear elasticity and an 8-nm working stroke of single myosin molecules in myofilaments. *Science* 329, 686–689 (2010).
- Wang, Y., Ajtai, K., Burghardt, T. P. Ventricular myosin modifies *in vitro* step-size when phosphorylated. *J. Mol. Cell. Cardiol.* 72, 231–237 (2014).
- Moretto, L., Ušaj, M., Matusovsky, O., Rassier, D. E., Friedman, R., Månsson, A. Multistep orthophosphate release tunes actomyosin energy transduction. *Nat Commun.* 13, 4575 (2022).
- Warnecke, A., Sandalova, T., Achour, A., Harris, R. PyTMs: a useful PyMOL plugin for modeling common post-translational modifications. *BMC Bioinformatics* 15, 370 (2014).
- Eastman, P., Swails, J., Chodera, J. D., McGibbon, R. T., Zhao, Y., Beauchamp, K. A. et al. OpenMM 7: Rapid development of high performance algorithms for molecular dynamics. *PLOS Comp. Biol.* 13, e1005659 (2017).
- Amyot, R., Flechsig, H. BioAFMviewer: An interactive interface for simulated AFM scanning of biomolecular structures and dynamics. *PLoS Comput. Biol.* 16, e1008444 (2020).
- Amyot, R., Marchesi, A., Franz, C. M., Casuso, I., Flechsig, H. Simulation atomic force microscopy for atomic reconstruction of biomolecular structures from resolution-limited experimental images. *PLoS Comput. Biol.* 18, e1009970 (2022).

- Uyeda, T. Q., Kron, S. J., Spudich, J. A. Myosin step size. Estimation from slow sliding movement of actin over low densities of heavy meromyosin. *J Mol Biol.* 214, 699–710 (1990).
- Capitanio, M., Canepari, M., Cacciafesta, P., Lombardi, V., Cicchi, R., Maffei, M. et al Two independent mechanical events in the interaction cycle of skeletal muscle myosin with actin. *Proc. Natl. Acad. Sci USA* 103, 87–92 (2006).
- Veigel, C., Molloy, J. E., Schmitz, S., Kendrick-Jones, J. Load-dependent kinetics of force production by smooth muscle myosin measured with optical tweezers. *Nat. Cell Biol.* 5, 980–986 (2003).
- Wang, Y., Yuan, C-C., Kazmierczak, K., Szczesna-Cordary, D., Burghardt, T. P. Single cardiac ventricular myosins are autonomous motors. *Open Biol.* 8, 170240 (2018).
- Månsson, A., Ušaj, M., Moretto, L., Rassier, D. E. Do Actomyosin Single-Molecule Mechanics Data Predict Mechanics of Contracting Muscle? *Int. J. Mol. Sci.* 19, 1863 (2018).
- Humphrey, W., Dalke, A., Schultem, K. VMD – Visual Molecular Dynamics. *J. Mol. Graphics* 14, 33–38, (1996).
- Ando, T., Kodera, N., Takai, E., Maruyama, D., Saito, K., Toda, A. A high-speed atomic force microscope for studying biological macromolecules. *Proc. Natl. Acad. Sci. USA* 98, 12468–72 (2001).
- Uchihashi, T., Kodera, N., Ando, T. Guide to video recording of structure dynamics and dynamic processes of proteins by high-speed atomic force microscopy. *Nat. Protoc.* 7, 1193–206 (2012).

Supplementary Materials

Supplementary file includes:

Python code for Molecular dynamics simulation

Python scripts for image analysis

Figures S1 to S5.

Other Supplementary Materials for this manuscript include the following:

The custom Python code used for Molecular dynamics (MD) simulation with OpenMM package and Amber forcefield.

OpenMM_Simulation.py

```
import numpy as np
import matplotlib.pyplot as plt
import mdtraj as md
import Bio.PDB
from Bio.PDB import PDBParser
import simtk.unit as unit
import openmm as mm
import openmm.app as app
from openmm.app import *
from openmm import *
from simtk import unit
from sys import stdout
import nglview as nv

# Load the PDB file
pdb = PDBFile(r'path\2zwh_fixed_pH_7.pdb')

k = 1.987e-3 # Boltzmann constant in kcal/mol/K
T = 300.0 # temperature in K
dt = 0.002 # integration timestep in ps
nsteps = 100000 # number of MD steps to run

# Define the force field
forcefield = app.ForceField('amber99sbildn.xml', 'tip3p.xml')

# Create the simulation system
system = forcefield.createSystem(pdb.topology, nonbondedMethod=app.PME,
nonbondedCutoff=1.2*unit.nanometers, constraints=app.HBonds)
box_vectors = np.diag([10, 10, 50]) * unit.nanometer
```

```

system.setDefaultPeriodicBoxVectors(*box_vectors)

# Add a Langevin thermostat
integrator = LangevinIntegrator(T*unit.kelvin, 1.0/unit.picosecond, dt*unit.picoseconds)
integrator.setRandomNumberSeed(42)

# Create the simulation object
platform = mm.Platform.getPlatformByName('CPU')
simulation = Simulation(pdb.topology, system, integrator, platform)

# Set the initial positions of the atoms
positions = pdb.getPositions()
simulation.context.setPositions(positions)

# Minimize the energy
print('Minimizing energy...')
#simulation.minimizeEnergy()
simulation.minimizeEnergy(tolerance=1.0*unit.kilojoule_per_mole, maxIterations=100) #change it to 100 from 1000
# Equilibrate the system
print('Equilibrating...')
simulation.context.setVelocitiesToTemperature(T*unit.kelvin)
simulation.step(100000)

#Create the DCD reporter to save the trajectory data
report_interval = 1
reporter = DCDReporter(r'path\trajectory.dcd', report_interval)
simulation.reporters.append(reporter)

# Run the production simulation and calculate the total potential energy at each frame
print('Running production simulation...')
potential_energy = []
for i in range(nsteps):
    simulation.step(1)
    state = simulation.context.getState(getEnergy=True)
    potential_energy.append(state.getPotentialEnergy().value_in_unit(unit.kilocalorie_per_mole))

# Save the force data to a csv file
np.savetxt('potential_energy.csv', potential_energy, delimiter=',')

# Plot the potential energy data
plt.plot(range(nsteps), potential_energy)
plt.xlabel('Time (ps)')
plt.ylabel('Potential energy (kcal/mol)')
plt.show()

```

PDF_Fixer.py

This script was used to correct PDB files of G-actin before MD simulation.

```
from pdbfixer import PDBFixer
```

```

from simtk.openmm.app import *
from simtk.openmm import *
from simtk.unit import *
import os

def fix_pdb(pdb_id):
    pdb = PDBFile(pdb_id)
    if len(pdb_id) != 4:
        print("Creating PDBFixer...")
        fixer = PDBFixer(pdb_id)
        print("Finding missing residues...")
        fixer.findMissingResidues()

        chains = list(fixer.topology.chains())
        keys = fixer.missingResidues.keys()
        for key in list(keys):
            chain = chains[key[0]]
            if key[1] == 0 or key[1] == len(list(chain.residues())):
                print("ok")
                del fixer.missingResidues[key]

        print("Finding nonstandard residues...")
        fixer.findNonstandardResidues()
        print("Replacing nonstandard residues...")
        fixer.replaceNonstandardResidues()
        print("Removing heterogens...")
        fixer.removeHeterogens(keepWater=True)

        print("Finding missing atoms...")
        fixer.findMissingAtoms()
        print("Adding missing atoms...")
        fixer.addMissingAtoms()
        print("Adding missing hydrogens...")
        fixer.addMissingHydrogens(7)
        print("Writing PDB file...")

        PDBFile.writeFile(
            fixer.topology,
            fixer.positions,
            open(os.path.join(".", "%s_fixed_pH_%s.pdb" % (pdb_id.split('.')[0], 7)),
                "w"),
            keepIds=True)
        return "%s_fixed_pH_%s.pdb" % (pdb_id.split('.')[0], 7)

```

**Python code for correlation of G-actin (PDB 2ZWH) and simulated HS-AFM G-actin structure.
Script to calculate the mean squared error using neural model to correlate a simulated HS-AFM image and a structure obtained from PDB file**

```

import numpy as np
import keras
from keras.models import Sequential
from keras.layers import Dense, Conv2D, Flatten

```

```

import matplotlib.pyplot as plt

# Load and preprocess the two images data
# tip radius for sim AFM = 2.0
# PDB obtained by Bio-AFM viewer
image1 = np.load('/content/image.npy')
image2 = np.load('/content/image_2zwh-VdW_pdb.npy')
image1 = image1 / 255.0 # normalize to [0, 1] range
image2 = image2 / 255.0 # normalize to [0, 1] range

# Reshape the images to 4-dimensional tensors
image1 = np.array(image1)
image1 = image1.reshape(100, 100, 1)
image2 = np.array(image2)
image2 = image2.reshape(100, 100, 1)

# Define the neural network model
model = Sequential()
model.add(Conv2D(32, kernel_size=(3,3), activation='relu', input_shape=(100,100,1)))

model.add(Flatten())
model.add(Dense(512, activation='relu'))
model.add(Dense(256, activation='relu'))
model.add(Dense(128, activation='relu'))
model.add(Dense(64, activation='relu'))
model.add(Dense(1, activation='linear'))

# Compile the model
model.compile(loss='mean_squared_error', optimizer='adam')

# Train the model
model.fit(np.array([image1, image2]), np.array([0, 1]), epochs=10, batch_size=32, validation_split=0.2)

# Use the model to predict the correlation between the two images
correlation_result = model.predict(np.array([image1, image2]))

# Plot the original images
plt.figure(figsize=(10,5))
plt.subplot(1,2,1)
plt.imshow(image1.reshape(100, 100), cmap='gray')
plt.title("Image 1")

plt.subplot(1,2,2)
plt.imshow(image2.reshape(100, 100), cmap='gray')
plt.title("Image 2")

# Print the correlation result
print("Correlation result: ", correlation_result)
## Normalize the images to [0, 1] range
# image1 = (image1 - np.min(image1)) / (np.max(image1) - np.min(image1))
# image2 = (image2 - np.min(image2)) / (np.max(image2) - np.min(image2))

# Predict the correlation between the two images
prediction = model.predict(np.array([image1, image2]))

```

```

# Merge the two images based on the predicted correlation
merged_image = image1 * prediction[0] + image2 * prediction[1]

# Plot the merged image
plt.imshow(merged_image.reshape(100, 100), cmap='plasma')

def mean_squared_error(image1, image2):
    return np.mean((image1 - image2)**2)

mse = mean_squared_error(image1, image2)
print("Mean Squared Error:", mse)
# Show the plot
plt.show()

```

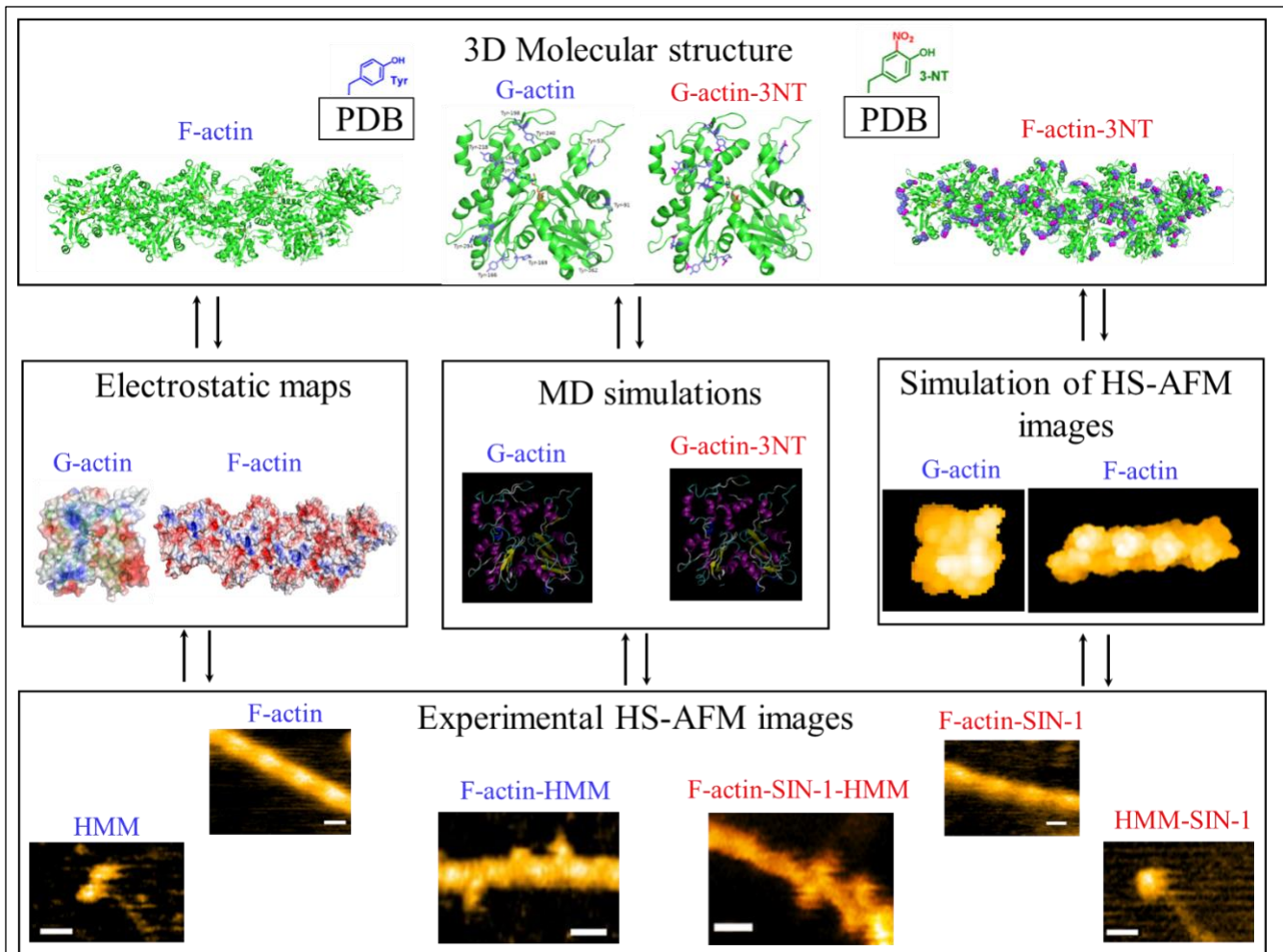
Results for correlation for G-actin (PDB 2ZWH) and simulated HS-AFM G-actin structure

```

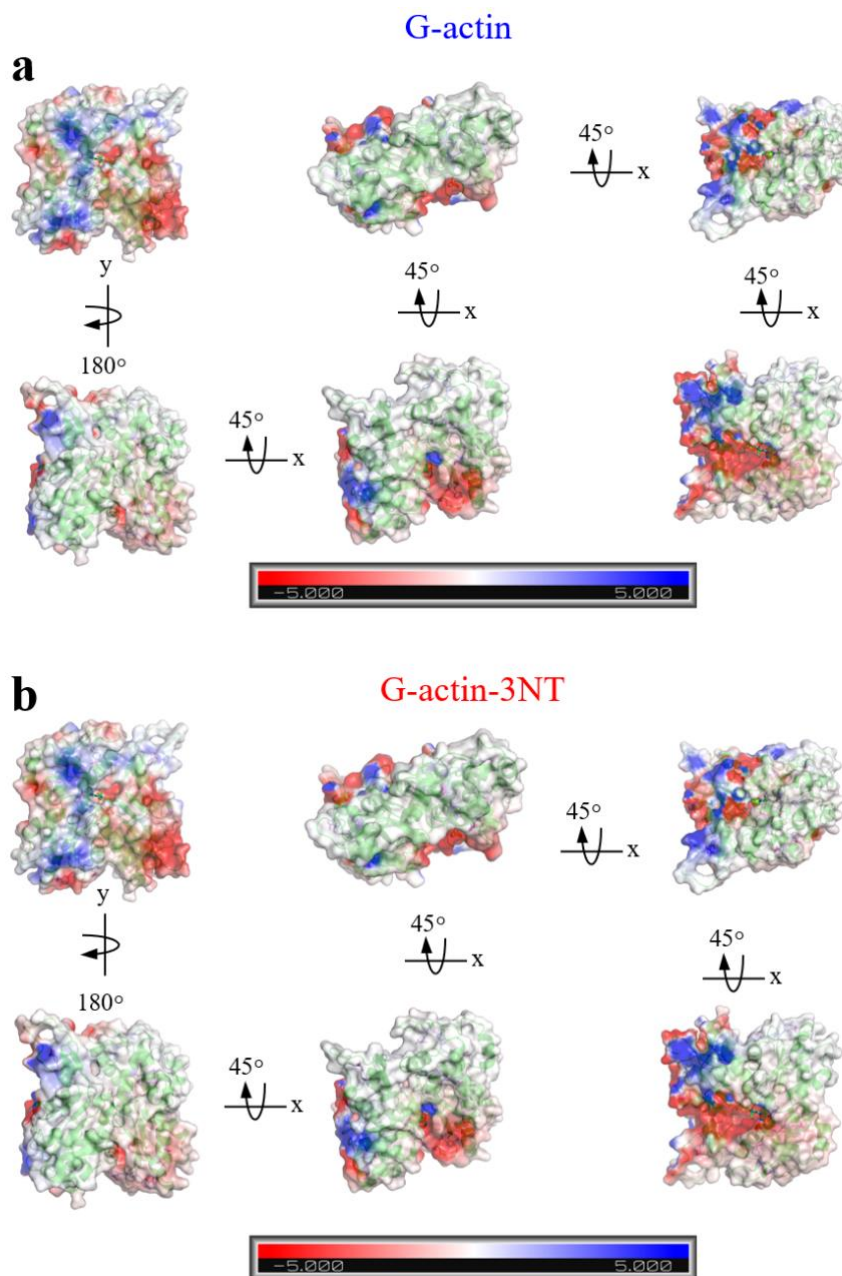
Epoch 1/10
1/1 [=====] - 2s 2s/step - loss: 2.8836e-11 - val_loss: 0.9950
Epoch 2/10
1/1 [=====] - 1s 762ms/step - loss: 7.2021e-06 - val_loss: 1.0028
Epoch 3/10
1/1 [=====] - 1s 786ms/step - loss: 2.0976e-06 - val_loss: 0.9979
Epoch 4/10
1/1 [=====] - 1s 768ms/step - loss: 1.1370e-06 - val_loss: 1.0043
Epoch 5/10
1/1 [=====] - 1s 771ms/step - loss: 4.7226e-06 - val_loss: 0.9984
Epoch 6/10
1/1 [=====] - 1s 769ms/step - loss: 6.4588e-07 - val_loss: 1.0097
Epoch 7/10
1/1 [=====] - 1s 756ms/step - loss: 2.4389e-05 - val_loss: 0.9929
Epoch 8/10
1/1 [=====] - 1s 763ms/step - loss: 1.2838e-05 - val_loss: 1.0021
Epoch 9/10
1/1 [=====] - 1s 764ms/step - loss: 1.1487e-06 - val_loss: 1.0008
Epoch 10/10
1/1 [=====] - 1s 778ms/step - loss: 1.7236e-07 - val_loss: 0.9975
1/1 [=====] - 0s 175ms/step
Correlation result: [[0.00126135]
 [0.00127196]]
1/1 [=====] - 0s 128ms/step

Mean Squared Error: 6.520016537572202e-07

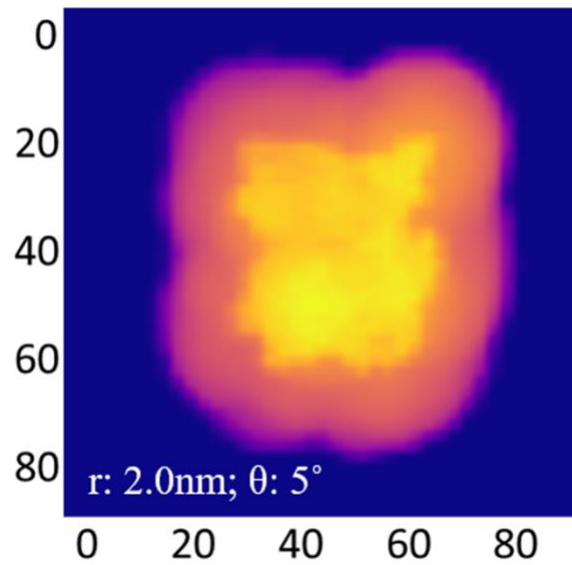
```



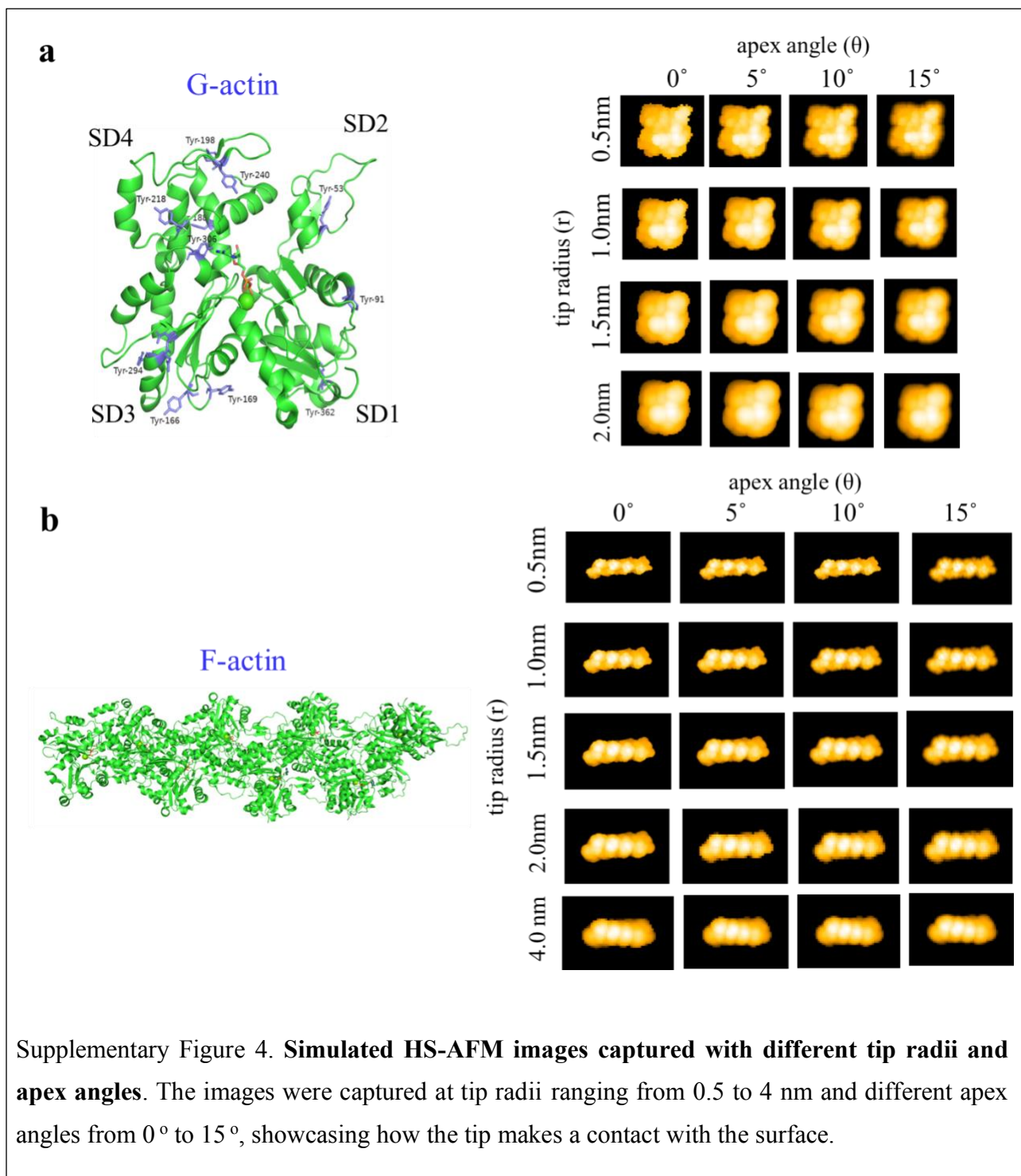
Supplementary Figure 1. **Flowchart of the project.**

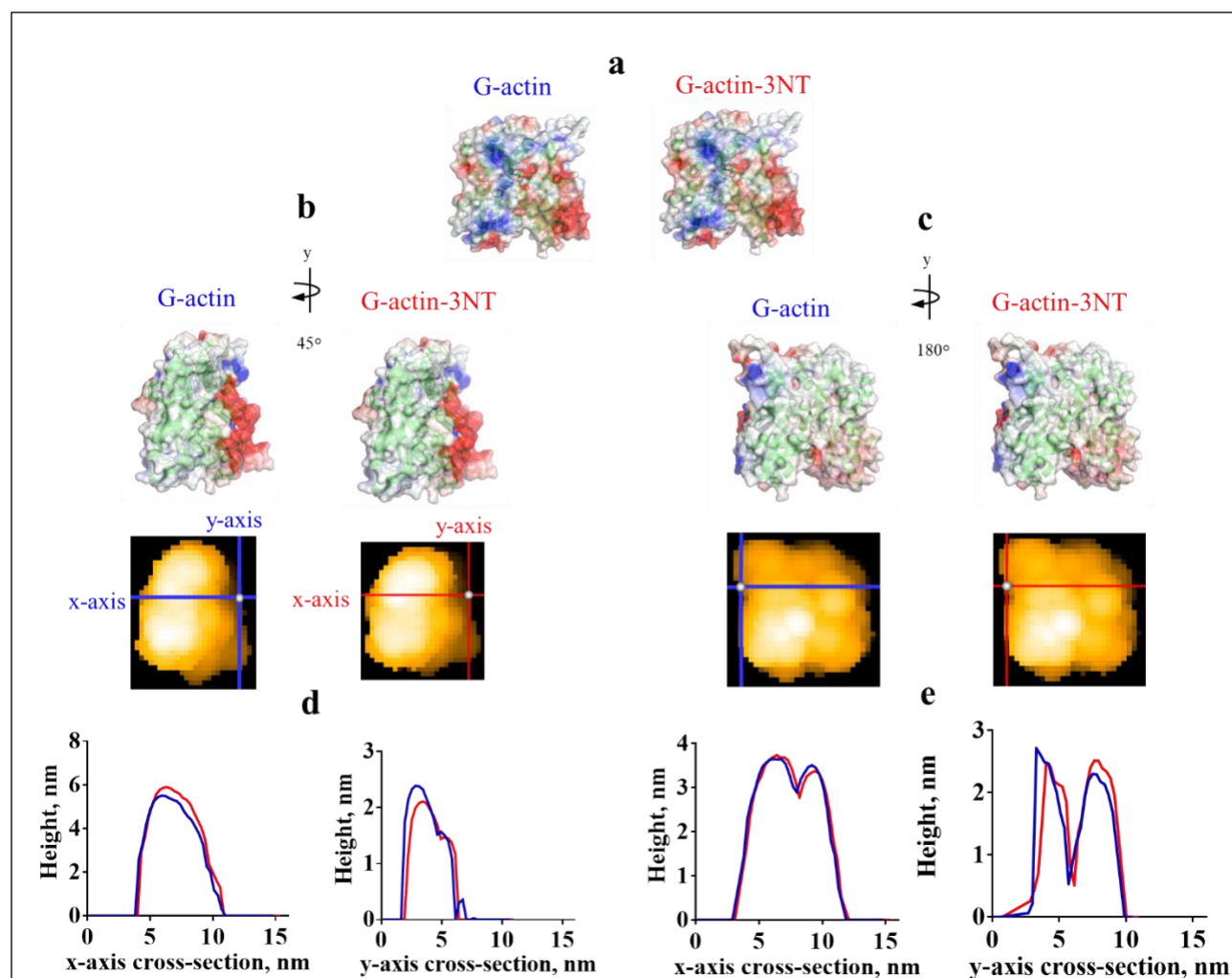


Supplementary Figure 2. **The successive x-axis rotation of the G-actin structures.** The non-oxidized G-actin (**a**) and the oxidized G-actin-3NT (**b**) structures with 45° step from initial position showed the local changes in the electrostatic potential energy around oxidized residues. The matched colored boxes for each orientation were magnified to show the charge differences more precisely. The map scale represents the electrostatic potential energy from -5.0 kBT (red) to 5.0 kBT (blue).



Supplementary Figure 3 **Correlation between pseudo-AFM G-actin image and G-actin structure using TensorFlow platform.** The pseudo-AFM images were obtained by BioAFM software (v.2.5) as described in the Methods using tip radii 2 nm. The mean squared error: 6.52×10^{-7} indicates the high correlation between pseudo-AFM image and G-actin atomic structure.





Supplementary Figure 5. **Local height measurements by cross-sectional analysis in the simulated G-actin and G-actin-3NT HS-AFM images.** (a-c) The initial conformation of the G-actin monomer structure (PDB: 2ZWH) rotated with 45° step around y-axis and corresponding simulated HS-AFM images obtained with BioAFM viewer with the tip radius 2 nm and the apex angle 5°. G-actin structures with non-oxidized Tyr and Tyr-3NT residues, indicating the x, y-axis used to obtain the local height values. (d, e) local height profiles for the G-actin structures with non-oxidized Tyr (blue) and Tyr-3NT (red) residues.

Supplementary References

- Steinz, M. M, Persson, M., Aresh, B., Olsson, K., Cheng A. J. et al. Oxidative hotspots on actin promote skeletal muscle weakness in rheumatoid arthritis, *JCI insight* 4 (2019).
- Warnecke, A., Sandalova, T., Achour, A., Harris, R. PyTMs: a useful PyMOL plugin for modeling common post-translational modifications. *BMC Bioinformatics* 15, 370 (2014).
- Humphrey, W., Dalke, A., Schultem, K. VMD – Visual Molecular Dynamics. *J. Mol. Graphics* 14, 33-38 (1996).

Thesis Discussion

Research Problem

The research problem at the heart of this thesis is the exploration of the effects of oxidation on actin, myosin and regulatory protein function, the most fundamental components of muscle contraction. While research had been undertaken on many of these components in whole and skinned muscle contexts, or assessing proteins individually, no studies analyzed the contractile apparatus across the experimental range used in this thesis. The novelty in our study comes from the comprehensiveness of the survey of oxidation, from amino acids assessed via MS, through structural and dynamic changes at the HS-AFM, to *in vitro* studies assessing velocity and force. Our review presents a seldom-espoused view: the complexity of the oxidative landscape leaves us with more questions than answers yet offers a foundational point for the entire survey of how contractile mechanics change as oxidative modifications accumulate. Following a summary of the findings, this section will discuss the implications of the entire thesis.

Summary of Findings

This thesis presents a comprehensive examination of the effects of oxidation on contractile muscle proteins at various levels of detail. At the smallest level, we validated the impact of SIN-1 oxidation on the amino acids of contractile proteins using MS, indicating widespread oxidation across all thin filament proteins. We then identified noticeable changes at the G-actin level, F-actin level, and in HMM under the HS-AFM, both experimentally and in simulated environments. We further assessed actin-myosin crossbridge turnover under SIN-1 oxidation using *in vitro* studies on actin, HMM, and actin plus HMM. We found decreases in sliding velocity when oxidation was present, which was reversible by antioxidant. Next, the study scope was expanded to the whole-filament level, where it was discovered that oxidation reduced filament force output when either actin or HMM were oxidized. Finally, we found that oxidation altered thin filament activity by shifting calcium sensitivity. Potentially, thin filament oxidation also caused a reduction in cross-bridge cycling, thus we also noted a reduction in velocities at all tested calcium concentrations. In sum, this data indicated a trail of effects across many scopes of actin-myosin interaction, from

smaller to larger levels. In the sections that follow we will explore the study aims from their conceptual genesis, which were updated as new data were uncovered. This allowed a wide evolution of study scope, which was both specific and wide-ranging, making for an ambitious attempt at understanding the oxidative map. We take the initial, traditional approach that while amino acid oxidative events are binary, events become collectively considered a redox “environment” (as often expressed in disease and aging studies (Berlett & Stadtman, 1997; Liguori et al., 2018; Squier, 2001; L. V. Thompson et al., 2006)) as larger contractile scopes are assessed. In this discussion we will attempt to bridge that conceptual gap, even though the events are one and the same.

Study Design and Interpretation of Results

Following initial suggestions that oxidative events in actin translated to contractile dysfunction in arthritis (Yamada et al., 2009; Yamada et al., 2017) and subsequent studies highlighting that actin oxidation was sufficient to induce contractile changes across experimental setups (Persson et al., 2019; Maarten Michiel Steinz, 2020; Maarten M Steinz et al., 2019), we launched an investigation into the effects of oxidation on actin. Previous research had demonstrated that using peroxide affects actin and regulated actin filaments, which was correlated to oxidation in ischemic conditions (J. H. Snook et al., 2008). Our initial surveys, focusing on the in vitro motility assay and preliminary HS-AFM data, corroborated these findings, revealing altered F-actin topology and reduced motility upon oxidation. Data indicated that these modifications were correlated to altered F-actin topology and reduced motility. Our results were in accordance with those who had shown that F-actin oxidation was also sufficient to reduce motility (Bansbach & Guilford, 2016). Intriguingly, studies indicated no changes or decreases in force depending on experimentation, oxidant species, or donor type, suggesting that many factors play a role in oxidant-induced force loss (Gao et al., 2012).

The original scope of our study, which aimed to exclusively evaluate actin in the controlled environment of the in vitro glass coverslip, evolved to incorporate heavy meromyosin (HMM). This shift underscored a pivotal realization: the intricate interplay among contractile proteins cannot be overlooked when assessing the overarching impact of oxidation on the contractile cycle. This revelation underscored the non-linear influence of contractile apparatus components on one

another. While the sequence of contractile responses is well-understood, from calcium binding to TnC culminating in cross-bridge formation, it's evident that each protein exerts reciprocal influences (Homsher et al., 2000; Pinto et al., 2008). It is known that conformational changes in Tm-Tn proteins affect the seemingly-distal actin-myosin interactions (Homsher et al., 2000), where the number and strength of cross-bridge attachments to the thin filament can significantly alter the binding of the TnC C-domain (Pinto et al., 2008). Therefore, it is plausible that oxidation on any of the thin filament components can have effects on cross bridging itself.

On the other hand, there are well characterized and purportedly directional oxidation events. Previous research has established that solely oxidizing HMM was sufficient to reduce filament contractile properties. Specifically, the oxidation of the highly reactive cysteines in the HMM head, SH1 and SH2, has been shown to impact ATPase activity and crossbridge formation. This suggests that oxidation events targeting specific amino acids might disproportionately influence protein function (Dutka et al., 2011; Gross & Lehman, 2013; Teresa Tiago et al., 2006). Thus, while there are many other studies showing several oxidation targets, (table 1 and table 2 in review), and some have proposed that cumulative, low level and cooperativity underlie the effects of oxidation (Bansbach & Guilford, 2016; J. H. Snook et al., 2008; Maarten M Steinz et al., 2019), a pivotal question remains: Which type of oxidation has a more pronounced impact - isolated oxidation events on key amino acids or the cumulative effect of numerous low-level oxidation events that cause indirect disruptions? This question warrants further investigation in future studies.

In our research, we observed pronounced effects of oxidation not only when actin or HMM were individually oxidized but also a synergistic decrease in velocity when both actin and myosin underwent oxidation. This observation was consistent with the filament force system output, where the combined oxidation of actin and myosin led to a reduction in filament force (study 1). Our study uniquely examined the force exerted by actin and myosin in their filamentous forms, a perspective rarely explored in existing literature due to the intricate nature of the isolation process. The findings from our study, while echoing the insights from years of prior research, offer a fresh perspective when contextualized within the broader scientific landscape. This segues into another theme of the thesis: the effects of oxidation appear to be cumulative. While HMM has traditionally been believed to predominantly influence crossbridge turnover (Teresa Tiago et al., 2010; T. Tiago

et al., 2006) our findings suggest that oxidation of actin alone can significantly reduce both crossbridge speed and force and when combined with HMM, there are further effects.

In tandem with Study 1, we were examining the impact of oxidation on actin under the AFM, which subsequently formed the basis for Study 3, focusing on actin and HMM assessments under the AFM.

We were encouraged by findings detailing how HA-AFM could be used to assess myosin V dynamics and biological structures in general (Ando et al., 2001; Koder, Yamamoto, Ishikawa, & Ando, 2010). We had also shown in another study that HS-AFM could be used to assess minute structural changes in calcium addition to thin filaments, indicating that not only could this be used to assess dynamics, but small structural changes could be directly associated with changes in function (Matusovsky et al., 2019). Our initial surveys had since then been published, indicating that even short lived dynamic events (~1 ms) of myosin II could be assessed and structurally implied using this technique (Matusovsky et al., 2020). While our preliminary data indicated that peak height was reduced in SIN-oxidized actin filaments (study 3), further exploration showed only minor changes in G-actin topology, again suggesting that as oxidation accumulates changes become more apparent at larger levels. We further validated this finding via comparisons with computational oxidative nitration of G-actin, which showed minor local changes in the electrostatic potential when only tyrosine was nitrosylated (Study 3, Figure 1). Interestingly, molecular dynamic simulation showed greater variability in G-actin with 3-NT additions, potentially indicating unstable molecules (Study 3, Figure 2), which could explain increased F-actin dissociation (Maarten M Steinz et al., 2019). Already, these data had shown that actin oxidation was sufficient to reduce functionality in in vitro studies, which as well-correlated with this computational data. G-actin nitrotyrosine was shown to influence local close-contact hydrogen bonding by introducing bulky steric groups, which are corroborated by our AFM and simulation data, and others who had shown that actin oxidation significantly reduces overall filament stability (Maarten M Steinz et al., 2019). This indicates the cumulative effect of oxidation in experimental data, likely, oxidation in the G actin accumulated and since G actins coil about each other, small changes resulted in larger changes along the F-actin. Thus, oxidation seems to have a cumulative effect, resulting in larger changes as we assess larger and larger scopes of contraction. Changes in actin topology, while not intuitively implying changes in myosin force production, nonetheless

bear ramifications for cross-bringing. Changes in actin shape would lead to changes in optimal cross bridge binding as well as whole filament cooperativity and could potentially imply changes in filament stiffness (Gittes, Mickey, Nettleton, & Howard, 1993; Wong, Sun, Cho, Lee, & Mak, 2015). Next, we decided to survey HMM structure and function in the same capacity.

Our investigations uncovered a notable difference in the inter-head distance of HMM, observing a significantly diminished distance between heads upon HMM oxidation (Study 3, Figure 6). This observation suggests that oxidation fosters interactions between adjacent HMM domains. Such interactions, primarily mediated through disulfide linkages, have been identified in various molecules of the contractile apparatus and have even been associated with augmented contractility (Gao et al., 2012). For instance, Tm oxidation has been shown to foster interactions with actin, leading to an initial enhancement in contractility, possibly due to increased stiffness, followed by a decline in function at elevated oxidant concentrations (Gao et al., 2012; Patel et al., 2013).

Furthermore, we identified a leftward shift in myosin head displacements in oxidized filaments relative to controls, indicating diminished displacement and, consequently, a reduced swinging arm movement in oxidized proteins. When extrapolating force from these displacements, the cumulative analysis of the oxidized lever arms revealed diminished force generation in oxidized HMM. While structural and lever arm alterations in the contractile apparatus have been previously suggested (Eisenberg & Hill, 1985; Prochniewicz, Lowe, et al., 2008; Thomas et al., 2002), our study stands as the first effort to visualize and correlate these changes specifically to the dynamics of myosin II using the HS-AFM. This is particularly significant given the non-processive nature of myosin II, rendering the capture of its dynamics a formidable challenge.

The implications of these studies are profound. These studies suggest that even minor and common modifications likely sum over a large contractile apparatus. Following this logic, the contractile dysfunction at the physiological level where excessive oxidation occurs in aging and disease cannot be ignored. Given the abundance of muscle and non-muscle contractile protein mass and the ubiquity of oxidation, this modification-protein pairing plays an outsize effect compared to the significance granted to single amino-acid modification events. This underscores the imperative of adopting a holistic perspective when evaluating post-translational modifications.

Complementing our HS-AFM findings, our direct assessment of oxidation via MS provided additional layers of insight and served to validate that oxidation was occurring within our samples. We identified oxidation on Tm, TnI, TnC, TnT, and actin. Intriguingly, despite detecting a broader spectrum of modifications on actin, other proteins displayed heightened oxidation under SIN-1 conditions compared to reduced conditions. Although all proteins exhibited considerable baseline oxidation, the levels were accentuated in oxidized conditions. This observation was further validated during our IVMA assessment, wherein the velocity of antioxidant-treated filaments was found to surpass that of controls (study 1, figure 2).

In broadening the scope of this thesis, we incorporated an examination of thin filament function under the IVMA (study 2). Notably, while numerous studies have investigated oxidative effects on actin and myosin, research focusing on the effects on thin filament proteins is comparatively sparse. It's a widely accepted that the principal thin and thick filament proteins, actin and myosin, are more susceptible to oxidation (Bobkov et al., 1997; Klein et al., 2011; Passarelli et al., 2008; Prochniewicz, Lowe, et al., 2008; Teresa Tiago et al., 2010), owing to their abundant cysteines and methionines. In spite of this, regulatory protein redox state is so critical that it has been used a marker for heart disease (La Vecchia et al., 2000) and has been shown to confer exercise adaptability low levels (De Palma et al., 2014; Merry & Ristow, 2016; Powers & Jackson, 2008) and contribute to dysfunction in disease and aging (Bai et al., 2013; Knott, Purcell, & Marston, 2002).

In alignment with this, we evaluated the calcium response of thin filaments in vitro, employing methodologies similar to those used for the velocity assessment in study 1. A salient observation was the consistent decrease in velocity across all tested calcium concentrations, underscoring the direct influence of TF oxidation on actin-myosin interactions. Emerging evidence suggests that the entire protein complex, rather than just actin and myosin in isolation, plays a role in cross-bridging. Consequently, perturbations in these proteins could precipitate pronounced contractile dysfunction. Some studies have posited that while velocity remains unaltered at lower calcium concentrations, more pronounced decreases manifest at elevated calcium levels (J. H. Snook et al., 2008). Intriguingly, our findings revealed that the oxidation of the regulated thin filament, when juxtaposed with unregulated actin, exhibited no discernible difference in velocity (study 2, figure 1). This indicates that while regulated filaments inherently slide faster than their unregulated

counterparts, oxidation diminishes this disparity. Potential underlying mechanisms could encompass complex dissociation, augmented stiffness, or cross-linking between subunits (Gao et al., 2012; Pinto et al., 2011; Wong et al., 2015).

Taken together, the *in vitro* motility and FFMS results from study 1 and 2 point to a consistent decrease in contractile output when oxidation is present. It should be noted however that oxidation was shown to result in increased contractility in some cases (Gao et al., 2012). This is possibly due to several factors, including the species of oxidant used, where SIN-1 predominantly donates peroxide, it was also shown to donate NO (shown in our MS data) and can also result in MDA modifications. More likely, the concentration or time exposure is critical to understanding functional outcomes. Some have moderate to little effect of oxidation on force when only actin is modified at moderate concentration (Bansbach & Guilford, 2016), while others have shown increases in contractility at low doses depending on whether there was rigor or relaxing solution, indicating the effect of subunit exposure (Gross & Lehman, 2013). As we have alluded to before, depending on the concentration and oxidant species, contractility, ATPase, and calcium sensitivity can even increase (Gao et al., 2012; Teresa Tiago et al., 2010). Our studies utilized large SIN-1 concentrations, mirroring those used earlier (Persson et al., 2019). At these concentrations, it is likely that there are unfolding effects on both actin and HMM, leading to whole-structural denaturation which are difficult to separate from the disruptions from modified amino acids themselves (Teresa Tiago et al., 2006). It should also be noted that there are sometimes no effects or unknown effects of oxidation on protein function (D. K. Polewicz, 2011; Prochniewicz, Lowe, et al., 2008). There are many forces within the protein, and one would assume that intramolecular redundancies would prevent modifications from having outsize effects.

Amino acid steric hindrances have been demonstrated to significantly influence molecular properties in isolation (Maarten M Steinz et al., 2019) and our findings in study 3 (figure 1) further underscore the impact of even a single type of modification. Considering this, over the course of this study we recognize that second-order effects likely surpass the consequences of individual modifications, which were difficult to capture with the tools used in this study. Consequently, models incorporating an escalating number of modifications, or a fully oxidized contractile apparatus might manifest amplified functional outcomes. it's noteworthy that residue exposure is modulated by solvent accessibility, particularly during various stages of the crossbridge cycle

(Gross & Lehman, 2013). The extended SIN-1 exposure in our MS studies, designed to ensure definitive oxidation, exceeded that used in the IVMA. Such prolonged exposure might have induced protein unfolding and denaturation (Teresa Tiago et al., 2006) potentially leading to the oxidation of residues that would remain unaffected under physiological conditions. On the other hand, due to the constraints of our experimental setup, characterized by high but still limited protein density, we couldn't achieve comprehensive protein coverage. This limitation precludes definitive conclusions about the full extent of potential oxidation sites in MS. Thus, while we can ascertain significant oxidation by SIN-1, the precise dynamics in a complex physiological environment remain elusive. Furthermore, we recognize the pivotal roles of other potentially-oxidized filament participants in contraction regulation which we regrettably could not incorporate, such as titin and MyBP-C (Balogh et al., 2014; Brennan et al., 2006; Herrero-Galán et al., 2022) which should be integrated in future research endeavors to expand on the foundational work done here for a more holistic understanding. While the complexities encountered in this study have provided invaluable insights, they also pave the way for intriguing questions and avenues for future research. A combination of *in vitro* and *in silico* modelling in the future would serve to answer exactly how protein function changes dynamically with fluxes in oxidative load. Correlating these changes with clinical studies promises exciting discoveries in the realm of molecular interactions and their physiological implications.

Meeting the Research Objectives

The primary objective of this research was to explore the effects of oxidation on the fundamental components of muscle contraction: actin, myosin, and regulatory proteins. Through a comprehensive survey spanning from amino acid assessment via MS to *in vitro* studies assessing velocity and force, this thesis follows oxidative events and their implications on contractile mechanics. The research has not only validated the impact of SIN-1 oxidation on amino acids of contractile proteins but has also highlighted the intricate interplay between different components of the contractile apparatus and how they influence each other.

Implications of the Findings

The findings underscore the profound influence of oxidation on muscle contraction. Oxidative modifications, even if minor, accumulate and manifest in significant changes across various scopes

of actin-myosin interaction. This research has shown that oxidation effects are cumulative, with both actin and myosin oxidation leading to a more than additive decrease in velocity and filament force. Furthermore, the research has illuminated the nuanced relationship between individual amino acid modifications and their collective impact on the larger contractile environment. The results have significant implications for understanding muscle dysfunction in conditions like aging and diseases where excessive oxidation occurs.

Future Directions

This research has provided a foundational understanding of the oxidative landscape in muscle contraction, unveiling exciting new avenues that beg further exploration. The contractile apparatus, with its intricate complexity, was necessarily distilled to a subset of its components for the scope of this study. As we look forward, it becomes imperative to broaden our lens. In the immediate future, endeavors should delve into the roles of other proteins in the contractile apparatus, such as titin, MyBP-C, α -actinin, and cofilin. Preliminary evidence suggests these proteins undergo oxidation, but the functional implications of such modifications remain enigmatic (Gao et al., 2012; Herrero-Galán et al., 2022; Patel et al., 2013). Additionally, there is a need to improve the resolution capabilities of Atomic Force Microscopy (AFM) to better visualize these oxidative modifications at the molecular level. Work with laser traps to investigate individual molecules could provide unprecedented insights into the mechanics of muscle contraction.

A pressing challenge and opportunity lie in bridging the chasm between micro-level experiments and macro-level physiological implications. While existing computational models have made strides in connecting individual cross-bridge dynamics to holistic muscle contractions (Månsson, 2016; Månsson et al., 2018), there's a compelling need to refine and expand these models. The advent of machine learning offers a tantalizing prospect: predicting and quantifying protein and organelle susceptibility to oxidation. Such advancements edge us closer to a comprehensive understanding of whole-tissue and organismal effects (R. L. Chang et al., 2020; Duan et al., 2020).

Looking further ahead, it is likely that there will be ground-breaking advancements in technology, such as intravital imaging and live super-resolution techniques, that could revolutionize our understanding of muscle physiology in whole tissues or organisms. Until then, comparative studies spanning *in vitro* setups, animal models, and computational simulations will be instrumental in

translating our findings to real-world applications (Maarten M Steinz et al., 2019). The integration of these technologies with advanced computational models could offer a comprehensive view of muscle contraction, from the molecular to the organismal level. The goal is to create a unified model that can explain muscle behavior under various oxidative conditions, thereby informing medical interventions for a range of diseases.

In conclusion, this research has taken an ambitious leap towards understanding the intricate oxidative landscape of muscle contraction. The nuanced interplay of the contractile apparatus's components underscores the need to view oxidation not as isolated redox states on individual amino acids but as dynamic environmental conditions across shifting populations of redox-susceptible molecules that shape muscle function. Embracing this holistic perspective is paramount as we endeavor to bridge the minutiae of biophysical systems with the grandeur of the entire contractile apparatus. This degree has imparted in me a dual sense of humility and motivation: first, in recognizing the profound complexities of translating molecular intricacies to whole-tissue phenomena; and second, in the realization that this endeavor is a distillation of a broader scientific aspiration. To model and comprehend complex systems, accounting for variations and unknown factors will allow the researcher of the future to integrate biophysical and chemical nuances into overarching effects. Such an endeavor demands nothing short of a comprehensive grasp of the human body; such an understanding lay beyond the frameworks offered by any singular academic discipline. Thus, we remain grounded by the enormity of tasks before us yet are invigorated by a future where integrative approaches are the norm in guiding us towards this bright future.

Appendices and Supplemental Information

Study II

Protein	Total number of Amino Acids	Total number of oxidizable residues	Proportion of oxidizable residues	Number of: C	M	R	K	Y	W	H
TnT	285	82	0.2877193	1	6	31	33	4	2	5
TnI	212	61	0.2877358	2	5	24	23	3	1	3
TnC	161	33	0.2049689	2	11	4	13	3	0	0
TM	284	68	0.2394366	1	6	14	39	6	0	2
Actin	377	89	0.2360743	6	17	18	19	16	4	9

Appendix Table 1. Number of Oxidizable residues for the most susceptible amino acids to oxidation in thin filament proteins. Numbers tabulated using scripts generated in R. Amino acids counted in bovine cardiac protein sequences listed in the supplementary tables from Study 2.

First Authorship Agreement for Study 3

This agreement is made this 07 day of August, 2023, between Oleg Matusovsky, hereinafter referred to as the "First Author", and Daren Elkrief, hereinafter referred to as the "Co-First Author".

WHEREAS, both parties have collaboratively contributed to Study 3, titled " Oxidation-induced structural changes in actin and myosin evaluated by computational simulation and high-speed AFM ", and wish to clarify the terms of co-first authorship and the use of the study in a manuscript-based thesis;

NOW, THEREFORE, in consideration of the mutual covenants contained herein and for other good and valuable consideration, the receipt and sufficiency of which is hereby acknowledged, the parties agree as follows:

1. **Co-First Authorship:** Both parties acknowledge and agree that Daren Elkrief is designated as a co-first author of Study 3, in recognition of his significant contributions to the project.
2. **Use in Thesis:** It is understood and agreed that Daren Elkrief, being a PhD student, will use Study 3 as part of his manuscript-based thesis at McGill University. Oleg Matusovsky, being a post-doc, will not use Study 3 for any thesis submission.
3. **No Further Use:** Oleg Matusovsky hereby confirms that he will not use the aforementioned study in more than one thesis or any other similar academic submission, in accordance with McGill University's guidelines.
4. **Intellectual Property:** Both parties acknowledge and respect the intellectual contributions of each other. Any intellectual property rights arising from the study will be dealt with as per McGill University's intellectual property guidelines and any other agreements in place between the parties.
5. **Entire Agreement:** This agreement contains the entire agreement between the parties relating to the subject matter hereof and supersedes any and all prior agreements or understandings, written or oral, between the parties related to the subject matter hereof.

6. **Amendments:** No modification or amendment to this agreement will be valid unless in writing and signed by both parties.

IN WITNESS WHEREOF, the parties hereto have executed this agreement as of the date first above written.

Oleg Matusovsky First Author 

Daren Elkrief Co-First Author 

Comprehensive Thesis Reference List

- Ackermann, M. A., & Kontrogianni-Konstantopoulos, A. (2011). Myosin binding protein-C: a regulator of actomyosin interaction in striated muscle. *Journal of Biomedicine and Biotechnology*, 2011.
- Ackermann, M. A., Patel, P. D., Valenti, J., Takagi, Y., Homsher, E., Sellers, J. R., & Kontrogianni-Konstantopoulos, A. (2013). Loss of actomyosin regulation in distal arthrogryposis myopathy due to mutant myosin binding protein-C slow. *The FASEB Journal*, 27(8), 3217.
- Ahmed, U., Anwar, A., Savage, R. S., Thornalley, P. J., & Rabbani, N. (2016). Protein oxidation, nitration and glycation biomarkers for early-stage diagnosis of osteoarthritis of the knee and typing and progression of arthritic disease. *Arthritis research & therapy*, 18, 1-11.
- Ait-Haddou, R., & Herzog, W. (2003). Brownian ratchet models of molecular motors. *Cell biochemistry and biophysics*, 38(2), 191-213.
- Aksenov, M., Aksenova, M., Butterfield, D., Geddes, J., & Markesbery, W. (2001). Protein oxidation in the brain in Alzheimer's disease. *Neuroscience*, 103(2), 373-383.
- Albet-Torres, N., Bloemink, M. J., Barman, T., Candau, R., Frölander, K., Geeves, M. A., . . . Piperio, C. (2009). Drug effect unveils inter-head cooperativity and strain-dependent ADP release in fast skeletal actomyosin. *Journal of Biological Chemistry*, 284(34), 22926-22937.
- Allingham, J. S., Smith, R., & Rayment, I. (2005). The structural basis of blebbistatin inhibition and specificity for myosin II. *Nature Structural & Molecular Biology*, 12(4), 378-379.
- Amyot, R., & Flechsig, H. (2020). BioAFMviewer: An interactive interface for simulated AFM scanning of biomolecular structures and dynamics. *PLoS computational biology*, 16(11), e1008444.
- Amyot, R., Marchesi, A., Franz, C. M., Casuso, I., & Flechsig, H. (2022). Simulation atomic force microscopy for atomic reconstruction of biomolecular structures from resolution-limited experimental images. *PLoS computational biology*, 18(3), e1009970.
- Ando, T., Kodera, N., Takai, E., Maruyama, D., Saito, K., & Toda, A. (2001). A high-speed atomic force microscope for studying biological macromolecules. *Proceedings of the National Academy of Sciences*, 98(22), 12468-12472. doi:10.1073/pnas.211400898

- Andrade, F. H., Reid, M. B., Allen, D. G., & Westerblad, H. (1998a). Effect of hydrogen peroxide and dithiothreitol on contractile function of single skeletal muscle fibres from the mouse. *The Journal of Physiology*, 509(Pt 2), 565.
- Andrade, F. H., Reid, M. B., Allen, D. G., & Westerblad, H. (1998b). Effect of nitric oxide on single skeletal muscle fibres from the mouse. *The Journal of Physiology*, 509(2), 577-586.
- Andrade, F. H., Reid, M. B., & Westerblad, H. (2001). Contractile response to low peroxide concentrations: myofibrillar calcium sensitivity as a likely target for redox-modulation of skeletal muscle function. *The FASEB Journal*, 15(2), 309-311.
- Andrey, P., & Boudier, T. (2006). Adaptive active contours (snakes) for the segmentation of complex structures in biological images. *Centre de Recherche Public Henri Tudor Copyright Notice*, 181.
- Antunes, F., & Cadenas, E. (2000). Estimation of H₂O₂ gradients across biomembranes. *FEBS letters*, 475(2), 121-126.
- Apple, F. S., Sandoval, Y., Jaffe, A. S., & Ordonez-Llanos, J. (2017). Cardiac troponin assays: guide to understanding analytical characteristics and their impact on clinical care. *Clinical chemistry*, 63(1), 73-81.
- Arstall, M. A., Yang, J., Stafford, I., Betts, W. H., & Horowitz, J. D. (1995). N-acetylcysteine in combination with nitroglycerin and streptokinase for the treatment of evolving acute myocardial infarction: safety and biochemical effects. *Circulation*, 92(10), 2855-2862.
- Ayala, A., Muñoz, M. F., & Argüelles, S. (2014). Lipid peroxidation: production, metabolism, and signaling mechanisms of malondialdehyde and 4-hydroxy-2-nonenal. *Oxidative medicine and cellular longevity*, 2014.
- Babu, A., Rao, V., Su, H., & Gulati, J. (1993). Critical minimum length of the central helix in troponin C for the Ca²⁺ switch in muscular contraction. *Journal of Biological Chemistry*, 268(26), 19232-19238.
- Baek, K., Liu, X., Ferron, F., Shu, S., Korn, E. D., & Dominguez, R. (2008). Modulation of actin structure and function by phosphorylation of Tyr-53 and profilin binding. *Proceedings of the National Academy of Sciences*, 105(33), 11748-11753.
- Bagni, M. A., Colombini, B., Nocella, M., Pregno, C., S. Cornachione, A., & Rassier, D. E. (2019). The effects of fatigue and oxidation on contractile function of intact muscle fibers and myofibrils isolated from the mouse diaphragm. *Scientific reports*, 9(1), 4422.

- Bai, F., Wang, L., & Kawai, M. (2013). A study of tropomyosin's role in cardiac function and disease using thin-filament reconstituted myocardium. *Journal of muscle research and cell motility*, *34*, 295-310.
- Balaz, M., & Månsson, A. (2005). Detection of small differences in actomyosin function using actin labeled with different phalloidin conjugates. *Analytical biochemistry*, *338*(2), 224-236.
- Balogh, Á., Santer, D., Pásztor, E. T., Tóth, A., Czuriga, D., Podesser, B. K., . . . Édes, I. (2014). Myofilament protein carbonylation contributes to the contractile dysfunction in the infarcted LV region of mouse hearts. *Cardiovascular research*, *101*(1), 108-119.
- Balta, E., Kramer, J., & Samstag, Y. (2020). Redox Regulation of the Actin Cytoskeleton in Cell Migration and Adhesion: On the Way to a Spatiotemporal View. *Frontiers in Cell and Developmental Biology*, *8*.
- Bansbach, H. M., & Guilford, W. H. (2016). Actin nitrosylation and its effect on myosin driven motility. *AIMS Molecular Science*, *3*(3), 426-438.
- Barford, D. (2004). The role of cysteine residues as redox-sensitive regulatory switches. *Current opinion in structural biology*, *14*(6), 679-686.
- Bates, G., Sigurdardottir, S., Kachmar, L., Zitouni, N. B., Benedetti, A., Petrof, B. J., . . . Lauzon, A.-M. (2013). Molecular, cellular, and muscle strip mechanics of the mdx mouse diaphragm. *American Journal of Physiology-Cell Physiology*, *304*(9), C873-C880.
- Beckman, J. S., Beckman, T. W., Chen, J., Marshall, P. A., & Freeman, B. A. (1990). Apparent hydroxyl radical production by peroxynitrite: implications for endothelial injury from nitric oxide and superoxide. *Proceedings of the National Academy of Sciences*, *87*(4), 1620-1624.
- Bell, M., Matta, J., Thomas, D., & Goldman, Y. (1995). Changes in cross-bridge kinetics induced by SH-1 modification in rabbit psoas fibers. *Biophysical journal*, *68*(4 Suppl), 360s.
- Berlett, B. S., & Stadtman, E. R. (1997). Protein oxidation in aging, disease, and oxidative stress. *Journal of Biological Chemistry*, *272*(33), 20313-20316.
- Bobkov, A. A., Bobkova, E. A., Homsher, E., & Reisler, E. (1997). Activation of regulated actin by SH1-modified myosin subfragment 1. *Biochemistry*, *36*(25), 7733-7738.
- Bobkova, E. A., Bobkov, A. A., Levitsky, D. I., & Reisler, E. (1999). Effects of SH1 and SH2 modifications on myosin similarities and differences. *Biophysical journal*, *76*(2), 1001-1007.

- Bonne, G., Carrier, L., Richard, P., Hainque, B., & Schwartz, K. (1998). Familial hypertrophic cardiomyopathy: from mutations to functional defects. *Circulation research*, *83*(6), 580-593.
- Borejdo, J., Shepard, A., Dumka, D., Akopova, I., Talent, J., Malka, A., & Burghardt, T. P. (2004). Changes in orientation of actin during contraction of muscle. *Biophysical journal*, *86*(4), 2308-2317. doi:10.1016/S0006-3495(04)74288-5
- Bowman, J. D., & Lindert, S. (2019). Computational studies of cardiac and skeletal troponin. *Frontiers in Molecular Biosciences*, *68*.
- Bradford, M. M. (1976). A rapid and sensitive method for the quantitation of microgram quantities of protein utilizing the principle of protein-dye binding. *Analytical biochemistry*, *72*(1-2), 248-254.
- Brennan, J. E., Chao, D. S., Xia, H., Aldape, K., & Bredt, D. S. (1995). Nitric oxide synthase complexed with dystrophin and absent from skeletal muscle sarcolemma in Duchenne muscular dystrophy. *Cell*, *82*(5), 743-752.
- Brennan, J. P., Miller, J. I., Fuller, W., Wait, R., Begum, S., Dunn, M. J., & Eaton, P. (2006). The utility of N, N-biotinyl glutathione disulfide in the study of protein S-glutathiolation. *Molecular & Cellular Proteomics*, *5*(2), 215-225.
- Brocca, L., McPhee, J. S., Longa, E., Canepari, M., Seynnes, O., De Vito, G., . . . Bottinelli, R. (2017). Structure and function of human muscle fibres and muscle proteome in physically active older men. *The Journal of Physiology*, *595*(14), 4823-4844.
- Burgoyne, J. R., Mongue-Din, H., Eaton, P., & Shah, A. M. (2012). Redox signaling in cardiac physiology and pathology. *Circulation research*, *111*(8), 1091-1106.
- Cadenas, E. (1989). Biochemistry of oxygen toxicity. *Annu Rev Biochem*, *58*, 79-110. doi:10.1146/annurev.bi.58.070189.000455
- Cadenas, E., & Boveris, A. (1980). Enhancement of hydrogen peroxide formation by protophores and ionophores in antimycin-supplemented mitochondria. *Biochemical Journal*, *188*(1), 31-37.
- Callahan, L. A., She, Z. W., & Nosek, T. M. (2001). Superoxide, hydroxyl radical, and hydrogen peroxide effects on single-diaphragm fiber contractile apparatus. *J Appl Physiol* (1985), *90*(1), 45-54. doi:10.1152/jappl.2001.90.1.45

- Canepari, M., Rossi, R., Pansarasa, O., Maffei, M., & Bottinelli, R. (2009). Actin sliding velocity on pure myosin isoforms from dystrophic mouse muscles. *Muscle & Nerve: Official Journal of the American Association of Electrodiagnostic Medicine*, *40*(2), 249-256.
- Canton, M., Menazza, S., & Di Lisa, F. (2014). Oxidative stress in muscular dystrophy: from generic evidence to specific sources and targets. *Journal of muscle research and cell motility*, *35*(1), 23-36.
- Canton, M., Menazza, S., Sheeran, F. L., de Laureto, P. P., Di Lisa, F., & Pepe, S. (2011). Oxidation of myofibrillar proteins in human heart failure. *Journal of the American College of Cardiology*, *57*(3), 300-309.
- Canton, M., Neverova, I., Menabò, R., Van Eyk, J., & Di Lisa, F. (2004). Evidence of myofibrillar protein oxidation induced by postischemic reperfusion in isolated rat hearts. *American Journal of Physiology-Heart and Circulatory Physiology*, *286*(3), H870-H877.
- Canton, M., Skyschally, A., Menabo, R., Boengler, K., Gres, P., Schulz, R., . . . Heusch, G. (2006). Oxidative modification of tropomyosin and myocardial dysfunction following coronary microembolization. *European Heart Journal*, *27*(7), 875-881.
- Capanni, C., Squarzoni, S., Petrini, S., Villanova, M., Muscari, C., Maraldi, N. M., . . . Caldarera, C. M. (1998). Increase of neuronal nitric oxide synthase in rat skeletal muscle during ageing. *Biochemical and biophysical research communications*, *245*(1), 216-219.
- Capitanio, D., Vasso, M., Fania, C., Moriggi, M., Viganò, A., Procacci, P., . . . Gelfi, C. (2009). Comparative proteomic profile of rat sciatic nerve and gastrocnemius muscle tissues in ageing by 2-D DIGE. *Proteomics*, *9*(7), 2004-2020.
- Capitanio, M., Canepari, M., Cacciafesta, P., Lombardi, V., Cicchi, R., Maffei, M., . . . Bottinelli, R. (2006). Two independent mechanical events in the interaction cycle of skeletal muscle myosin with actin. *Proceedings of the National Academy of Sciences*, *103*(1), 87-92.
- Carballal, S., Bartesaghi, S., & Radi, R. (2014). Kinetic and mechanistic considerations to assess the biological fate of peroxynitrite. *Biochimica et Biophysica Acta (BBA)-General Subjects*, *1840*(2), 768-780.
- Chance, B., Sies, H., & Boveris, A. (1979). Hydroperoxide metabolism in mammalian organs. *Physiological reviews*, *59*(3), 527-605.
- Chang, R. L., Stanley, J. A., Robinson, M. C., Sher, J. W., Li, Z., Chan, Y. A., . . . Matallana-Surget, S. (2020). Protein structure, amino acid composition and sequence determine proteome vulnerability to oxidation-induced damage. *The EMBO journal*, *39*(23), e104523.

- Chang, T.-C., Chou, W.-Y., & Chang, G.-G. (2000). Protein oxidation and turnover. *Journal of biomedical science*, 7(5), 357-363.
- Chen, F. C., & Ogut, O. (2006). Decline of contractility during ischemia-reperfusion injury: actin glutathionylation and its effect on allosteric interaction with tropomyosin. *American Journal of Physiology-Cell Physiology*, 290(3), C719-C727.
- Cheng, A. J., Bruton, J. D., Lanner, J. T., & Westerblad, H. (2015). Antioxidant treatments do not improve force recovery after fatiguing stimulation of mouse skeletal muscle fibres. *The Journal of physiology*, 593(2), 457-472.
- Cheng, A. J., Yamada, T., Rassier, D. E., Andersson, D. C., Westerblad, H., & Lanner, J. T. (2016). Reactive oxygen/nitrogen species and contractile function in skeletal muscle during fatigue and recovery. *The Journal of Physiology*, 594(18), 5149-5160.
- Cheng, Y.-S., de Souza Leite, F., & Rassier, D. E. (2020). The load dependence and the force-velocity relation in intact myosin filaments from skeletal and smooth muscles. *American Journal of Physiology-Cell Physiology*, 318(1), C103-C110.
- Cheng, Y.-S., Matusovskiy, O. S., & Rassier, D. E. (2019). Cleavage of loops 1 and 2 in skeletal muscle heavy meromyosin (HMM) leads to a decreased function. *Archives of Biochemistry and Biophysics*, 661, 168-177. doi:<https://doi.org/10.1016/j.abb.2018.11.002>
- Cheung, H. C., Gryczynski, I., Malak, H., Wiczak, W., Johnson, M. L., & Lakowicz, J. R. (1991). Conformational flexibility of the Cys 697-Cys 707 segment of myosin subfragment-1: distance distributions by frequency-domain fluorometry. *Biophysical chemistry*, 40(1), 1-17.
- Coirault, C., Guellich, A., Barbry, T., Samuel, J. L., Riou, B., & Lecarpentier, Y. (2007). Oxidative stress of myosin contributes to skeletal muscle dysfunction in rats with chronic heart failure. *American Journal of Physiology-Heart and Circulatory Physiology*, 292(2), H1009-H1017.
- Coirault, C., Lambert, F., Marchand-Adam, S., Attal, P., Chemla, D., & Lecarpentier, Y. (1999). Myosin molecular motor dysfunction in dystrophic mouse diaphragm. *American Journal of Physiology-Cell Physiology*, 277(6), C1170-C1176.
- Coirault, C., Lambert, F., Pourny, J.-C., & Lecarpentier, Y. (2002). Velocity of actomyosin sliding in vitro is reduced in dystrophic mouse diaphragm. *American Journal of Respiratory and Critical Care Medicine*, 165(2), 250-253.

- Cooper, C. E., Patel, R. P., Brookes, P. S., & Darley-Usmar, V. M. (2002). Nanotransducers in cellular redox signaling: modification of thiols by reactive oxygen and nitrogen species. *Trends Biochem Sci*, 27(10), 489-492.
- Cornachione, A. S., Leite, F. S., Wang, J., Leu, N. A., Kalganov, A., Volgin, D., . . . Yates III, J. R. (2014). Arginylation of myosin heavy chain regulates skeletal muscle strength. *Cell reports*, 8(2), 470-476.
- Cremonese, C., Grammer, J., & Yount, R. (1989). Direct chemical evidence that serine 180 in the glycine-rich loop of myosin binds to ATP. *Journal of Biological Chemistry*, 264(12), 6608-6611.
- Crowder, M., & Cooke, R. (1984). The effect of myosin sulphhydryl modification on the mechanics of fibre contraction. *Journal of Muscle Research & Cell Motility*, 5(2), 131-146.
- Cuello, F., Wittig, I., Lorenz, K., & Eaton, P. (2018). Oxidation of cardiac myofibrillar proteins: Priming for dysfunction? *Molecular Aspects of Medicine*, 63, 47-58.
- Cunha-Oliveira, T., Montezinho, L., Mendes, C., Firuzi, O., Saso, L., Oliveira, P. J., & Silva, F. S. (2020). Oxidative stress in amyotrophic lateral sclerosis: pathophysiology and opportunities for pharmacological intervention. *Oxidative medicine and cellular longevity*, 2020.
- D'Oria, R., Schipani, R., Leonardini, A., Natalicchio, A., Perrini, S., Cignarelli, A., . . . Giordano, F. (2020). The role of oxidative stress in cardiac disease: from physiological response to injury factor. *Oxidative medicine and cellular longevity*, 2020.
- Dalle-Donne, I., Giustarini, D., Rossi, R., Colombo, R., & Milzani, A. (2003). Reversible S-glutathionylation of Cys 374 regulates actin filament formation by inducing structural changes in the actin molecule. *Free Radic Biol Med*, 34(1), 23-32.
- Dalle-Donne, I., Rossi, R., Giustarini, D., Gagliano, N., Di Simplicio, P., Colombo, R., & Milzani, A. (2002). Methionine oxidation as a major cause of the functional impairment of oxidized actin. *Free Radical Biology and Medicine*, 32(9), 927-937.
- Dalle-Donne, I., Rossi, R., Giustarini, D., Gagliano, N., Di Simplicio, P., Colombo, R., & Milzani, A. (2002). Methionine oxidation as a major cause of the functional impairment of oxidized actin. *Free Radic Biol Med*, 32(9), 927-937.
- Dalle-Donne, I., Rossi, R., Giustarini, D., Gagliano, N., Lusini, L., Milzani, A., . . . Colombo, R. (2001). Actin carbonylation: from a simple marker of protein oxidation to relevant signs of severe functional impairment. *Free Radical Biology and Medicine*, 31(9), 1075-1083.

- De Palma, C., Morisi, F., Pambianco, S., Assi, E., Touvier, T., Russo, S., . . . Clementi, E. (2014). Deficient nitric oxide signalling impairs skeletal muscle growth and performance: involvement of mitochondrial dysregulation. *Skeletal muscle*, 4(1), 22-22. doi:10.1186/s13395-014-0022-6
- Dean, R. T., Fu, S., Stocker, R., & Davies, M. J. (1997). Biochemistry and pathology of radical-mediated protein oxidation. *Biochemical Journal*, 324(1), 1-18.
- Digerness, S. B., Harris, K. D., Kirklin, J. W., Urthaler, F., Viera, L., Beckman, J. S., & Darley-Usmar, V. (1999). Peroxynitrite irreversibly decreases diastolic and systolic function in cardiac muscle. *Free Radic Biol Med*, 27(11-12), 1386-1392.
- Disatnik, M.-H., Dhawan, J., Yu, Y., Beal, M. F., Whirl, M. M., Franco, A. A., & Rando, T. A. (1998). Evidence of oxidative stress in mdx mouse muscle: studies of the pre-necrotic state. *Journal of the neurological Sciences*, 161(1), 77-84.
- Dominguez, R., Freyzon, Y., Trybus, K. M., & Cohen, C. (1998). Crystal structure of a vertebrate smooth muscle myosin motor domain and its complex with the essential light chain: Visualization of the pre-power stroke state. *Cell*, 94(5), 559-571.
- Doroszko, A., Polewicz, D., Cadete, V. J., Sawicka, J., Jones, M., Szczesna-Cordary, D., . . . Sawicki, G. (2010). Neonatal asphyxia induces the nitration of cardiac myosin light chain 2 (MLC2) which is associated with cardiac systolic dysfunction. *Shock (Augusta, Ga.)*, 34(6), 592.
- Doroszko, A., Polewicz, D., Sawicka, J., Richardson, J. S., Cheung, P.-Y., & Sawicki, G. (2009). Cardiac dysfunction in an animal model of neonatal asphyxia is associated with increased degradation of MLC1 by MMP-2. *Basic research in cardiology*, 104(6), 669.
- Dos Santos, S. L., Baraibar, M. A., Lundberg, S., Eeg-Olofsson, O., Larsson, L., & Friguet, B. (2015). Oxidative proteome alterations during skeletal muscle ageing. *Redox biology*, 5, 267-274.
- Droge, W. (2002). Free radicals in the physiological control of cell function. *Physiological reviews*, 82(1), 47-95.
- Du, J., Wang, X., Miereles, C., Bailey, J. L., Debigare, R., Zheng, B., . . . Mitch, W. E. (2004). Activation of caspase-3 is an initial step triggering accelerated muscle proteolysis in catabolic conditions. *The Journal of clinical investigation*, 113(1), 115-123.
- Duan, J., Zhang, T., Gaffrey, M. J., Weitz, K. K., Moore, R. J., Li, X., . . . Qian, W.-J. (2020). Stoichiometric quantification of the thiol redox proteome of macrophages reveals subcellular compartmentalization and susceptibility to oxidative perturbations. *Redox biology*, 36, 101649.

- Duke, J., Takashi, R., Ue, K., & Morales, M. (1976). Reciprocal reactivities of specific thiols when actin binds to myosin. *Proceedings of the National Academy of Sciences*, *73*(2), 302-306.
- Durham, W. J., Aracena-Parks, P., Long, C., Rossi, A. E., Goonasekera, S. A., Boncompagni, S., . . . Hamilton, S. L. (2008). RyR1 S-nitrosylation underlies environmental heat stroke and sudden death in Y522S RyR1 knockin mice. *Cell*, *133*(1), 53-65. doi:10.1016/j.cell.2008.02.042
- Dutka, T. L., Mollica, J. P., & Lamb, G. D. (2011). Differential effects of peroxynitrite on contractile protein properties in fast- and slow-twitch skeletal muscle fibers of rat. *Journal of applied physiology*, *110*(3), 705-716. doi:10.1152/jappphysiol.00739.2010
- Eastman, P., Swails, J., Chodera, J. D., McGibbon, R. T., Zhao, Y., Beauchamp, K. A., . . . Stern, C. D. (2017). OpenMM 7: Rapid development of high performance algorithms for molecular dynamics. *PLoS computational biology*, *13*(7), e1005659.
- Eaton, P., Byers, H. L., Leeds, N., Ward, M. A., & Shattock, M. J. (2002). Detection, quantitation, purification, and identification of cardiac proteins S-thiolated during ischemia and reperfusion. *Journal of Biological Chemistry*, *277*(12), 9806-9811.
- Eisenberg, E., & Hill, T. L. (1985). Muscle contraction and free energy transduction in biological systems. *Science*, *227*(4690), 999-1006.
- El-Shafey, A. F., Armstrong, A. E., Terrill, J. R., Grounds, M. D., & Arthur, P. G. (2011). Screening for increased protein thiol oxidation in oxidatively stressed muscle tissue. *Free Radical Research*, *45*(9), 991-999.
- Elkrief, D., Cheng, Y.-S., Matusovsky, O. S., & Rassier, D. E. (2022). Oxidation alters myosin-actin interaction and force generation in skeletal muscle filaments. *American Journal of Physiology-Cell Physiology*, *323*(4), C1206-C1214.
- Evangelista, A. M., Rao, V. S., Filo, A. R., Marozkina, N. V., Doctor, A., Jones, D. R., . . . Guilford, W. H. (2010). Direct regulation of striated muscle myosins by nitric oxide and endogenous nitrosothiols. *PloS one*, *5*(6), e11209.
- Fabian, F., & Mühlrad, A. (1968). Effect of trinitrophenylation on myosin ATPase. *Biochimica et Biophysica Acta (BBA)-Bioenergetics*, *162*(4), 596-603.
- Farah, M. E., Sirotkin, V., Haarer, B., Kakhniashvili, D., & Amberg, D. C. (2011). Diverse protective roles of the actin cytoskeleton during oxidative stress. *Cytoskeleton (Hoboken, N.J.)*, *68*(6), 340-354. doi:10.1002/cm.20516

- Fauver, M. E., Dunaway, D. L., Lilienfeld, D. H., Craighead, H. G., & Pollack, G. H. (1998). Microfabricated cantilevers for measurement of subcellular and molecular forces. *IEEE transactions on biomedical engineering*, *45*(7), 891-898.
- Fedorova, M., Kuleva, N., & Hoffmann, R. (2010). Identification of cysteine, methionine and tryptophan residues of actin oxidized in vivo during oxidative stress. *J Proteome Res*, *9*(3), 1598-1609. doi:10.1021/pr901099e
- Fedorova, M., Todorovsky, T., Kuleva, N., & Hoffmann, R. (2010). Quantitative evaluation of tryptophan oxidation in actin and troponin I from skeletal muscles using a rat model of acute oxidative stress. *Proteomics*, *10*(14), 2692-2700.
- Ferreira, L. F., & Reid, M. B. (2008). Muscle-derived ROS and thiol regulation in muscle fatigue. *J Appl Physiol (1985)*, *104*(3), 853-860. doi:10.1152/jappphysiol.00953.2007
- Finer, J. T., Simmons, R. M., & Spudich, J. A. (1994). Single myosin molecule mechanics: piconewton forces and nanometre steps. *Nature*, *368*(6467), 113-119.
- Fisher, A. J., Smith, C. A., Thoden, J., Smith, R., Sutoh, K., Holden, H. M., & Rayment, I. (1995a). Structural studies of myosin: nucleotide complexes: a revised model for the molecular basis of muscle contraction. *Biophysical journal*, *68*(4 Suppl), 19S.
- Fisher, A. J., Smith, C. A., Thoden, J., Smith, R., Sutoh, K., Holden, H. M., & Rayment, I. (1995b). X-ray structures of the myosin motor domain of dictyostelium discoideum complexed with MgADP. cntdot. BeFx and MgADP. cntdot. AIF4. *Biochemistry*, *34*(28), 8960-8972.
- Forman, H. J., & Zhang, H. (2021). Targeting oxidative stress in disease: Promise and limitations of antioxidant therapy. *Nature Reviews Drug Discovery*, *20*(9), 689-709.
- Förstermann, U., Closs, E. I., Pollock, J. S., Nakane, M., Schwarz, P., Gath, I., & Kleinert, H. (1994). Nitric oxide synthase isozymes. Characterization, purification, molecular cloning, and functions. *Hypertension*, *23*(6_pt_2), 1121-1131.
- Fraser, I. D., & Marston, S. B. (1995). In Vitro Motility Analysis of Actin-Tropomyosin Regulation by Troponin and Calcium: THE THIN FILAMENT IS SWITCHED AS A SINGLE COOPERATIVE UNIT (*). *Journal of Biological Chemistry*, *270*(14), 7836-7841.
- Fujii, T., Iwane, A. H., Yanagida, T., & Namba, K. (2010). Direct visualization of secondary structures of F-actin by electron cryomicroscopy. *Nature*, *467*(7316), 724-728. doi:10.1038/nature09372

- Fujii, T., & Namba, K. (2017). Structure of actomyosin rigour complex at 5.2 Å resolution and insights into the ATPase cycle mechanism. *Nat Commun*, 8, 13969. doi:10.1038/ncomms13969
- Furch, M., Fujita-Becker, S., Geeves, M. A., Holmes, K. C., & Manstein, D. J. (1999). Role of the salt-bridge between switch-1 and switch-2 of Dictyostelium myosin. *Journal of molecular biology*, 290(3), 797-809.
- Galińska-Rakoczy, A., Engel, P., Xu, C., Jung, H., Craig, R., Tobacman, L. S., & Lehman, W. (2008). Structural basis for the regulation of muscle contraction by troponin and tropomyosin. *Journal of molecular biology*, 379(5), 929-935.
- Galler, S., Hilber, K., & Göbesberger, A. (1997). Effects of nitric oxide on force-generating proteins of skeletal muscle. *Pflügers Archiv*, 434(3), 242-245.
- Gannon, J., Doran, P., Kirwan, A., & Ohlendieck, K. (2009). Drastic increase of myosin light chain MLC-2 in senescent skeletal muscle indicates fast-to-slow fibre transition in sarcopenia of old age. *European journal of cell biology*, 88(11), 685-700.
- Gao, W. D., Liu, Y., & Marban, E. (1996). Selective effects of oxygen free radicals on excitation-contraction coupling in ventricular muscle: implications for the mechanism of stunned myocardium. *Circulation*, 94(10), 2597-2604.
- Gao, W. D., Murray, C. I., Tian, Y., Zhong, X., DuMond, J. F., Shen, X., . . . King, S. B. (2012). Nitroxyl-mediated disulfide bond formation between cardiac myofilament cysteines enhances contractile function. *Circulation research*, 111(8), 1002-1011.
- Gasmi-Seabrook, G. M., Howarth, J. W., Finley, N., Abusamhadneh, E., Gaponenko, V., Brito, R. M., . . . Rosevear, P. R. (1999). Solution structures of the C-terminal domain of cardiac troponin C free and bound to the N-terminal domain of cardiac troponin I. *Biochemistry*, 38(26), 8313-8322.
- Geeves, M. A., & Holmes, K. C. (2005). The molecular mechanism of muscle contraction. *Advances in protein chemistry*, 71, 161-193.
- Gelfi, C., Viganò, A., Ripamonti, M., Pontoglio, A., Begum, S., Pellegrino, M. A., . . . Cerretelli, P. (2006). The human muscle proteome in aging. *J Proteome Res*, 5(6), 1344-1353.
- Giordano, F. J. (2005). Oxygen, oxidative stress, hypoxia, and heart failure. *The Journal of clinical investigation*, 115(3), 500-508.
- Gittes, F., Mickey, B., Nettleton, J., & Howard, J. (1993). Flexural rigidity of microtubules and actin filaments measured from thermal fluctuations in shape. *J Cell Biol*, 120(4), 923-934.

- Gollub, J., Cremo, C. R., & Cooke, R. (1996). ADP release produces a rotation of the neck region of smooth myosin but not skeletal myosin. *Nature structural biology*, 3(9), 796-802.
- Gomes, A. V., Potter, J. D., & Szczesna-Cordary, D. (2002). The role of troponins in muscle contraction. *IUBMB life*, 54(6), 323-333.
- Gomez-Cabrera, M. C., Close, G. L., Kayani, A., McArdle, A., Vina, J., & Jackson, M. J. (2010). Effect of xanthine oxidase-generated extracellular superoxide on skeletal muscle force generation. *American Journal of Physiology-Regulatory, Integrative and Comparative Physiology*, 298(1), R2-R8.
- Gordon, A. M., Homsher, E., & Regnier, M. (2000). Regulation of contraction in striated muscle. *Physiological reviews*, 80(2), 853-924.
- Gordon, A. M., LaMadrid, M. A., Chen, Y., Luo, Z., & Chase, P. B. (1997). Calcium regulation of skeletal muscle thin filament motility in vitro. *Biophysical journal*, 72(3), 1295-1307.
- Grammer, J., & Yount, R. (1991). Photochemical evidence that Ser-243 of myosin's heavy chain is near the phosphate binding site for ATP. *Biophys. J*, 59, 226a.
- Greenberg, M. J., & Moore, J. R. (2010). The molecular basis of frictional loads in the in vitro motility assay with applications to the study of the loaded mechanochemistry of molecular motors. *Cytoskeleton*, 67(5), 273-285.
- Gross, S. M., & Lehman, S. L. (2013). Accessibility of myofilament cysteines and effects on ATPase depend on the activation state during exposure to oxidants. *PLoS One*, 8(7).
- Guellich, A., Negroni, E., Decostre, V., Demoule, A., & Coirault, C. (2014). Altered cross-bridge properties in skeletal muscle dystrophies. *Frontiers in physiology*, 5, 393.
- Harris, S. P., Lyons, R. G., & Bezold, K. L. (2011). In the thick of it: HCM-causing mutations in myosin binding proteins of the thick filament. *Circulation research*, 108(6), 751-764.
- Hayakawa, Y., Takaine, M., Ngo, K. X., Imai, T., Yamada, M. D., Behjat, A. B., . . . Kodera, N. (2023). Actin-binding domain of Rng2 sparsely bound on F-actin strongly inhibits actin movement on myosin II. *Life Science Alliance*, 6(1).
- Haycock, J. W., Jones, P., Harris, J. B., & Mantle, D. (1996). Differential susceptibility of human skeletal muscle proteins to free radical induced oxidative damage: a histochemical, immunocytochemical and electron microscopical study in vitro. *Acta neuropathologica*, 92(4), 331-340.
- Heather, M. B., & William, H. G. (2016). Actin nitrosylation and its effect on myosin driven motility. *AIMS Molecular Science*, 3(3), 426-438.

- Herrero-Galán, E., Martínez-Martín, I., Sánchez-González, C., Vicente, N., Bonzón-Kulichenko, E., Calvo, E., . . . Velázquez-Carreras, D. (2022). Basal oxidation of conserved cysteines modulates cardiac titin stiffness and dynamics. *Redox biology*, *52*, 102306.
- Hertelendi, Z., Toth, A., Borbely, A., Galajda, Z., Van Der Velden, J., Stienen, G. J., . . . Papp, Z. (2008). Oxidation of myofilament protein sulfhydryl groups reduces the contractile force and its Ca²⁺ sensitivity in human cardiomyocytes. *Antioxid Redox Signal*, *10*(7), 1175-1184.
- Hitchcock-DeGregori, S. E., & Barua, B. (2017). Tropomyosin structure, function, and interactions: a dynamic regulator. *Fibrous proteins: structures and mechanisms*, 253-284.
- Holmes, K. C. (1997). The swinging lever-arm hypothesis of muscle contraction. *Current Biology*, *7*(2), R112-R118.
- Homsher, E., Lee, D. M., Morris, C., Pavlov, D., & Tobacman, L. S. (2000). Regulation of force and unloaded sliding speed in single thin filaments: effects of regulatory proteins and calcium. *The Journal of Physiology*, *524*(Pt 1), 233.
- Hong, S. J., Gokulrangan, G., & Schöneich, C. (2007). Proteomic analysis of age dependent nitration of rat cardiac proteins by solution isoelectric focusing coupled to nanoHPLC tandem mass spectrometry. *Experimental gerontology*, *42*(7), 639-651.
- Höök, P., Li, X., Sleep, J., Hughes, S., & Larsson, L. (1999). In vitro motility speed of slow myosin extracted from single soleus fibres from young and old rats. *The Journal of Physiology*, *520*(2), 463-471.
- Höök, P., Sriramoju, V., & Larsson, L. (2001). Effects of aging on actin sliding speed on myosin from single skeletal muscle cells of mice, rats, and humans. *American Journal of Physiology-Cell Physiology*, *280*(4), C782-C788.
- Hool, L. C. (2009). The L-type Ca²⁺ channel as a potential mediator of pathology during alterations in cellular redox state. *Heart, Lung and Circulation*, *18*(1), 3-10.
- Horwitz, J., Bullard, B., & Mercola, D. (1979). Interaction of troponin subunits. The interaction between the inhibitory and tropomyosin-binding subunits. *Journal of Biological Chemistry*, *254*(2), 350-355.
- Houdusse, A., Szent-Györgyi, A. G., & Cohen, C. (2000). Three conformational states of scallop myosin S1. *Proceedings of the National Academy of Sciences*, *97*(21), 11238-11243.
- Houk Jr, T. W., & Ue, K. (1974). The measurement of actin concentration in solution: a comparison of methods. *Analytical biochemistry*, *62*(1), 66-74.

- Hozumi, T., & Muhrad, A. (1981). Reactive lysyl of myosin subfragment 1: location on the 27K fragment and labeling properties. *Biochemistry*, *20*(10), 2945-2950.
- Humphrey, W., Dalke, A., & Schulten, K. (1996). VMD: visual molecular dynamics. *Journal of molecular graphics*, *14*(1), 33-38.
- Hutchinson, K. R., Stewart Jr, J. A., & Lucchesi, P. A. (2010). Extracellular matrix remodeling during the progression of volume overload-induced heart failure. *Journal of molecular and cellular cardiology*, *48*(3), 564-569.
- Huxley, A. F. (1957). Muscle structure and theories of contraction. *Prog. Biophys. Biophys. Chem*, *7*, 255-318.
- Huxley, A. F., & Niedergerke, R. (1954). Structural Changes in Muscle During Contraction: Interference Microscopy of Living Muscle Fibres. *Nature*, *173*(4412), 971-973. doi:10.1038/173971a0
- Huxley, H., & Hanson, J. (1954). Changes in the Cross-Striations of Muscle during Contraction and Stretch and their Structural Interpretation. *Nature*, *173*(4412), 973-976. doi:10.1038/173973a0
- Hvid, L. G., Ørtenblad, N., Aagaard, P., Kjaer, M., & Suetta, C. (2011). Effects of ageing on single muscle fibre contractile function following short-term immobilisation. *The Journal of Physiology*, *589*(19), 4745-4757.
- Hvid, L. G., Suetta, C., Aagaard, P., Kjaer, M., Frandsen, U., & Ørtenblad, N. (2013). Four days of muscle disuse impairs single fiber contractile function in young and old healthy men. *Experimental gerontology*, *48*(2), 154-161.
- Ijpm, G., Balassy, Z., & Lauzon, A.-M. (2018). Rapid time-stamped analysis of filament motility. *Journal of muscle research and cell motility*, *39*(5), 153-162.
- Jackson, M., Edwards, R., & Symons, M. (1985). Electron spin resonance studies of intact mammalian skeletal muscle. *Biochimica et Biophysica Acta (BBA)-Molecular Cell Research*, *847*(2), 185-190.
- Kabsch, W., Mannherz, H. G., Suck, D., Pai, E. F., & Holmes, K. C. (1990). Atomic structure of the actin:DNase I complex. *Nature*, *347*(6288), 37-44. doi:10.1038/347037a0
- Kalaganov, A., Novinger, R., & Rassier, D. E. (2010). A technique for simultaneous measurement of force and overlap between single muscle filaments of myosin and actin. *Biochemical and biophysical research communications*, *403*(3-4), 351-356.

- Kalganov, A., Shalabi, N., Zitouni, N., Kachmar, L. H., Lauzon, A.-M., & Rassier, D. E. (2013). Forces measured with micro-fabricated cantilevers during actomyosin interactions produced by filaments containing different myosin isoforms and loop 1 structures. *Biochimica et Biophysica Acta (BBA)-General Subjects*, *1830*(3), 2710-2719.
- Kalganov, A., Shalabi, N., Zitouni, N., Kachmar, L. H., Lauzon, A. M., & Rassier, D. E. (2013). Forces measured with micro-fabricated cantilevers during actomyosin interactions produced by filaments containing different myosin isoforms and loop 1 structures. *Biochim Biophys Acta*, *1830*(3), 2710-2719.
- Kanski, J., Behring, A., Pelling, J., & Schoneich, C. (2005). Proteomic identification of 3-nitrotyrosine-containing rat cardiac proteins: effects of biological aging. *American Journal of Physiology-Heart and Circulatory Physiology*, *288*(1), H371-H381.
- Kanski, J., Hong, S. J., & Schöneich, C. (2005). Proteomic analysis of protein nitration in aging skeletal muscle and identification of nitrotyrosine-containing sequences in vivo by nanoelectrospray ionization tandem mass spectrometry. *Journal of Biological Chemistry*, *280*(25), 24261-24266.
- Kapchinsky, S., Vuda, M., Miguez, K., Elkrief, D., de Souza, A. R., Baglolle, C. J., . . . Hepple, R. T. (2018). Smoke-induced neuromuscular junction degeneration precedes the fibre type shift and atrophy in chronic obstructive pulmonary disease. *J Physiol*, *596*(14), 2865-2881. doi:10.1113/jp275558
- Kaya, M., & Higuchi, H. (2010). Nonlinear elasticity and an 8-nm working stroke of single myosin molecules in myofilaments. *Science*, *329*(5992), 686-689.
- Kellermayer, M. S., & Granzier, H. L. (1996). Calcium-dependent inhibition of in vitro thin-filament motility by native titin. *FEBS letters*, *380*(3), 281-286.
- Khaitlina, S. Y. (2001). Functional specificity of actin isoforms. In *International Review of Cytology* (Vol. 202, pp. 35-98): Academic Press.
- Khassaf, M., McArdle, A., Esanu, C., Vasilaki, A., McArdle, F., Griffiths, R., . . . Jackson, M. (2003). Effect of vitamin C supplements on antioxidant defence and stress proteins in human lymphocytes and skeletal muscle. *The Journal of Physiology*, *549*(2), 645-652.
- Kirsch, M., Lomonosova, E. E., Korth, H.-G., Sustmann, R., & de Groot, H. (1998). Hydrogen Peroxide Formation by Reaction of Peroxynitrite with HEPES and Related Tertiary Amines IMPLICATIONS FOR A GENERAL MECHANISM. *Journal of Biological Chemistry*, *273*(21), 12716-12724.

- Kirshenbaum, K., Papp, S., & Highsmith, S. (1993). Cross-linking myosin subfragment 1 Cys-697 and Cys-707 modifies ATP and actin binding site interactions. *Biophysical journal*, *65*(3), 1121-1129.
- Klein, J. C., Moen, R. J., Smith, E. A., Titus, M. A., & Thomas, D. D. (2011). Structural and functional impact of site-directed methionine oxidation in myosin. *Biochemistry*, *50*(47), 10318-10327.
- Knott, A., Purcell, I., & Marston, S. (2002). In vitro motility analysis of thin filaments from failing and non-failing human hearts induces slower filament sliding and higher Ca²⁺-sensitivity. *J Mol Cell Cardiol*, *34*, 469-482.
- Kobayashi, T., Jin, L., & de Tombe, P. P. (2008). Cardiac thin filament regulation. *Pflügers Archiv-European Journal of Physiology*, *457*, 37-46.
- Kobayashi, T., & Solaro, R. J. (2005). Calcium, thin filaments, and the integrative biology of cardiac contractility. *Annu. Rev. Physiol.*, *67*, 39-67.
- Kobzik, L., Reid, M. B., Bredt, D. S., & Stamler, J. S. (1994). Nitric oxide in skeletal muscle. *Nature*, *372*(6506), 546-548.
- Kodera, N., Yamamoto, D., Ishikawa, R., & Ando, T. (2010). Video imaging of walking myosin V by high-speed atomic force microscopy. *Nature*, *468*(7320), 72-76.
- Kopylova, G., Katsnelson, L., Ovsyannikov, D., Bershitsky, S. Y., & Nikitina, L. (2006). Application of in vitro motility assay to studying the calcium-mechanical relationship in skeletal and cardiac muscles. *Biophysics*, *51*, 687-691.
- Korff, S., Katus, H. A., & Giannitsis, E. (2006). Differential diagnosis of elevated troponins. *Heart*, *92*(7), 987-993.
- Kovács, M., Tóth, J., Hetényi, C., Málnási-Csizmadia, A., & Sellers, J. R. (2004). Mechanism of blebbistatin inhibition of myosin II. *Journal of Biological Chemistry*, *279*(34), 35557-35563.
- Kress, M., Huxley, H., Faruqi, A., & Hendrix, J. (1986). Structural changes during activation of frog muscle studied by time-resolved X-ray diffraction. *Journal of molecular biology*, *188*(3), 325-342.
- Kron, S. J., Toyoshima, Y. Y., Uyeda, T. Q., & Spudich, J. A. (1991a). [33] Assays for actin sliding movement over myosin-coated surfaces. In *Methods in enzymology* (Vol. 196, pp. 399-416): Elsevier.

- Kron, S. J., Toyoshima, Y. Y., Uyeda, T. Q., & Spudich, J. A. (1991b). Assays for actin sliding movement over myosin-coated surfaces. In *Methods in enzymology* (Vol. 196, pp. 399-416): Elsevier.
- Kubo, S., Tokura, S., & Tonomura, Y. (1960). On the active site of myosin A-adenosine triphosphatase I. Reaction of the enzyme with trinitrobenzenesulfonate. *Journal of Biological Chemistry*, *235*(10), 2835-2839.
- La Vecchia, L., Mezzena, G., Zanolla, L., Paccanaro, M., Varotto, L., Bonanno, C., & Ometto, R. (2000). Cardiac troponin I as diagnostic and prognostic marker in severe heart failure. *The Journal of heart and lung transplantation*, *19*(7), 644-652.
- Lamb, G. D., & Posterino, G. S. (2003). Effects of oxidation and reduction on contractile function in skeletal muscle fibres of the rat. *J Physiol*, *546*(Pt 1), 149-163.
- Lamb, G. D., & Westerblad, H. (2011). Acute effects of reactive oxygen and nitrogen species on the contractile function of skeletal muscle. *The Journal of physiology*, *589*(9), 2119-2127.
- Lambole, C., Wyckelsma, V., Dutka, T., McKenna, M., Murphy, R., & Lamb, G. (2015). Contractile properties and sarcoplasmic reticulum calcium content in type I and type II skeletal muscle fibres in active aged humans. *The Journal of Physiology*, *593*(11), 2499-2514.
- Larsson, L., Li, X., & Frontera, W. (1997). Effects of aging on shortening velocity and myosin isoform composition in single human skeletal muscle cells. *American Journal of Physiology-Cell Physiology*, *272*(2), C638-C649.
- Lawler, J. M. (2011). Exacerbation of pathology by oxidative stress in respiratory and locomotor muscles with Duchenne muscular dystrophy. *The Journal of Physiology*, *589*(9), 2161-2170.
- Le Moal, E., Pialoux, V., Juban, G., Groussard, C., Zouhal, H., Chazaud, B., & Mounier, R. (2017). Redox control of skeletal muscle regeneration. *Antioxid Redox Signal*, *27*(5), 276-310.
- Lee, B. C., Péterfi, Z., Hoffmann, F. W., Moore, R. E., Kaya, A., Avanesov, A., . . . Fomenko, D. E. (2013). MsrB1 and MICALs regulate actin assembly and macrophage function via reversible stereoselective methionine oxidation. *Molecular cell*, *51*(3), 397-404.
- Lewis, W. G., & Smillie, L. B. (1980). The amino acid sequence of rabbit cardiac tropomyosin. *Journal of Biological Chemistry*, *255*(14), 6854-6859.
- Li, M., Ogilvie, H., Ochala, J., Artemenko, K., Iwamoto, H., Yagi, N., . . . Larsson, L. (2015). Aberrant post-translational modifications compromise human myosin motor function in old age. *Aging cell*, *14*(2), 228-235.

- Li, X., & Larsson, L. (1996). Maximum shortening velocity and myosin isoforms in single muscle fibers from young and old rats. *American Journal of Physiology-Cell Physiology*, *270*(1), C352-C360.
- Lian, D., Chen, M.-M., Wu, H., Deng, S., & Hu, X. (2022). The Role of Oxidative Stress in Skeletal Muscle Myogenesis and Muscle Disease. *Antioxidants*, *11*(4), 755.
- Liguori, I., Russo, G., Curcio, F., Bulli, G., Aran, L., Della-Morte, D., . . . Abete, P. (2018). Oxidative stress, aging, and diseases. *Clinical interventions in aging*, *13*, 757-772. doi:10.2147/CIA.S158513
- Linari, M., Caremani, M., Piperio, C., Brandt, P., & Lombardi, V. (2007). Stiffness and fraction of myosin motors responsible for active force in permeabilized muscle fibers from rabbit psoas. *Biophysical journal*, *92*(7), 2476-2490.
- Liu, R., Warner, R. D., Zhou, G., & Zhang, W. (2018). Contribution of nitric oxide and protein S-nitrosylation to variation in fresh meat quality. *Meat Science*, *144*, 135-148.
- Liu, X., Shu, S., Hong, M.-S. S., Levine, R. L., & Korn, E. D. (2006). Phosphorylation of actin Tyr-53 inhibits filament nucleation and elongation and destabilizes filaments. *Proceedings of the National Academy of Sciences*, *103*(37), 13694-13699.
- Liu, X., Shu, S., Hong, M.-S. S., Yu, B., & Korn, E. D. (2010). Mutation of actin Tyr-53 alters the conformations of the DNase I-binding loop and the nucleotide-binding cleft. *Journal of Biological Chemistry*, *285*(13), 9729-9739.
- Lombardi, V., Piazzesi, G., & Linari, M. (1992). Rapid regeneration of the actin-myosin power stroke in contracting muscle. *Nature*, *355*(6361), 638-641.
- Louie, J. L., Kappahn, R. J., & Ferrington, D. A. (2002). Proteasome function and protein oxidation in the aged retina. *Experimental eye research*, *75*(3), 271-284.
- Lovelock, J. D., Monasky, M. M., Jeong, E.-M., Lardin, H. A., Liu, H., Patel, B. G., . . . Pokhrel, N. (2012). Ranolazine improves cardiac diastolic dysfunction through modulation of myofilament calcium sensitivity. *Circulation research*, *110*(6), 841-850.
- Lowe, D. A., Surek, J. T., Thomas, D. D., & Thompson, L. V. (2001). Electron paramagnetic resonance reveals age-related myosin structural changes in rat skeletal muscle fibers. *American Journal of Physiology-Cell Physiology*, *280*(3), C540-C547.
- Lowe, D. A., Warren, G. L., Snow, L. M., Thompson, L. V., & Thomas, D. D. (2004). Muscle activity and aging affect myosin structural distribution and force generation in rat fibers. *Journal of applied physiology*, *96*(2), 498-506.

- Lu, J., Katano, T., Uta, D., Furue, H., & Ito, S. (2011). Rapid S-nitrosylation of actin by NO-generating donors and in inflammatory pain model mice. *Molecular pain*, 7, 1744-8069-1747-1101.
- Luo, J., Xuan, Y.-T., Gu, Y., & Prabhu, S. D. (2006). Prolonged oxidative stress inverts the cardiac force–frequency relation: role of altered calcium handling and myofilament calcium responsiveness. *Journal of molecular and cellular cardiology*, 40(1), 64-75.
- Luther, P. K. (2009). The vertebrate muscle Z-disc: sarcomere anchor for structure and signalling. *Journal of muscle research and cell motility*, 30(5-6), 171-185.
- Maack, C., Kartes, T., Kilter, H., Schäfers, H.-J., Nickenig, G., Böhm, M., & Laufs, U. (2003). Oxygen free radical release in human failing myocardium is associated with increased activity of rac1-GTPase and represents a target for statin treatment. *Circulation*, 108(13), 1567-1574.
- MacFarlane, N., & Miller, D. (1992). Depression of peak force without altering calcium sensitivity by the superoxide anion in chemically skinned cardiac muscle of rat. *Circulation research*, 70(6), 1217-1224.
- Mahmood, R., Elzinga, M., & Yount, R. G. (1989). Serine-324 of myosin's heavy chain is photoaffinity-labeled by 3'(2')-O-(4-benzoylbenzoyl) adenosine triphosphate. *Biochemistry*, 28(9), 3989-3995.
- Mair, J., Dienstl, F., & Puschendorf, B. (1992). Cardiac troponin T in the diagnosis of myocardial injury. *Critical reviews in clinical laboratory sciences*, 29(1), 31-57.
- Maita, T., Yajima, E., Nagata, S., Miyanishi, T., Nakayama, S., & Matsuda, G. (1991). The primary structure of skeletal muscle myosin heavy chain: IV. Sequence of the rod, and the complete 1,938-residue sequence of the heavy chain. *The Journal of Biochemistry*, 110(1), 75-87.
- Málnási-Csizmadia, A., Tóth, J., Pearson, D. S., Hetényi, C., Nyitray, L., Geeves, M. A., . . . Kovács, M. (2007). Selective perturbation of the myosin recovery stroke by point mutations at the base of the lever arm affects ATP hydrolysis and phosphate release. *Journal of Biological Chemistry*, 282(24), 17658-17664.
- Månsson, A. (2016). Actomyosin based contraction: one mechanokinetic model from single molecules to muscle? *Journal of muscle research and cell motility*, 37(6), 181-194.
- Månsson, A., & Tågerud, S. (2003). Multivariate statistics in analysis of data from the in vitro motility assay. *Analytical biochemistry*, 314(2), 281-293.

- Månsson, A., Ušaj, M., Moretto, L., & Rassier, D. E. (2018). Do actomyosin single-molecule mechanics data predict mechanics of contracting muscle? *Int J Mol Sci*, *19*(7), 1863.
- Marechal, G., & Gailly, P. (1999). Effects of nitric oxide on the contraction of skeletal muscle. *Cell Mol Life Sci*, *55*(8-9), 1088-1102.
- Margossian, S. S., & Lowey, S. (1982). [7] Preparation of myosin and its subfragments from rabbit skeletal muscle. *Methods in enzymology*, *85*, 55-71.
- Markus, B., Narkis, G., Landau, D., Birk, R. Z., Cohen, I., & Birk, O. S. (2012). Autosomal recessive lethal congenital contractural syndrome type 4 (LCCS4) caused by a mutation in MYBPC1. *Human mutation*, *33*(10), 1435-1438.
- Martin-Romero, F. J., Gutiérrez-Martin, Y., Henao, F., & Gutiérrez-Merino, C. (2004). Fluorescence measurements of steady state peroxynitrite production upon SIN-1 decomposition: NADH versus dihydrodichlorofluorescein and dihydrorhodamine 123. *Journal of fluorescence*, *14*(1), 17-23.
- Masuko, K. (2014). Rheumatoid cachexia revisited: a metabolic co-morbidity in rheumatoid arthritis. *Frontiers in nutrition*, *1*, 20-20. doi:10.3389/fnut.2014.00020
- Matecki, S., Fauconnier, J., & Lacampagne, A. (2014). Reactive oxygen species and muscular dystrophy. In (pp. 3055-3079): Springer: Berlin Heidelberg.
- Matusovsky, O. S., Kodera, N., MacEachen, C., Ando, T., Cheng, Y.-S., & Rassier, D. E. (2020). Millisecond conformational dynamics of skeletal myosin II power stroke studied by high-speed atomic force microscopy. *ACS nano*, *15*(2), 2229-2239.
- Matusovsky, O. S., Månsson, A., Persson, M., Cheng, Y.-S., & Rassier, D. E. (2019). High-speed AFM reveals subsecond dynamics of cardiac thin filaments upon Ca²⁺ activation and heavy meromyosin binding. *Proceedings of the National Academy of Sciences*, *116*(33), 16384-16393.
- Matusovsky, O. S., Månsson, A., & Rassier, D. E. (2023). Cooperativity of myosin II motors in the non-regulated and regulated thin filaments investigated with high-speed AFM. *Journal of General Physiology*, *155*(3), e202213190.
- McArdle, A., Dillmann, W. H., Mestril, R., Faulkner, J., & Jackson, M. J. (2004). Overexpression of HSP70 in mouse skeletal muscle protects against muscle damage and age-related muscle dysfunction.

- McArdle, F., Spiers, S., Aldemir, H., Vasilaki, A., Beaver, A., Iwanejko, L., . . . Jackson, M. (2004). Preconditioning of skeletal muscle against contraction-induced damage: the role of adaptations to oxidants in mice. *The Journal of Physiology*, *561*(1), 233-244.
- Mehra, A., Shotan, A., Ostrzega, E., Hsueh, W., Vasquez-Johnson, J., & Elkayam, U. (1994). Potentiation of isosorbide dinitrate effects with N-acetylcysteine in patients with chronic heart failure. *Circulation*, *89*(6), 2595-2600.
- Menazza, S., Aponte, A., Sun, J., Gucek, M., Steenbergen, C., & Murphy, E. (2015). Molecular signature of nitroso–redox balance in idiopathic dilated cardiomyopathies. *Journal of the American Heart Association*, *4*(9), e002251.
- Menazza, S., Blaauw, B., Tiepolo, T., Toniolo, L., Braghetta, P., Spolaore, B., . . . Canton, M. (2010). Oxidative stress by monoamine oxidases is causally involved in myofiber damage in muscular dystrophy. *Human molecular genetics*, *19*(21), 4207-4215.
- Menon, S., & Goswami, P. (2007). A redox cycle within the cell cycle: ring in the old with the new. *Oncogene*, *26*(8), 1101-1109.
- Merry, T. L., & Ristow, M. (2016). Do antioxidant supplements interfere with skeletal muscle adaptation to exercise training? *The Journal of physiology*, *594*(18), 5135-5147.
- Mihm, M. J., Coyle, C. M., Schanbacher, B. L., Weinstein, D. M., & Bauer, J. A. (2001). Peroxynitrite induced nitration and inactivation of myofibrillar creatine kinase in experimental heart failure. *Cardiovascular research*, *49*(4), 798-807.
- Mihm, M. J., Yu, F., Reiser, P. J., & Bauer, J. A. (2003). Effects of peroxynitrite on isolated cardiac trabeculae: selective impact on myofibrillar energetic controllers. *Biochimie*, *85*(6), 587-596.
- Mihm, M. J., Yu, F., Weinstein, D. M., Reiser, P. J., & Bauer, J. A. (2002). Intracellular distribution of peroxynitrite during doxorubicin cardiomyopathy: evidence for selective impairment of myofibrillar creatine kinase. *Br J Pharmacol*, *135*(3), 581-588. doi:10.1038/sj.bjp.0704495
- Miki, M., & Remedios, C. G. d. J. T. J. o. B. (1988). Fluorescence quenching studies of fluorescein attached to Lys-61 or Cys-374 in actin: effects of polymerization, myosin subfragment-1 binding, and tropomyosin-troponin binding. *104*(2), 232-235.
- Milzani, A., Rossi, R., Di Simplicio, P., Giustarini, D., Colombo, R., & DalleDonne, I. (2000). The oxidation produced by hydrogen peroxide on Ca-ATP-G-actin. *Protein science : a publication of the Protein Society*, *9*(9), 1774-1782. doi:10.1110/ps.9.9.1774

- Missov, E., & Mair, J. (1999). A novel biochemical approach to congestive heart failure: cardiac troponin T. *American heart journal*, *138*(1), 95-99.
- Moen, R. J., Cornea, S., Oseid, D. E., Binder, B. P., Klein, J. C., & Thomas, D. D. (2014). Redox-sensitive residue in the actin-binding interface of myosin. *Biochemical and biophysical research communications*, *453*(3), 345-349.
- Mollica, J., Dutka, T., Merry, T., Lambole, C. R., McConell, G., McKenna, M. J., . . . Lamb, G. (2012). S-Glutathionylation of troponin I (fast) increases contractile apparatus Ca²⁺ sensitivity in fast-twitch muscle fibres of rats and humans. *The Journal of Physiology*, *590*(6), 1443-1463.
- Molloy, J., Burns, J., Kendrick-Jones, J., Tregear, R., & White, D. (1995). Movement and force produced by a single myosin head. *Nature*, *378*(6553), 209-212.
- Moretto, L., Ušaj, M., Matusovsky, O., Rassier, D. E., Friedman, R., & Månsson, A. (2022). Multistep orthophosphate release tunes actomyosin energy transduction. *Nature communications*, *13*(1), 4575.
- Mornet, D., Pantel, P., Bertrand, R., Audemard, E., & Kassab, R. (1980). Localization of the reactive trinitrophenylated lysyl residue of myosin ATPase site in the NH₂-terminal (27 k domain) of S1 heavy chain. *FEBS letters*, *117*(1-2), 183-188.
- Morrison, R., Miller 3rd, C., & Reid, M. B. (1996). Nitric oxide effects on shortening velocity and power production in the rat diaphragm. *Journal of applied physiology*, *80*(3), 1065-1069.
- Muhlrad, A. (1983). Mechanism of adenosine triphosphatase activity of trinitrophenylated myosin subfragment 1. *Biochemistry*, *22*(15), 3653-3660.
- Münzel, T., Camici, G. G., Maack, C., Bonetti, N. R., Fuster, V., & Kovacic, J. C. (2017). Impact of oxidative stress on the heart and vasculature: part 2 of a 3-part series. *Journal of the American College of Cardiology*, *70*(2), 212-229.
- Murphy, M. P. (2009). How mitochondria produce reactive oxygen species. *Biochemical Journal*, *417*(1), 1-13.
- Murphy, R., Dutka, T., & Lamb, G. (2008). Hydroxyl radical and glutathione interactions alter calcium sensitivity and maximum force of the contractile apparatus in rat skeletal muscle fibres. *The Journal of Physiology*, *586*(8), 2203-2216.
- Murray, C. I., Gao, W. D., Zhong, X., Stanley, B. A., Foster, D. B., King, S. B., . . . Paolucci, N. (2009). HNO Induces a Disulfide Bond Between Cysteine Residues on Actin (Cys 257) and

- Tropomyosin (Cys 190) Increasing Cardiac Force Development: A Novel, Redox-based Mechanism for Contractile Regulation. In: Am Heart Assoc.
- Muthuchamy, M., Pajak, L., Howles, P., Doetschman, T., & Wieczorek, D. F. (1993). Developmental analysis of tropomyosin gene expression in embryonic stem cells and mouse embryos. *Molecular and cellular biology*.
- Nag, S., Trivedi, D. V., Sarkar, S. S., Adhikari, A. S., Sunitha, M. S., Sutton, S., . . . Spudich, J. A. (2017). The myosin mesa and the basis of hypercontractility caused by hypertrophic cardiomyopathy mutations. *Nature Structural & Molecular Biology*, *24*(6), 525-533.
- Nakamura, T., Prikhodko, O. A., Pirie, E., Nagar, S., Akhtar, M. W., Oh, C.-K., . . . Lipton, S. A. (2015). Aberrant protein S-nitrosylation contributes to the pathophysiology of neurodegenerative diseases. *Neurobiology of disease*, *84*, 99-108.
- Nethery, D., Callahan, L., Stofan, D., Mattera, R., DiMarco, A., & Supinski, G. (2000). PLA2 dependence of diaphragm mitochondrial formation of reactive oxygen species. *Journal of applied physiology*, *89*(1), 72-80.
- Ngo, K. X., Kodera, N., Katayama, E., Ando, T., & Uyeda, T. Q. (2015). Cofilin-induced unidirectional cooperative conformational changes in actin filaments revealed by high-speed atomic force microscopy. *Elife*, *4*, e04806.
- Nogueira, L., Figueiredo-Freitas, C., Casimiro-Lopes, G., Magdesian, M. H., Assreuy, J., & Sorenson, M. M. (2009). Myosin is reversibly inhibited by S-nitrosylation. *Biochem J*, *424*(2), 221-231. doi:10.1042/bj20091144
- Nuttall, S., Kendall, M., & Martin, U. (1999). Antioxidant therapy for the prevention of cardiovascular disease. *QJM*, *92*(5), 239-244.
- Offer, G., & Ranatunga, K. (2020). The Location and Rate of the Phosphate Release Step in the Muscle Cross-Bridge Cycle. *Biophysical journal*, *119*(8), 1501-1512.
- Oh-Ishi, M., Ueno, T., & Maeda, T. (2003). Proteomic method detects oxidatively induced protein carbonyls in muscles of a diabetes model Otsuka Long-Evans Tokushima Fatty (OLETF) rat. *Free Radic Biol Med*, *34*(1), 11-22.
- Okamoto, Y., & Sekine, T. (1985). A streamlined method of subfragment one preparation from myosin. *The Journal of Biochemistry*, *98*(4), 1143-1145.
- Orlova, A., & Egelman, E. H. (1997). Cooperative rigor binding of myosin to actin is a function of F-actin structure. *Journal of molecular biology*, *265*(5), 469-474. doi:10.1006/jmbi.1996.0761

- Ostap, E. M., & Thomas, D. D. (1991). Rotational dynamics of spin-labeled F-actin during activation of myosin S1 ATPase using caged ATP. *Biophys J*, 59(6), 1235-1241. doi:10.1016/s0006-3495(91)82338-4
- Ostap, E. M., White, H. D., & Thomas, D. D. (1993). Transient detection of spin-labeled myosin subfragment 1 conformational states during ATP hydrolysis. *Biochemistry*, 32(26), 6712-6720.
- Otten, E. (1988). Concepts and models of functional architecture in skeletal muscle. *Exercise and sport sciences reviews*, 16(1), 89-138.
- Oztug Durer, Z. A., Kamal, J. K. A., Benchaar, S., Chance, M. R., & Reisler, E. (2011). Myosin binding surface on actin probed by hydroxyl radical footprinting and site-directed labels. *Journal of molecular biology*, 414(2), 204-216. doi:10.1016/j.jmb.2011.09.035
- Pal, R., Thakur, P. B., Li, S., Minard, C., & Rodney, G. G. (2013). Real-time imaging of NADPH oxidase activity in living cells using a novel fluorescent protein reporter. *PLoS one*, 8(5), e63989.
- Pardee, J. D., & Spudich, J. (1982). [18] Purification of muscle actin. *Methods in enzymology*, 85, 164-181.
- Passarelli, C., Di Venere, A., Piroddi, N., Pastore, A., Scellini, B., Tesi, C., . . . Poggesi, C. (2010). Susceptibility of isolated myofibrils to in vitro glutathionylation: potential relevance to muscle functions. *Cytoskeleton*, 67(2), 81-89.
- Passarelli, C., Petrini, S., Pastore, A., Bonetto, V., Sale, P., Gaeta, L. M., . . . Rossi, R. (2008). Myosin as a potential redox-sensor: an in vitro study. *Journal of muscle research and cell motility*, 29(2-5), 119-126.
- Pastore, A., Tozzi, G., Gaeta, L. M., Bertini, E., Serafini, V., Di Cesare, S., . . . Federici, G. (2003). Actin glutathionylation increases in fibroblasts of patients with Friedreich's ataxia: a potential role in the pathogenesis of the disease. *Journal of Biological Chemistry*, 278(43), 42588-42595.
- Pate, E., Nakamaye, K., Franks-Skiba, K., Yount, R., & Cooke, R. (1991). Mechanics of glycerinated muscle fibers using nonnucleoside triphosphate substrates. *Biophysical journal*, 59(3), 598-605.
- Patel, B. G., Wilder, T., & Solaro, R. J. (2013). Novel control of cardiac myofilament response to calcium by S-glutathionylation at specific sites of myosin binding protein C. *Frontiers in physiology*, 4, 336.

- Peoples, J. N., Saraf, A., Ghazal, N., Pham, T. T., & Kwong, J. Q. (2019). Mitochondrial dysfunction and oxidative stress in heart disease. *Experimental & molecular medicine*, 51(12), 1-13.
- Perkins, W. J., Han, Y.-S., & Sieck, G. C. (1997). Skeletal muscle force and actomyosin ATPase activity reduced by nitric oxide donor. *Journal of applied physiology*, 83(4), 1326-1332.
- Persson, M., Steinz, M. M., Westerblad, H., Lanner, J. T., & Rassier, D. E. (2019). Force generated by myosin cross-bridges is reduced in myofibrils exposed to ROS/RNS. *American Journal of Physiology-Cell Physiology*, 317(6), C1304-C1312.
- Peyser, Y. M., Muhlrud, A., & Werber, M. M. (1990). Tryptophan-130 is the most reactive tryptophan residue in rabbit skeletal myosin subfragment-1. *FEBS letters*, 259(2), 346-348.
- Pfeilschifter, J., Eberhardt, W., & Huwiler, A. (2001). Nitric oxide and mechanisms of redox signalling: matrix and matrix-metabolizing enzymes as prime nitric oxide targets. *Eur J Pharmacol*, 429(1-3), 279-286.
- Phillips, L., Separovic, F., Cornell, B. A., Barden, J. A., & dos Remedios, C. G. (1991). Actin dynamics studied by solid-state NMR spectroscopy. *European Biophysics Journal*, 19(3), 147-155. doi:10.1007/BF00185455
- Pinto, J. R., de Sousa, V. P., & Sorenson, M. M. (2011). Redox state of troponin C cysteine in the D/E helix alters the C-domain affinity for the thin filament of vertebrate striated muscle. *Biochimica et Biophysica Acta (BBA)-General Subjects*, 1810(4), 391-397.
- Pinto, J. R., Veltri, T., & Sorenson, M. M. (2008). Modulation of troponin C affinity for the thin filament by different cross-bridge states in skinned skeletal muscle fibers. *Pflügers Archiv-European Journal of Physiology*, 456, 1177-1187.
- Pizarro, G. O., & Ogut, O. (2009). Impact of actin glutathionylation on the actomyosin-S1 ATPase. *Biochemistry*, 48(31), 7533-7538.
- Polewicz, D., Cadete, V. J., Doroszko, A., Hunter, B. E., Sawicka, J., Szczesna-Cordary, D., . . . Sawicki, G. (2011). Ischemia induced peroxynitrite dependent modifications of cardiomyocyte MLC1 increases its degradation by MMP-2 leading to contractile dysfunction. *Journal of cellular and molecular medicine*, 15(5), 1136-1147.
- Polewicz, D. K. (2011). *Oxidative stress-induced, peroxynitrite-dependent, modifications of myosin light chain 1 lead to its increased degradation by matrix metalloproteinase-2*. Citeseer,

- Potter, J. D., Seidel, J. C., Leavis, P., Lehrer, S. S., & Gergely, J. (1976). Effect of Ca²⁺ binding on troponin C. Changes in spin label mobility, extrinsic fluorescence, and sulfhydryl reactivity. *Journal of Biological Chemistry*, *251*(23), 7551-7556.
- Powers, S. K., & Jackson, M. J. (2008). Exercise-induced oxidative stress: cellular mechanisms and impact on muscle force production. *Physiological reviews*, *88*(4), 1243-1276.
- Prochniewicz, E., Lowe, D. A., Spakowicz, D. J., Higgins, L., O'Connor, K., Thompson, L. V., . . . Thomas, D. D. (2008). Functional, structural, and chemical changes in myosin associated with hydrogen peroxide treatment of skeletal muscle fibers. *American Journal of Physiology-Cell Physiology*, *294*(2), C613-C626.
- Prochniewicz, E., Spakowicz, D., & Thomas, D. D. (2008). Changes in actin structural transitions associated with oxidative inhibition of muscle contraction. *Biochemistry*, *47*(45), 11811-11817. doi:10.1021/bi801080x
- Prochniewicz, E., Thompson, L. V., & Thomas, D. D. (2007). Age-related decline in actomyosin structure and function. *Experimental gerontology*, *42*(10), 931-938. doi:10.1016/j.exger.2007.06.015
- Pye, D., Palomero, J., Kabayo, T., & Jackson, M. J. (2007). Real-time measurement of nitric oxide in single mature mouse skeletal muscle fibres during contractions. *The Journal of physiology*, *581*(1), 309-318.
- Quinlan, C. L., Treberg, J. R., Perevoshchikova, I. V., Orr, A. L., & Brand, M. D. (2012). Native rates of superoxide production from multiple sites in isolated mitochondria measured using endogenous reporters. *Free Radical Biology and Medicine*, *53*(9), 1807-1817.
- Radi, R. (2004). Nitric oxide, oxidants, and protein tyrosine nitration. *Proceedings of the National Academy of Sciences*, *101*(12), 4003-4008.
- Radi, R. (2012). Protein tyrosine nitration: biochemical mechanisms and structural basis of functional effects. *Accounts of chemical research*, *46*(2), 550-559.
- Ragusa, R. J., Chow, C. K., & Porter, J. D. (1997). Oxidative stress as a potential pathogenic mechanism in an animal model of Duchenne muscular dystrophy. *Neuromuscular disorders*, *7*(6-7), 379-386.
- Rahman, M. A., Salhotra, A., & Månsson, A. (2018). Comparative analysis of widely used methods to remove nonfunctional myosin heads for the in vitro motility assay. *Journal of muscle research and cell motility*, *39*(5), 175-187.

- Rahman, M. A., Ušaj, M., Rassier, D. E., & Månsson, A. (2018). Blebbistatin effects expose hidden secrets in the force-generating cycle of actin and myosin. *Biophysical journal*, *115*(2), 386-397.
- Ramakrishnan, S., & Hitchcock-DeGregori, S. E. (1995). Investigation of the structural requirements of the troponin C central helix for function. *Biochemistry*, *34*(51), 16789-16796.
- Ramamurthy, B., & Larsson, L. (2013). Detection of an aging-related increase in advanced glycation end products in fast-and slow-twitch skeletal muscles in the rat. *Biogerontology*, *14*(3), 293-301.
- Rando, T. A., Disatnik, M.-H., Yu, Y., & Franco, A. (1998). Muscle cells from mdx mice have an increased susceptibility to oxidative stress. *Neuromuscular disorders*, *8*(1), 14-21.
- Rayment, I., Holden, H. M., Whittaker, M., Yohn, C. B., Lorenz, M., Holmes, K. C., & Milligan, R. A. (1993). Structure of the actin-myosin complex and its implications for muscle contraction. *Science*, *261*(5117), 58-65.
- Reid, M. B. (2001). Invited Review: redox modulation of skeletal muscle contraction: what we know and what we don't. *Journal of applied physiology*, *90*(2), 724-731.
- Reid, M. B., & Durham, W. J. (2002). Generation of reactive oxygen and nitrogen species in contracting skeletal muscle: potential impact on aging. *Annals of the New York Academy of Sciences*, *959*(1), 108-116.
- Reid, M. B., Khawli, F., & Moody, M. R. (1993). Reactive oxygen in skeletal muscle. III. Contractility of unfatigued muscle. *Journal of applied physiology*, *75*(3), 1081-1087.
- Reid, M. B., & Moylan, J. S. (2011). Beyond atrophy: redox mechanisms of muscle dysfunction in chronic inflammatory disease. *The Journal of Physiology*, *589*(9), 2171-2179.
- Reynoso, J., Bobkov, A., Muhrad, A., & Reisler, E. (2001). Solution properties of full length and truncated forms of myosin subfragment 1 from Dictyostelium discoideum. *Journal of Muscle Research & Cell Motility*, *22*, 657-664.
- Salhotra, A., Zhu, J., Surendiran, P., Meinecke, C. R., Lyttleton, R., Ušaj, M., . . . Månsson, A. (2021). Prolonged function and optimization of actomyosin motility for upscaled network-based biocomputation. *New Journal of Physics*, *23*(8), 085005.
- Samengo, G., Avik, A., Fedor, B., Whittaker, D., Myung, K. H., Wehling-Henricks, M., & Tidball, J. G. (2012). Age-related loss of nitric oxide synthase in skeletal muscle causes reductions in

- calpain S-nitrosylation that increase myofibril degradation and sarcopenia. *Aging cell*, 11(6), 1036-1045. doi:10.1111/ace1.12003
- Santolini, J., Adak, S., Curran, C. M., & Stuehr, D. J. (2001). A kinetic simulation model that describes catalysis and regulation in nitric-oxide synthase. *Journal of Biological Chemistry*, 276(2), 1233-1243.
- Schiaffino, S., & Reggiani, C. (1996). Molecular diversity of myofibrillar proteins: gene regulation and functional significance. *Physiological reviews*, 76(2), 371-423.
- Schlossarek, S., Mearini, G., & Carrier, L. (2011). Cardiac myosin-binding protein C in hypertrophic cardiomyopathy: mechanisms and therapeutic opportunities. *Journal of molecular and cellular cardiology*, 50(4), 613-620.
- Schoenmakers, T. J., Visser, G. J., Flik, G., & Theuvenet, A. P. (1992). CHELATOR: an improved method for computing metal ion concentrations in physiological solutions.
- Schulz, R., Dodge, K. L., Lopaschuk, G. D., & Clanachan, A. S. (1997). Peroxynitrite impairs cardiac contractile function by decreasing cardiac efficiency. *American Journal of Physiology-Heart and Circulatory Physiology*, 272(3), H1212-H1219.
- Scott, B., Deman, A., Peeters, P., Van den Branden, C., Stolear, J. C., Van Camp, G., & Verbeelen, D. (2003). Cardiac troponin T and malondialdehyde modified plasma lipids in haemodialysis patients. *Nephrology Dialysis Transplantation*, 18(4), 737-742.
- Seddon, M., Looi, Y. H., & Shah, A. M. (2007). Oxidative stress and redox signalling in cardiac hypertrophy and heart failure. *Heart*, 93(8), 903-907.
- Seidel, J. (1969). Similar effects on enzymic activity due to chemical modification of either of two sulfhydryl groups of myosin. *Biochimica et Biophysica Acta (BBA)-Bioenergetics*, 180(1), 216-219.
- Serra, A. J., Pinto, J. R., Prokić, M. D., Arsa, G., & Vasconsuelo, A. (2020). Oxidative stress in muscle diseases: current and future therapy 2019. In (Vol. 2020): Hindawi.
- Sheeran, F. L., & Pepe, S. (2006). Energy deficiency in the failing heart: linking increased reactive oxygen species and disruption of oxidative phosphorylation rate. *Biochimica et Biophysica Acta (BBA)-Bioenergetics*, 1757(5-6), 543-552.
- Shenouda, S. K., Lord, K. C., McIlwain, E., Lucchesi, P. A., & Varner, K. J. (2008). Ecstasy produces left ventricular dysfunction and oxidative stress in rats. *Cardiovascular research*, 79(4), 662-670.

- Shishkin, S., Kovalyov, L., & Kovalyova, M. (2004). Proteomic studies of human and other vertebrate muscle proteins. *Biochemistry (Moscow)*, *69*(11), 1283-1298.
- Silveira, L. R., Pereira-Da-Silva, L., Juel, C., & Hellsten, Y. (2003). Formation of hydrogen peroxide and nitric oxide in rat skeletal muscle cells during contractions. *Free Radical Biology and Medicine*, *35*(5), 455-464.
- Singh, R. J., Hogg, N., Joseph, J., Konorev, E., & Kalyanaraman, B. (1999). The peroxynitrite generator, SIN-1, becomes a nitric oxide donor in the presence of electron acceptors. *Archives of biochemistry and biophysics*, *361*(2), 331-339.
- Slupsky, C. M., & Sykes, B. D. (1995). NMR solution structure of calcium-saturated skeletal muscle troponin C. *Biochemistry*, *34*(49), 15953-15964.
- Snook, J. H., Li, J., Helmke, B. P., & Guilford, W. H. (2008). Peroxynitrite inhibits myofibrillar protein function in an in vitro assay of motility. *Free Radic Biol Med*, *44*(1), 14-23. doi:10.1016/j.freeradbiomed.2007.09.004
- Snook, J. H., Li, J., Helmke, B. P., & Guilford, W. H. (2008). Peroxynitrite inhibits myofibrillar protein function in an in vitro assay of motility. *Free Radical Biology and Medicine*, *44*(1), 14-23.
- Snow, L. M., Fugere, N. A., & Thompson, L. V. (2007). Advanced glycation end-product accumulation and associated protein modification in type II skeletal muscle with aging. *The Journals of Gerontology Series A: Biological Sciences and Medical Sciences*, *62*(11), 1204-1210.
- Šochman, J., & Peregrin, J. H. (1992). Total recovery of left ventricular function after acute myocardial infarction: comprehensive therapy with streptokinase, N-acetylcysteine and percutaneous transluminal coronary angioplasty. *Int J Cardiol*, *35*(1), 116-118.
- Šochman, J., Vrbská, J., Musilová, B., & Roček, M. (1996). Infarct size limitation: acute N-acetylcysteine defense (ISLAND trial): preliminary analysis and report after the first 30 patients. *Clinical cardiology*, *19*(2), 94-100.
- Squier, T. C. (2001). Oxidative stress and protein aggregation during biological aging. *Experimental gerontology*, *36*(9), 1539-1550.
- Stadtman, E. R., & Levine, R. L. (2000). Protein oxidation. *Annals of the New York Academy of Sciences*, *899*(1), 191-208.
- Stamler, J. S., Lamas, S., & Fang, F. C. (2001). Nitrosylation. the prototypic redox-based signaling mechanism. *Cell*, *106*(6), 675-683.

- Stehle, R., Solzin, J., Iorga, B., & Poggesi, C. (2009). Insights into the kinetics of Ca²⁺-regulated contraction and relaxation from myofibril studies. *Pflügers Archiv-European Journal of Physiology*, *458*, 337-357.
- Steinberg, S. F. (2013). Oxidative stress and sarcomeric proteins. *Circulation research*, *112*(2), 393-405.
- Steinhorn, B., Sorrentino, A., Badole, S., Bogdanova, Y., Belousov, V., & Michel, T. (2018). Chemogenetic generation of hydrogen peroxide in the heart induces severe cardiac dysfunction. *Nature communications*, *9*(1), 4044.
- Steinz, M. M. (2020). Oxidative stress and muscle weakness associated with rheumatoid arthritis.
- Steinz, M. M., Persson, M., Aresh, B., Olsson, K., Cheng, A. J., Ahlstrand, E., . . . Möller, K. Ä. (2019). Oxidative hotspots on actin promote skeletal muscle weakness in rheumatoid arthritis. *JCI insight*, *4*(9).
- Stewart, T. J., Murthy, V., Dugan, S. P., & Baker, J. E. (2021). Velocity of myosin-based actin sliding depends on attachment and detachment kinetics and reaches a maximum when myosin-binding sites on actin saturate. *Journal of Biological Chemistry*, *297*(5).
- Straight, C. R., Ades, P. A., Toth, M. J., & Miller, M. S. (2018). Age-related reduction in single muscle fiber calcium sensitivity is associated with decreased muscle power in men and women. *Experimental gerontology*, *102*, 84-92.
- Sun, M., Rose, M. B., Ananthanarayanan, S. K., Jacobs, D. J., & Yengo, C. M. J. (2008). Characterization of the pre-force-generation state in the actomyosin cross-bridge cycle. *PNAS*. *105*(25), 8631-8636.
- Sundaralingam, M., Bergstrom, R., Strasburg, G., Rao, S., Roychowdhury, P., Greaser, M., & Wang, B. (1985). Molecular structure of troponin C from chicken skeletal muscle at 3-angstrom resolution. *Science*, *227*(4689), 945-948.
- Sundberg, M., Rosengren, J. P., Bunk, R., Lindahl, J., Nicholls, I. A., Tågerud, S., . . . Månsson, A. (2003). Silanized surfaces for in vitro studies of actomyosin function and nanotechnology applications. *Anal Biochem*, *323*(1), 127-138.
- Supinski, G., Stofan, D., Callahan, L. A., Nethery, D., Nosek, T. M., & DiMarco, A. (1999). Peroxynitrite induces contractile dysfunction and lipid peroxidation in the diaphragm. *J Appl Physiol (1985)*, *87*(2), 783-791. doi:10.1152/jappl.1999.87.2.783

- Tahara, E. B., Navarete, F. D., & Kowaltowski, A. J. (2009). Tissue-, substrate-, and site-specific characteristics of mitochondrial reactive oxygen species generation. *Free Radical Biology and Medicine*, *46*(9), 1283-1297.
- Takeda, S., Kobayashi, T., Taniguchi, H., Hayashi, H., & Maéda, Y. (1997). Structural and functional domains of the troponin complex revealed by limited digestion. *Eur J Biochem*, *246*(3), 611-617.
- Takeda, S., Yamashita, A., Maeda, K., & Maéda, Y. (2003). Structure of the core domain of human cardiac troponin in the Ca²⁺-saturated form. *Nature*, *424*(6944), 35-41.
- Takimoto, E., & Kass, D. A. (2007). Role of oxidative stress in cardiac hypertrophy and remodeling. *Hypertension*, *49*(2), 241-248.
- Taldone, F. S., Tummala, M., Goldstein, E. J., Ryzhov, V., Ravi, K., & Black, S. M. (2005). Studying the S-nitrosylation of model peptides and eNOS protein by mass spectrometry. *Nitric Oxide*, *13*(3), 176-187.
- Terman, J. R., & Kashina, A. (2013). Post-translational modification and regulation of actin. *Curr Opin Cell Biol*, *25*(1), 30-38. doi:10.1016/j.ceb.2012.10.009
- Thomas, D. D., Prochniewicz, E., & Roopnarine, O. (2002). Changes in actin and myosin structural dynamics due to their weak and strong interactions. In *Molecular Interactions of Actin* (pp. 7-19): Springer.
- Thompson, L. V. (2009). Age-related muscle dysfunction. *Experimental gerontology*, *44*(1-2), 106-111.
- Thompson, L. V., Durand, D., Fugere, N. A., & Ferrington, D. A. (2006). Myosin and actin expression and oxidation in aging muscle. *J Appl Physiol (1985)*, *101*(6), 1581-1587. doi:10.1152/jappphysiol.00426.2006
- Thomson, M. J., Frenneaux, M. P., & Kaski, J. (2009). Antioxidant treatment for heart failure: friend or foe? *QJM: An International Journal of Medicine*, *102*(5), 305-310.
- Tiago, T., Palma, P. S., Gutierrez-Merino, C., & Aureliano, M. (2010). Peroxynitrite-mediated oxidative modifications of myosin and implications on structure and function. *Free Radical Research*, *44*(11), 1317-1327.
- Tiago, T., Ramos, S., Aureliano, M., & Gutierrez-Merino, C. (2006). Peroxynitrite induces F-actin depolymerization and blockade of myosin ATPase stimulation. *Biochem Biophys Res Commun*, *342*(1), 44-49. doi:10.1016/j.bbrc.2006.01.112

- Tiago, T., Simao, S., Aureliano, M., Martín-Romero, F. J., & Gutiérrez-Merino, C. (2006). Inhibition of skeletal muscle S1-myosin ATPase by peroxynitrite. *Biochemistry*, *45*(11), 3794-3804.
- Tidball, J. G., & Wehling-Henricks, M. (2007). The role of free radicals in the pathophysiology of muscular dystrophy. *Journal of applied physiology*, *102*(4), 1677-1686.
- Tien, M., Berlett, B. S., Levine, R. L., Chock, P. B., & Stadtman, E. R. (1999). Peroxynitrite-mediated modification of proteins at physiological carbon dioxide concentration: pH dependence of carbonyl formation, tyrosine nitration, and methionine oxidation. *Proceedings of the National Academy of Sciences*, *96*(14), 7809-7814.
- Tokuraku, K., Uyeda, T. Q. P. J. J. o. M. R., & Motility, C. (2001). Phalloidin affects the myosin-dependent sliding velocities of actin filaments in a bound-divalent cation dependent manner. *22*(4), 371-378. doi:10.1023/a:1013120127602
- Tsaturyan, A. K., Koubassova, N., Ferenczi, M. A., Narayanan, T., Roessle, M., & Bershtitsky, S. Y. (2005). Strong binding of myosin heads stretches and twists the actin helix. *Biophysical journal*, *88*(3), 1902-1910.
- Turrens, J. F., & Boveris, A. (1980). Generation of superoxide anion by the NADH dehydrogenase of bovine heart mitochondria. *Biochemical Journal*, *191*(2), 421-427.
- Uchida, K. (2003). Histidine and lysine as targets of oxidative modification. *Amino acids*, *25*(3-4), 249-257.
- Uchihashi, T., Kodera, N., & Ando, T. (2012). Guide to video recording of structure dynamics and dynamic processes of proteins by high-speed atomic force microscopy. *Nature protocols*, *7*(6), 1193-1206.
- Umanskaya, A., Santulli, G., Xie, W., Andersson, D. C., Reiken, S. R., & Marks, A. R. (2014). Genetically enhancing mitochondrial antioxidant activity improves muscle function in aging. *Proceedings of the National Academy of Sciences*, *111*(42), 15250-15255.
- Uyeda, T. Q., Kron, S. J., & Spudich, J. A. (1990). Myosin step size: estimation from slow sliding movement of actin over low densities of heavy meromyosin. *Journal of molecular biology*, *214*(3), 699-710.
- Vaage, J., Antonelli, M., Bufi, M., Irtun, Ö., DeBlasi, R. A., Corbucci, G. G., . . . Semb, A. G. (1997). Exogenous reactive oxygen species deplete the isolated rat heart of antioxidants. *Free Radical Biology and Medicine*, *22*(1-2), 85-92.

- van der Pol, A., van Gilst, W. H., Voors, A. A., & van der Meer, P. (2019). Treating oxidative stress in heart failure: past, present and future. *European Journal of Heart Failure*, 21(4), 425-435.
- van der Veen, R. C., & Roberts, L. J. (1999). Contrasting roles for nitric oxide and peroxynitrite in the peroxidation of myelin lipids. *J Neuroimmunol*, 95(1-2), 1-7. doi:10.1016/s0165-5728(98)00239-2
- Van Dijk, S. J., Bezold, K. L., & Harris, S. P. (2014). Earning stripes: myosin binding protein-C interactions with actin. *Pflügers Archiv-European Journal of Physiology*, 466(3), 445-450.
- Varland, S., Vandekerckhove, J., & Drazic, A. (2019). Actin Post-translational Modifications: The Cinderella of Cytoskeletal Control. *Trends Biochem Sci*. doi:10.1016/j.tibs.2018.11.010
- Vasilaki, A., Mansouri, A., Van Remmen, H., Van Der Meulen, J., Larkin, L., Richardson, A. G., . . . Jackson, M. J. (2006). Free radical generation by skeletal muscle of adult and old mice: effect of contractile activity. *Aging cell*, 5(2), 109-117.
- Vassilyev, D. G., Takeda, S., Wakatsuki, S., Maeda, K., & Maéda, Y. (1998). Crystal structure of troponin C in complex with troponin I fragment at 2.3-Å resolution. *Proceedings of the National Academy of Sciences*, 95(9), 4847-4852.
- Veigel, C., Molloy, J. E., Schmitz, S., & Kendrick-Jones, J. (2003). Load-dependent kinetics of force production by smooth muscle myosin measured with optical tweezers. *Nature cell biology*, 5(11), 980-986.
- Verrastro, I., Pasha, S., Tveen Jensen, K., Pitt, A. R., & Spickett, C. M. (2015). Mass spectrometry-based methods for identifying oxidized proteins in disease: advances and challenges. *Biomolecules*, 5(2), 378-411.
- Vikhorev, P. G., Vikhoreva, N. N., & Månsson, A. (2008). Bending flexibility of actin filaments during motor-induced sliding. *Biophysical journal*, 95(12), 5809-5819. doi:10.1529/biophysj.108.140335
- Vikhoreva, N. N., Vikhorev, P. G., Fedorova, M. A., Hoffmann, R., Månsson, A., & Kuleva, N. V. (2009). The in vitro motility assay parameters of actin filaments from *Mytilus edulis* exposed in vivo to copper ions. *Archives of biochemistry and biophysics*, 491(1-2), 32-38.
- Walcott, S., Warshaw, D. M., & Debold, E. P. (2012). Mechanical coupling between myosin molecules causes differences between ensemble and single-molecule measurements. *Biophysical journal*, 103(3), 501-510.
- Walsmith, J., & Roubenoff, R. (2002). Cachexia in rheumatoid arthritis. *Int J Cardiol*, 85(1), 89-99.

- Wang, L., Lopaschuk, G. D., & Clanachan, A. S. (2008). H₂O₂-induced left ventricular dysfunction in isolated working rat hearts is independent of calcium accumulation. *Journal of molecular and cellular cardiology*, *45*(6), 787-795.
- Wang, Y., Ajtai, K., & Burghardt, T. P. (2014). Ventricular myosin modifies in vitro step-size when phosphorylated. *Biophysical journal*, *106*(2), 563a.
- Wang, Y., Yuan, C.-C., Kazmierczak, K., Szczesna-Cordary, D., & Burghardt, T. P. (2018). Single cardiac ventricular myosins are autonomous motors. *Open biology*, *8*(4), 170240.
- Ward, D. G., Ashton, P. R., Trayer, H. R., & Trayer, I. P. (2001). Additional PKA phosphorylation sites in human cardiac troponin I. *Eur J Biochem*, *268*(1), 179-185.
- Warnecke, A., Sandalova, T., Achour, A., & Harris, R. A. (2014). PyTMs: a useful PyMOL plugin for modeling common post-translational modifications. *BMC bioinformatics*, *15*(1), 1-12.
- Watanabe, H., Ogasawara, M., Suzuki, N., Nishizawa, N., & Ambo, K. (1992). Glycation of myofibrillar protein in aged rats and mice. *Bioscience, biotechnology, and biochemistry*, *56*(7), 1109-1112.
- Wehling, M., Spencer, M. J., & Tidball, J. G. (2001). A nitric oxide synthase transgene ameliorates muscular dystrophy in mdx mice. *The Journal of cell biology*, *155*(1), 123-132.
- Wei, B., & Jin, J.-P. (2011). Troponin T isoforms and posttranscriptional modifications: Evolution, regulation and function. *Archives of biochemistry and biophysics*, *505*(2), 144-154.
- Weitzberg, E., Hezel, M., & Lundberg, J. O. (2010). Nitrate-nitrite-nitric oxide PathwayImplications for anesthesiology and intensive care. *Anesthesiology: The Journal of the American Society of Anesthesiologists*, *113*(6), 1460-1475.
- Westerblad, H., & Allen, D. G. (2011). Emerging roles of ROS/RNS in muscle function and fatigue. *Antioxidants & redox signaling*, *15*(9), 2487-2499.
- Williams Jr, D. L., & Swenson, C. A. (1982). Disulfide bridges in tropomyosin: effect on ATPase activity of actomyosin. *Eur J Biochem*, *127*(3), 495-499.
- Wink, D. A., Cook, J. A., Pacelli, R., Liebmann, J., Krishna, M. C., & Mitchell, J. B. (1995). Nitric oxide (NO) protects against cellular damage by reactive oxygen species. *Toxicology letters*, *82*, 221-226.
- Winkler, B. S., Boulton, M. E., Gottsch, J. D., & Sternberg, P. (1999). Oxidative damage and age-related macular degeneration. *Molecular vision*, *5*, 32.
- Wolska, B. M., & Wieczorek, D. F. (2003). The role of tropomyosin in the regulation of myocardial contraction and relaxation. *Pflügers Archiv*, *446*, 1-8.

- Wong, S. W., Sun, S., Cho, M., Lee, K. K., & Mak, A. F. (2015). H₂O₂ Exposure Affects Myotube Stiffness and Actin Filament Polymerization. *Ann Biomed Eng*, *43*(5), 1178-1188. doi:10.1007/s10439-014-1178-2
- Wu, A. H., Feng, Y.-J., Moore, R., Apple, F. S., McPherson, P. H., Buechler, K. F., . . . Standardization, C. C. S. o. c. (1998). Characterization of cardiac troponin subunit release into serum after acute myocardial infarction and comparison of assays for troponin T and I. *Clinical chemistry*, *44*(6), 1198-1208.
- Wulf, S. F., Ropars, V., Fujita-Becker, S., Oster, M., Hofhaus, G., Trabuco, L. G., . . . Schröder, R. R. (2016). Force-producing ADP state of myosin bound to actin. *Proceedings of the National Academy of Sciences*, *113*(13), E1844-E1852.
- Yamada, T., Abe, M., Lee, J., Tatebayashi, D., Himori, K., Kanzaki, K., . . . Lanner, J. T. (2015). Muscle dysfunction associated with adjuvant-induced arthritis is prevented by antioxidant treatment. *Skeletal muscle*, *5*(1), 1-10.
- Yamada, T., Fedotovskaya, O., Cheng, A. J., Cornachione, A. S., Minozzo, F. C., Aulin, C., . . . Lanner, J. T. (2015). Nitrosative modifications of the Ca²⁺ release complex and actin underlie arthritis-induced muscle weakness. *Annals of the rheumatic diseases*, *74*(10), 1907-1914. doi:10.1136/annrheumdis-2013-205007
- Yamada, T., Mishima, T., Sakamoto, M., Sugiyama, M., Matsunaga, S., & Wada, M. (2006). Oxidation of myosin heavy chain and reduction in force production in hyperthyroid rat soleus. *J Appl Physiol (1985)*, *100*(5), 1520-1526. doi:10.1152/jappphysiol.01456.2005
- Yamada, T., Place, N., Kosterina, N., Ostberg, T., Zhang, S. J., Grundtman, C., . . . Westerblad, H. (2009). Impaired myofibrillar function in the soleus muscle of mice with collagen-induced arthritis. *Arthritis Rheum*, *60*(11), 3280-3289. doi:10.1002/art.24907
- Yamada, T., Steinz, M. M., Kenne, E., & Lanner, J. T. (2017). Muscle Weakness in Rheumatoid Arthritis: The Role of Ca²⁺ and Free Radical Signaling. *EBioMedicine*, *23*, 12-19. doi:10.1016/j.ebiom.2017.07.023
- Yamaguchi, M., & Sekine, T. (1966). Sulfhydryl groups involved in the active site of myosin A adenosine triphosphatase. *The Journal of Biochemistry*, *59*(1), 24-33.
- Yasui, B., Fuchs, F., & Briggs, F. (1968). The role of the sulfhydryl groups of tropomyosin and troponin in the calcium control of actomyosin contractility. *Journal of Biological Chemistry*, *243*(4), 735-742.

- Yount, R. G., Cremo, C. R., Grammer, J. C., & Kerwin, B. A. (1992). Photochemical mapping of the active site of myosin. *Philosophical Transactions of the Royal Society of London. Series B: Biological Sciences*, 336(1276), 55-61.
- Zhong, S., Lowe, D. A., & Thompson, L. V. (2006). Effects of hindlimb unweighting and aging on rat semimembranosus muscle and myosin. *Journal of applied physiology*, 101(3), 873-880.
- Zima, A. V., & Blatter, L. A. (2006). Redox regulation of cardiac calcium channels and transporters. *Cardiovascular research*, 71(2), 310-321.
- Zinellu, E., Zinellu, A., Fois, A. G., Carru, C., & Pirina, P. (2016). Circulating biomarkers of oxidative stress in chronic obstructive pulmonary disease: a systematic review. *Respiratory research*, 17, 1-11.